

UNIVERSIDADE FEDERAL DE MINAS GERAIS
INSTITUTO DE CIÊNCIAS BIOLÓGICAS
DEPARTAMENTO DE BIOLOGIA GERAL
PROGRAMA DE PÓS-GRADUAÇÃO EM GENÉTICA



Tese de Doutorado

**Estudo do genoma funcional de *Corynebacterium pseudotuberculosis*
através de diferentes estratégias proteômicas**

Orientado: Wanderson Marques da Silva

Orientadores: Prof./Dr. Vasco Ariston de Carvalho Azevedo

Dr. Yves Le Loir

**Belo Horizonte
2015**



THESE / AGROCAMPUS OUEST

Sous le label de l'Université Européenne de Bretagne

pour obtenir le diplôme de :

DOCTEUR DE L'INSTITUT SUPERIEUR DES SCIENCES AGRONOMIQUES, AGRO-ALIMENTAIRES, HORTICOLES ET DU PAYSAGE

Spécialité : Biochimie, Biologie moléculaire et cellulaire

Ecole Doctorale : Vie Agro Santé

présentée par :

Wanderson Marques da Silva

Étude fonctionnelle du génome de *Corynebacterium pseudotuberculosis* par différentes stratégies protéomiques

soutenue le 11 mars 2015 devant la commission d'Examen

Composition du jury :

Rapporteurs :

Dr. Monique Zagorec (INRA, Oniris, Nantes, France)

Pr. Walter Lilenbaum (UFF, Niteroi, Brasil)

Membres :

Pr. Michel Gautier (Agrocampus Ouest, Rennes, France)

Pr. Jacques Nicoli (UFMG, Belo Horizonte, Brasil)

Directeurs de thèse :

Pr. Vasco Ariston de Carvalho Azevedo (UFMG, Belo Horizonte, Brasil)

Dr. Yves Le Loir (INRA, UMR STLO, Rennes, France)



Wanderson Marques Silva

**Estudo do genoma funcional de *Corynebacterium pseudotuberculosis*
através de diferentes estratégias proteômicas**

Tese apresentada ao programa de Pós-Graduação em Genética do Departamento de Biologia Geral do Instituto de Ciências Biológicas da Universidade Federal de Minas Gerais como requisito parcial para obtenção do título de Doutor em Genética.

Orientadores:

Prof./Dr. Vasco Ariston de Carvalho Azevedo

Dr. Yves Le Loir

**Belo Horizonte
2015**

043 Silva, Wanderson Marques da.
Estudo do genoma funcional de *Corynebacterium pseudotuberculosis* através de diferentes estratégias proteômicas [manuscrito] / Wanderson Marques da Silva. – 2015.

246 f. : il. ; 29,5 cm.

Orientadores: Vasco Ariston de Carvalho Azevedo; Yves Le Loir.

Tese (doutorado) – Universidade Federal de Minas Gerais, Departamento de Biologia Geral.

1. *Corynebacterium pseudotuberculosis* - Teses. 2. Genômica - Teses. 3. Proteômica- Teses. 4. Virulência bacteriana - Teses. 5. Linfadenite caseosa - Teses. 6. Linfagite ulcerativa. 7. Genética - Teses. I. Azevedo, Vasco Ariston de Carvalho. II. Le Loir, Yves. III. Universidade Federal de Minas Gerais. Departamento de Biologia Geral. IV. Título.

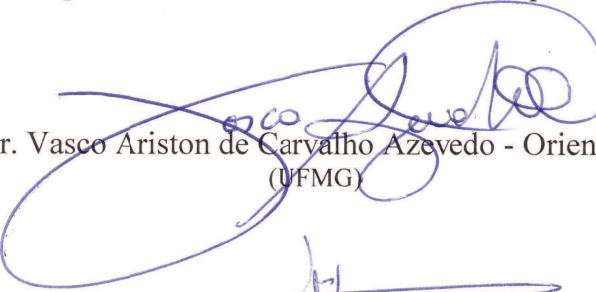
CDU: 575



**"Estudo do genoma funcional de *Corynebacterium pseudotuberculosis*
através de diferentes estratégias proteômicas"**

Wanderson Marques da Silva

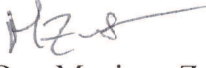
Tese aprovada pela banca examinadora constituída pelos Professores:

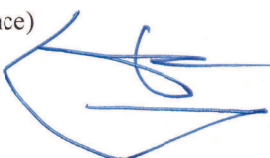

Dr. Vasco Ariston de Carvalho Azevedo - Orientador
(UFMG)


Yves Le Loir - Orientador
(INRA, Rennes, France)


Dr. Jacques Robert Nicoli
(UEMG)


Dr. Walter Lilenbaum
(UFF, Niteroi, Brasil)


Dra. Monique Zagorec
(INRA, Oniris, Nantes, France)


Dr. Michel Gautier
(Agrocampus Ouest, Rennes, France)

Belo Horizonte, 11 de março de 2015.

RESUMO

Corynebacterium pseudotuberculosis é um patógeno intracelular facultativo, que se subdivide em dois biovaries: *C. pseudotuberculosis ovis*, agente etiológico da linfadenite caseosa em pequenos ruminantes, e *C. pseudotuberculosis equi*, que é responsável pela linfagite ulcerativa em equinos, mastite em bovinos e doença de pele edematosas em bubalinos. Estudos *in silico* do genoma de *C. pseudotuberculosis* identificaram vários genes que poderiam desempenhar papel importante, tanto na fisiologia quanto na virulência deste patógeno. Em complemento a genômica estrutural, a genômica funcional visa elucidar a função que cada gene exerce no organismo, bem como a interação destes genes entre si, dentro de uma rede biológica. Assim, neste presente trabalho, nós utilizamos diferentes estratégias proteômicas para avaliar o genoma funcional de *C. pseudotuberculosis* em nível proteico, para complementar prévio estudo *in silico*. Primeiramente, foi caracterizado o proteoma extracelular das linhagens 1002_*ovis* e C231_*ovis*, que permitiu a caracterização total de 60 diferentes proteínas de *C. pseudotuberculosis*. Além disso, 18 proteínas foram diferencialmente reguladas entre as duas linhagens. Posteriormente o proteoma da linhagem 1002_*ovis* foi avaliado em resposta ao estresse nitrosativo, o qual possibilitou a caracterização de 835 proteínas, correspondendo a aproximadamente 41% do genoma predito desta linhagem. Além disso, foram identificadas 58 proteínas diferencialmente reguladas, envolvidas em diferentes processos biológicos que podem favorecer o processo de sobrevivência deste patógeno na presença do estresse nitrosativo. Em um terceiro estudo foi realizado uma análise comparativa, entre o proteoma extracelular das linhagens 1002_*ovis* e 258_*equi*. Neste estudo, a análise proteômica realizada após um processo de passagem serial das linhagens em camundongos, permitiu a identificação de 250 proteínas diferencialmente reguladas de *C. pseudotuberculosis*, envolvidas em sistemas de transportes, detoxificação, virulência, adesão celular e resposta geral a estresse. Por fim, este trabalho de doutorado promoveu a geração de um banco de dados proteicos, assim como a validação de genes preditos anteriormente *in silico*. Além disso, pela primeira vez foi demonstrado um estudo proteômico comparativo, entre linhagens pertencentes aos biovaries *ovis* (1002_*ovis*) e *equi* (258_*equi*). Os resultados gerados nestes estudos forneceram informações importantes, acerca de fatores que favorecem processos fisiológicos básicos, quanto envolvidos na virulência e na patogênese de *C. pseudotuberculosis*.

ABSTRACT

Corynebacterium pseudotuberculosis is a facultative intracellular pathogenic species, subdivided into two biovars: *C. pseudotuberculosis ovis*, etiologic agent of caseous lymphadenitis in small ruminants, and *C. pseudotuberculosis equi*, which causes ulcerative lymphangitis in equines, mastitis in bovine, and oedematous skin disease in buffalos. *In silico* analysis of the genome of *C. pseudotuberculosis* revealed genes that can play an important role in both physiology and virulence of this pathogen. As a complement to structural genomics, functional genomics aims to elucidate the role that each gene plays in organism, as well as interaction of these genes into a biological network. Thus, in this PhD work, we used different proteomic approaches to evaluate the functional genome of *C. pseudotuberculosis* at the protein level to complement these previous *in silico* studies. First, the analysis of the exoproteome of strains 1002_*ovis* and C231_*ovis*, enable the characterization total of 60 proteins of *C. pseudotuberculosis*. In addition, 18 differentially regulated proteins were detected between the two strains. In a second study, the proteome of the strain 1002_*ovis* was evaluated in response to nitrosative stress, a stress encountered by the bacteria during the onset of the infection. A total of 845 proteins were analyzed, representing approximately 41% of the predicted proteome of this strain. A set of 58 proteins were found differentially regulated when compared to the control conditions. These 58 proteins are involved in different biological processes, and their induction may favor the survival of this pathogen under exposition to nitrosative stress. In a third study, the strains 1002_*ovis* and 258_*equi*, which represent the biovars *ovis* and *equi* of *C. pseudotuberculosis*, respectively, were used in a murine model of experimental infection. A comparative analysis of their extracellular proteomes before and after passage in the murine host revealed that 250 proteins were differentially regulated in *C. pseudotuberculosis*. These proteins are involved in transport pathways, virulence, cell adhesion and stress general response. Altogether, this PhD work allowed the generation of a protein data base, as well as the validation of several genes previously predicted *in silico*. In addition, this work reports the first comparative proteomic study of the biovars *ovis* and *equi* of *C. pseudotuberculosis*. The results generated in this study provide information about of factors that favor the physiology, virulence and pathogenesis of *C. pseudotuberculosis*.

RÉSUMÉ

Corynebacterium pseudotuberculosis est une espèce de pathogène intracellulaire facultatif, divisée en deux biovars : *C. pseudotuberculosis ovis*, agent étiologique de la lymphadénite caséuse chez les petits ruminants, et *C. pseudotuberculosis equi*, responsable de lymphangites ulcérées chez les chevaux, de mammites chez les bovins et d'œdèmes cutanés chez les buffles. Des travaux antérieurs de caractérisation *in silico* du génome de *C. pseudotuberculosis* ont mis en évidence plusieurs gènes qui pourraient jouer un rôle important dans la physiologie et la virulence de cet agent pathogène. En complément de la génomique structurale, la génomique fonctionnelle a pour but d'élucider le rôle que joue chaque gène dans l'organisme, ainsi que l'interaction de ces gènes dans un réseau biologique. Au cours de ce travail de thèse, nous avons appliquée différentes stratégies protéomiques à l'étude fonctionnelle du génome de *C. pseudotuberculosis*, afin de compléter ces données antérieures, obtenues *in silico*. Tout d'abord, nous avons caractérisé le protéome extracellulaire des souches 1002_*ovis* et C231_*ovis* qui a permis la caractérisation totale de 60 protéines différentes de *C. pseudotuberculosis*. En outre, 18 protéines ont été régulées différemment entre les deux souches. Dans une deuxième étude, le protéome de la souche 1002_*ovis* a été analysé en réponse au stress nitrosant. Au total, 835 protéines ont été identifiées, ce qui représente environ 41% du génome prédict de cette souche. Parmi elles, 58 protéines différentiellement régulées ont été identifiées et sont impliquées dans différents processus biologiques susceptibles de favoriser la survie de cet agent pathogène en présence d'un stress nitrosant. Dans une troisième étude, les souches 1002_*ovis* (représentative du biovar *ovis*) et 258_*equi* (biovar *equi*) ont été utilisées pour induire des infections expérimentales sur modèle souris. Les protéomes extracellulaires des deux souches ont été analysés avant et après passage en série sur l'hôte murin. L'analyse en protéomique comparative a permis d'identifier 250 protéines différentiellement régulées dont les fonctions touchent aux systèmes de transport, à la désintoxication, la virulence, l'adhérence cellulaire et la réponse générale au stress. Pour conclure, à travers différentes stratégies protéomiques, ce travail a permis de générer une base de données de protéines et de valider la fonctionnalité de différents gènes jusqu'alors prédicts *in silico*, seulement. En outre, ce travail constitue la première étude protéomique comparative des souches de biovars *ovis* et *equi*. L'ensemble de ces résultats fournit des informations importantes sur les facteurs qui favorisent les processus physiologiques et infectieux de *C. pseudotuberculosis*.

Sumário

LISTA DE TABELAS/ LISTE DES TABLEAUX	10
LISTA DE FIGURAS/ LISTE DES FIGURES	12
1. Apresentação/Présentation	13
1.1 Colaborações	14
Collaborations	16
1.2 Introdução Geral.....	18
Introduction générale.....	21
1.3 Estrutura do manuscrito.....	24
Structure du manuscrit.....	26
2. Revisão da Literatura	28
2.1 <i>Corynebacterium pseudotuberculosis</i> e as enfermidades: linfadenite caseosa e linfagite ulcerativa	29
2.1.1 Patogenia	32
2.1.2 Determinantes de virulência.....	32
2.1.3 Genômica de <i>C. pseudotuberculosis</i>	34
2.2 Genômica funcional: Proteômica	38
2.2.1 Estado da arte.....	38
2.2.2 Emprego da proteômica no estudo da patogênese bacteriana	43
2.3 Proteômica no Gênero <i>Corynebacterium</i>	47
2.3.1 Proteoma de <i>Corynebacterium</i> não patogênicas	48
2.3.2 Proteoma de <i>Corynebacterium</i> patogênicas	52
3. Objetivos/objectifs	58
3.1 Objetivo Geral	59
Objectif Général	59

3.2	Objetivos específicos.....	60
	Objectifs spécifiques	60
4.	Capítulo 1: Caracterização do proteoma extracelular de linhagens de <i>C. pseudotuberculosis ovis</i>, através da proteômica comparativa.	62
	Chapitre 1 : Caractérisation du proteome extracellulaire des souches de <i>C. pseudotuberculosis ovis</i> par protéomique comparative.....	62
4.1	Introdução.....	63
	Introduction.....	64
4.2	Artigo 1: Identification of 11 new exoproteins in <i>Corynebacterium pseudotuberculosis</i> by comparative analysis of the exoproteome.....	65
	4.2.1 Supplementary file.....	72
4.3	Artigo 2: Differential Exoproteome analysis of two <i>Corynebacterium pseudotuberculosis</i> biovar <i>ovis</i> strains isolated from goat (1002) and sheep (C231).	90
	4.3.1 Supplementary file.....	97
5.	Capítulo 2: Caracterização funcional do genoma de <i>C. pseudotuberculosis ovis</i> 1002 em resposta ao estresse utilizando uma abordagem proteômica.	101
	Chapitre 2 : Caractérisation fonctionnelle du génome de <i>C. pseudotuberculosis</i> 1002 en réponse au stress nitrosant par une approche protéomique.	101
5.1	Introdução.....	102
	Introduction	103
5.2	Artigo 3: Label-free proteomic analysis to confirm the predicted proteome of <i>Corynebacterium pseudotuberculosis</i> under nitrosative stress mediated by nitric oxide.. ..	104
	5.2.1 Supplementary file.....	120
6.	Capítulo 3: Alteração do potencial de virulência de <i>C. pseudotuberculosis</i> demonstrado por análise proteômica	128
	Chapitre 3 : Modification du potentiel de virulence de <i>C. pseudotuberculosis</i> révélée par analyse protéomique.....	128

6.1	Introdução.....	129
	Introduction	130
6.2	Artigo 4: A shift in the virulence potential of <i>Corynebacterium pseudotuberculosis</i> biovars <i>ovis</i> and <i>equi</i> after passage in a murine host demonstrated through comparative proteomics.	132
6.2.1	Introduction	133
6.2.2	Materials and Methods	135
6.2.3	Results	140
6.2.4	Discussion.....	153
6.2.5	Conclusion.....	159
6.2.6	References	161
6.2.7	Supplementary data	169
7.	Discussão geral.....	189
	Discussion générale.....	194
8.	Conclusão/Conclusion	198
9.	Perspectivas/Perspectives.....	200
10.	Referências/Reference.....	202
11.	Anexos/ Annexe.....	217
	Anexo 1: Proteínas diferencias presentes em mais de um experimento proteômico em que foi aplicado estresse.....	218
	Annexe 1: Protéines différentiellement produites dans au moins deux études au cours desquelles une condition de stress a été appliquée.....	218
	Anexo/Annexe 2: Suplementary data (Paper 3; Table S.1)	219
	Anexo/Annexe 3: Subjected Publications / Evidence Submission	241
	Anexo/Annexe 4: <i>Curriculum vitae</i>	243

LISTA DE TABELAS/ LISTE DES TABLEAUX

Revisão da literatura/Révision de la littérature

Tabela 1: Lista das linhagens de <i>C. pseudotuberculosis</i> que foram sequenciadas.....	36
Tableaux 1: Liste des souches de <i>C. pseudotuberculosis</i> qui ont été séquencés.....	38

Capítulo 1/Chapitre 1

Paper 1

Additional file 1: Table S1: List of the extracellular proteins common to 1002 and C231 <i>C. pseudotuberculosis</i> strains.....	72
Additional file 2: Table S2: List of the extracellular unique proteins 1002 <i>C. pseudotuberculosis</i> strain.....	76
Additional file 3: Table S3: List of the extracellular unique proteins to C231 <i>C. pseudotuberculosis</i> strain	79
Additional file 4: Table S4: List of 104 extracellular proteins of <i>C. pseudotuberculosis</i> detected by both approaches (2-DE-MALDI-TOF/TOF and TPP-LC/MS ^E)	80

Paper 2

Supplementary file 1: List of proteins differentially produced in strain 1002, identified by MALDI-TOF-MS/MS	97
Supplementary file 2: List of proteins differentially produced in strain C231, identified by MALDI-TOF-MS/MS	99

Capítulo 2/Chapitre 2

Paper 3

Table S.2: Unique proteins identified in strain 1002_ DETA/NO	120
Table S.3: Unique proteins identified in strain 1002 control condition	125

Capítulo 3/Chapitre 3

Table 1: Proteins differentially produced between the recovered and control conditions for strain 1002_ <i>ovis</i>	148
Table 2: Proteins differentially produced between the recovered and control conditions for strain 258_ <i>equi</i>	151
Supplementary file 1: Table S.1: List of proteins identified in the exclusive proteome of <i>Cp1002_ovis</i>	169
Supplementary file 2: Table S.2: List of proteins identified in the exclusive proteome of strain 258_ <i>equi</i>	172
Supplementary file 3: Table S.3: Complet list of proteins differentially produced among the recovered and control condition of strain 1002_ <i>ovis</i>	174
Supplementary file 4: Table S.4: Functional classification of the total proteins differentially produced between the recovered and control conditions of <i>strain 258_equi</i>	180
Supplementary file 5: Table S.5 : Proteins identified in the pathogenicity island	187

LISTA DE FIGURAS/ LISTE DES FIGURES

Figura 1: Diferentes estratégias com base na proteômica para a identificação de proteínas, associadas à fisiologia quanto à virulência bacteriana.....	45
Figure 1: Différentes stratégies protéomique pour identifier des protéines associées à la physiologie et la virulence bactérienne.....	47
Capítulo 3/Chapitre 3	
Figure 1: Survival of Balb/C mice infected with strain 1002_ <i>ovis</i> or strain 258_ <i>equi</i>	142
Figure 2: 2D nanoUPLC HDMS ^E analysis showing MS/MS data.....	145
Figure 3: Biological processes differentially regulated in strain 1002_ <i>ovis</i> after passage in mice.	147
.....	
Figure 4: Biological processes differentially regulated in strain 258_ <i>equi</i> after passage in mice.	150
.....	
Figure 5: Comparison of biological processes in the strains 1002_ <i>ovis</i> and 258_ <i>equi</i>	153

1. Apresentação/Présentation

1.1 Colaborações

O presente trabalho de tese foi desenvolvido através de um programa de Cotutela Internacional de Tese, devido ao convênio estabelecido entre a Universidade Federal de Minas Gerais (UFMG) (Belo Horizonte, Brasil) e o Instituto Superior de Ciências Agrícolas, Agro-Alimentares, Hortícolas e de Paisagem (*Agrocampus Oeste*) (Rennes, França). Este programa permite que alunos possam obter duplo diploma reconhecido por ambas as instituições, além de promover aos estudantes um contato com a comunidade científica internacional.

O trabalho de tese desenvolvido esteve sob a supervisão do Prof./Dr. Vasco Azevedo do Programa de Pós-Graduação em Genética do Depto. de Biologia Geral (ICB-UFMG), localizado na cidade de Belo Horizonte, Brasil. Além da supervisão do Dr. Yves Le Loir do *Laboratoire de la Science et Technologie du Lait et de l'Oeuf (STLO)* no *Institut National de la Recherche Agronomique (INRA)*, localizado na cidade de Rennes, França.

Este trabalho contou com colaboração de vários laboratórios localizados em diferentes instituições.

- ❖ Instituto de Ciências Biológicas da Universidade Federal de Minas Gerais (UFMG)
 - Laboratório de Genética Celular e Molecular (LGCM),
 - Laboratório de Venenos e Toxinas (LVTA).
- ❖ Instituto de Ciências Biológicas da Universidade Federal do Pará (UFPA)
 - Laboratório de Polimorfismo de DNA (LPDNA)
- ❖ *Waters Corporation*, São Paulo, Brasil

- *MS Applications and Development Laboratory*

❖ *Institut National de la Recherche Agronomique (INRA), Rennes, França*

- *Laboratoire de la Science et Technologie du Lait et de l'Oeuf (STLO).*

O trabalho desenvolvido durante o período de doutoramento, contou com o apoio financeiro das seguintes agências de fomento:

- ❖ Coordenação de Aperfeiçoamento de Pessoal de Nível Superior (CAPES),
- ❖ Conselho Nacional de Desenvolvimento Científico e Tecnológico (CNPq),
- ❖ Fundação de Amparo à Pesquisa do Pará (FAPESPA),
- ❖ Programa Institucional de Doutorado Sanduíche no Exterior (PDSE).

Collaborations

Cette thèse a été développée avec la collaboration du programme de co-tutelle de thèse internationale, dans le cadre de l'accord établi entre l'Université Fédérale de Minas Gerais (UFMG) (Belo Horizonte, Brésil) et l'Institut Supérieur des Sciences Agronomiques, Agro-Alimentaires, Horticoles et du Paysage (Agrocampus Ouest) (Rennes, France). Ce programme permet aux étudiants d'obtenir un double diplôme reconnu par les deux institutions, de plus il favorise le contact des étudiants avec la communauté scientifique internationale.

Le travail de thèse a été élaboré sous la direction du Prof. / Dr. Vasco Azevedo du Programme d'Etudes Supérieures de Génétique au Département de Biologie Générale (ICB-UFMG), situé à Belo Horizonte, Brésil, ainsi que sous la supervision du Dr. Yves Le Loir du Laboratoire de la Science et Technologie du Lait et de l'Oeuf (STLO) à l'Institut National de la Recherche Agronomique (INRA), situé à Rennes, France.

Ce travail a bénéficié de la collaboration de divers laboratoires situés dans différentes institutions :

- ❖ Institut des Sciences Biologiques, Université Fédérale de Minas Gerais (UFMG)
 - Laboratoire de Génétique Cellulaire et Moléculaire (LGCM),
 - Laboratoire de Venins et Toxines.
- ❖ Institut des Sciences Biologiques, Université Fédérale du Pará (UFPA)
 - Laboratoire de Polymorphisme de l'ADN (LPDNA)
- ❖ *Waters Corporation*, São Paulo, Brésil

- *MS Applications and Development Laboratory*
- ❖ Institut National de la Recherche Agronomique (INRA), Rennes, France
- Laboratoire de la Science et Technologie du Lait et de l'Oeuf (STLO).

Le travail développé au cours de la période de doctorat a reçu le soutien financier des organismes suivants:

- ❖ Coordination de perfectionnement du personnel de l'enseignement supérieur (CAPES)
- ❖ Conseil National de Développement Scientifique et Technologique (CNPq)
- ❖ Fondation pour la Recherche de l'état de Pará (FAPESPA)
- ❖ Programme de Doctorat sandwich à l'étranger (PDSE).

1.2 Introdução Geral

Corynebacterium pseudotuberculosis é uma bactéria Gram-positiva, parasita intracelular facultativo e subdivide-se em dois biovares: *C. pseudotuberculosis ovis* (nitrato negativo) e *C. pseudotuberculosis equi* (nitrato positivo). As linhagens pertencentes ao biovar *ovis* causam linfadenite caseosa em pequenos ruminantes e mastite em bovinos. Já as linhagens biovar *equi* causam linfangite ulcerativa em equinos e doença de pele edematosas em bubalinos. Ambas as enfermidades são infecto-contagiosa crônicas, distribuídas mundialmente, e acarretam grandes perdas econômicas na produção de leite, carne, lã e couro (Dorella et al., 2006; Baird & Fontainde, 2007).

Até o presente momento poucos fatores de virulência de *C. pseudotuberculosis* foram caracterizados, como a fosfolipase D, associada à disseminação deste patógeno no hospedeiro (McKean et al., 2007); lipídeos da parede celular, que favorecem a sobrevivência bacteriana dentro de macrófagos (Hard, 1982) e um sistema de aquisição de ferro: o sistema *fagABC* (Billington et al., 2002).

Devido à escassez de informações sobre fatores que favorecem o processo patogênico de *C. pseudotuberculosis*, o nosso grupo de pesquisa do Laboratório de Genética Celular e Molecular (LGCM/ICB/UFMG) em colaboração com Laboratório de Polimorfismo de DNA (LPDNA/ICB/UFPA), vem realizando o sequenciamento do genoma de linhagens de *C. pseudotuberculosis ovis* e *equi*, isoladas de diferentes hospedeiros e provenientes de diversas partes do mundo. Os dados provenientes do sequenciamento destas linhagens revelam vários genes, envolvidos tanto na virulência, quanto a processos fisiológicos básicos deste patógeno. Além disso, quando realizada análise comparativa, entre linhagens *ovis* e *equi*, observa-se uma

variabilidade genica que poderia influenciar no processo de patogenicidade de cada biovar (Soares et al., 2013).

No entanto, como estes dados obtidos a partir do sequenciamento genômico representam apenas uma análise estrutural do genoma de *C. pseudotuberculosis*, torna-se necessário realizar uma análise funcional do genoma deste patógeno para elucidar a função exercida por cada gene, bem como a interação destes genes entre si, dentro de uma rede biológica. Para tal, nosso grupo de pesquisa vem realizando estudos transcriptomicos e proteômicos de *C. pseudotuberculosis*. Em relação ao transcriptoma, recentemente foi caracterizado o perfil transcricional de *C. pseudotuberculosis ovis* 1002 em resposta a diferentes tipos de estresses abióticos (térmico, osmótico e ácido), o que possibilitou a identificação de vários genes que podem contribuir para sobrevivência e adaptação deste patógeno na presença destes estresses (Pinto et al., 2013).

Estudos demonstram que proteínas extracelulares desempenham um papel importante na virulência bacteriana, esta fração proteica está associada à adesão e invasão celular, adaptação e sobrevivência dentro da célula hospedeira, além de modular o sistema imune do hospedeiro (Hilbi & Haas, 2012; Schneewind, & Missiakas, 2012). Neste contexto, o nosso grupo caracterizou tanto o proteoma extracelular, quanto o imunoproteoma extracelular de duas linhagens de *C. pseudotuberculosis ovis* (1002 e C231), (Pacheco et al., 2011; Pacheco et al., 2012; Seyffert et al., 2014). Os resultados obtidos nestes estudos promoveram a identificação de proteínas envolvidas na virulência de *C. pseudotuberculosis*, além de alvos para o desenvolvimento de testes de imunodiagnóstico.

Além destes estudos, recentemente o proteoma de superfície celular de linhagens de *C. pseudotuberculosis ovis*, isoladas diretamente de linfonodos de ovinos infectados foi caracterizado. Este estudo promoveu a identificação de fatores que podem contribuir para

sobrevivência de *C. pseudotuberculosis* no estado crônico da infecção (Rees et al., 2014). Contudo, estes trabalhos foram realizados apenas com linhagens pertencentes ao biovar *ovis*; com respeito a linhagens pertencentes ao biovar *equi*, até o presente momento não foi realizado nenhum estudo funcional do seu genoma.

Assim seguimos com o objetivo de continuar explorando o genoma funcional de *C. pseudotuberculosis*. Neste presente trabalho, foram empregadas diferentes estratégias proteomicas para caracterizar o genoma funcional de linhagens de *C. pseudotuberculosis ovis* (1002_*ovis* e C231_*ovis*) e *C. pseudotuberculosis equi* (258_*equi*), isoladas de um caprino e equino, respectivamente. Assim, pela primeira vez foi realizado um estudo proteômico comparativo, entre linhagens *ovis* e *equi* de *C. pseudotuberculosis*. Além disso, os resultados obtidos neste estudo permitiram a complementação de prévios estudos, genómicos, transcriptómicos e proteómicos de *C. pseudotuberculosis*. Além de ampliar o nosso conhecimento a cerca da biologia e de fatores que contribuem para o processo patogênico de cada biovar.

Introduction générale

Corynebacterium pseudotuberculosis est une bactérie à Gram positif, parasite intracellulaire facultatif, et l'espèce est subdivisé en deux biovars : *C. pseudotuberculosis ovis* (nitrate négative) et *C. pseudotuberculosis equi* (nitrate positive). Les souches appartenant au biovar *ovis*, sont l'agent étiologique de la lymphadénite caséeuse, une maladie qui touche principalement les petits ruminants, et les souches du biovar *equi* causent la lymphangite ulcéreuse chez les chevaux, des mammites chez les bovins et des maladies de la peau œdémateuses chez les buffles (Dorella et al., 2006; Baird & Fontainde, 2007).

À ce jour, peu de facteurs de virulence de *C. pseudotuberculosis* ont été caractérisés : (i) la phospholipase D, qui est associée à la propagation de ce pathogène dans l'hôte (McKean et al., 2007) ; (ii) les lipides de la paroi cellulaire qui favorisent la survie des bactéries dans les macrophages (Hard, 1982) et (iii) un système d'acquisition du Fer: le système *fagABC* (Billington et al., 2002).

En raison du manque d'informations sur les facteurs qui favorisent le processus pathogène de *C. pseudotuberculosis*, notre groupe de recherche, le Laboratoire de Génétique Cellulaire et Moléculaire, en collaboration avec le laboratoire Polymorphisme de l'ADN a mis en œuvre le séquençage du génome des souches de *C. pseudotuberculosis ovis* et *equi*, qui ont été isolées partir de différents hôtes et dans différentes parties du monde. Les données du séquençage de ces souches ont révélé plusieurs gènes impliqués dans la virulence autant que dans les processus physiologiques de base de ce pathogène. En outre, l'analyse comparative des souches *equi* et *ovis*, a permis d'observer une variation génétique qui pourrait affecter le processus pathogène de chaque biovar (Soares et al., 2013).

Toutefois, les données obtenues à partir de la séquence du génome ne représentent qu'une analyse structurelle du génome de *C. pseudotuberculosis*. Ainsi, il est nécessaire de procéder à l'analyse fonctionnelle du génome de ce pathogène pour élucider non seulement la fonction remplie par chacun des gènes, mais encore l'interaction de ces gènes entre eux dans un réseau biologique. À cette fin, notre groupe de recherche a mené des études transcriptomiques et protéomiques de *C. pseudotuberculosis*. En ce qui concerne le transcriptome le profil transcriptionnel de *C. pseudotuberculosis ovis* en 1002, a été récemment caractériser en réponse à différents types de stress abiotiques (thermique, osmotique et acide), ce qui a permis l'identification de plusieurs gènes qui peuvent contribuer à la survie et à l'adaptation de ce pathogène en présence de ces stress (Pinto et al., 2013).

Des études ont montré que les protéines extracellulaires jouent un rôle important dans la virulence bactérienne, qu'elles sont associées à l'adhésion cellulaire, à l'invasion, à l'adaptation et la survie au sein de la cellule hôte, et à la modulation du système immunitaire de l'hôte (Hilbi & Haas, 2012; Schneewind, & Missiakas, 2012). Dans ce contexte, notre groupe a caractérisé à la fois le protéome extracellulaire et l'immunoprotéome extracellulaire de deux souches de *C. pseudotuberculosis ovis* (1002 e C231), (Pacheco et al., 2011; Pacheco et al., 2012; Seyffert et al., 2014). Les résultats de ces études ont permis l'identification de protéines impliquées dans la virulence de *C. pseudotuberculosis*, ainsi que des cibles pour le développement de tests de diagnostic immunologique.

En plus de ces études, le protéome de surface cellulaire des souches de *C. pseudotuberculosis*, isolé directement à partir de ganglion lymphatique de moutons infectés, a été récemment caractérisé. Cette étude a permis l'identification de facteurs qui peuvent contribuer à la survie de *C. pseudotuberculosis* dans un état chronique de l'infection (Rees et al., 2014).

Toutefois, ces études ont été réalisées avec des souches appartenant uniquement au biovar *ovis*.

En ce qui concerne, les souches appartenant au biovar *equi*, il n'y a pas eu à ce jour d'étude fonctionnelle de son génome.

Ainsi, afin de continuer à explorer le génome fonctionnel de *C. pseudotuberculosis*.

Dans ce travail, nous avons utilisé différentes stratégies protéomiques pour caractériser le génome fonctionnel des souches de *C. pseudotuberculosis ovis* (1002_*ovis* e C231_*ovis*) e *C. pseudotuberculosis equi* (258_*equi*), qui ont été isolées à partir d'une chèvre et d'un cheval, respectivement. C'est par la première fois qu'une telle étude protéomique comparative entre les souches de *C. pseudotuberculosis ovis* et *equi* a été réalisée. En outre, les résultats obtenus dans cette étude ont permis l'achèvement des études génomiques, transcriptomiques et protéomiques de *C. pseudotuberculosis* précédentes, en plus d'élargir nos connaissances sur la biologie et les facteurs qui contribuent au processus pathogène de chaque biovar.

1.3 Estrutura do manuscrito

O presente manuscrito de tese encontra-se subdivido em seções de acordo com os assuntos a serem abordados, como se segue:

- I.** A primeira parte deste manuscrito apresenta, uma revisão da literatura sobre os seguintes temas: (i) *Corynebacterium pseudotuberculosis*, onde serão abordados aspectos gerais deste patógeno como: as enfermidades causadas por *C. pseudotuberculosis*, processo patogênico e *status* atual do seu genoma; (ii) uma descrição de técnicas e aplicações da proteômica no campo da microbiologia de patógenos bacterianos e (iii) uma breve revisão dos estudos proteômicos no gênero *Corynebacterium*.
- II.** A segunda parte será apresentada em forma de artigo científico. Neste capítulo será descrito a caracterização do proteoma extracelular das linhagens *C. pseudotuberculosis ovis* 1002 e *C. pseudotuberculosis ovis* C231, utilizando sistemas baseados em géis para gerar mapas proteicos do exoproteoma de ambas as linhagens.
- III.** A terceira parte será apresentada em forma de artigo científico, que demonstra o estudo proteômico da linhagem *C. pseudotuberculosis ovis* 1002 em resposta ao estresse nitrosativo. No qual permitiu a identificação de fatores que contribuem para o processo adaptativo desta linhagem durante a exposição ao óxido nítrico. Além disso, este estudo permitiu a validação de prévios dados preditos *in silico*.

- IV.** A quarta parte deste trabalho, será apresentada em forma de artigo científico. Nesta seção será descrito uma análise proteômica comparativa entre o proteoma extracelular das linhagens 1002_*ovis* e 258_*equi* de *C. psedotuberculosis*, após a passagem das mesmas em um modelo murino de infecção experimental.
- V.** Por último, será abordada uma discussão geral dos trabalhos realizados, seguido de uma conclusão geral e perspectivas.

Structure du manuscrit

Ce manuscrit de thèse est subdivisé en sections correspondant aux questions à traiter, comme suit :

- I.** La première partie présente une revue de la littérature sur les sujets suivants: (i) *Corynebacterium pseudotuberculosis*, cette partie examinera les aspects généraux de ce pathogène, comme : les maladies provoquées par *C. pseudotuberculosis*, le processus pathogène et l'état actuel des connaissances sur son génome; (ii) une brève description des techniques et applications de la protéomique en ce qui concerne la microbiologie des pathogènes et (iii) une brève revue de la protéomique du genre *Corynebacterium*.

- II.** La deuxième section sera présentée sous forme d'article scientifique. Ce chapitre, décrira la caractérisation du protéome extracellulaire des souches *C. pseudotuberculosis ovis* 1002 et *C. pseudotuberculosis ovis* C231, en utilisant les systèmes basés sur des gels pour générer des cartes de protéines de l'exoprotéome de ces deux souches.

- III.** La troisième partie sera présentée sous forme d'article scientifique, présentant l'étude protéomique de la souche de *C. pseudotuberculosis ovis* 1002 en réponse au stress nitrosant. Ceci a permis l'identification des facteurs qui contribuent au processus d'adaptation de cette souche pendant l'exposition à l'oxyde nitrique. Ainsi, cette étude a permis la validation de données (précédentes) prédictives *in silico*.

IV. La quatrième section de cette thèse sera présentée sous forme d'article scientifique. Cette section décrira une analyse protéomique comparative entre le protéome extracellulaire des souches 1002_*ovis* et 258_*equi* de *C. psedotuberculosis*, après le passage de ces souches dans un modèle murin d'infection expérimentale.

V. Enfin, une discussion générale sur le travail sera effectuée, suivie d'une conclusion générale et de perspectives.

2. Revisão da Literatura

2.1 *Corynebacterium pseudotuberculosis* e as enfermidades: linfadenite caseosa e linfangite ulcerativa

Corynebacterium pseudotuberculosis é um patógeno intracelular facultativo, que pertence ao gênero *Corynebacterium* que juntamente com os gêneros *Mycobacterium* ssp., *Nocardia* ssp e *Rhodococcus* formam o grupo CMNR. As principais características do grupo CMNR são: organização da parede celular composta por peptideoglicano, arabinogalactano e ácidos micólicos e alto conteúdo G+C (47–74%) no seu genoma (Dorella et al., 2006).

C. pseudotuberculosis se subdivide em dois biovaras: *C. pseudotuberculosis ovis*, que é o agente etiológico da linfadenite caseosa principalmente em pequenos ruminantes, e *C. pseudotuberculosis equi*, que causa linfangite ulcerativa em equinos, mastite em bovinos e doença de pele edematosa em bubalinos. *C. pseudotuberculosis ovis* e *equi* podem ser distinguidos através de um simples teste bioquímico, onde linhagens biovar *equi* reduzem nitrato a nitrito (nitrato positivo) e linhagens biovar *ovis* não possuem esta habilidade sendo nitrato negativo (Dorella et al., 2006a).

A linfadenite caseosa e a linfangite ulcerativa são enfermidades descritas como infecto-contagiosas crônicas e caracterizadas pela formação de abscessos em nódulos linfáticos e órgãos internos (Aleman et al., 1996; Dorella et al., 2006a). Em alguns casos, a infecção produz poucos sinais clínicos no animal, impossibilitando identificá-los até sua morte (Paton et al., 1994). Na linfadenite caseosa, a progressão desses abscessos gera distintos nódulos com diferentes tamanhos contendo material caseoso (Baird; Fontaine, 2007). Em relação à linfangite ulcerativa, esta progressão promove a ruptura dos abscessos nodulares e consequentemente a formação de úlceras com diferentes formas e tamanhos (Aleman et al., 1996).

Estas enfermidades causadas por *C. pseudotuberculosis* são distribuídas mundialmente e acarretam grandes perdas econômicas associadas na produção de leite, carne, lã, couro e condenação de carcaças (Paton et al., 2003; Foley et al., 2004). No Brasil, os Estados da Região Nordeste são os mais afetados pela linfadenite caseosa, em razão de possuírem a maior concentração de rebanhos caprinos do país (Ribeiro et al., 2001). Minas Gerais, apesar de ainda possuir um rebanho reduzido, tem apresentado crescimento na atividade de ovinocultura, e a linfadenite caseosa já tem sido observada com alta frequência principalmente nos criatórios da região Norte do Estado (Guimarães et al., 2009; Seyffert et al., 2010). As perdas econômicas acarretadas pela linfadenite caseosa estão evidenciadas em diminuição na produção de leite, carne e lã, além da desvalorização da pele devido às cicatrizes (Dorella et al., 2006; Baird; Fontaine, 2007).

Em relação à linfangite ulcerativa, esta enfermidade apresenta-se bastante frequente nos Estados Unidos. Estudos descrevem o relato da linfangite ulcerativa em 23 Estados, dentre estes, o Estado da Califórnia é relatado como uma área endêmica para esta doença (Aleman et al., 1996; Doherr et al., 1998). Além disso, um recente estudo demonstra um aumento no número de casos de equinos infectados por *C. pseudotuberculosis* nos últimos 10 anos (Kilocoyne et al., 2014).

O contágio por *C. pseudotuberculosis* é facilitado por lesões na pele dos animais e o contato direto destes animais com secreções oro nasais, abcessos dos linfonodos ou materiais contaminados favorecem a infecção por este patógeno (Williamson, 2001). Contudo, a principal fonte de infecção por *C. pseudotuberculosis* são os abcessos que supuram e contaminam o ambiente, uma vez que esta bactéria pode sobreviver no solo por até oito meses, o que contribui para a disseminação no rebanho (Alves et al., 1997). A infecção de *C. pseudotuberculosis* em humanos é caracterizada como zoonose *ocupacional*, mas há relatos descritos que a enfermidade

pode ocorrer por meio da ingestão de carne caprina crua e leite de ovinos contaminados (Schreuder; ter-Laak; de-Gee, 1990; Mills et al., 1997; Peel et al., 1997).

O diagnóstico dos animais infectados com *C. pseudotuberculosis* é através da observação macroscópica dos abcessos superficiais formados, associado a cultura bacteriológica e testes bioquímicos (Ribeiro et al., 2001, Williamson, 2001). Com o intuito de obter um diagnóstico mais rápido e eficiente, nosso grupo de pesquisa do Laboratório de Genética Celular e Molecular, desenvolveu um ensaio multiplex PCR. Esta PCR multiplex demonstrou boa especificidade analítica e obteve uma sensibilidade de 94%, o que demonstra sua eficácia diagnóstica (Pacheco et al., 2007). Entretanto, até o presente momento não há um método de diagnóstico que seja capaz de identificar a infecção por *C. pseudotuberculosis* em estágios sub-clínicos da infecção, sendo assim os animais são diagnosticados em estágios tardios da infecção, o que contribui para a disseminação no rebanho.

Atualmente, não existe um tratamento que seja realmente eficaz para controle da linfadenite caseosa e linfangite ulcerativa. Apesar de testes *in vitro* demonstrarem a sensibilidade de *C. pseudotuberculosis* a vários antibióticos, o uso destas drogas geralmente não é efetivo. Isto é devido à incapacidade destas drogas penetrarem a rígida cápsula do abscesso onde a bactéria está localizada intracelularmente, durante o estágio de infecção (Adamson et al., 1985; Judson; Songer et al., 1991).

A respeito da imunoprofilaxia, diferentes estratégias foram testadas na tentativa de combater a infecção por *C. pseudotuberculosis*, entretanto nenhuma ofereceu proteção eficaz contra infecções experimentais (LeaMaster et al., 1987; Brogden et al., 1990; Eggleton et al., 1991; Ellis, 1991). Recentemente, nosso grupo de pesquisa demonstrou que a imunização de camundongos com uma linhagem defectiva para um gene relacionado à aquisição de ferro (*ciiA*),

promove proteção de 81% contra o desafio experimental com a linhagem selvagem (Ribeiro et al., 2014). Estes resultados sugerem a utilização desta linhagem mutante como alvo promissor na obtenção de uma vacina contra a linfadenite caseosa.

2.1.1 Patogenia

O processo patogênico de *C. pseudotuberculosis* é dividido em duas etapas: (i) colonização inicial e replicação em nódulos linfáticos, onde ocorre a formação de piogranulomas, (ii) no estágio seguinte de infecção, ocorre um novo ciclo de replicação e disseminação via sistema linfático e circulatório. Esta disseminação é promovida pela ação da exotoxina fosfolipase D (PLD), que permite a instalação deste patógeno em órgãos viscerais e nódulos linfáticos, e consequentemente a formação de lesões (Batey, 1986; McKean et al., 2007).

Durante este processo patogênico, ao contrário de outros patógenos intracelulares como *Mycobacterium tuberculosis*, *C. pseudotuberculosis* demonstra capacidade em sobreviver dentro do fagolisossomo de macrófagos (Stefańska et al., 2010). Estudos demonstram que este processo é mediado pelos lipídeos presentes na parede celular de *C. pseudotuberculosis* (Hard, 1975) e pela ação da PLD (McKean et al., 2007). Além destes, outros fatores como: o complexo de aquisição de ferro *fagABCD* (Billington et al., 2002) e o fator extracitoplasmático (ECF) sigma σ^E que apresenta papel na resistência deste patógeno ao estresse nitrosativo (Pacheco et al., 2012), contribuem para o processo de infecção de *C. pseudotuberculosis*.

2.1.2 Determinantes de virulência

Fosfolipase D

A fosfolipase D é descrita como o principal fator de virulência de *C. pseudotuberculosis*. Devido a sua atividade esfingomielinase, esta potente exotoxina promove micro lesões nas células endoteliais, o que resulta na permeabilidade dos vasos sanguíneos e linfáticos do hospedeiro. Esta permeabilidade vascular favorece a disseminação de *C. pseudotuberculosis* do sítio primário de infecção para outros órgãos como fígado, baço, rins e pulmões (Songer, 1990; McKean et al., 2007).

Com o objetivo de avaliar o papel da PLD na virulência de *C. pseudotuberculosis*, estudos realizados com linhagens mutantes para o gene *pld* demonstraram incapacidade destas linhagens em disseminarem no hospedeiro. Entretanto, quando avaliado seu potencial vacinal estas linhagens não foram capazes de induzirem uma resposta imune protetora contra o desafio com a linhagem selvagem (Hodgson et al., 1992).

Lipídeos da parede celular

A estrutura da parede celular de *C. pseudotuberculosis* apresenta uma camada externa de lipídeos, semelhantes aos ácidos micólicos presentes na parede celular de *M. tuberculosis* (Hard, 1975). De acordo com Jolly (1966), esta camada lipídica tem papel importante na virulência de *C. pseudotuberculosis*, pois esta confere resistência à ação de células fagocíticas, além de induzir a morte de macrófagos, devido ao seu efeito citotóxico. A toxicidade do material lipídico foi demonstrada pela indução de necrose hemorrágica, após injeção intradérmica em cobaias (Jolly, 1966). Além disso, outros estudos sugerem que há uma relação direta entre a porcentagem de lipídeos de superfície e a indução de abscessos crônicos (Muckle & Gyles, 1982).

Sistemas de aquisição de ferro

O ferro é um dos principais nutrientes que são essências para a vida microbiana, assim diversos patógenos, necessitam da aquisição de ferro para favorecer seu crescimento e estabelecer em exitoso processo de infecção (Cassat; Skaar, 2013). Em *C. pseudotuberculosis*, foram identificados dois sistemas envolvidos na aquisição de ferro: sistema *fagABCD* e o sistema *ciuABCDEF*.

O sistema *fagABCD*, está organizado em forma de um operon *fagABC*, localizado a montante do gene *pld*. Estudos realizados em linhagens conduzindo a fusão *fagA-LacZ*, demonstraram aumento na expressão do operon *fagABC* quando cultivadas em meio contendo baixa concentração de ferro. Além disso, estas linhagens *fagBC* mutantes apresentaram virulência reduzida quando comparada com a linhagem selvagem (Billington et al., 2002).

Utilizando a estratégia de mutagênese aleatória, através da inserção de um transposon (TnFuZ), nosso grupo de pesquisa gerou uma linhagem mutante para o gene *ciuA*, que é um componente do sistema *ciuABCDEF*. A proteína ciuA é descrita como um sideróforo, e atua na aquisição de ferro presente no meio extracelular. As linhagens defectivas para o gene *ciuA*, demonstraram viabilidade intracelular reduzida, nos ensaios *in vitro* com células JJ774, além de apresentarem virulência reduzida em camundongos. Quando foram realizados ensaios imunológicos com estas linhagens, observou-se a indução de níveis significativos de IgG e IgG2a, o que caracteriza uma resposta imune do tipo Th1, responsável por combater a infecção por patógenos intracelulares, como *C. pseudotuberculosis* (Ribeiro et al., 2014).

2.1.3 Genômica de *C. pseudotuberculosis*

Com o objetivo de desvendar as bases moleculares da virulência e patogenicidade de *C. pseudotuberculosis* e ampliar o conhecimento acerca da biologia deste patógeno, em 2006 o

Laboratório de Genética Celular e Molecular inserido na Rede Genômica de Minas Gerais, deu início ao projeto Genoma de *C. pseudotuberculosis*. No qual foi proposto o sequenciamento da linhagem *C. pseudotuberculosis ovis* 1002, isolada de um caprino no Estado da Bahia. A finalização do genoma da linhagem 1002, ou seja, o seu processo de anotação, ocorreu em paralelo com o genoma da linhagem *C. pseudotuberculosis ovis* C231, isolada de um ovino na Austrália e sequenciada pelo Prof. Robert Moore (Ruiz et al., 2011).

Atualmente 18 genomas de diferentes linhagens de *C. pseudotuberculosis* foram completamente sequenciados (Tabela 1), dentre estes, 15 genomas foram sequenciados, através da colaboração estabelecida, entre o LGCM e o Laboratório de Polimorfismo de DNA (LPDA) que está inserido na Rede Paraense de Genômica e Proteômica. Estas linhagens sequenciadas foram isoladas de distintos hospedeiros e provenientes de diferentes países. Assim os resultados obtidos nestes estudos, promoveram a predição *in silico* de vários genes que podem estar associados, a diferentes processos fisiológicos, bem como envolvidos na virulência destas linhagens. Além disso, foi possível determinar o número médio de genes para linhagens *ovis* e *equi* que é de aproximadamente 2,098 genes e 2,047 genes, respectivamente.

Tabela 1: Lista das linhagens de *C. pseudotuberculosis* que foram sequenciadas

Linhagens	Biovar	Hospedeiro	País de isolamento	Descrição clínica	Tamanho genoma (Mb)	Número de genes	Número de proteínas	GenBank	Referência
FRC41	<i>ovis</i>	Humano	França	Linfadenite necrotizante	2.33	2.171	2.171	CP002097	Trost et al., 2010
CIP52.97	<i>equi</i>	Cavalo	Quénia	Linfagite ulcerativa	2.32	2.194	2.060	CP003061	Cerdeira et al., 2011
19	<i>ovis</i>	Vaca	Israel	Abscesso mastite bovina	2.33	2.213	2.095	CP002251	Silva et al., 2011
1002	<i>ovis</i>	Cabra	Brasil	Abcessos	2.33	2.203	2.090	CP001809	Ruiz et al., 2011
PAT10	<i>ovis</i>	Ovelha	Argentina	Abcessos Pulmão	2.33	2.200	2.200	P002924	Cerdeira et al., 2011
Cp162	<i>equi</i>	Camelo	Inglaterra	Abcessos cervical	2.29	2.150	1.997	P003652	Hassan et al., 2012
1/06-A	<i>equi</i>	Cavalo	EUA	Abcessos	2.27	2.127	1.963	CP003082	Pethick et al., 2012
316	<i>equi</i>	Cavalo	EUA	Abcessos	2.31	2.234	2.106	P003077	Ramos et al., 2012
31	<i>equi</i>	Búfalo	Egito	Abcessos	2.29	2.170	2.063	P003421	Silva et al., 2012
258	<i>equi</i>	Cavalo	Bélgica	Linfagite ulcerativa	2.31	2.195	2.088	CP003540	Soares et al., 2012
267	<i>ovis</i>	Lhama	EUA	Abcessos	2.33	2.249	2.148	CP003407	Lopes et al., 2012
42/02-A	<i>ovis</i>	Ovelha	Australia	Abcessos	2.33	2.164	2.051	CP003062	Pethick et al., 2012
3/99-5	<i>ovis</i>	Ovelha	Escócia	Abcessos	2.33	2.239	2.142	CP003152	Pethick et al., 2012
C231	<i>ovis</i>	Ovelha	Australia	Abcessos	2.32	2.204	2.091	P001829	Ruiz et al., 2012
Ft_2193/67	<i>ovis</i>	Cabra	Noruega	Pus	2.33	2.303	2.242	CP008924	Havelsrud et al., 2014
CS_10	<i>ovis</i>	Cabra	Noruega	Laboratório	2.33	2.293	2.232	CP008923	Havelsrud et al., 2014

48252	<i>ovis</i>	Humano	Noruega	Abcessos	2.33	2.288	2.227	CP008922	Havelsrud et al., 2014
P54B96	<i>ovis</i>	Antilope	África do Sul	Abcessos	2.33	2.205	2.084	CP003385	-

A partir dos dados obtidos com sequenciamento do genoma destas linhagens, recentemente foi realizado um estudo do pan genoma de 15 linhagens de *C. pseudotuberculosis* pertencentes aos biovaras *ovis* e *equi* (Soares et al., 2013). Neste estudo, identificou-se o core genoma entre linhagens *ovis* e *equi* (1,504 genes), além do core-genoma específico para cada biovar, sendo 314 genes para o biovar *ovis* e 95 genes para o biovar *equi* (Soares et al., 2013).

Os genes identificados no core-genoma das 15 linhagens *C. pseudotuberculosis* foram agrupados em processos biológicos, e grande parte destes genes estão envolvidos em processos de metabolismo celular (produção de energia, metabolismo de carboidratos, amino ácidos, nucleotídeos, coenzimas, lipídeos, íons orgânicos e metabolitos secundários) e armazenamento e processos de informações (tradução, biogênese de ribossomos, transcrição, replicação, recombinação e reparo do DNA) (Soares et al., 2013).

Além disso, 16 ilhas de patogenicidade foram identificadas em todas as 15 linhagens, contendo diversos genes envolvidos na virulência bacteriana. Entretanto, uma variabilidade gênica tanto inter quanto intra biovar foi observada nas ilhas identificadas. Contudo, esta análise do pan-genoma de *C. pseudotuberculosis*, sugere que a variação gênica observada entre os dois biovaras poderia influenciar na virulência e patogenicidade de cada biovar (Soares et al., 2013).

2.2 Genômica funcional: Proteômica

2.2.1 Estado da arte

Atualmente, devido aos grandes avanços tecnológicos observados no campo da genômica, principalmente com introdução de novas tecnologias, baseadas em sequenciamentos de nova geração, do inglês – “*Next Generation Sequence*”, houve um crescente aumento, na geração dados em diferentes áreas como: médica, veterinária e biotecnológica. No campo da

microbiologia, o elevado número de genomas bacterianos sequenciados tem gerado informações importantes a respeito das bases moleculares de virulência e patogenicidade de vários patógenos, bem como o conhecimento sobre aspectos fisiológicos básicos que favorecem o processo de adaptação bacteriano. Além disso, informações a respeito de alvos para o desenvolvimento de vacinas e diagnósticos também podem ser obtidos com dados provenientes do sequenciamento de genomas.

Entretanto, os resultados obtidos a partir do sequenciamento de genoma revelam poucas informações de como as proteínas de um organismo operam, individualmente ou em conjunto, para exercerem suas funções. Assim, em complemento a genômica estrutural, a genômica funcional, através de estudos transcriptomicos e proteômicos, busca elucidar a função que cada gene exerce no organismo, além da interação destes genes dentro de uma rede biológica (Gstaiger & Aebersold, 2009; Altelaar; Munoz; Heck, 2013).

O estudo proteômico busca avaliar a expressão global proteica de uma célula em uma determinada condição. Neste contexto, uma análise proteômica promove informações importantes a respeito da síntese proteica, análise quantitativas e qualitativas de produtos proteicos, modificações pós-traducionais, interação proteína-proteína e localização subcelular (Pandey & Mann, 2000; Gstaiger & Aebersold, 2009).

A proteômica permite a análise em larga escala de proteínas presentes em misturas complexas. Este estudo é dividido basicamente em duas etapas: (i) separação do extrato proteico, através das características intrínseca de cada proteína, esta separação poderá ser feita utilizando sistemas dependente de gel ou sistemas livre de gel, (ii) identificação das proteínas, através do sequenciamento dos peptídeos pré-digeridos enzimaticamente, geralmente feito por

espectrometria de massa, do inglês – “*mass spectrometry*” (MS) (Van Oudenhove & Devreese, 2013).

Espectrometria de massa é uma técnica utilizada para medir a relação entre massa/carga (*m/z*) de íons na fase gasosa. Nas últimas décadas, tornou-se um método valioso para estudos proteômicos, devido à capacidade de identificar e caracterizar proteínas intactas e desconhecidas, determinar modificações pós-traducionais e possibilitar a quantificação de proteínas (Xan; Aslanian; Yates, 2008; Pan et al., 2009).

Contudo, o sucesso de um estudo proteômico é devido ao desenvolvimento de ferramentas de bioinformática, onde vários *softwares* são utilizados para auxiliar na análise dos dados proteômicos. Principalmente na correlação com dados genômicos, busca pela ontologia genética, análise de dados quantitativos, além de permitir a análise no campo da biologia de sistemas que permite a criação de redes de interação proteína-proteína (Altelaar; Munoz; Heck, 2013).

Análise proteômica baseada em sistemas dependente de gel

Métodos baseado em géis, como eletroforese em gel de poliacrilamida, são usados rotineiramente na análise proteômica para separação de moléculas ou peptídeos. Eletroforese bidimensional (2-DE) é uma técnica proteômica clássica, aplicada para a resolução de proteínas presentes em misturas complexas. A 2-DE, é utilizada para separar proteínas em duas dimensões: (i) durante o processo de focalização isoelétrica, do inglês – “*isoelectric focalization*” (IEF), as proteínas são separadas de acordo com seu ponto isoelétrico (*pI*), e (ii) posteriormente utilizando um gel de poliacrilamida (SDS-PAGE), as proteínas são separadas de acordo com seu peso molecular (Görg et al., 2004). Assim, a combinação da 2-DE com a técnica de espectrometria de

massas do tipo MALDI-TOF-MS (*matrix-assisted laser desorption/ionization – time of flight*) possibilitou vários avanços no campo da proteômica baseada em sistema dependente de gel (Görg et al., 2004).

A 2-DE permite a geração de mapas proteicos, onde *spots* proteicos são visualizados diferencialmente expressos, bem como a presença de modificações pós-tradicionalis e isoformas de proteínas. Entretanto, uma das desvantagens desta técnica proteômica clássica é a variação de gel para gel. Assim para suprir esta deficiência observada na 2-DE, foi desenvolvida a eletroforese bidimensional de fluorescência diferencial, do inglês – “*two-dimensional fluorescence difference gel electrophoresis*” (2D-DIGE) (Unlu et al., 1997).

Esta técnica, permite a separação simultânea de duas amostras diferentes pré-marcadas com fluoroforos *cyanine dye* (*CyDye*) na mesma 2-DE. Além disso, o grande avanço desta técnica é a realização de um ensaio multiplex, onde um padrão interno é usado para a normalização dos dados, assim minimizando a variação experimental entre géis, e favorecendo uma análise quantitativa mais precisa das proteínas (Arentz et al., 2014). Apesar deste avanço em estudos proteômicos quantitativos baseado em 2-DE, a resolução de proteínas de caráter hidrofóbico, ainda segue sendo uma das grandes limitações desta técnica (Görg et al., 2004).

Análise proteômica baseada em sistemas livre de gel

O desenvolvimento de métodos baseados em sistemas livre de gel, como o sistema de cromatografia líquida, do inglês – “*liquid chromatography*” (LC), associado à espectrometria de massa (LC-MS/MS), promoveu um avanço na pesquisa proteômica. Nesta técnica, os fragmentos tripticos, provenientes da digestão enzimática do extrato proteico, são separados por uma micro-coluna de fase reversa, do inglês – “*reverse phase*” (RP) e *in tandem*, analisado por MS/MS. A

análise por espectrometria de massa é feita por espectrômetros, equipados com ionização do tipo ESI (*electrospray ionization*), associada a quatro analisadores de massas (*time-of-flight* (TOF), quadrupolo, *orbitrap* e *ion trap*) (Roe & Griffin, 2006).

No entanto, com o objetivo de aumentar a eficiência da técnica LC-MS/MS, foi desenvolvido um sistema de cromatografia bidimensional de alto desempenho, do inglês “*high performance liquid chromatography* (HPLC)”. Este sistema é composto por duas colunas microcapilares bifásica com RP ou com uma fase com troca catiônica, do inglês “*strong cation exchange* (SCX)”, acoplado a um espectrômetro de massa. Esta nova abordagem é denominada MudPit (*multidimensional protein identification technology*) (Washburn, 2004). Assim, a utilização da abordagem MudPit, associada à análise bioinformática tem promovido uma análise proteômica de alta eficiência, do inglês – “*high-throughput proteomics*” (Roe and Griffin, 2006).

O estudo quantitativo de proteínas presentes em amostras biológicas complexas é um dos grandes desafios no estudo proteômico. Assim, com a introdução de métodos baseados em sistema livre de gel, vários *workflows* para a quantificação em proteômica foram desenvolvidos, como a quantificação dependente de ligação, do inglês – “*label-based*” e independente de ligação, do inglês “*label-free*”.

A quantificação *label-based* pode ser subdividida em: (1) ligação química: através da técnica ICAT (*isotope-coded affinity tag*), onde os resíduos de cisteínas das proteínas são marcados covalentemente por *tags thiol* específicas. Outro método utilizando na ligação química, é através da técnica iTRAQ (*isobaric tags for relative and absolute quantitation*), onde as extremidade *N-terminal* da cadeia lateral e porções aminas das proteínas são marcadas por isótopos estáveis. (2) Ligação metabólica: através da técnica SILAC (*stable isotope labeling by/with amino acids in cell culture*) precursores metabólicos (amino ácidos, carboidratos, sais

orgânicos), contendo isótopos estáveis pesados (^{13}C , ^{15}N) são introduzidos no meio de cultura e ligam-se covalentemente as proteínas (Otto et al., 2012; Otto et al., 2014).

Na quantificação *label free*, nenhum tipo de ligação é usada para quantificar as proteínas presentes em uma amostra proteica complexa. Esta abordagem é subdividida em: (i) contagem espectral, do inglês – “*spectral counting*”, onde a quantificação é obtida pelo número total de espectros MS/MS para uma proteína, e (ii) pela intensidade da área do pico cromatográfico, sob a área da curva, onde a intensidade do *ion* precursor do espectro MS1 é contada (Otto et al., 2014).

2.2.2 Emprego da proteômica no estudo da patogênese bacteriana

A elucidação de moléculas e de mecanismos subjacentes à patogenia bacteriana em humanos, animais e plantas, é um dos principais focos da pesquisa microbiológica que visa aplicações práticas na prevenção e tratamento de várias enfermidades. Este tipo de pesquisa baseia-se no desenvolvimento de diagnósticos precisos, novos tipos de drogas e vacinas mais eficazes. Além disso, o conhecimento sobre as bases da patogênese bacteriana tem permitido a expansão do nosso conhecimento, a cerca das interações entre patógenos e seus hospedeiros, seja em nível celular ou molecular (Hueck, 1998).

Durante o processo de infecção, patógenos expressam diversas moléculas que favorecem a adaptação e sobrevivência dentro da célula hospedeira. Estas moléculas são denominadas fatores de virulência, e estes, quando expressos durante o processo de infecção bacteriano, permitem ao patógeno resistir, evadir, ou mesmo sistematicamente modular os efetores da imunidade inata do hospedeiro (Ziebuhr et al., 1999; Ohl; Miller, 2001).

Neste contexto, diversos grupos de pesquisa vêm aplicando a proteômica no estudo de patógenos bacterianos, tendo como um dos principais objetivos a identificação de fatores de

virulência, que é um importante passo para a compreensão da patogênese bacteriana e sua interação com o hospedeiro (Wu; Wang; Jennings, 2008). Portanto, a utilização de uma abordagem ou a combinação de distintas abordagens proteômica, associadas a estudos *in vitro* e/ou *in vivo*, torna-se uma estratégia atrativa para investigar a biologia bacteriana (Figura 1).

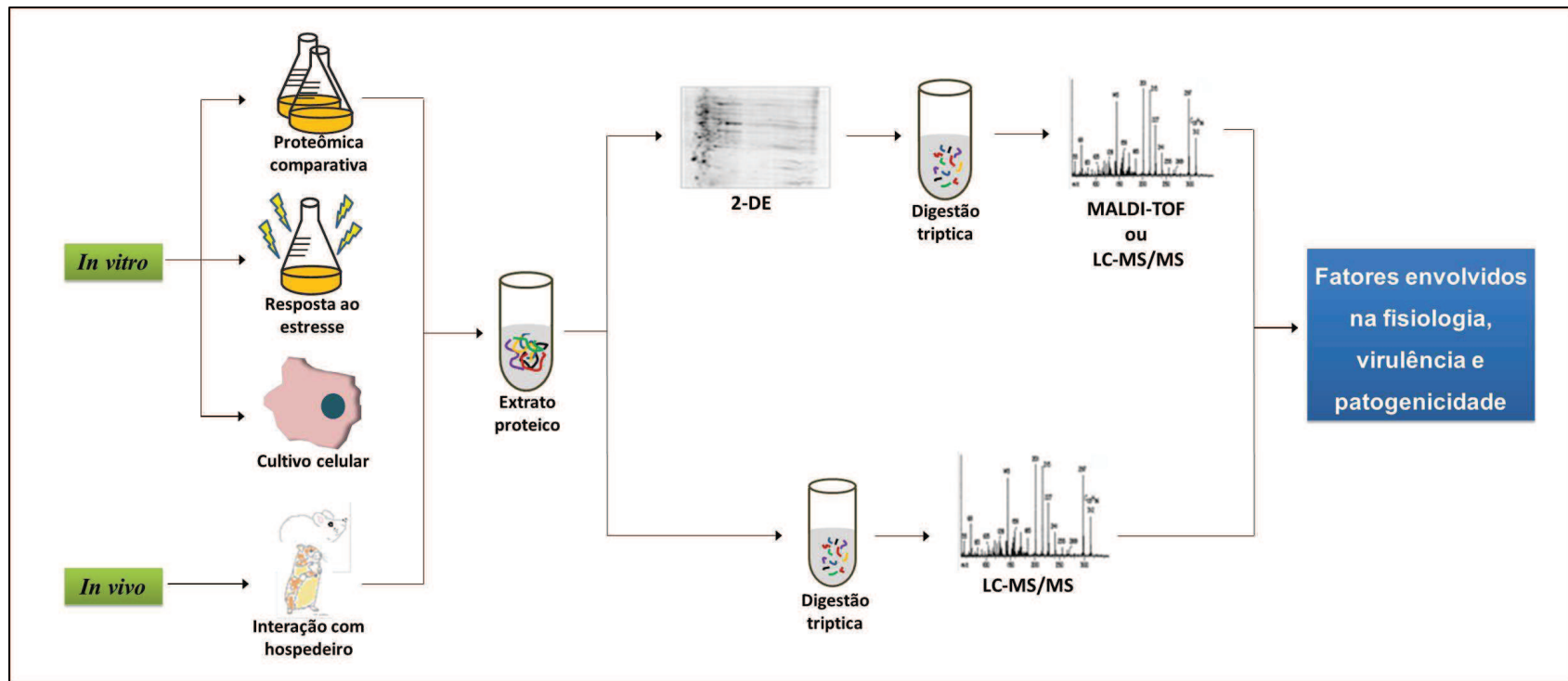


Figura 1: Workflow das diferentes estratégias e abordagens proteômicas para a identificação de proteínas, associadas tanto à fisiologia quanto à virulência bacteriana.

Dentro das abordagens *in vitro*, a análise proteômica comparativa é uma estratégia utilizada principalmente para explorar diferenças ou fatores compartilhados entre linhagens bacterianas pertencentes à mesma espécie. Por exemplo, a análise proteômica comparativa entre os sorovares *Gallinarum* e *Enteriditidis* de *Salmonella enterica*, permitiu a identificação de proteínas que podem influenciar no processo patogênico e adaptação a hospedeiros específicos de cada sorovar (Osman et al., 2009). Em *Staphylococcus aureus*, a análise comparativa entre linhagens enterotoxigênicas e não enterotoxigênicas possibilitou identificar no core proteoma destes dois patógenos, que foi composto por proteínas associadas tanto a virulência quanto a processos fisiológicos básicos (Pocsfalvi et al., 2008).

A caracterização do proteoma de patógenos bacterianos, em resposta a condições de estresse é uma estratégia *in vitro* que visa mimetizar as diferentes condições ambientais encontradas por patógenos durante o processo de infecção, como: alteração do pH, temperatura, escassetes nutricional, além de espécies reativas de oxigênio e nitrogênio. Estas modificações ambientais atuam diretamente na expressão gênica e consequentemente, alteram a coordenação de diferentes processos celulares. Assim, a análise proteomica promove uma avaliação em nível proteico desta alteração na expressão gênica, identificando fatores que contribuem para a adaptação e resistência bacteriana a diferentes situações de estresse (Renzone et., 2005).

Outra estratégia *in vitro* que demonstra bastante eficiência na identificação de fatores de virulência bacteriana é a análise do proteoma de patógenos, associado ao co-cultivo com diferentes linhagens celulares. A utilização de cultivo celular e posterior análise proteômica visa mimetizar as condições encontradas pelo patógeno durante o processo de infecção dentro da célula hospedeira. Além disso, este modelo de estudo pode promover a formação de compartimentos específicos da célula hospedeira em que patógenos intracelulares como

Mycobacterium, *Salmonella* ssp. e *C. pseudotuberculosis* utilizam para a proliferação celular (Bumann, 2010). A análise do proteoma de *Staphylococcus aureus*, após internalização em diferentes tipos células epiteliais (pulmão, rim) demonstrou níveis diminuídos de proteínas ribossomais e enzimas metabólicas, entretanto proteínas envolvidas na biossíntese de arginina e lisina, proteínas de resposta a estresse e reguladores transcripcionais foram altamente reguladas (Surmann et al., 2014). Assim, estes resultados demonstram um rearranjo na expressão genica de *S. aureus* durante a infecção em células epiteliais.

A utilização de modelos *in vivo* no estudo de doenças infecciosas vem sendo aplicado com o objetivo de tentar suprir algumas limitações do estudo *in vitro*. Assim uma das vantagens em utilizar sistemas *in vivo* é a possibilidade de gerar um confronto que ocorre entre o patógeno e a rede dinâmica do sistema imune do hospedeiro (Shi et al., 2006). Neste tipo de abordagem utiliza-se, principalmente cobaios (porcos-da-índia) e camundongos como hospedeiros, em muitos casos, estes modelos representam o hospedeiro definitivo ou é o modelo que mais se aproxima do hospedeiro definitivo. Em *Clostridium perfringens*, utilizou-se camundongos como modelos para o estudo da gangrena gasosa. A análise do imunoproteoma deste patógeno, após o contato com o hospedeiro murino, permitiu identificar um *set* de proteínas antigênicas. Outro resultado interessante foi que o perfil proteomico observado neste estudo apresentou-se diferente de estudos prévios, onde foi avaliado o proteoma *C. perfringens*, após internalização em células epiteliais (Sengupta & Alam, 2011).

2.3 Proteômica no Gênero *Corynebacterium*

O gênero *Corynebacterium* é composto por espécies não patogênicas de interesse biotecnológico como: *Corynebacterium glutamicum*, *Corynebacterium efficiens*

Corynebacterium ammoniagenes e que são utilizadas principalmente na produção de amino ácidos (Shirai et al., 2005); e espécies patogênicas como: *Corynebacterium diphtheriae*, *Corynebacterium jeikeium* e *Corynebacterium pseudotuberculosis* sendo agentes etiológicos da difteria, doenças nosocomiais, e linfadenite caseosa e linfagite ulcerativa, respectivamente (Riegel, 1998; Baird & Fontaine, 2007; Rogers et al., 2011).

Devido ao grande interesse biotecnológico e médico-veterinário do gênero *Corynebacterium*, o genoma de várias linhagens pertencentes às diferentes espécies deste gênero foram sequenciadas. Os dados provenientes destes trabalhos *in silico*, demonstram uma grande perda genética na maioria das espécies patogênicas (Sangal et al., 2014). Além disso, foi observado uma variabilidade genética entre espécies patogênicas e não patogênicas, onde linhagens patogênicas apresentam um conteúdo genético médio de aproximadamente 2.277 genes, enquanto que espécies não patogênicas demonstram aproximadamente 3.003 genes (Dorella et al., 2007).

Além de estudos *in silico* do genoma de *Corynebacterium*, diversos estudos funcionais do genoma de espécies pertencentes a este gênero veem sendo realizados. Onde estudos proteômicos, são aplicados com o objetivo de avaliar o genoma funcional de espécies não patogênicas e patogênicas em nível proteico para obter informações a respeito da biologia destas bactérias.

2.3.1 Proteoma de *Corynebacterium* não patogênicas

Corynebacterium glutamicum

C. glutamicum é a espécie de interesse biotecnológico mais importante dentro do gênero *Corynebacterium*, sendo utilizada principalmente na produção de aminoácidos como: L-lisina, L-arginina, L-histidina e L-valina. Devido a esta importância no cenário biotecnológico, é a espécie

mais estudada deste gênero, tanto em nível genético quanto fisiológico. A linhagem modelo de estudos pertencente a esta espécie é *C. glutamicum* ATCC13032, a qual possui um genoma de aproximadamente 3,3 Mb, e 3058 regiões codificantes de proteína (Kalinowski et al., 2003).

Dentre as frações proteicas que compõe a célula bacteriana, as frações citoplasmáticas e de membrana são as mais exploradas em *C. glutamicum*. Nestes compartimentos, estão alocadas várias proteínas que desempenham papel importante no metabolismo desta bactéria, o que favorece a produção de aminoácidos. Assim, vários esforços são realizados para caracterizar estas frações, através de estudos descritivos ou em situações que mimetizam condições ambientais encontradas por *C. glutamicum*.

Entretanto, devido à baixa resolução de proteínas de caráter hidrofóbico pela 2-DE, vários esforços veem sendo realizados com o objetivo de padronizar abordagens que permitam a caracterização do proteoma de membrana de *C. glutamicum*. Assim vários protocolos foram estabelecidos para obtenção desta fração proteica. Além disso, a combinação destes métodos com técnicas como: cromatografia de troca aniônica, associado à SDS-PAGE e MALDI-TOF e a utilização da *high-throughput proteomics* tem promovido um alto nível de identificação de proteínas de membrana de *C. glutamicum* (Schluesener et al., 2005; Fischer et al., 2006; Fränzel et al., 2009; Rietschel et al., 2009; Arrey et al., 2010).

O primeiro trabalho proteômico realizado com *C. glutamicum* foi um estudo descritivo do proteoma citoplasmático e de membrana da linhagem ATCC13032, o qual caracterizou 10 proteínas. Neste trabalho, foram combinadas as técnicas de eletroforese bidimensional (2-DE) para resolução do extrato proteico e a técnica de sequenciamento de Edman para identificação dos *spots* proteicos (Hermann et al., 1998). A partir deste estudo outros trabalhos foram realizados para caracterizar o proteoma de *C. glutamicum*

Li et al. (2007) utilizando 2-DE e MALDI-TOF/MS, geraram um mapa proteico para o proteoma citoplasmático de uma linhagem produtora de *L*-glutamato, o que possibilitou caracterização de 139 proteínas de *C. glutamicum* ATCC 14067. Quando comparado o proteoma da linhagem ATCC 14067 com a linhagem referência ATCC13032, foram identificadas 87 proteínas exclusivas para a linhagem produtora de aminoácido. Assim, estas diferenças observadas demonstram um *set* de proteínas produzidas por esta linhagem envolvida na produção de glutamato.

A análise proteômica comparativa entre a linhagem DM1730 produtora de *L*-lisina e a linhagem ATCC13032, permitiu a quantificação significativa de 347 proteínas que foram agrupadas em 21 processos biológicos (Franzel et al., 2010). A linhagem produtora de *L*-lisina demonstrou proteínas menos abundantes envolvidas na síntese proteica e que participam do processo de crescimento e divisão celular. Além disso, a detecção de baixos níveis de proteínas, associadas ao processo de homeostase de ferro e a indução de proteínas envolvidas na aquisição de ferro demonstram limitação de ferro durante a produção de lisina. Outro resultado interessante foi à presença de um alto número de proteínas envolvidas em estresse oxidativo reguladas positivamente, sugerindo que esta linhagem encontra este tipo de estresse durante a síntese de *L*-lisina. Assim, neste estudo foi demonstrado que o processo de produção de lisina pode ser positivo, mesmo devido à baixa abundância de proteínas envolvidas em processos fisiológicos básicos (Franzel et al., 2010).

Devido as diferentes condições ambientais encontradas por *C. glutamicum*, alguns estudos proteômicos foram aplicados para avaliar a resposta desta bactéria a diferentes situações de estresse, como: estresse térmico (30 °C e 40 °C) (Barreiro et al., 2005), diferentes condições de pH (6 e 9) (Barriuso-Iglesias et al., 2008; Follman et al., 2009), osmótico (NaCl 750 mM) (Fränzel et al., 2009), metais pesados (Fanous et al., 2008; Fanous et al., 2010) e hipoclorito (Chi

et al., 2014). Além destes estudos que mimetizam diferentes condições de estresse, diversos trabalhos proteômicos foram realizados para avaliar o metabolismo de carbono (Claes et al., 2002; Polen, et al., 2007; Qi et al., 2007; Haussmann et al., 2009; Haussmann & Poetsch, 2012; Koch-Koerfges et al., 2012; Voges & Noack, 2012) e nitrogênio (Beckers et al., 2005; Silberbach et al., 2005) em *C. glutamicum*.

Sendo assim, estes estudos proteômicos realizados tem promovido um conhecimento, acerca de fatores e mecanismos envolvidos em diferentes processos fisiológicos de *C. glutamicum*, o que favorece o desenvolvimento de meios ou condições de cultivo para aprimorar a síntese de aminoácidos por esta bactéria.

Corynebacterium efficiens

C. efficiens é uma bactéria de interesse biotecnológico, contudo a principal característica desta bactéria é a sua capacidade de produzir L-glutamato em temperaturas próximas de 40 °C. Assim, este fator quando avaliado em escala industrial, torna-se importante para a redução de custos relacionados à utilização de mecanismos para resfriamento do calor durante o processo de fermentação (Nishio et al., 2003).

A respeito da proteômica de *C. efficiens*, apenas um estudo foi realizado, onde uma análise proteômica comparativa foi conduzida, entre o proteoma de *C. efficiens* YS-314 e *C. glutamicum* ATCC13032 (Hansmeier et al., 2006). Neste estudo, através da 2-DE foram estabelecidos mapas proteicos para a fração citoplasmática, superfície celular e extracelular de *C. efficiens* YS-314. Além disso, 177 diferentes proteínas desta linhagem foram caracterizadas por MALDI-TOF-MS. Quando comparado o proteoma das linhagens YS-314 e ATCC13032, foi observado diferença entre proteínas envolvidas no metabolismo de inositol, envelope celular,

além de proteínas associadas à adesão celular (fimbrias e *surface layer*), o que pode sugerir diferenças entre processos de colonização de cada linhagem (Hansmeier et al., 2006a).

Corynebacterium ammoniagenes

C. ammoniagenes é uma bactéria utilizada na produção de nucleotídeos e pouco foi explorado sobre o proteoma desta bactéria. A análise proteomica (SDS-PAGE/ESI), da parede celular de uma linhagem mutante para o gene *ramA*, gene que participa de processos envolvidos na biossíntese do envelope bacteriano celular, permitiu a caracterização de sete proteínas. Além disso, nesta análise proteômica a baixa intensidade de bandas proteicas no gel da linhagem mutante, referente a proteínas associadas ao envelope celular, demonstra a importância do gene *ramA*, na síntese da parede celular de *C. ammoniagenes* (Lee et al., 2010).

2.3.2 Proteoma de *Corynebacterium* patogênicas

Ao contrário dos estudos protêomicos de espécies não patogênicas que visam principalmente à caracterização das frações citoplasmática e de membrana, os estudos realizados com espécies patogênicas de *Corynebacterium* tem como o principal objetivo o estudo com proteínas presentes na superfície celular bacteriana e proteínas extracelulares. Bactérias possuem vários sistemas que permitem a translocação de diferentes fatores em torno da membrana celular, estes produtos quando exportados desempenham um papel importante na patogênese bacteriana. Na qual permitem, a adesão e invasão da célula hospedeira, bem como a aquisição de nutrientes para a sobrevivência bacteriana. Além disso, muitos destes fatores exportados favorecem o processo de defesa contra o sistema imune (Schneewind & Missiakas, 2012; Chang et al., 2014). Assim a caracterização destas frações proteicas, além de favorecer um conhecimento acerca da

virulência bacteriana, podem representar alvos para o desenvolvimento de vacinas e testes de imunodiagnóstico.

Corynebacterium diphtheriae

C. diphtheriae é o agente etiológico da difteria, uma doença infectocontagiosa causada pela ação da exotoxina diftérica produzida por este patógeno. A difteria é caracterizada pela formação de lesões, contendo pseudomembranas na pele e vias respiratórias. Em alguns casos, a toxina pode atingir a via circulatória, e consequentemente promover lesões em alguns órgãos como o coração, o que pode resultar no óbito de alguns pacientes. A principal via de transmissão da difteria é através do contato direto, tosse e espirros. O diagnóstico normalmente é realizado clinicamente ou através da cultura bacteriológica associada a exames bioquímicos ou a partir de teste sanguíneos (Hadfield et al., 2000).

Uma análise pan-genômica de 13 linhagens de *C. diphtheriae*, demonstrou um tamanho médio do genoma destas linhagens de aproximadamente 2,4 Mb, além do número médio de 2.294 genes, codificantes de proteína (Trost et al., 2012). Entretanto, apesar da importância deste patógeno na saúde pública, apenas dois estudos protêomicos de *C. diphtheriae* foram realizados (Hansmeier et al., 2006b; Ott et al., 2010).

Hansmeier et al. (2006b) conduziram uma análise do proteoma extracelular e de superfície celular de *C. diphtheriae*, no qual foi possível estabelecer mapas proteicos para estas duas frações. A combinação das técnicas de 2-DE e MALDI-TOF-MS permitiu a identificação de 107 proteínas extracelulares e 58 proteínas de superfície. Contudo, apenas 85 diferentes proteínas de *C. diphtheriae* foram caracterizadas. Em suma, esta análise proteômica de *C. diphtheriae*

permitiu identificar várias proteínas que favorecem tanto a virulência e patogenicidade, quanto processos fisiológicos básicos deste patógeno.

Um estudo foi conduzido com uma linhagem mutante de *C. diphtheriae* para o gene que codifica uma proteína hipotética (DIP1281), com o objetivo de confirmar a hipótese de que esta proteína poderia estar associada à invasão celular. Entretanto, neste estudo, foi demonstrado que esta proteína não desempenha papel no processo patogênico de *C. diphtheriae*, no entanto está envolvida na organização da parede celular de *C. diphtheriae*. Além disso, a análise do proteôma de superfície celular da linhagem DIP1281, utilizando SDS-PAGE, *Western blotting* e 2-DE, demonstrou alteração no perfil eletroforético da linhagem mutante, quando comparado com a linhagem selvagem (Ott et al., 2010).

Corynebacterium jeikeium

C. jeikeium é um dos mais frequentes *Corynebacterium* isolados dentro de ambientes hospitalares. Esta bactéria é isolada principalmente de pacientes imunodeprimidos, dispositivos médicos, longo período hospitalar e terapia com espectro de antibióticos. O espectro clínico das manifestações causadas por *C. jeikeium* é bastante amplo, sendo bastante reportada por causar endocardites, septicemia, meningites, pneumonia e osteomielite (Funke et al., 1997).

C. jeikeium apresenta um genoma de aproximadamente 2,4 Mb, contendo 2.104 genes, além de um plasmídeo (pKW4) produtor de bacteriocina (Tauch et al., 2005). A respeito da proteômica desta bactéria, um estudo conduzido por Hansmeier et al. (2007) permitiu gerar mapas proteicos para as seguintes frações celulares: citoplasmática, superfície celular e extracelular. Esta análise proteômica, caracterizou 358 diferentes proteínas de *C. jeikeium*, que foram agrupadas em 17 processos biológicos. Além disso, este estudo permitiu a reconstituição

de vias metabólicas que favorece processos fisiológicos desta bactéria, além de proteínas que podem desempenhar papel importante na virulência e patogenicidade de *C. jeikeium* (Hansmeier et al., 2007).

Corynebacterium pseudotuberculosis

O primeiro genoma complemento sequenciado de *C. pseudotuberculosis* foram os das linhagens 1002_*ovis*, isolada de um caprino no Brasil e C231_*ovis* isolada de um ovino na Austrália (Ruiz et al., 2011). Estas linhagens possuem um genoma de aproximadamente 2,3 Mb, e o proteoma predito para estas linhagens foram de 2.059 e 2.053 proteínas para 1002_*ovis* e C231_*ovis*, respectivamente (Ruiz et al., 2011).

Com o objetivo de complementar os prévios estudos *in silico* do genoma das linhagens 1002_*ovis* e C231_*ovis*, uma análise comparativa do proteoma extracelular destas linhagens foi conduzido (Pacheco et al., 2011). Neste estudo, utilizando a abordagem LC-MS/MS foram caracterizadas 70 proteínas de 1002_*ovis* e 67 proteínas de C231_*ovis*, totalizando 93 diferentes proteínas extracelulares de *C. pseudotuberculosis*. A análise quantitativa do core-proteoma de 1002_*ovis* e C231_*ovis*, revelou diferenças principalmente em proteínas envolvidas no envelope celular, o que pode influenciar em fatores que contribuem para adesão e invasão celular bem como em mecanismos de transporte celular. Além disso, no proteoma de 1002_*ovis* não foi possível detectar alguns fatores de virulência como a PLD, principal fator de virulência de *C. pseudotuberculosis*, sugerindo que esta linhagem poderia apresentar baixo potencial de virulência. Contudo, esta análise do proteoma extracelular das linhagens 1002_*ovis* e C231_*ovis*, permitiu a validação de dados preditos anteriormente *in silico* (Pacheco et al., 2011).

Outra análise proteômica comparativa foi realizada entre o proteoma extracelular das linhagens 1002_*ovis* e C231_*ovis*. Seyffert et al., (2014) com o objetivo de identificar proteínas antigênicas, além de marcadores para o desenvolvimento de testes de imunodiagnóstico contra a linfadenite caseosa, utilizaram a abordagem SERPA (*serological proteome analysis*) para caracterizar o imunoproteoma extracelular destas duas linhagens. O *core*-imunoproteoma foi composto por 11 proteínas imunorreativas, e o imunoproteoma acessório apresentou três proteínas para C231_*ovis* e duas proteínas para 1002_*ovis*. Esta análise permitiu a caracterização total de 16 proteínas antigênicas de *C. pseudotuberculosis*.

Um estudo realizado com uma linhagem mutante para o gene *sigE* (1002 Δ *sigE*), demonstrou que o fator extracitoplasmático σ^E , é mais suscetível ao estresse nitrosativo. Quando caracterizado o exoproteoma das linhagens selvagem 1002 e mutante 1002 Δ *sigE* em resposta ao estresse nitrosativo, um total de 104 diferentes proteínas de *C. pseudotuberculosis* foram identificadas. No proteoma da linhagem selvagem 1002 após exposição ao estresse nitrosativo, foram detectadas proteínas envolvidas em transporte celular, resposta ao estresse nitrosativo e metabolismo celular. Entretanto, o proteoma exclusivo da linhagem 1002 Δ *sigE* após exposição ao estresse nitrosativo, foi composto principalmente por proteínas envolvidas no crescimento celular, transporte de metais e envolvidas na resposta ao estresse nitrosativo/oxidativo. Os resultados obtidos neste estudo, além de demonstrarem o papel do fator σ^E na resistência de *C. pseudotuberculosis* ao estresse nitrosativo, demonstraram um grupo de proteínas que podem favorecer o processo de resistência e adaptação deste patógeno, na presença do estresse nitrosativo (Pacheco et al., 2012).

Outro estudo que contribuiu para a identificação de fatores que contribuem para o processo infecioso de *C. pseudotuberculosis* foi à caracterização do proteoma de superfície

celular de linhagens biovar *ovis*, isoladas diretamente de linfonodos de animais infectados naturalmente. Um total de 247 proteínas de superfície celular de *C. pseudotuberculosis* foram caracterizadas. Quando analisado o proteoma das linhagens na condição recuperada, este foi composto por proteínas envolvidas na virulência bacteriana como: chaperonas, proteases, transportadores, resposta ao estresse oxidativo. Além disso, foram detectadas proteínas envolvidas na síntese da parede celular e que participam de processos fisiológicos básicos essenciais para crescimento bacteriano. Este trabalho ainda conseguiu demonstrar um repertório de fatores que podem contribuir para a sobrevivência e adaptação de *C. pseudotuberculosis*, durante o estágio crônico da infecção, uma vez que esta análise proteômica foi feita a partir de linhagens isoladas de animais com a doença já estabelecida (Rees, et al., 2014).

3. Objetivos/objectifs

3.1 Objetivo Geral

Este trabalho de Tese teve como objetivo geral, avaliar o genoma funcional de *C. pseudotuberculosis* através de diferentes estratégias proteômicas para identificar fatores que contribuem para os processos fisiológicos básicos, bem como aqueles envolvidos na patogênese e virulência deste patógeno.

Objectif général

Ce travail de thèse vise à évaluer le génome fonctionnel de *C. pseudotuberculosis* par différentes stratégies protéomiques pour identifier les principaux facteurs qui contribuent aux processus physiologiques de base, ainsi que ceux impliqués dans la pathogenèse et la virulence de cet agent pathogène.

3.2 Objetivos específicos

- ✓ Caracterizar o exoproteoma das linhagens *C. pseudotuberculosis ovis* 1002 e *C. pseudotuberculosis ovis* C231.
- ✓ Identificar exoproteínas diferencialmente expressas entre as linhagens *C. pseudotuberculosis ovis* 1002 e *C. pseudotuberculosis ovis* C231.
- ✓ Caracterizar o proteoma da linhagem *C. pseudotuberculosis ovis* 1002, em resposta ao estresse nitrosativo.
- ✓ Identificar e comparar os fatores que podem estar envolvidos na virulência de *C. pseudotuberculosis ovis* 1002 e *C. pseudotuberculosis equi* 258, utilizando ensaios de infecção experimental em modelo murino, associada à análise proteômica.
- ✓ Correlacionar os resultados obtidos nas análises proteômicas com dados genômicos de *C. pseudotuberculosis* para validação de prévios dados *in silico*.

Objectifs spécifiques

- ✓ Caractériser l'exoprotéome des souches *C. pseudotuberculosis ovis* 1002 et *C. pseudotuberculosis ovis* C231.
- ✓ Identifier les exoprotéines qui sont exprimées de manière différentielle, entre les souches, *C. pseudotuberculosis ovis* 1002 et *C. pseudotuberculosis ovis* C231.
- ✓ Caractériser le protéome de la souche *C. pseudotuberculosis ovis* 1002, en réponse au stress nitrosant.
- ✓ Identifier les facteurs qui peuvent être impliqués dans la virulence de *C. pseudotuberculosis ovis* 1002 e *C. pseudotuberculosis equi* 258, en utilisant des essais d'infection expérimentale chez la souris, associés à l'analyse protéomique.

- ✓ Corréler les résultats obtenus dans l'analyse protéomique avec des données génomiques de *C. pseudotuberculosis* pour valider les données *in silico* précédentes.

4. Capítulo 1: Caracterização do proteoma extracelular de linhagens de *C. pseudotuberculosis ovis*, através da proteômica comparativa.

Chapitre 1 : Caractérisation du proteome extracellulaire des souches de *C. pseudotuberculosis ovis* par protéomique comparative.

4.1 Introdução

Este primeiro capítulo é apresentado em formato de artigo científico, onde serão apresentados dois artigos que exploram o proteoma extracelular de duas linhagens de *C. pseudotuberculosis*, pertencentes ao biovar *ovis*: C231_*ovis* e 1002_*ovis*, isoladas de um ovino e um caprino, respectivamente. Devido ao papel desempenhado por proteínas extracelulares na virulência bacteriana, a caracterização do exoproteoma destas linhagens nos permitiu obter um conhecimento de um repertório de moléculas que poderiam estar associadas à virulência e fisiologia destes patógenos. No primeiro estudo, foi utilizada a técnica 2-DE para caracterizar qualitativamente o exoproteoma das linhagens C231_*ovis* e 1002_*ovis*. No segundo estudo, utilizando a técnica 2D-DIGE, foi realizado uma análise quantitativa entre o proteoma extracelular destas duas linhagens. As proteínas foram detectadas por espectrometria de massa do tipo MALDI-TOF-MS/MS. Além disso, nós associamos o crescimento bacteriano em um meio quimicamente definido a um protocolo otimizado para obter as proteínas extracelulares.

Os resultados obtidos nestes estudos possibilitaram a caracterização do proteoma extracelular de *C. pseudotuberculosis* e o estabelecimento de mapas proteicos para as linhagens 1002_*ovis* e C231_*ovis*. Além disso, um resultado interessante foi a não detecção de alguns fatores de virulência em 1002_*ovis*. Como por exemplo, a PLD principal fator de virulência de *C. pseudotuberculosis*, sugerindo que esta linhagem poderia apresentar baixo potencial de virulência. No entanto, os resultados obtidos nestes trabalhos foram capazes de complementar prévios estudos do proteoma extracelular destas linhagens, como estudos *in silico* do genoma de *C. pseudotuberculosis*.

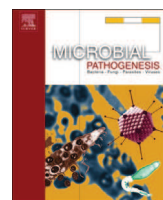
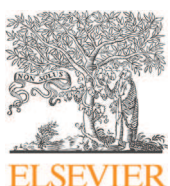
Introduction

Ce premier chapitre est présenté sous forme d'article scientifique qui compare le protéome extracellulaire de deux souches de *C. pseudotuberculosis* biovar *ovis*, 1002_*ovis* et C231_*ovis*, isolées à partir d'un caprin et un ovin, respectivement. En raison du rôle des protéines extracellulaires dans la virulence bactérienne, nous avons caractérisé l'exoprotéome de ces souches ce qui nous a permis d'acquérir des connaissances sur le répertoire de protéines qui pourraient être associées à la virulence et à la physiologie de ce pathogène. Dans la première étude, nous avons utilisé l'électrophorèse bi-dimensionnelle (2-DE) pour caractériser qualitativement l'exoproteome des souches 1002_*ovis* et C231_*ovis*. Dans la deuxième étude, en utilisant la technique 2D-DIGE, nous avons réalisé une analyse quantitative du protéome extracellulaire des deux souches. Les protéines ont été identifiées par spectrométrie de masse de type MALDI-TOF-MS/MS. En outre, nous avons adapté et combiné un milieu chimiquement défini pour la culture de ces bactéries et un protocole pour obtenir des protéines extracellulaires.

Les résultats obtenus dans cette étude ont permis la caractérisation du protéome extracellulaire de *C. pseudotuberculosis* et l'établissement de cartes de protéines pour les souches 1002_*ovis* et C231_*ovis*. Un résultat intéressant issu de ce travail est l'absence (non-détection) de certains facteurs de virulence, dans le protéome extracellulaire de 1002_*ovis*. A titre d'exemple, la phospholipase D, principal facteur de virulence de *C. pseudotuberculosis*, n'a pas été identifiée chez 1002 suggérant que la souche 1002 pourrait présenter une virulence moindre. Par ailleurs, les résultats obtenus dans ce travail ont permis de compléter les études précédentes du protéome extracellulaire des souches 1002_*ovis* et C231_*ovis*, ainsi que des travaux antérieurs *in silico* sur le génome de *C. pseudotuberculosis*.

4.2 Artigo 1: Identification of 11 new exoproteins in *Corynebacterium pseudotuberculosis* by comparative analysis of the exoproteome. *Microb Pathog.* v. 61-62, p. 37-42. 2013. doi: 10.1016/j.micpath.2013.05.004.

Silva, W.M., Seyffert, N., Santos, A.V., Castro, T.L., Pacheco, L.G., Santos, A.R., Ciprandi, A., Dorella, F.A., Andrade, H.M., Barh, D., Pimenta, A.M., Silva, A., Miyoshi, A., Azevedo, V.



Identification of 11 new exoproteins in *Corynebacterium pseudotuberculosis* by comparative analysis of the exoproteome

Wanderson M. Silva^a, Núbia Seyffert^a, Agenor V. Santos^b, Thiago L.P. Castro^a, Luis G.C. Pacheco^c, Anderson R. Santos^a, Alessandra Ciprandi^b, Fernanda A. Dorella^a, Hélida M. Andrade^d, Debmalya Barh^f, Adriano M.C. Pimenta^e, Artur Silva^b, Anderson Miyoshi^a, Vasco Azevedo^{a,*}

^a Departamento de Biologia Geral, Instituto de Ciências Biológicas, Universidade Federal de Minas Gerais, Av. Antonio Carlos, 6627 – Pampulha, CP 486, CEP 31.270-901 Belo Horizonte-MG, Brazil

^b Instituto de Ciências Biológicas, Universidade Federal do Pará, Rua Augusto Corrêa, 01 – Guamá, Belém, PA, Brazil

^c Instituto de Ciências da Saúde, Universidade Federal da Bahia, Av. Reitor Miguel Calmon, s/n – Vale do Canela, CEP 40110100 Salvador-BA, Brazil

^d Departamento de Parasitologia, Instituto de Ciências Biológicas, Universidade Federal de Minas Gerais, Av. Antonio Carlos, 6627 – Pampulha, CP 486, CEP 31.270-901 Belo Horizonte-MG, Brazil

^e Departamento de Bioquímica e Imunologia, Instituto de Ciências Biológicas, Universidade Federal de Minas Gerais, Av. Antonio Carlos, 6627 – Pampulha, CP 486, CEP 31.270-901 Belo Horizonte-MG, Brazil

^f Centre for Genomics and Applied Gene Technology, Institute of Integrative Omics and Applied Biotechnology (IIOAB), Purba Medinipur, WB 721172, India

ARTICLE INFO

Article history:

Received 3 October 2012

Received in revised form

23 April 2013

Accepted 6 May 2013

Available online 16 May 2013

Keywords:

Corynebacterium pseudotuberculosis

Proteomics

Extracellular proteins

Two-dimensional electrophoresis (2-DE)

Caseous lymphadenitis

ABSTRACT

This study involves the comparison between the exoproteomes of two different strains of *Corynebacterium pseudotuberculosis*, the etiologic agent of caseous lymphadenitis in small ruminants. In a previous study, based on a gel-free system (TPP-LC/MS^E), 70 exoproteins for the strain 1002 and 67 for the strain C231, totaling 93 different extracellular proteins for *C. pseudotuberculosis*, were identified. In the present work, we have used 2D gel electrophoresis to resolve the extracellular proteins of both strains, which were then digested with trypsin, analyzed by MALDI-TOF/TOF and identified with the software MASCOT®. A total of 45 extracellular proteins of *C. pseudotuberculosis* were identified by this approach. The comparative analysis between the strains 1002 and C231 identified 13 and 3 strain-specific proteins, respectively, 11 of which are novel. These newly identified proteins may play an important role in the physiology and virulence of *C. pseudotuberculosis*.

Crown Copyright © 2013 Published by Elsevier Ltd. All rights reserved.

1. Introduction

Corynebacterium pseudotuberculosis is a Gram-positive, facultative, intracellular pathogen, responsible for caseous lymphadenitis (CLA) in small ruminants [1] and causes great economic losses in the goat and sheep industries worldwide [2]. Currently, there are no efficient tests, vaccines, or drugs available for early diagnosis, effective prevention, or treatment.

The phospholipase D (PLD), a potent exotoxin with sphingomyelinase activity, is the main virulence factor of *C. pseudotuberculosis* [3]. Other virulence factors include ABC type iron transporters (important for disease progression) [4] and a serine protease [5]. Extracellular and secreted proteins are important virulence factors, associated with cell adhesion, cell invasion, survival and proliferation in the host cell, and escape from the immune system; and have high potential for the development of drugs or vaccines to target bacterial pathogens [6]. Therefore, the exoproteome and secretome of *C. pseudotuberculosis* are of interest for developing effective drugs or vaccines to combat CLA.

Here, using two-dimensional electrophoresis (2-DE) along with mass spectrometry MALDI-TOF/TOF, we have generated exoproteome maps for the *C. pseudotuberculosis* 1002 (Cp 1002) and *C. pseudotuberculosis* C231 (Cp C231) strains. Based on this methodology it was possible to identify 11 extracellular proteins of *C. pseudotuberculosis* that had not been detected in the previous

Abbreviations: CLA, caseous lymphadenitis; LC-MS, liquid chromatography – mass spectrometry; PLD, phospholipase D; PSE, potentially surface exposed; TPP, three-Phase partitioning; 2-DE, two-dimensional electrophoresis; MALDI-TOF, matrix-assisted laser desorption/ionization – time-of-flight; MS, mass spectrometer; HSP, heat shock protein; RT, room temperature.

* Corresponding author. Tel./fax: +55 31 3409 2610.

E-mail addresses: vasco@icb.ufmg.br, vascoariston@gmail.com (V. Azevedo).

study, based on gel-free approach TPP-LC/MS^E [7]. After combining the results (93 extracellular proteins) obtained from TPP-LC/MS^E, and 2-DE-MALDI-TOF/TOF methodologies, a total of 104 extracellular proteins were successfully characterized in *C. pseudotuberculosis*.

2. Materials and methods

2.1. Bacterial strains and culture conditions

The wild-type *C. pseudotuberculosis* strains *Cp 1002* and *Cp C231* were routinely maintained in Brain Heart Infusion (BHI) broth or bacteriological agar plates at 37 °C. To extract extracellular proteins, the strains were cultured in chemically defined medium (CDM) [(Na₂HPO₄·7H₂O (12.93 g/L), KH₂PO₄ (2.55 g/L), NH₄Cl (1 g/L), MgSO₄·7H₂O (0.20 g/L), CaCl₂ (0.02 g/L), and 0.05% (v/v) Tween 80]; 4% (v/v) MEM Vitamins Solution 100× (Invitrogen); 1% (v/v) MEM Amino Acids Solution 50× (Invitrogen); 1% (v/v) MEM Non Essential Amino Acids Solution 100× (Invitrogen); and 1.2% (w/v) filter-sterilized glucose) at 37 °C [8] until the set point of exponential growth (DO_{600nm} = 1.3) was reached.

2.2. Three-phase partitioning

An optimized TPP protocol was used to extract extracellular proteins [9]. The cultures were centrifuged for 20 min at 2700 × g. Supernatants were filtered using 0.22 µm filters, ammonium sulfate was added to the samples at 30% (w/v) and the pH of the mixtures was adjusted to 4.0. Next, an equal volume of N-butanol was added to each sample. The samples were vigorously vortexed and left to rest for 1 h at room temperature, then centrifuged for 10 min at 1350 × g at 4 °C. The interfacial precipitate was collected in 1.5 mL microcentrifuge tubes and re-suspended in 1 mL Tris 20 mM + 10 µL protease inhibitor. The protein concentration was determined using a standard curve [10].

2.3. Two-dimensional electrophoresis (2-DE)

Approximately 300 µg of protein was dissolved in 450 µL of rehydration buffer (Urea 7 M, thiourea 2 M, 3-[*N*-(3-Cholamidopropyl) dimethylammonio]-1-propanesulfonate 2%, Tris 40 mM, bromophenol blue 0.002%, DTT 75 mM, IPG Buffer 1%). Samples were applied to 18 cm pH 3–10 NL strips (GE Healthcare). Isoelectric focusing (IEF) was performed using the apparatus IPGphor 2 (GE Healthcare) under the following voltages: 100 V 1 h, 500 V 2 h, 1000 V 2 h, 10000 V 3 h, 10000 V 6 h, 500 V 4 h. The strips were kept at equilibrium for 15 min in 10 mL of equilibration buffer I (Tris–HCl 50 mM pH 8.8, Urea 6 M, Glycerol 30%, SDS 2%, bromophenol blue 0.002%, 100 mg dithiothreitol) and an additional 15 min in 10 mL of equilibration buffer II (Tris–HCl 50 mM pH 8.8, urea 6 M, Glycerol 30%, SDS 2%, bromophenol blue 0.002%, iodoacetamide 250 mg). The isolated proteins were separated in 12% acrylamide/bis-acrylamide gels with an Ettan DaltSix II system (GE Healthcare). To visualize the separated proteins, gels were stained with Coomassie blue G-250 staining solution. Three biological replicates of 2-DE gels were scanned using an Image Scanner (GE Healthcare), and the Image Master 2D Platinum 7 (GE Healthcare) software was used to analyze the generated images. Reproducible images detected by the software were manually analyzed to eliminate possible artifacts.

2.4. In-gel tryptic digestion of proteins

Protein spots were excised from the gels using an *Ettan Spot Picker* (GE Healthcare), and fragments containing the excised spots were washed with ultra-sterile water for 5 min and dehydrated with acetonitrile (ACN) for 20 min. Subsequently, the fragments were

dried in a speed vac. Protein digestion was performed by adding 10 µL of a stock solution of trypsin (Promega, Sequencing Grade Modified Trypsin) (33 ng/mL—ca. 1.5 µM) to each tube for 60 min at 4 °C. After removal of excess trypsin, samples were incubated at 58 °C for 30 min. Digestion was interrupted by adding 1 mL of 5% formic acid (v/v). The extraction of peptides was performed using 30 mL of formic acid solution (5%–50% ACN), and the sample was subjected to ultrasound. The peptides were concentrated to a volume of 10 mL by a speed vac and desalinated and concentrated using ZIP-TIP C18 tips (Eppendorf) [11]. Finally, the samples were stored at –20 °C for subsequent analysis by mass spectrometry.

2.5. Mass spectra and database search

Analyses by MS and MS/MS modes were performed using a MALDI-TOF/TOF mass spectrometer Autoflex III™ (Bruker Daltonics, Billerica USA). The equipment was controlled in a positive/reflector using the FlexControl™ software. Calibration was performed using samples of standard peptides (Angiotensin II, Angiotensin I, Substance P, Bombesin, ACTH clip 1–17, ACTH clip 18–39, Somatostatin 28, Bradykinin Fragment 1–7, Renin Substrate tetradecapeptide porcine) (Bruker Daltonics, Billerica, USA). The peptides were added to the alpha-cyano-4-hydroxycinnamic acid matrix, applied on an AnchorChipTM 600 plate (Bruker Daltonics, Billerica, USA) and analyzed by Autoflex III. The search parameters included peptide mass fingerprint; enzyme; trypsin; fixed modification, carbamido methylation (Cys); variable modifications, oxidation (Met); mass values, monoisotopic; maximum missed cleavages, 1; and peptide mass tolerance of 0.05% Da (50 ppm). The results obtained by MS/MS were used for identifying proteins with the program MASCOT® (<http://www.matrixscience.com>) and compared with the NCBI databases.

2.6. In silico predictions of protein sub-cellular localization

To predict the sub-cellular localization of proteins, we used the following programs: SurfG+ v1.0 [12], SecretomeP v2.0 [13] and TatP v1.0 [14].

3. Results

3.1. The proteome reference maps of two *C. pseudotuberculosis* strains and protein identifications by MALDI-TOF/TOF

After 2-DE, 85 spots for *Cp 1002* and 80 spots for *Cp C231* were detected in the extracellular proteome. The electrophoretic patterns of the proteins were similar between the strains, with the majority of spots concentrated in the acidic range of the gels (p.I3–5). After acquiring the results from images of the gels, spots were excised from the gels, submitted to tryptic digestion and analyzed by MALDI-TOF MS/MS. MASCOT software identified 55 of the 85 protein spots (65%) in *Cp 1002* (Fig. 1) and 45 (56%) in *Cp C231* (Fig. 2). Because of low amounts or post-translational modifications of the proteins, some spots could not be identified. Altogether, we identified 45 proteins, 29 of which are common to both strains (Supplementary file 1), 13 of which are unique to *Cp 1002* (Supplementary file 2) and 3 of which are exclusive to *Cp C231* (Supplementary file 3). Some protein spots were identified as the same protein, possibly revealing the presence of isoforms because of post-translational modifications.

3.2. Comparative analysis between the strains exoproteomes

The exclusive proteins to *Cp 1002* are involved in several molecular functions (Supplementary file 2), acting on distinct

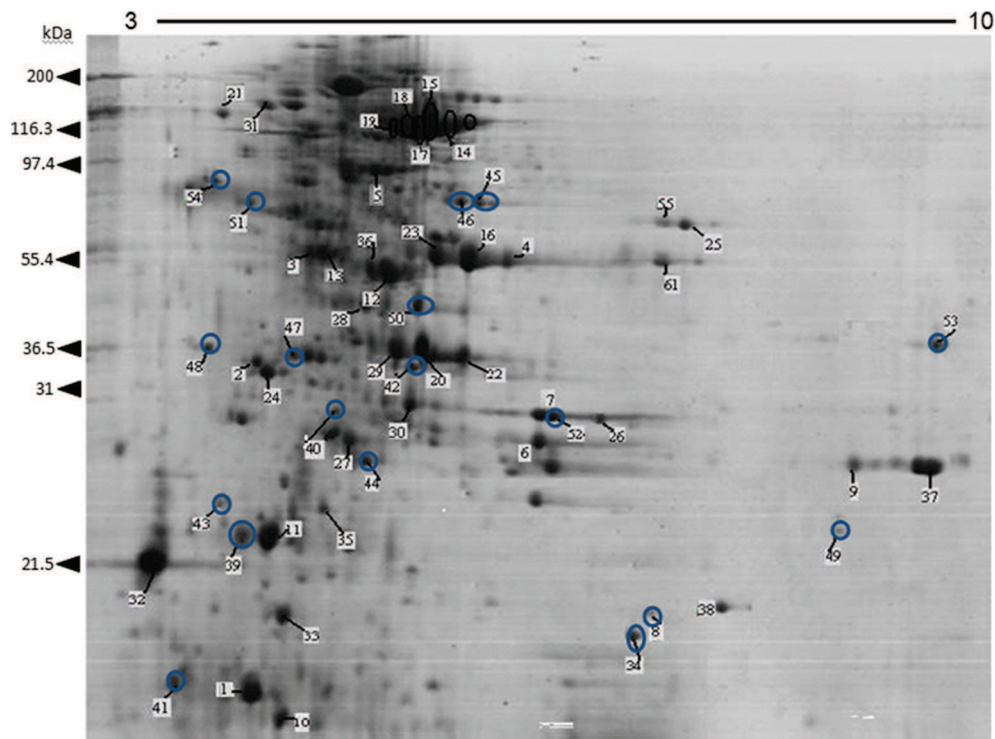


Fig. 1. 2-DE of extracellular proteins of strain 1002 stained with colloidal Coomassie. Electrophoretic profile using 3–10 NL strips. Spots with numbers were identified by MS. Spots with blue circles indicate protein spots taken exclusively from strain 1002. (For interpretation of the references to color in this figure legend, the reader is referred to the web version of this article.)

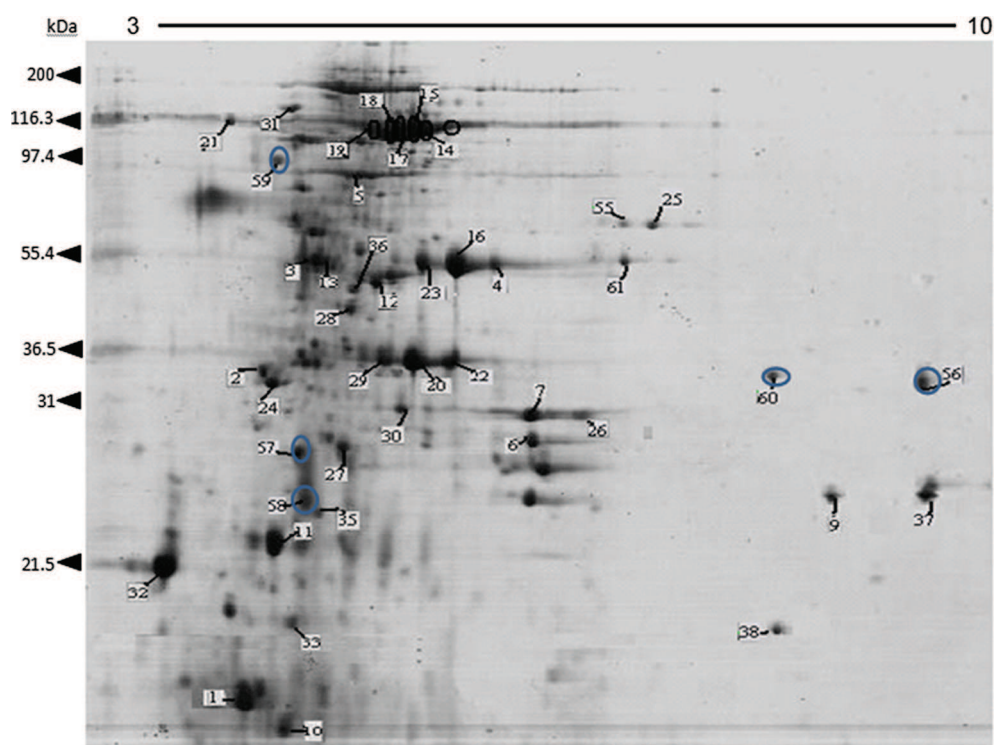


Fig. 2. 2-DE of extracellular proteins of strain C231 stained with colloidal Coomassie. Electrophoretic profile using 3–10 NL strips. Spots with numbers were identified by MS. Spots with blue circles indicate protein spots taken exclusively from strain C231. (For interpretation of the references to color in this figure legend, the reader is referred to the web version of this article.)

biological processes. The predominant functional group among the proteins detected is predicted to be involved in stress oxidative and cellular metabolism. Others process such as: transcription, translation, transport and biosynthesis were also identified. The set exclusive proteins to *Cp C231* (Supplementary file 3) are likely related to virulence, biosynthesis and cell wall biogenesis. Proteins with unknown functions were also identified for both strains. According to the NCBI database, one specific hypothetical protein (ADL09626) showed no similarity to any other protein in the *Corynebacterium* genus or other bacterial genera, suggesting that it is unique to the *C. pseudotuberculosis* species. This observation motivates further studies to explore the role of ADL09626 in *C. pseudotuberculosis* physiology and pathogenesis.

Bioinformatics analyses revealed that among the set of exclusive proteins *Cp 1002*, only the Open Reading Frames (ORF) which encodes for a putative DsbG protein (ADL21555) is not present in the genome of *Cp C231*, this protein belongs to the superfamily of thioredoxin and acts as a chaperone in the formation of disulfide bonds in proteins secreted by *Escherichia coli* [15]. However, DNA sequences encoding for all proteins present in exclusive proteome *Cp C231*, are present in the genome of *Cp 1002*.

Identical proteins with unknown functions were also identified for both strains. According to the NCBI database, one specific hypothetical protein (ADL09626) showed no similarity to any other protein in the *Corynebacterium* genus or other bacterial genera, suggesting that it is unique to the *C. pseudotuberculosis* species. This observation motivates further studies to explore the role of ADL09626 in *C. pseudotuberculosis* physiology and pathogenesis.

3.3. Analysis of *C. pseudotuberculosis* extracellular proteins using different approaches

Pacheco et al. [7] detected 70 and 67 (for a total of 93) proteins, respectively, from the exoproteomes of strains *Cp 1002* and *Cp C231* using the TPP/LC-MS^E method. This combined method of 2-DE and MALDI-TOF/TOF techniques allowed us to identify 42 proteins in *Cp 1002* and 32 proteins in *Cp C231*, resulting in a total of 45 different extracellular proteins identified for *C. pseudotuberculosis*. Despite our lower number of identifications, it is possible to demonstrate the presence of 11 proteins that were not previously detected by Pacheco et al. [7] (Table 1). Combining the results obtained by both studies, 81 and 73 extracellular proteins were characterized for strains *Cp 1002* and *Cp C231*, respectively, totaling 104 exported proteins for *C. pseudotuberculosis* (Supplementary file 4). Fig. 3 shows the distribution of proteins identified by the different approaches.

Table 1

List of the 11 proteins not identified by TPP/LC-MS^E.

Protein	ID (NCBI) ^a of strains		Gel identification	
	1002	C231	1002	C231
Chaperone GroEL	ADL21673	ADL11255	Yes	Yes
Chaperone protein DnaK	ADL21757	ADL11343	Yes	Yes
Hypothetical protein	ADL21702	ADL11289	Yes	Yes
Hypothetical protein	ADL21703	ADL11290	Yes	Yes
Hypothetical protein	ADL21704	ADL11291	Yes	Yes
Elongation factor P	ADL21021	ADL10611	Yes	Yes
Enolase	ADL20605	ADL10195	Yes	No
Glyceraldehyde-3-phosphate dehydrogenase	ADL20991	ADL10581	Yes	No
ABC-type transporter	ADL20391	ADL09988	Yes	No
Carbonic anhydrase	ADL20477	ADL20477	Yes	No
Manganese superoxide dismutase	ADL21849	ADL11437	Yes	No

^a Access number of proteins (NCBI genome project at 40687 and 40875).

4. Discussion

In this study, a comparative analysis between the extracellular proteins of *C231* and *1002* *C. pseudotuberculosis* strains was performed. Exoproteome differences observed between these strains may result from differences in hosts and geographic locations (*Cp 1002* was isolated from goats in Brazil and *Cp C231* from sheep in Australia). We could not detect spots referent to PLD and CP40 proteins in *Cp 1002* gels, similar to the findings by Pacheco et al. [7]. PLD is the most important virulence factor in *C. pseudotuberculosis*, the non-production of this exotoxin in *Cp 1002* can promote the inability this strain to spread in host, directly influencing in pathogenesis process of this pathogen [16].

The cytoplasmic proteins identified in the extracellular extracts may be exported by non-classical secretion. According to previous work, the detected proteins, elongation factor Tu, GroEL, Enolase, Glyceraldehyde-3-phosphate dehydrogenase and superoxide dismutase (SodA), were found to be dependent on a non-classical secretion pathway via SecA [13,17–19]. After sequencing the genomes of strains *Cp 1002* and *Cp C231*, it was observed that both carry two SecA genes (*SecA1* and *SecA2*), possibly involved in the *C. pseudotuberculosis* secretion systems [20]. *SecA2* has been described in *Bacillus subtilis* [17] and pathogenic bacteria, such as *Listeria monocytogenes* [18] and *Mycobacterium tuberculosis* [19].

A classic proteomics technique, based on 2-DE, led us to identify 11 proteins not detected using the TPP-LC/MS (gel-independent) approach in a previous study [7]. The combination of both techniques was found to be complementary, as it increased the previous number of identified extracellular proteins from 93 to 104. The differences observed in both studies may be associated with the separation methods, which involve distinct buffers for sample solubilization, and the physical–chemical properties of each protein. Another question that deserves attention for proteomics involving prokaryotes is the growth phase in which the studies are held. This growth phase issue is a possible explanation for the non-identification by Pacheco et al. [7] of 11 proteins described in the present work, as the extractions of proteins in our study occurred at the late-exponential growth phase, whereas Pacheco et al. [7] performed their extractions in the early exponential phase.

Among the 11 proteins newly identified in this study (Table 1), 3 have unknown functions (hypothetical proteins) and 8 have been related to various physiological functions and virulence factors. GroEL (HSP60) and DnaK (HSP70) are 2 of the major and best-studied chaperone proteins that play a key role in bacterial physiology and infection [21]. Elongation factor P (EFP) is a highly conserved protein in prokaryotes that stimulates the peptidyl-transferase activity of 70S ribosomes and enhances the synthesis of certain dipeptides initiated by *N*-formylmethionine [22]. The *efp* gene is essential for *E. coli* growth and protein synthesis [22]. In *Salmonella enterica*, it is involved in virulence and stress response [23]. Enolase is an enzyme of the glycolytic pathway that catalyzes the reversible conversion of 2-phosphoglycerate (2-PGE) into phosphoenolpyruvate (PEP). Bacterial enolases exhibit fibronectin-binding activity and influence colonization, invasion and persistence in host tissues [24]. In *Bacillus anthracis*, this protein acts as an immunodominant antigen [25] and may contribute to raising the invasive potential of the pathogen [26]. Glyceraldehyde-3-phosphate dehydrogenase (GAPDH) is present in cellular surfaces and secretomes of various pathogens; it is also associated with the *Streptococcus agalactiae* virulence mechanism because of its ability to modulate the host immune system during infection [27]. ABC-type transporters are essential for nutrient uptake and the secretion of various molecules, and they are involved in translation of mRNA and DNA repair [28]. ABC transporters can also play important roles in cell viability, virulence and bacterial

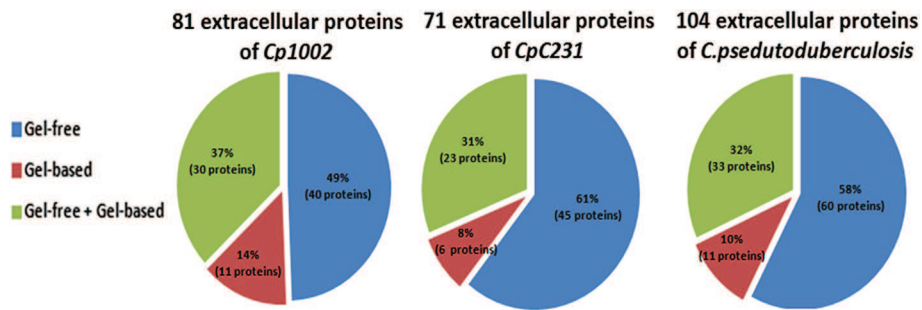


Fig. 3. Distribution of the identification of extracellular proteins of *C. pseudotuberculosis* by different approaches. Proteins detected by both techniques (2DE/MALDI-TOF/TOF + TPP-LC-MS^E) are in blue; proteins identified by the 2DE/MALDI-TOF/TOF technique are in red; and proteins identified by Pacheco et al. (2011) (TPP-LC-MS^E) are in green.

pathogenicity, such as the iron ABC uptake system [29]. Carbonic anhydrase maintains pH homeostasis and is involved in respiration, ion transportation, and bacterial growth [30,31]. Manganese superoxide dismutase (MnSOD) is an isoform of the superoxide dismutase family and an important component of the antioxidant defense mechanism that acts to eliminate reactive oxygen species (ROS) [32,33]. In *Enterococcus faecalis*, the MnSOD contributes to survival of the bacterium in macrophages, which is potentially important during the pathogenesis process [34].

In conclusion, the observed difference between the exoproteome of the strains *Cp 1002* and *Cp C231*, can influence in pathogenesis, antigenicity and adaptation specific-hosp of each isolated. Therefore, our data demonstrated which use of complementary proteomic techniques is an efficient strategy for the characterization of bacterial exoproteomes. These new identified proteins increase the extracellular protein catalog of *C. pseudotuberculosis* and validate former *in silico* predictions. In addition, these proteins may represent new potential targets for use in prophylaxis against CLA.

Conflict of interest

The authors declare that they have no competing interests.

Acknowledgments

The current work was supported by CNPq, FAPEMIG and FAPESPA.

Appendix A. Supplementary data

Supplementary data related to this article can be found at <http://dx.doi.org/10.1016/j.micpath.2013.05.004>.

References

- Dorella FA, Pacheco LG, Oliveira SC, Miyoshi A, Azevedo V. *Corynebacterium pseudotuberculosis*: microbiology, biochemical properties, pathogenesis and molecular studies of virulence. *Vet Res* 2006;37:201–18.
- Williamson LH. Caseous lymphadenitis in small ruminants. *Vet Clin North Am Food Anim Pract* 2001;17:359–71.
- Songer JG. Bacterial phospholipases and their role in virulence. *Trends Microbiol* 1997;5:156–60.
- Billington SJ, Esmay PA, Songer JG, Jost BH. Identification and role in virulence of putative iron acquisition genes from *Corynebacterium pseudotuberculosis*. *J Bacteriol* 2002;180:3233–6.
- Wilson MJ, Brandon MR, Walker J. Molecular and biochemical characterization of a Protective 40-Kilodalton antigen from *Corynebacterium pseudotuberculosis*. *Infect Immun* 1995;63:206–11.
- Wu Z, Zhang W, Lu C. Comparative proteome analysis of secreted proteins of *Streptococcus suis* serotype 9 isolates from diseased and healthy pigs. *Microb Pathog* 2008;45:159–66.
- Pacheco LG, Slade SE, Seyffert N, Santos AR, Castro TL, Silva WM, et al. A combined approach for comparative exoproteome analysis of *Corynebacterium pseudotuberculosis*. *BMC Microbiol* 2011;11:12.
- Moura-Costa LF, Paule BJA, Freire SM, Nascimento I, Schaer R, Regis LF, et al. Meio sintético químico definido para o cultivo de *Corynebacterium pseudotuberculosis*. *Rev Bras Saúde Prod* 2002;3:1–9.
- Paule BJ, Meyer R, Moura-Costa LF, Bahia RC, Carminati R, Regis LF, et al. Three-phase partitioning as an efficient method for extraction/concentration of immunoreactive excreted-secreted proteins of *Corynebacterium pseudotuberculosis*. *Protein Expr Purif* 2004;34:311–6.
- Simpson RJ. Proteins and proteomics. New York: Cold Spring Harbor Laboratory Press; 2003.
- Havlis J, Thomas H, Sebela M, Shevchenko A. Fast-response proteomics by accelerated in-gel digestion of proteins. *Analyti Chemist* 2003;75:1300–6.
- Barinov A, Loux V, Hammani A, Nicolas P, Langella P, Maquin E, et al. Prediction of surface exposed proteins in *Streptococcus pyogenes*, with a potential application to other gram-positive bacteria. *Proteomics* 2009;9:61–73.
- Bendtsen JD, Kierner L, Fausboll A, Brunak S. Non-classical protein secretion in bacteria. *BMC Microbiol* 2005;5:58.
- Bendtsen JD, Nielsen H, Widdick D, Palmer T, Brunak S. Prediction of twinarginine signal peptides. *BMC Bioinformatics* 2005;6:167.
- Bessette PH, Cotto JJ, Gilbert HF, Georgiou G. *In vivo* and *in vitro* function of the *Escherichia coli* periplasmic cysteine oxidoreductase DsbG. *J Biol Chem* 1999;274:7784–92.
- Hodgson AL, Krywult J, Corner LA, Rothel JS, Radford AJ. Rational attenuation of *Corynebacterium pseudotuberculosis*: potential cheesy gland vaccine and live delivery vehicle. *Infect Immun* 1992;60:2900–5.
- Hirose I, Sano K, Shioda I, Kumano M, Nakamura K, Yamane K. Proteome analysis of *Bacillus subtilis* extracellular proteins: a two-dimensional protein electrophoretic study. *Mycrobioiology* 2000;146:65–75.
- Lenz LL, Mohammadi S, Geissler A, Portnoy DA. SecA2-dependent secretion of autolytic enzymes promotes *Listeria monocytogenes* pathogenesis. *Proc Natl Acad Sci U S A* 2003;14:12432–7.
- Braunstein M, Espinosa BJ, Chan J, Belisle JT, Jacobs Jr WR. SecA2 functions in the secretion of superoxide dismutase A and in the virulence of *Mycobacterium tuberculosis*. *Mol Microbiol* 2003;48:453–64.
- Ruiz JC, D'Afonseca V, Silva A, Ali A, Pinto AC, Santos AR, et al. Evidence for reductive genome evolution and lateral acquisition of virulence functions in two *Corynebacterium pseudotuberculosis* strains. *Plos One* 2011;6:e18551.
- Craig EA, Cambill BD, Nelson RJ. Heat shock proteins: molecular chaperones of protein biogenesis. *Microbiol Rev* 1993;57:402–14.
- Aoki H, Dekany K, Adams SL, Ganoza MC. The gene encoding the elongation factor P protein is essential for viability and is required for protein synthesis. *J Biol Chem* 1997;272:32254–9.
- Navarre WW, Zou SB, Roy H, Xie JL, Savchenko A, Singer A, et al. PoxA, YjeK and elongation factor P coordinately modulate virulence and drug resistance in *Salmonella enterica*. *Mol Cell* 2010;30:209–21.
- Pancholi V, Fischetti VA. Alpha-enolase, a novel strong plasmin (ogen) binding protein on the surface of pathogenic streptococci. *J Biol Chem* 1998;273:14503–15.
- Chitlari T, Gat O, Grosfeld H, Inbar I, Gozlan Y, Shafferman A. Identification of in vivo-expressed immunogenic proteins by serological proteome analysis of the *Bacillus anthracis* secretome. *Infect Immun* 2007;6:2841–52.
- Agarwal S, Kulshreshtha P, Bambah MD, Bhatnagar R. α -Enolase binds to human plasminogen on the surface of *Bacillus anthracis*. *Biochim Biophys Acta* 2008;1784:986–94.
- Madureira P, Baptista M, Vieira M, Magalhães V, Camelo A, Oliveira L, et al. *Streptococcus agalactiae* GAPDH is a virulence-associated immunomodulatory protein. *J Immunol* 2007;178:1379–87.
- Davidson AL, Dassa E, Orelle C, Chen J. Structure, function, and evolution of bacterial ATP-binding cassette systems. *Microbiol Mol Biol Rev* 2008;72:317–64.
- Henderson DP, Payne SM. *Vibrio cholerae* iron transport systems: roles of heme and siderophore iron transport in virulence and identification of a gene associated with multiple iron transport systems. *Infect Immun* 1994;62:5120–5.
- Hewett-Emmett D, Tashian RE. Functional diversity, conservation, and convergence in the evolution of the alpha-, beta-, and gamma-carbonic anhydrase gene families. *Mol Phylogenet Evol* 1996;5:50–77.

- [31] Burghout P, Cron LE, Gradstedt H, Quintero B, Simonetti E, Bijlsma JJ, et al. Carbonic anhydrase is essential for *Streptococcus pneumoniae* growth in environmental ambient air. *J Bacteriol* 2010;192:4054–62.
- [32] Poyart C, Berche P, Trieu-Cuot P. Characterization of superoxide dismutase genes from gram-positive bacteria by polymerase chain reaction using degenerate primers. *FEMS Microbiol Lett* 1995;131:41–5.
- [33] Sanders JW, Leenhouwers KJ, Haandrikman AJ, Venema G, Kok J. Stress response in *Lactococcus lactis*: cloning, expression analysis and mutation of the lactococcal superoxide dismutase gene. *J Bacteriol* 1995;177:5254–60.
- [34] Peppoloni S, Posteraro B, Colombari B, Manca L, Hartke A, Giard JC, et al. Role of the (Mn)superoxide dismutase of *Enterococcus faecalis* in the in vitro interaction with microglia. *Microbiology* 2011;157:1816–22.

4.2.1 Supplementary file

Additional file 1: Table S1: List of the extracellular proteins common to 1002 and C231 *C. pseudotuberculosis* strains.

Spot	Databank identified protein	ID (NCBI) ^P of strains 1002	ID (NCBI) ^P of strains C231	MW(kDa) /p.I	Sequence of peptide identified	Mascot Score	Molecular function	Predicted localization
1	Hypothetical protein	ADL21925	ADL11512	14.54/4.88	R.EVGPEGNSYIHSYFYK.F K.GEPFSPTGETELGTQLTLPSGR.V R.EVGPEGNSYIHSYGYKFYGTQK.S	334	Unknown	S
2,3	Hypothetical protein	ADL21714	ADL11301	40.90/5.05	R.LSDTTTEMQWSVNNR.A K.TANLLGVCTVGYVDTENNR.V R.NPLNLREPLPYHDFDR.L	190	Catalytic activity	S
4,28	Cytochrome c oxidase subunit 2	ADL21302	ADL10895	40.33/6.03	K.VTVDDVTAYQWNWK.F K.SIGEEPYATTTHPFNSER.A	155	Cytochrom e-c oxidase activity	PSE
5	Hypothetical protein	ADL20097	ADL09691	51.41/5.43	R.ISEGLTVTMLDDLFGGR.G K.DGKEFAIIFGDSFTGER.L K.GLDKFFNITPKPADAQPTPR.A	241	Unknown	S [#]
6,29	Trypsin-like serine protease	ADL20653	ADL10245	25.72/6.49	R.AVEQIPHPTADIALIK.L R.HAVLIEQWISQGILR.Q	167	Peptidase activity	S
7,26	L,D-transpeptidase catalytic domain, region YkuD	ADL20288	ADL09881	26.80/9.07	K.QSVDNAVNFAFPGLIWER.T R.SWLQNNGQVSYGAVPISSGR.V R.TAPPVVPPAPAPAPVPTPPAFDTGSCPAFAR.A	273	Peptidase activity	S [#]
9	Hypothetical protein	ADL09626	ADL09626	24.30/9.24	K.VAGWNATSQADR.V K.AITLDTTLEYTYTVGVR.A K.IHSQGGYTEFSELTEFVPSVGR.L	228	Unknown	S
10	Hypothetical protein	ADL21703	ADL11290	87.79/5.09	K.FLTPLFGESFESVK.K K.FLTPLFGESFESVKK.V	138	Unknown	S
11	Resuscitation-promoting factor	ADL20487	ADL10080	21.52/6.07	K.GFGGGQQYAPTADK.A K.GFGGGQQYAPTADKATR.E K.VLASQGWGAWPSCSAK.L	218	Unknown	S

12	Lysozyme M1	ADL19973	ADL09563	40.28/5.58	K.TPQELVNWTR.D K.FASINLPELADLGK.N K.VGSYHYARPGADAR.Q R.ADELNIDANQVAQVLR.S K.ATEGLWTNDFYASDITQAAAQGLK.V R.HYANVISHTPNHSLPPVLDEVAEGK.T	491	Hydrolase activity	S [#]
13,16	Surface layer protein A	ADL20140	ADL09734	38.67/5.90	R.LQSLNIPADFNLR.N R.NTGTHSWSYWQDDL.R.A R.LQSLNIPADFNLR.N R.NTGTHSWSYWQDDL.R.A K.ASSPDRPTVYLLNGGDGGEGR.A R.GTEVYVSNASGVAGGHDILANPR.F K.TPAQISNGTALADVHFGATPDISPVWR.E	496	Transferase activity	S
14,15, 19,23	Trehalose corynomycolyl transferase C	ADL21812	ADL11400	70.34/5.61	R.GNIYWSPER.G R.TFPSVWALDGLR.A K.LKDNVVAFAQFER.G R.AYWSPATGHALGGR.V K.NQGTYAGIGLEVISR.M R.AVVGLSMGGTAAVNLAER.R K.SAAPGNPIQVQVLLAR.D K.TYVSAGSGRDDYQQPGSVAK.N K.FGSFSGYLDTTSIGMTAIR.A K.GGQVGTCVNNEDIAGGKAEDFVDGR.A	800	Transferase activity, transferring acyl groups other than	S [#]
17	Cell-wall peptidase NIpC/P60 protein	ADL21293	ADL10887	36.63/5.62	R.GAVIDPLTNAVSAENPQNAIDR.A	101	Hydrolase activity	S
18	Invasion-associated protein p60	ADL10547	ADL10547	63.17/5.59	K.ALVDYHDAQSSAQQAR.D K.ATAQQAIADDSSAKLEDNR.K R.AYIGTPYAWGGGNASGPTLGIR.D	217	Hydrolase activity	S
20,61	Corynomycolyl transferase	ADL21610	ADL11196	41.80/7.05	K.GGVHDWPLFNR.Q K.AAHVAQSIGFPGWRL K.GVFGISGYATQEPVGR.I	123	Transferase activity, transferring acyl groups other than	S ^{\$}
21	GroEL chaperonin	ADL21673	ADL11255	57.12/4.72	K.SWGAPITNDGVSIAR.E	134	Folding	C

					R.KVVVTKDETTIVEGAGSPEQIEGR.V			protein
22	Trehalose corynomycolyl transferase B	ADL21814	ADL11402	36.67/6.90	R.GGNAALYLLDGAR.A R.RIELDPLFNMR.G R.RIELDPLFNMR.G K.WETFLTQELPAYLEAHFGVAR.N R.DWLRPDATGTCEWDAANYWVQR.C	245	Transferase activity, transferring acyl groups other than	S
24	Hypothetical protein	ADL20770	ADL10365	30.07/5.19	K.SLYSLTVTTR.E K.LVDPYTGNTVDFVR.G K.GKLVDPTYTGNTVDFVR.G R.NFANDPINLIATSLEANR.M R.DQFGQAWSDDVEVEGGHNGCDTR.N	466	Unknown	S
25	Secreted hydrolase	ADL20134	ADL09728	29.04/8.83	R.IQIVGYPTIVTGSR.I R.VVITHGFNDTYFNGGESEGATRA.	91	Hydrolase activity	S
27	Resuscitation-promoting factor RpfB	ADL20574	ADL10163	40.31/5.06	K.VQASQGWGAWPACTSK.L K.AGVTVGDKDIVYPGLTEK.I K.TVFTQIAATVKDVLAER.G	298	Hydrolase activity	S
30	Chaperone protein DnaK	ADL21757	ADL11343	65.61/4.68	K.LLGSFELGGIAPAR.G R.DAESYLGDEVTDAVITVPAYFSDAQR.Q	118	ATP binding	C
31	Sialidase precursor	ADL20287	ADL09880	74.86/5.05	R.VLLYSAPIDTR.I R.SNGWVMASCDDGR.S K.SAAQDAIAAAEANAR.V R.IPAIATAVDGTLVAFDNR.Y K.AGGTDNTENKGFWQELLR.I	415	Hydrolase activity	S
32	Hypothetical protein	ADL19922	ADL09511	19.86/4.30	K.VSVSASPDAKPGDTYTVK.V K.VVDLDGKVTVWAEAPFTVGE.-	145	Calcium ion binding	S
33	Hypothetical protein	ADL21702	ADL11289	10.89/5.16	K.TIEQPGSNWINWFYETSK.H	90	Unknown	S
35	Elongation factor P	ADL21021	ADL10611	20.57/5.24	K.NYEQVELAPHILGDAAR.F	108	Translation elongation factor activity	S
36	Serine protease	ADL20555	ADL10144	48.98/5.29	K.QIGINSVIASLSQR.Q K.ATQPMIGIQLVSNAR.V	93	Peptidase	S

					R.QSQSGAQAGSIGLGFIPSNFAR.R			activity
37	Secreted hydrolase	ADL20429	ADL10025	31.47/9.59	R.SVSLQIDQAAAQR.T R.RSVSLQIDQAAAQR.T	108	Hydrolase activity	S
38	Uncharacterized metalloprotease	ADL20536	ADL10125	24.83/7.23	K.IVVHTPAMGTLTSPYGM.R.W	64	Metalloendopeptidase activity	PSE
55	Hypothetical protein	ADL20466	ADL10062	41.34/8.52	K.AFEPIIDGPNYHWR.T R.VAGSWFNSPDVPAESLAAEKR.G	99	Hydrolase activity	S [#]

E = extracytoplasmic; S = secreted; PSE = potentially surface exposed; C = cytoplasmic; M = membrane.

(#) Predicted Tat-associated signal peptide.

(\\$) Predicted lipoprotein

(P) Accession numbers in Entrez Protein (NCBI Genome Projects 40687 and 40875).

Theoretical molecular weights (Mr) and isoelectric points (pI), calculated by the Compute pI/MW tool (ExPASY tools).

Additional file 2: Table S2: List of the extracellular unique proteins 1002 *C. pseudotuberculosis* strain.

Spot	Databank identified protein	ID (NCBI) ^P 1002	MW (kDa) /p.I	Sequence of peptides identified	Masco t score	Molecular function	Subcellular localization
8	^K Hypothetical protein	ADL09626	24.30/9.24	K.VAGWNATSQADR.V K.AITLDTTLEYTYTVGVR.A K.IHSQGGYTEFSELTEFVPSVGR.L	228	Unknown	S
34	Hypothetical protein	ADL21704	8.97/5.82	K.NLATINDFIAR.G K.SVFHFFHQWLTTGSSAPATAPAEK.A	90	Unknown	S
39	Thiol peroxidase	ADL21047	15.85/4.56	R.FCAAEGLDNVIPASAFR.S R.IVFNIFPSVDTDVCAASVR.R	120	Peroxidase activity	C
40	Manganese superoxide dismutase	ADL21849	22.08/5.07	K.AVWNVFNWEDVAAR.Y	109	Oxidoreductase activity	C
41	Chaperonin	ADL20318	10.60/4.49	K.YNGEEYLLLNR.D K.YGGTELKYNEEYLLLNR.D	219	ATP binding	C
42	Carbonic anhydrase	ADL20477	26.17/6.24	K.KLPATHDWLTR.S R.IDAETLLSAKPGELFHRL.N R.AANAAQLENLMSHPFVSDR.V	155	Carbonate dehydratase activity	S
43	DsbG protein	ADL21555	26.67/5.43	K.WSNEDFANAAK.N R.TLLMEEQNSIYGK.W K.KIDLYEDYSCSHCAELGK.A	198	Unknown	C
44	Elongation factor Tu	ADL20240	44.14/4.83	K.STQTTVTGIEMFR.K R.HYAHVDAPGHADYIK.N K.LLDYTEAGDNCGLLR.G R.GITINISHVEYQTEKR.H R.KLLDYTEAGDNCGLLR.G R.GQVVVKPGAYTPHTEFEGSVYVLSK.D K.VLADAYPDLNEAFADIAIDKAPEEKER.G	466	Translation elongation factor activity	C
45	^K Surface layer protein A	ADL20140	38.67/5.90	R.LQSLNIPADFNLR.N R.NTGTHSWSYWQDDL.R.A K.FSYYTDWVSNAALGGK.Q K.ASSPDERPTVYLLNGGDGGEGR.A	526	Transferase activity	S

				R.GTEVYVSNASGVAGGHDILANPR.F K.TPAQISNGTALADVHFGATPDISPVWR.E			
46	^K Resuscitation-promoting factor RpfB	ADL20574	40.31/5.06	K.VQASQGWGAWPACTSK.L K.TVFTQIAAATVKDVLAER.G	197	Hydrolase activity	S
47	Phosphoglycerate kinase	ADL20990	44.11/4.61	R.SDFNVPPLNDAR.E K.RLPHYAGALVEK.E K.TLKDLIAEGVEGR.H K.SLLQEDQIANCQR.L R.ANGLNDGVLENVR.F K.AVESPERYVVVLGGAK.V	391	ATP binding	C
48	ABC-type transporter	ADL20391	46.01/4.80	K.SLENAAPRVSPFYPAISK.A K.ATVESATYNGTLYALPQNTNGQLLFR.N	175	Transporter activity	S\$
49	^K Putative cytochrome c oxidase subunit 2	ADL21302	40.33/6.03	K.VTVDTVTAYQWNWK.F K.FGYSDIAADLSPTGAEYK.G	216	Cytochrome-c oxidase activity	PSE
50	Glyceraldehyde-3-phosphate dehydrogenase (GPDAH)	ADL20991	36.37/5.35	R.VPVITGSATDLTFYASK.E R.LGKDVTDYDDESITVDGHR.I R.GADVEVVAINDLTDNHTLHLLK.Y	362	Oxidoreductase activity; binding	C
51	Enolase	ADL20605	45.17/4.68	K.AAAESAGLPLYR.Y K.VQIVGDDFFVTNPVR.L K.VNQIGTLTETFDAVDLAHR.N	271	Phosphopyruvate hydratase activity	S
52	^K L,D-transpeptidase catalytic domain, region YkuD	ADL20288	26.80/9.07	K.QSVDNAVNFAPGLIQER.T R.SWLQNNGQVSYGAVPISGR.V R.TAPPVPAPAPAPVPTPPAFDTGSCPAFAR.A	431	Peptidase activity	S#
53	Hypothetical protein	ADL20508	31.62/9.52	K.GRPIYVAIDDNPTR.A R.LGSFFWQHDWGSGNRI.	66	Unknown	S#
54	Secretory lipoase	ADL21667	44.17/5.03	R.EPIHNFLNTR.G R.LTLSISDDVFQR.A R.GPGPPRVALLAPGTQGAGDSCAPS.K.	116	Triglyceride lipase activity	S

E = extracytoplasmic; S = secreted; PSE = potentially surface exposed; C = cytoplasmic; M = membrane.

(#) Predicted Tat-associated signal peptide.

(\$) Predicted lipoprotein

(P) Accession numbers in Entrez Protein (NCBI Genome Projects 40687).

(K) Protein characterized as isoform.

Theoretical molecular weights (Mr) and isoelectric points (pI) calculated by the Compute pI/MW tool (ExPASY tools).

Additional file 3: Table S3: List of the extracellular unique proteins to C231 *C. pseudotuberculosis* strain

Spot	Databank identified protein	ID (NCBI) ^P C231	MW (kDa) /p.I	Sequence of peptide identified	Mascot Score	Molecular function	Predicted Localization
56	Phospholipase D precursor	ADL09524	34.09/8.91	K.TFGWTIATGQDAR.V R.DGEAVALSGPAQDVNLNDFAR.S K.IADYGYYNINQGFGNCYGTWNR.T	286	Sphingomyelin phosphodiesterase D activity	S
57	Serine proteinase precursor (CP40)	ADL11339	43.04/6.48	K.ESVTQVWNGFR.D K.GGTFAVYALDRDGR.T	65	Catalytic activity	S
58	Hypothetical protein	ADL10248	24.39/5.34	K.DFADTLPEPLR.N K.AKDFATLPEPLR.N K.EGETAFVFTALGTGK.L	169	Unknown	S ^{\$}
59	^K Putative secreted protein	ADL09691	51.31/5.35	K.HVDGAHLTPILNSVK.A R.ISEGGLTVTMLDDLFGR.G K.FFNITPKPADAQPTPR.A K.IQIVRPLNEGEKAEQLIK.Y	143	Unknown	S [#]
60	^K Corynomycolyl transferase	ADL11196	41.80/7.05	K.GGVHDWPLFNR.Q K.GVFGISGCYATQEPVGR.I	79	Transferase activity, transferring acyl groups other than	S ^{\$}

E = extracytoplasmic; S = secreted; PSE = potentially surface exposed; C = cytoplasmic; M = membrane.

(#) Predicted Tat-associated signal peptide.

(\\$) Predicted lipoprotein

(P) Accession numbers in Entrez Protein (NCBI Genome Projects 40875).

(K) Protein characterized as isoform.

Theoretical molecular weights (Mr) and isoelectric points (pI), calculated by the Compute pI/MW tool (ExPASY tools).

Additional file 4: Table S4: List of 104 extracellular proteins of *C. pseudotuberculosis* detected by both approaches (2-DE-MALDI-TOF/TOF and TPP-LC/MS^E)

Protein	Nomenclature update	ID (NCBI) ^P of the strains		<u>MW(kDa)</u> <u>P.I</u>	Prediting SurfG+	Molecular function	Reference
		<u>1002</u>	<u>C231</u>				
1 Putative secreted protein	Hypothetical protein	ADL21925	ADL11512	14.54/4.88	S	Unknown	This work and Pacheco et al., 2011
2 Putative secreted protein	Hypothetical protein	ADL21714	ADL11301	40.90/5.05	S	Catalytic activity	This work and Pacheco et al., 2011
3 Cytochrome c oxidase subunit 2		ADL21302	ADL10895	40.33/6.03	PSE	Cytochrome-c oxidase activity	This work and Pacheco et al., 2011
4 Trypsin-like serine protease	Serine protease	ADL20555	ADL10144	48.98/5.29	S	Peptidase activity	This work and Pacheco et al., 2011
5 Putative trypsin-like serine protease	Trypsin-like serine protease	ADL20653	ADL10245	25.72/6.49	S	Peptidase activity	This work and Pacheco et al., 2011
6 Putative secreted protein	L,D-transpeptidase catalytic domain, region YkuD	ADL20288	ADL09881	26.80/9.07	S [#]	Peptidase activity	This work and Pacheco et al., 2011
7 Hypothetical protein		ADL09626	ADL09626	24.30/9.24	S	Unknown	This work and Pacheco et al., 2011
8 Conserved hypothetical protein	Hypothetical protein	ADL19922	ADL09511	19.86/4.30	S	Calcium ion binding	This work and Pacheco et al., 2011
9 Resuscitation-promoting factor A	Resuscitation-promoting factor	ADL20487	ADL10080	21.52/6.07	S	Unknown	This work and Pacheco et al., 2011
10 Putative hydrolase	Lysozyme M1	ADL19973	ADL09563	40.28/5.58	S [#]	Hydrolase activity	This work and Pacheco et al.,

								2011
11	Surface layer protein A		ADL20140	ADL09734	38.67/5.90	S	Transferase activity	This work and Pacheco et al., 2011
12	NLP/P60 protein	Cell-wall peptidase NlpC/P60 protein	ADL21293	ADL10887	36.63/5.62	S	Hydrolase activity	This work and Pacheco et al., 2011
13	Putative protein secreted	Invasion-associated protein p60	ADL10547	ADL10547	63.17/5.59	S	Hydrolase activity	This work and Pacheco et al., 2011
14	Putative serine protease	Secreted hydrolase	ADL20429	ADL10025	31.47/9.59	S	Hydrolase activity	This work and Pacheco et al., 2011
15	Trehalose corynomycolyl transferase B		ADL21814	ADL11402	36.67/6.90	S	Transferase activity, transferring acyl groups other than	This work and Pacheco et al., 2011
16	Trehalose corynomycolyl transferase C		ADL21812	ADL11400	70.34/5.61	S [#]	Transferase activity, transferring acyl groups other than	This work and Pacheco et al., 2011
17	Putative secreted protein	Hypothetical protein	ADL20770	ADL10365	30.07/5.19	S	Unknown	This work and Pacheco et al., 2011
18	Putative secreted hydrolase	Secreted hydrolase	ADL20134	ADL09728	29.04/8.83	S	Hydrolase activity	This work and Pacheco et al., 2011
19	Resuscitation-promoting factor RpfB		ADL20574	ADL10163	40.31/5.06	S	Hydrolase activity	This work and Pacheco et al., 2011
20	Putative secreted metalloendopeptidase	Uncharacterized metalloprotease	ADL20536	ADL10125	24.83/7.23	PSE	Metalloendopeptidase activity	This work and Pacheco et al.,

								2011
21	Corynomycolyl transferase		ADL21610	ADL11196	41.80/7.05	S ^{\$}	Transferase activity, transferring acyl groups other than	This work and Pacheco et al., 2011
22	Putative twin-arginine translocation pathway signal protein	Hypothetical protein	ADL20508	ADL10099	31.65/9.52	S [#]	Unknown	This work and Pacheco et al., 2011
23	Putative trypsin-like serine protease	Hypothetical protein	ADL20466	ADL10062	41.00/ 8.53	S [#]	Hydrolase activity	This work and Pacheco et al., 2011
24	Putative exported lipoase	Secretory lipoase	ADL21667	ADL11248	44.04/ 5.03	E	Triglyceride lipase activity	This work and Pacheco et al., 2011
25	co-chaperonin GroES	Chaperonin	ADL20318	ADL09912	10.60/ 4.49	C	ATP binding	This work and Pacheco et al., 2011
26	Elongation factor Tu		ADL20240	ADL09833	44.00/ 4.86	C	Translation elongation factor activity	This work and Pacheco et al., 2011
27	Peroxiredoxin	Thiol peroxidase	ADL21047	ADL10638	15.70/4.56	C	Peroxidase activity	This work and Pacheco et al., 2011
28	Phosphoglycerate kinase		ADL20990	ADL10580	42.60/ 4.68	C	ATP binding	This work and Pacheco et al., 2011
29	Phospholipase D (PLD)		ADL19935	ADL09524	32.45/ 8.77	E	Sphingomyelin phosphodiesterase D activity	This work and Pacheco et al., 2011
30	Serine proteinase precursor (CP40)	Hypothetical protein	ADL21753	ADL11339	43.00/ 6.48	E	Catalytic activity	This work and Pacheco et al., 2011

31 Putative secreted protein	Hypothetical protein	ADL20097	ADL09691	51.41/5.43	S [#]	Unknown	This work and Pacheco et al., 2011
32 Putative secreted protein	Hypothetical protein	ADL20656	ADL10248	24.39/5.34	S ^{\$}	Unknown	This work and Pacheco et al., 2011
33 *Putative DsbG protein	*DsbG protein	ADL21555		26.67/5.43	C	Unknown	This work and Pacheco et al., 2011
34 GroEL chaperonin		ADL21673	ADL11255	57.12/4.72	C	Folding protein	This work
35 Hypothetical protein		ADL21702	ADL11289	10.89/5.16	S	Unknown	This work
36 Hypothetical protein		ADL21704	ADL11291	8.97/5.82		Unknown	This work
37 Elongation factor P		ADL21021	ADL10611	20.57/5.24	S	Translation elongation factor activity	This work
38 Hypothetical protein		ADL21703	ADL11290	87.79/5.09	S	Unknown	This work
39 Chaperone protein DnaK		ADL21757	ADL11343	65.61/4.68	C	ATP binding	This work
40 Manganese superoxide dismutase		ADL21849	ADL11437	22.08/5.07	C	Metal ion binding	This work
41 Carbonic anhydrase		ADL20477	ADL10071	26.17/6.24	S	Carbonate dehydratase activity	This work
42 ABC-type transporter		ADL20391	ADL09988	46.01/4.80	S ^{\$}	Transporter activity	This work
43 Glyceraldehyde-3-phosphate dehydrogenase (GPDAH)		ADL20991	ADL10581	36.37/5.35	C	Oxidoreductase activity; nucleotide binding	This work

44	Enolase		ADL20605	ADL10195	45.17/4.68	S	Phosphopyruvate hydratase activity Unknown	This work
45	Hypothetical protein		ADL20222	ADL09817	44.1 / 9.24	PSE		Pacheco et al., 2011
46	Putative exported esterase hydrolase	Poly(3-hydroxybutyrate) depolymerase	ADL20788	ADL10383	32.90/ 6.20	C	Hydrolase activity	Pacheco et al., 2011
47	Putative heme transport associated protein	Cell-surface hemin receptor	ADL20347	ADL09942	64.00/ 5.82	PSE	Receptor activity	Pacheco et al., 2011
48	Putative efflux system protein	Secretion protein HlyD	ADL21747	ADL11333	59.60/ 5.60	PSE	Protein transporter activity	Pacheco et al., 2011
49	Putative phosphatase	PAP2 superfamily protein	ADL09864	ADL09864	44.31/ 7.76	E	Catalytic activity	Pacheco et al., 2011
50	Putative surface-anchored membrane protein	Surface antigen	ADL20074	ADL09668	118.41/5.68	PSE [¶]	Protein binding	Pacheco et al., 2011
51	Putative sialidase precursor	Neuraminidase (sialidase)	ADL20287	ADL09880	75.00 / 5.05	E	Hydrolase activity	Pacheco et al., 2011
52	Putative peptide transport system secreted protein	Oligopeptide-binding protein oppA	ADL20650	ADL10241	57.30/ 4.88	PSE ^{\$}	Transporter activity	Pacheco et al., 2011
53	Putative membrane protein	Hypothetical protein	ADL21840	ADL11428	41.30/5.83	PSE	Unknown	Pacheco et al., 2011
54	Putative peptidoglycan recognition protein	Peptidoglycan recognition protein	ADL21828	ADL11416	70.00 / 5.00	S	N-acetylmuramoyl-L-alanine amidase activity	Pacheco et al., 2011

55	Secreted subtilisin-like peptidase	Peptidase, S8A (subtilisin) family protein	ADL21499	ADL11094	64.54/ 5.38	S	Hydrolase activity	Pacheco et al., 2011
56	Putative peptidyl prolyl cis trans isomerase A	Peptidyl-prolyl cis-trans isomerase A	ADL19928	ADL09517	19.30 / 4.82	S	Peptidyl-prolyl cis-trans isomerase activity	Pacheco et al., 2011
57	Hemin receptor precursor	Hemin-binding periplasmic protein hmuT	ADL20348	ADL09943	40.50 / 4.96	PSE ^{\$}	Iron ion transmembrane transporter activity	Pacheco et al., 2011
58	Putative membrane protein	Hypothetical protein	ADL21275	ADL10868	24.61/10.24	PSE	Unknown	Pacheco et al., 2011
59	Cell-surface hemin receptor	Hypothetical protein	ADL21841	ADL11429	71.00 / 5.47	PSE	Unknown	Pacheco et al., 2011
60	Conserved hypothetical protein	Lipoprotein LpqE	ADL21628	ADL11211	19.50 / 5.30	S [#]	Unknown	Pacheco et al., 2011
61	*PAP2 phosphatase	*PAP2 superfamily protein		ADL09864	44.21 / 7.90	E	Unknown	Pacheco et al., 2011
62	Putative cell-surface hemin receptor	Cell-surface hemin receptor	ADL21338	ADL10936	84.15 / 5.40	PSE	Unknown	Pacheco et al., 2011
63	Putative secreted protein	Trypsin	ADL20455	ADL10051	22.00 / 6.59	E	Catalytic activity	Pacheco et al., 2011
64	Putative amino deoxychorismate lyase	Amino deoxychorismate lyase	ADL21028	ADL10619	41.10 / 5.12	S ^{\$}	Lyase activity	Pacheco et al., 2011

65 Putative secreted protein	Hypothetical protein	ADL21239	ADL10832	23.07 / 4.59	PSE ^{\$}	Unknown	Pacheco et al., 2011
66 ABC superfamily ATP binding cassette transporter	ABC-type metal ion transport system, periplasmic component/surface adhesin	ADL20218	ADL09813	57.80 / 5.15	PSE ^{\$}	Metal ion binding	Pacheco et al., 2011
67 Putative membrane protein	Hypothetical protein	ADL20351	ADL09946	32.54 / 8.58	PSE	Unknown	Pacheco et al., 2011
68 Phosphoglyceromutase		ADL20161	ADL09755	27.51 / 5.25	C	2,3-Bisphosphoglycerate-dependent phosphoglycerate	Pacheco et al., 2011
69 Putative HtaA family protein	Uncharacterized protein htaC	ADL21337	ADL10935	32.00 / 8.55	PSE	DNA-directed RNA polymerase activity	Pacheco et al., 2011
70 Elongation factor Ts		ADL21187	ADL10779	29.40 / 5.06	C	Translation elongation factor activity	Pacheco et al., 2011
71 Transcription elongation factor GreA		ADL20612	ADL10202	19.01 / 4.83	C [%]	Transcription elongation regulator activity	Pacheco et al., 2011
72 Conserved hypothetical protein	Hypothetical protein	ADL20222	ADL09817	15.35 / 8.72	C [%]	Unknown	Pacheco et al., 2011
73 Conserved hypothetical protein	Hypothetical protein	ADL21049	ADL10640	11.60 / 9.30	M	Unknown	Pacheco et al., 2011

74	Triosephosphate isomerase		ADL20989	ADL10579	27.35 / 4.99	C	Triose-phosphate isomerase activity	Pacheco et al., 2011
75	Conserved hypothetical protein	Hypothetical protein	ADL21342	ADL10940	7.26 / 4.62	C%	Unknown	Pacheco et al., 2011
76	Putative carbohydrate carrier protein	Phosphocarrier protein HPr	ADL21114	ADL10706	9.1 / 4.06	C	Kinase activity	Pacheco et al., 2011
77	FHA domain protein (OdhI)	Oxoglutarate dehydrogenase inhibitor	ADL20881	ADL10473	15.34 / 4.80	C	Unknown	Pacheco et al., 2011
78	Putative methylmalonyl CoA epimerase	Methylmalonyl-CoA epimerase	ADL20739	ADL10334	16.70 / 4.89	C	Lyase activity	Pacheco et al., 2011
79	Putative lipoprotein	Hypothetical protein	ADL19972	ADL09562	48.50 / 4.71	C	Unknown	Pacheco et al., 2011
80	Hypothetical protein	Cell wall channel	AEK49210	ADL11253	6.64 / 4.93	C	Unknown	Pacheco et al., 2011
81	NLP/P60 family secreted protein	Hypothetical protein	ADL21294	ADL10888	21.41 / 7.00	E	Unknown	Pacheco et al., 2011
82	Substrate-binding protein	Hypothetical protein	ADL21914	ADL11501	123.00/ 5.04	PSE&	Unknown	Pacheco et al., 2011
83	Putative penicillin-binding protein	Penicillin-binding protein	ADL21890	ADL11477	77.16 / 8.67	PSE	Peptidoglycan Glycosyltransferase activity	Pacheco et al., 2011
84	Putative surface-anchored protein	Hypothetical protein	ADL21911	ADL11498	90.60 / 5.10	PSE	Unknown	Pacheco et al., 2011
85	Hypothetical protein		ADL20404	ADL10001	27.21 / 4.77	E	Unknown	Pacheco et al., 2011
86	Putative secreted protein	Hypothetical protein	ADL09871	ADL20404	16.80 / 8.30	E	Unknown	Pacheco et al., 2011
87	*Conserved hypothetical exported protein	*Hypothetical protein		ADL10384	49.61 / 8.69	E	Hydrolase activity	Pacheco et al., 2011
88	Hypothetical protein		ADL11213	ADL21630	33.55 / 4.48	E	Unknown	Pacheco et al.,

								2011
89	Putative secreted protein	Hypothetical protein	ADL21537	AEK49277	23.4 / 9.36	E	Unknown	Pacheco et al., 2011
90	Putative secreted protein	Protein yceI	ADL20898	ADL10489	24.73 / 5.07	E	Unknown	Pacheco et al., 2011
91	Secreted penicillin-binding protein	Penicillin-binding protein A	ADL09532	ADL19443	50.75 / 5.67	E	Carboxypeptidase activity	Pacheco et al., 2011
92	Putative surface-anchored protein	Hypothetical protein (fimbrial subunit)	ADL11344	ADL21758	27.85 / 9.24	E	Unknown	Pacheco et al., 2011
93	Putative penicillin-binding secreted protein	Penicillin binding protein transpeptidase	ADL09697	ADL20103	83.00 / 5.38	E	Penicillin binding	Pacheco et al., 2011
94	Putative membrane anchored protein	Membrane protein	ADL11338	ADL21752	21.15 / 9.59	E	Unknown	Pacheco et al., 2011
95	Hypothetical protein		ADL11326	ADL21739	34.65 / 5.85	E	Unknown	Pacheco et al., 2011
96	Transcriptional regulator	Transcriptional regulator lytR	ADL09990	ADL20393	55.05 / 4.97	PSE	Unknown	Pacheco et al., 2011
97	Putative serine threonine protein kinase	Serine/threonine protein kinase	ADL10880	ADL21286	80.10 / 4.80	PSE	ATP binding	Pacheco et al., 2011
98	Putative extracellular solute-binding protein	Oligopeptide-binding protein oppA	ADL09852	ADL20259	61.54 / 5.31	PSE	Transporter activity	Pacheco et al., 2011
99	Maltotriose-binding protein		ADL09872	ADL20278	43.93 / 5.07	PSE ^{\$}	Transporter activity	Pacheco et al., 2011
10	Putative zinc metallopeptidase	Zinc metallopeptidase	ADL10626	ADL26425	35.38 / 5.29	PSE	Peptidase activity	Pacheco et al., 2011
10	Putative iron transport system binding (secreted) protein	Iron ABC transporter substrate-binding protein	ADL10460	ADL20866	30.05 / 5.16	PSE ^{\$}	Iron ion transmembrane transporter activity	Pacheco et al., 2011
10	Glycerophosphoryl		ADL11410	ADL21822	40.28 / 5.13	PSE ^{\$}	Phosphoric	Pacheco et al.,

diesterphosphodiesterase							diester hydrolase activity	2011
10 Putative metal-binding like protein	Lipoprotein		ADL10663	ADL21072	20.81 / 5.48	PSE ^{\$}	Unknown	Pacheco et al., 2011
10 Iron siderophore binding protein – FagD	Iron siderophore binding protein		ADL09528	ADL19939	37.47 / 5.05	PSE ^{\$}	Unknown	Pacheco et al., 2011

E = extracytoplasmic; S = secreted; PSE = potentially surface exposed; C = cytoplasmic; M = membrane.

(#)Predicted Tat-associated signal peptide.

(\$)Predicted lipoprotein.

(&) Predicted LPXTG cell wall-anchoring motif.

(%) SecretomeP prediction of non-classical secretion.

(*) ORF detected only of the genome of one strain.

(P) Accession numbers in Entrez Protein (NCBI Genome Projects 40875).

Theoretical molecular weights (Mr) and isoelectric points (pI), calculated by the Compute pI/MW tool (ExPASY tools).

Cellular function has been established in accordance with the program Blast2Go.

4.3 Artigo 2: Differential Exoproteome analysis of two *Corynebacterium pseudotuberculosis* biovar *ovis* strains isolated from goat (1002) and sheep (C231).

Curr Microbiol. v. 67, p. 460-465. 2013. doi: 10.1007/s00284-013-0388-4.

Silva, W.M., Seyffert, N., Ciprandi, A., Santos, A.V., Castro, T.L., Pacheco, L.G., Barh, D., Le Loir, Y., Pimenta, A.M., Miyoshi, A., Silva, A., Azevedo, V.

Differential Exoproteome Analysis of Two *Corynebacterium pseudotuberculosis* Biovar *Ovis* Strains Isolated from Goat (1002) and Sheep (C231)

Wanderson M. Silva · Núbia Seyffert · Alessandra Ciprandi · Agenor V. Santos · Thiago L. P. Castro · Luis G. C. Pacheco · Debmalya Barh · Yves Le Loir · Adriano M. C. Pimenta · Anderson Miyoshi · Artur Silva · Vasco Azevedo

Received: 19 February 2013 / Accepted: 17 April 2013
© Springer Science+Business Media New York 2013

Abstract *Corynebacterium pseudotuberculosis* is the etiologic agent of caseous lymphadenitis a chronic infectious disease affecting small ruminants. The 2D-DIGE technique was used to compare the exoproteomes of two *C. pseudotuberculosis* biovar *ovis* strains isolated from goat (strain 1002) and sheep (strain C231). Seventeen proteins differentially produced were identified here. Nine proteins appeared over-produced in the exoproteome of 1002 goat strain and 8 in that of C231 sheep strain. These proteins were related to various biological functions, such as the cell envelope, respiratory metabolism and proteolysis. This proteomic analysis revealed strain-specific exoproteins although each of the corresponding genes was found in both strain genomes. Such differential expression pattern may reflect inter-strain differences in adaptation to a specific host, in pathogenicity and or in antigenicity of this pathogenic bacterium.

Electronic supplementary material The online version of this article (doi:10.1007/s00284-013-0388-4) contains supplementary material, which is available to authorized users.

W. M. Silva · N. Seyffert · T. L. P. Castro · A. Miyoshi · V. Azevedo (✉)
Departamento de Biologia Geral, Instituto de Ciências Biológicas, Universidade Federal de Minas Gerais, Av. Antonio Carlos, 6627, Pampulha, CP 486, Belo Horizonte, MG CEP 31.270-901, Brazil
e-mail: vasco@icb.ufmg.br

A. Ciprandi · A. V. Santos · A. Silva
Instituto de Ciências Biológicas, Universidade Federal do Pará, Rua Augusto Corrêa, 01, Guamá, Belém, PA, Brazil

L. G. C. Pacheco
Instituto de Ciências da Saúde, Universidade Federal da Bahia, Av. Reitor Miguel Calmon, s/n, Vale do Canela, Salvador, BA CEP 40110100, Brazil

Introduction

Corynebacterium pseudotuberculosis is a Gram-positive, facultative intracellular pathogen, and the etiologic agent of caseous lymphadenitis (CLA), a chronic infectious disease affecting small ruminants [9]. Despite a huge impact of CLA in small ruminant herds, *C. pseudotuberculosis* is still poorly documented and our understanding of its pathogenesis is partial. A few virulence factors of *C. pseudotuberculosis* were identified in previous works, including phospholipase D [15], toxic cell wall lipids [12], iron transporters belonging to the ABC proteins family [5] and a serine protease [32].

Comparative proteomics has been used to identify virulence factors and to gain further information about the physiology of various pathogens such as *Listeria monocytogenes* [29], *Staphylococcus aureus* [17] or *Clostridium perfringens* [27]. These studies took account of secreted/extracellular proteins, a protein fraction which indeed contains factors involved in adhesion and invasion of the

D. Barh
Centre for Genomics and Applied Gene Technology, Institute of Integrative Omics and Applied Biotechnology (IIOAB), Purba Medinipur, WB 721172, India

Y. Le Loir
INRA, UMR1253 STLO, 35042 Rennes, France

Y. Le Loir
Agrocampus Ouest, UMR1253 STLO, 35042 Rennes, France

A. M. C. Pimenta
Departamento de Bioquímica e Imunologia, Instituto de Ciências Biológicas, Universidade Federal de Minas Gerais, Av. Antonio Carlos, 6627, Pampulha, CP 486, Belo Horizonte, MG CEP 31.270-901, Brazil

host cell, and in survival, persistence and intracellular proliferation [29].

We recently reported the use of a gel-free proteomic approach to compare the exoproteomes of two *C. pseudotuberculosis* strains 1002 and C231 that both belong to the biovar *ovis*, but were isolated from different hosts: goat and sheep, respectively. This study enabled detection of qualitative and quantitative changes between the exoproteome of the two strains. Proteins identified were associated with bacterial physiology and included putative virulence factors [22]. However, such approach only gives a partial view of the protein sample contents. More sensitive techniques, such as the two-dimensional differential in-gel electrophoresis (2D-DIGE), have been described and allow to achieve a more complete analysis of proteomes. This multiplex technique allows analyzing differences between protein samples resolved on the same gel, in the presence of an internal standard, enabling more accurate results. 2D-DIGE demonstrated advantages over the conventional 2-DE in quantitative studies [1]. Here, 2D-DIGE was used to identify quantitative changes in the exoproteomes of *C. pseudotuberculosis* 1002 and C231.

Materials and Methods

Bacterial Strains and Culture Conditions

Corynebacterium pseudotuberculosis biovar *ovis* strain 1002, isolated from a caprine host in Brazil, and *C. pseudotuberculosis* biovar *ovis* strain C231, isolated from an ovine host in Australia, were maintained in brain-heart-infusion broth (BHI—HiMedia Laboratories Pvt. Ltd., India) at 37 °C. For proteomic analysis, both strains were cultivated in chemically defined medium (CDM) [(Na₂HPO₄·7H₂O (12.93 g/L), KH₂PO₄ (2.55 g/L), NH₄Cl (1 g/L), MgSO₄·7H₂O (0.20 g/L), CaCl₂ (0.02 g/L) and 0.05 % (v/v) Tween 80]; 4 % (v/v) MEM Vitamins Solution 100× (Invitrogen, Gaithersburg, MD, USA); 1 % (v/v) MEM Amino Acids Solution 50× (Invitrogen); 1 % (v/v) MEM Non-Essential Amino Acids Solution 100× (Invitrogen); and 1.2 % (w/v) filter-sterilized glucose) [19].

Three-Phase Partitioning

The three-phase partitioning protocol (TPP) was used to extract extracellular proteins [24]. Briefly, each strain was cultivated in triplicate on CDM and after reaching late exponential growth (DO_{600nm} = 1.3). Bacterial cells were pelleted by centrifugation for 20 min at 2,700×g, and culture supernatants were filtered using 0.22 μm filters. Ammonium sulfate 6 g/L was added to supernatant samples, and the pH was set to 4.0. N-butanol 20 mL/L was

then added to each 20 mL of sample, left 1 h at room temperature and centrifuged for 10 min at 1,350×g at 4 °C. The interfacial precipitate was re-suspended in 1 mL Tris-HCl (20 mM, pH 7.2) + 10 μL Protease Inhibitor Mix (GE Healthcare, Piscataway, NJ, USA).

2D-DIGE

For 2D-DIGE experiment, the protein samples (50 μg) of each strain were labeled separately with 400 pmol of either Cy3 or Cy5 CyDye DIGE Fluor minimal dyes (GE Healthcare, Piscataway, NJ, USA), and an internal standard was prepared using 25 μg of each bacterial protein extract (*Cp1002* + *CpC231*) and labeled with 400 pmol of Cy2 (GE Healthcare). The labeled samples were then mixed and combined with a sample buffer containing 7 M urea, 2 M thiourea, 4 % CHAPS, 0.2 % DTT and 0.002 % bromophenol blue and applied to 18 cm pH 3–10 NL strips (GE Healthcare). Isoelectric focusing was performed using the IPGphor 2 (GE Healthcare) for a total of 60,000 Vh. The strips were then brought to equilibrium for 15 min in 10 mL of equilibration buffer I (Tris-HCl 50 mM pH 8.8, urea 6 M, glycerol 30 %, SDS 2 %, bromophenol blue 0.002 %, 100 mg dithiothreitol) followed by 15 min in 10 mL of equilibration buffer II (Tris-HCl 50 mM pH 8.8, urea 6 M, glycerol 30 %, SDS 2 %, bromophenol blue 0.002 %, iodoacetamide 250 mg). After equilibration, proteins were separated in 12 % acrylamide/bis-acrylamide gels with an Ettan DaltSix II system (GE Healthcare), and the gels were then scanned between low fluorescence glass plates at a 50 nm resolution. The three fluorophores were imaged at excitation wavelengths of Cy3/580 nm, Cy5/670 nm and Cy2/520 nm, and gel images were cropped and analyzed using the Image Master 2D Platinum 7.0 DIGE Software (GE Healthcare). Spots with at least a 2.0-fold volume ratio change and ANOVA *t* test *P* value less than 0.01 were selected for identification.

In-Gel Trypsin Digestion, Mass Spectrometry and Protein Identification

Protein spots were excised from the gels using an Ettan Spot Picker (GE Healthcare) and in-gel digestion was carried out using trypsin enzyme (Promega, Sequencing Grade Modified Trypsin, Madison, WI, USA). The peptides were then concentrated to a volume of 10 μL using a speed vacuum, desalinated and concentrated using ZIP-TIP C18 tips (Eppendorf, Hamburg, Germany). The samples were subsequently analyzed by MS and MS/MS modes, using a MALDI-TOF/TOF mass spectrometer Autoflex III™ (Bruker Daltonics, Billerica USA). The equipment was controlled in a positive/reflector way using the FlexControlTM software (Bruker Daltonics), and calibration

was performed using standard peptide samples (angiotensin II, angiotensin I, substance P, bombesin, ACTH clip 1–17, ACTH clip 18–39, somatostatin 28, bradykinin Fragment 1–7, renin Substrate tetradecapeptide porcine) (Bruker Daltonics). The peptides were added to the alpha-cyano-4-hydroxycinnamic acid matrix, applied on an AnchorChipTM 600 plate (Bruker Daltonics) and analyzed by Autoflex III. The search parameters were as follows: peptide mass fingerprint; enzyme; trypsin; fixed modification, carbamido methylation (Cys); variable modifications, oxidation (Met); mass values, monoisotopic; maximum missed cleavages, 1; and peptide mass tolerance of 0.05 % Da (50 ppm). The results obtained by MS/MS were used to identify proteins utilizing the MASCOT® (<http://www.matrixscience.com>) program and compared to NCBI databases.

Bioinformatics Analysis

The Blast2GO program was used to classify the protein's functionality [8]. To predict the sub-cellular localization of proteins, we used the following programs: SurfG+v1.0 [2], SecretomeP v2.0 [3] and TatP v1.0 [4].

Results and Discussion

2D-DIGE and Mass Spectrometry

In this study, the 2D-DIGE was used for a quantitative analysis and a comparison of the exoproteomes of *C. pseudotuberculosis* 1002 and C231, isolated from of goat and sheep, respectively (Fig. 1). Using this technique, 18 spots were found differentially produced, selected and subjected to mass spectrometry analysis. Nine out of these 18 proteins were specifically found over-produced in strain 1002 supernatants (Supplementary file 1 and Fig. 2) and 8 were over-produced in strain C231 supernatants (Supplementary file 2 and Fig. 2). Of note, the genes corresponding to each of these proteins are found in both 1002 and C231 genomes suggesting that the differences observed at the proteome level are due to strain-specific abilities in expressing these particular genes, rather than differences in gene content.

Interestingly, various selected spots actually contained the same unique protein. For example, trehalose corynomycolyl transferase C was found at the expected molecular mass in C231 (spot 53; Supplementary file 2) and at a lower observed mass in 1002 (spot 87; Supplementary file 1), suggesting a proteolytic cleavage occurred in strain 1002. Cytochrome c oxidase sub-unit 2 was found over-produced in C231 in two different spots, at the expected size but significantly lower pI (spot 147; Supplementary

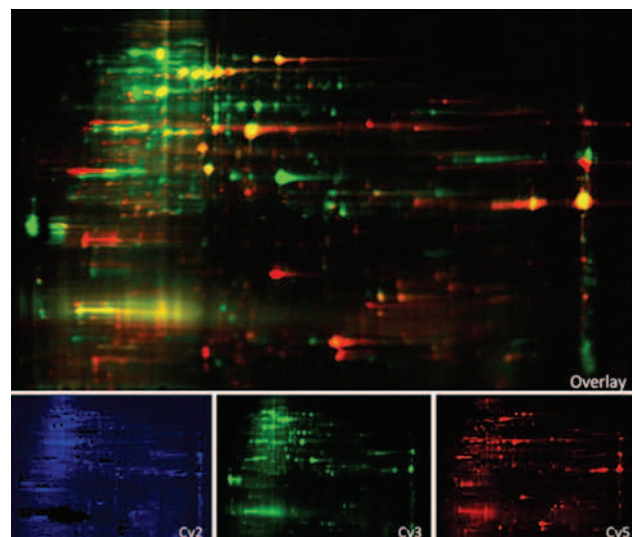


Fig. 1 Comparative display of differential in-gel electrophoresis (DIGE) of the extracellular fractions of strains 1002 and C231 of *C. pseudotuberculosis*. Overlay of the three color images Cy3 (colored green), Cy5 (colored red) and Cy2 (colored blue) derived from a single gel

file 2) and at an observed mass slightly higher than the theoretical mass (spot 125; Supplementary file 2). These observations suggest the occurrence of post-translational modifications, which are commonly detected in studies based in gel-dependent system [25]. Such post-translational modifications were shown to regulate several cellular functions, for example, in *S. aureus*, post-translational modifications (phosphorylation) play a key role in pathogenesis, through modulation of adhesion to and invasion of host cells [21]. The exact nature of the putative post-translational modifications observed here is still to be determined. Whether and how such modifications can affect pathogenesis and or host specificity in *C. pseudotuberculosis* remains unknown.

Predicting the Sub-Cellular Localization of Identified Exoproteins

In silico predictions of sub-cellular localization of *C. pseudotuberculosis*, extracellular proteins were performed using the software SurfG+ [2]. The predictions point out the presence of 13 secreted proteins, 2 proteins possibly associated with the cell wall and 1 cytoplasmic protein. The protein predicted as cytoplasmatic was glyceraldehyde-3-phosphate dehydrogenase (GAPDH) (spot 101, Supplementary file 1); this protein is associated with the lipid biosynthesis, carbohydrate metabolism and oxireduction process. However, despite being predicted as a cytoplasmic protein, several studies have detected GAPDH in different sub-cellular locations (membrane, cell surface and extracellular) and developing different functions; due to these features, this

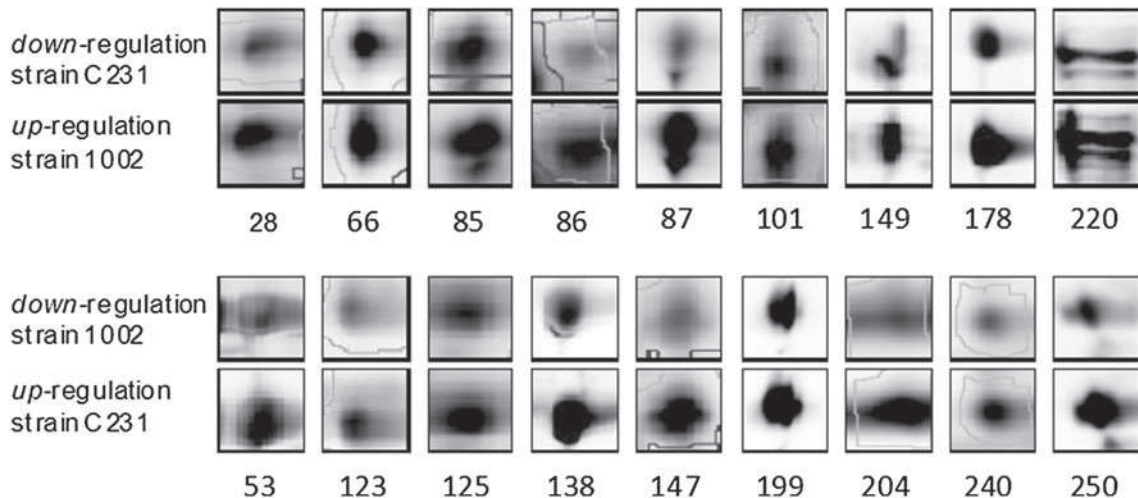


Fig. 2 Differential expression pattern of the proteins spots. Expanded views of the proteins spots differentially produced, between the strains 1002 and C231, identified by MS/MS

protein is classified as moonlighting proteins; these proteins show distinct functional behavior depending on the cell type, cellular localization and multiple binding sites [14]. Several of the moonlighting functions of GAPDH have been studied in different Gram-positive and Gram-negative pathogens, showing that this protein plays important role during the adhesion and invasion process to host cell [11, 18, 23]. The functional prediction of GPDH by Blast2GO in *C. pseudotuberculosis* shows the presence of two distinct functions: (1) oxireduction activity and (2) binding nucleotide showed the moonlight behavior this protein in this pathogen (Supplementary file 1). However, further studies are needed to uncover the true moonlighting role of GPDH in *C. pseudotuberculosis*.

Functional Classification of Differentially Produced Proteins

The differentially produced proteins identified here were related to various physiological functions. Two proteins (spots 204 and 250) found in strain C231, and one protein (spot 149) found in 1002 were of unknown function when submitted to a Blast2GO search [8]. Their putative role in the physiology and/or virulence of *C. pseudotuberculosis* thus remains to be determined. Four proteins detected in 1002 strain (spot 28, 66, 85 and 86, Supplementary file 1) and one protein detected in C231 strain (spot 199, Supplementary file 2) are associated with cell envelope and have a hydrolase activity. Such hydrolases partially digest the cell wall during the bacterial growth and thus participate in the turnover of peptidoglycan during the cell growth, in cell division or in cell autolysis [31]. Peptidoglycan is essential for cell viability and shape. It also

controls the internal osmotic pressure [13]. Among, the detected proteins with hydrolases activity, spot 28 (Supplementary file 1) was identified as a neuraminidase in 1002 supernatants. This protein acts in the hydrolysis process of glycoproteins by cleaving sialic acid residues. Moreover, it was shown to be involved in the virulence of pathogens like *Pseudomonas aeruginosa* and *Streptococcus pneumoniae*, by promoting cell adhesion and cell invasion [7, 30].

Other proteins are found differentially produced and are also associated with cell envelope: Mycolyltransferases (spot 87, 178, Supplementary file 1; spot 53, 123, Supplementary file 2) were previously shown to be associated with the cell envelope in *Mycobacterium tuberculosis*. This class of proteins is involved in the biosynthesis of corynemycolyl components that are associated with the envelope structure. These components are formed from high molecular weight chain fatty acids and are the largest cell wall constituents of *Mycobacterium*, *Nocardia* and *Corynebacterium* [28]. Changes in the quantity and structure of these fatty acids can affect the permeability, fluidity and other physical characteristics of the bilayer membrane of these bacteria and consequently may influence bacterial growth [33]. Furthermore, these constituents of the cell envelope also play important roles in the mechanisms of pathogenicity, due to their ability to form an impermeable asymmetric lipid bilayer that contributes to the resistance and survival of the bacteria in the hostile environment of macrophages [10].

A hypothetical protein (spot 225, Supplementary file 1) showed conserved domains the calcium ion binding. Calcium and calcium-binding proteins are involved in numerous bacterial processes, such as chemotaxis, sporulation, virulence, molecules transport, phosphorylation,

septation and stability of the cell envelope [20]. Several studies showed that calcium also influences the formation of biofilms. Thickness of *P. aeruginosa* biofilm increase in the presence of CaCl₂ compared to growth in medium without CaCl₂ supplementation [26]. The formation of biofilm by *V. cholerae* is dependent upon calcium and biofilms dissolve when the medium is depleted of calcium [16].

Bacteria that show characteristics of aerobic or anaerobic facultative growth, such as *C. pseudotuberculosis*, need oxygen as exogenous electron acceptor for respiration. The Cytochrome c oxidase sub-unit 2 (spot 125, 147, Supplementary file 2) is involved in this process [6], and was detected in this work.

Exploring *C. pseudotuberculosis* Exoproteome by Different Proteomics Approaches

The results obtained here were compared to those obtained by Pacheco et al. [22] in a previous study. Most of the differentially produced proteins identified in this work were shown over-produced as well in Pacheco et al. [22]. However, this study revealed some discrepancies with this previous study. Proteins ADL20134, ADL20574 and ADL21814 were indeed found over-produced in 1002 here (Table 1), whereas they were previously reported over-produced in C231 [22] and vice versa for proteins ADL11400 and ADL10895. We also identified some additional proteins, for example, lysozyme M1 (spot 86,

Supplementary file 1), GPDH (spot 101, Supplementary file 1) and hypothetical protein (spot 250, Supplementary file 2) that were not previously detected. Such differences may be linked to the experimental procedure used: these differentially produced or additional proteins may indeed be revealed in samples prepared, in this work, from cultures in late exponential growth phase whereas they did not appear in Pacheco et al. [22] where proteins were prepared from cultures in early exponential phase. On the other hand, sensitivity of the 2D-DIGE technique (as compared to the gel-free approach adopted in Pacheco et al. [22]) might also explain the additional proteins that were identified here. These results demonstrated that comparative analysis, combining different proteomic approaches, is a powerful strategy to characterize a proteome.

Conclusions

Exoproteome analysis of *C. pseudotuberculosis* strains 1002 and C231 revealed differential production patterns, which may be related to differences in host adaptation, pathogenicity or antigenicity of this pathogen. The genes corresponding to the differentially produced proteins are present in both strains, suggesting differences related to the ability of each strain to express these genes in these growth conditions. The results obtained here complement previous comparative genomic and proteomic studies, adding data regarding the biology and virulence of *C. pseudotuberculosis*. Investigating the proteomes of *C. pseudotuberculosis* strains isolated from various hosts will help understand how bacteria are able to adapt to specific hosts, and provide excellent candidates for targeted studies of the molecular basis of *C. pseudotuberculosis* pathogenesis in small ruminant.

Acknowledgments We are thankful to the Center for Study of Structure and Function of Biomolecules of the Institute of Biological Sciences of the Federal University of Minas Gerais and to the Genomic and Proteomic network of the State of Pará. The current work was supported by CNPq, FAPEMIG and FAPESPA.

References

1. Alban A, David SO, Bjorkesten L, Andersson C, Sloge E, Lewis S, Currie I (2003) A novel experimental design for comparative two-dimensional gel analysis: two-dimensional difference gel electrophoresis incorporating a pooled internal standard. *Proteomics* 3:36–44
2. Barinov A, Loux V, Hammani A, Nicolas P, Langella P, Maquin E, van de Guchte M (2009) Prediction of surface exposed proteins in *Streptococcus pyogenes*, with a potential application to other gram-positive bacteria. *Proteomics* 9:61–73
3. Bendtsen JD, Kierner L, Fausbøll A, Brunak S (2005) Non-classical protein secretion in bacteria. *BMC Microbiol* 5:58

Table 1 Analysis comparative between the results obtained by TPP/LC–MS^E

Protein	In this work	Pacheco et al. [22]
Secreted hydrolase	Over-produced in 1002 strain	Over-produced in C231 strain
Resuscitation-promoting factor RpfB		
Trehalose corynomycolyl transferase B		
Trehalose corynomycolyl transferase C	Over-produced in C231 strain	Over-produced in 1002 strain
Cytochrome c oxidase sub-unit 2		
Neuraminidase	Significant expression ^b	Not significant expression ^a
Hypothetical protein		
Metalloendopeptidase		
Lysozyme	Detected	Not detected ^c
M1 GPDH		
Hypothetical protein		

^a Proteins not differentially expressed according to the *t* test and *P* value

^b Proteins differentially expressed according to the *t* test and *P* value

^c Proteins not detected in the exoproteome analysis by TPP-LC/MS^E (Pacheco et al. [22])

4. Bendtsen JD, Nielsen H, Widdick D, Palmer T, Brunak S (2005) Prediction of twin-arginine signal peptides. *BMC Bioinformatics* 6:167
5. Billington SJ, Esmay PA, Songer JG, Jost BH (2002) Identification and role in virulence of putative iron acquisition genes from *Corynebacterium pseudotuberculosis*. *J Bacteriol* 180: 3233–3236
6. Bott M, Niebisch A (2003) The respiratory chain of *Corynebacterium glutamicum*. *J Biotechnol* 4:129–153
7. Cacalano G, Kays M, Saiman L, Prince A (1992) Production of the *Pseudomonas aeruginosa* neuraminidase is increased under hyperosmolar conditions and is regulated by genes involved in alginate expression. *J Clin Invest* 89:1866–1874
8. Conesa A, Gotz S, Garica-Gomez JM, Terol J, Talon M, Robles M (2005) Blast2GO: a universal tool for annotation, visualization and analysis in functional genomics research. *Bioinformatics* 21:3674–3676
9. Dorella FA, Pacheco LG, Oliveira SC, Miyoshi A, Azevedo V (2006) *Corynebacterium pseudotuberculosis*: microbiology, biochemical properties, pathogenesis and molecular studies of virulence. *Vet Res* 37:201–218
10. Dubnau E, Chan J, Raynaud C, Mohan VP, Lanéelle MA, Yu K, Quémard A, Smith I, Daffé M (2000) Oxygenated mycolic acids are necessary for virulence of *Mycobacterium tuberculosis* in mice. *Mol Microbiol* 36:630–637
11. Egéa L, Aguilera L, Giménez R, Sorolla MA, Aguilar J, Badía J, Baldoma L (2007) Role of secreted glyceraldehyde-3-phosphate dehydrogenase in the infection mechanism of enterohemorrhagic and enteropathogenic *Escherichia coli*: interaction of the extracellular enzyme with human plasminogen and fibrinogen. *Int J Biochem Cell Biol* 39:1190–1203
12. Hard GC (1975) Comparative toxic effect on the surface lipid of *Corynebacterium ovis* on peritoneal macrophages. *Infect Immun* 12:1439–1449
13. Hayhurst EJ, Kailas L, Hobbs JK, Foster SJ (2008) Cell wall peptidoglycan architecture in *Bacillus subtilis*. *Proc Natl Acad Sci USA* 23:14603–14608
14. Henderson B, Martin A (2011) Bacterial virulence in the moonlight: multitasking bacterial moonlighting proteins are virulence determinants in infectious disease. *Infect Immun* 79:3476–3491
15. Hodgson AL, Bird P, Nisbet IT (1990) Cloning, nucleotide sequence, and expression in *Escherichia coli* of the phospholipase D gene from *Corynebacterium pseudotuberculosis*. *J Bacteriol* 172:1256–1261
16. Kierek K, Watnick PI (2003) The *Vibrio cholerae* O139 O-antigen polysaccharide is essential for Ca²⁺-dependent biofilm development in sea water. *Proc Natl Acad Sci USA* 100:14357–14362
17. Le Maréchal C, Seyffert N, Jardin J et al (2011) Molecular basis of virulence in *Staphylococcus aureus* mastitis. *PLoS ONE* 6:e27354
18. Modun B, Williams P (1999) The staphylococcal transferrin-binding protein is a cell wall glyceraldehyde-3-phosphate dehydrogenase. *Infect Immun* 67:1086–1092
19. Moura-Costa LF, Paule BJA, Freire SM et al (2002) Meio sintético quimicamente definido para o cultivo de *Corynebacterium pseudotuberculosis*. *Rev Bras Saúde Prod An* 3:1–9
20. Norris V, Chen M, Goldberg M, Voskuil J, McGurk G, Holland IB (1991) Calcium in bacteria: a solution to which problem? *Mol Microbiol* 5:775–778
21. Ohlsson K, Donat S (2010) The impact of serine/threonine phosphorylation in *Staphylococcus aureus*. *Int J Med Microbiol* 300:137–141
22. Pacheco LG, Slade SE, Seyffert N et al (2011) A combined approach for comparative exoproteome analysis of *Corynebacterium pseudotuberculosis*. *BMC Microbiol* 11:12
23. Pancholi V, Fischetti VA (1992) A major surface protein on group A streptococci is a glyceraldehyde-3-phosphate-dehydrogenase with multiple binding activity. *J Exp Med* 176: 415–426
24. Paule BJ, Meyer R, Moura-Costa LF et al (2004) Three-phase partitioning as an efficient method for extraction/concentration of immunoreactive excreted-secreted proteins of *Corynebacterium pseudotuberculosis*. *Protein Expr Purif* 34:311–316
25. Rosen R, Sacher A, Shechter N, Becher D, Büttner K, Biran D, Hecker M, Ron EZ (2004) Two-dimensional reference map of *Agrobacterium tumefaciens* proteins. *Proteomics* 4:1061–1073
26. Sarkisova S, Patrauchan MA, Berglund D, Nivens DE, Franklin MJ (2005) Calcium-induced virulence factors associated with the extracellular matrix of mucoid *Pseudomonas aeruginosa* biofilms. *J Bacteriol* 187:4327–4337
27. Sengupta N, Alam SI, Kumar B, Kumar RB, Gautam V, Kumar S, Singh L (2010) Comparative proteomic analysis of extracellular proteins of *Clostridium perfringens* type A and type C strains. *Infect Immun* 78:3957–3968
28. Shimakata T, Minatogawa Y (2000) Essential role of trehalose in the synthesis and subsequent metabolism of corynomycolic acid in *Corynebacterium matruchotii*. *Arch Biochem Biophys* 380: 331–338
29. Trost M, Wehmhöner D, Kärs U, Dieterich G, Wehland J, Jansch L (2005) Comparative proteome analysis of secretory proteins from pathogenic and nonpathogenic *Listeria* species. *Proteomics* 5:1544–1557
30. Uchiyama S, Carlin AF, Khosravi A, Weiman S, Banerjee A, Quach D, Hightower G, Mitchell TJ, Doran KS, Nizet V (2009) The surface-anchored NanA protein promotes pneumococcal brain endothelial cell invasion. *J Exp Med* 31:1845–1852
31. Vollmer W, Bernard J, Charlier P, Foster S (2008) Bacterial peptidoglycan (murein) hydrolases. *FEMS Microbiol Rev* 32: 259–286
32. Wilson MJ, Brandon MR, Walker J (1995) Molecular and biochemical characterization of a protective 40-kilodalton antigen from *Corynebacterium pseudotuberculosis*. *Infect Immun* 63: 206–211
33. Winder FG, Collins PB (1970) Inhibition by isoniazid of synthesis of mycolic acids in *Mycobacterium tuberculosis*. *J Gen Microbiol* 66:41–48

4.3.1 Supplementary file:

Supplementary file 1: List of proteins differentially produced in strain 1002, identified by MALDI-TOF-MS/MS

Spot	Databank identified protein	ID (NCBI) ^P 1002	Theoretical Mr(kDa)/pI	Observed Mr(kDa)/pI	Sequence of peptide identified	Mascot Score	Cellular Function	^(k) Fold change	Sub-cellular Localization
28	Neuraminidase	ADL20287	74.86/5.05	69.79/4.48	R.VLLYSAPIDTR.I R.SNGWVMASCDDGR.S K.SAAQDAIAAAEANAR.V R.IPAIATAVDGTLVAFDNR.Y K.AGGTDNTENKGFWQELL.R	415	Hydrolase activity	+ 2,05	S
66	Secreted hydrolase	ADL20134	29.04/8.83	56.87/6.93	R.IQIVGYPTIVTGSR.I R.VVITHGFNDTYFNGGESEGATR.A	91	Hydrolase activity	+ 2,54	S
85	Resuscitation-promoting factor RpfB	ADL20574	40.31 / 5.06	50.66/5.35	K.VQASQGWGAWPACTSK.L K.AGVTVGDKDIVYPGLTEK.I K.TVFTQIAAATVKDVLAER.G	298	Hydrolase activity	+ 8,09	S
86	Lysozyme M1	ADL19973	40.28/5.58	49.44/5.39	K.TPQELVNWTR.D K.FASINLPELADLGK.N K.VGSYHYARPGADAR.Q R.ADELNIDANQVAQVLR.S K.ATEGLGWTNDFYASDITQAAAQGLK.V R.HYANVISHTPNHSLPPVLDEVAEGK.T	491	Hydrolase activity	+ 8,23	S [#]
87	Trehalose corynomycolyl transferase C	ADL21812	70.34 / 5.61	51.88/5.79	R.GNIYWSPER.G R.TFPSVWALDGLR.A K.LKDNVVAAQFER.G R.AYWSPATGAHALGGR.V K.NQGTYAGIGLEVISR.M R.AVVGLSMGGTAAVNLAER.R	417	Transferase activity, transferring acyl groups	+ 5,34	S [#]
101	Glyceraldehyde-3-phosphate dehydrogenase (GPDH)	ADL20991	36.37/5.35	48.63/5.21	R.VPVITGSATDLTFYASK.E R.LGKDVTYDDESITVDGHR.I R.GADVEVVAINDLTDNHTLSHLLK.Y	362	^(a) oxidoreductase activity; acting on the aldehyde or oxo group of donors,	+ 2,01	C

								NAD or NADP as acceptor	NADP binding; NAD binding;	(b) nucleotide binding	
149	Hypothetical protein	ADL20508	31.62/9.52	37.24/9.87	K.GRPIYVAIDDNPTR.A R.LGSFFWQHDWGSNGR.I	66	Unknown function	+ 2,55	S [#]		
178	Trehalose corynomycetyl transferase B	ADL21814	36.67/6.90	35.89/6.28	R.GGNAALYLLDGAR.A R.RIELDPLFNMR.G R.RIELDPLFNMR.G K.WETFLTQELPAYLEAHFGVAR.N R.DWLRRPDATGTCEWDAANYWVQR.C	245	Transferase activity, transferring acyl groups	+ 2,61	S		
220	Hypothetical protein	ADL19922	19.86 / 4.30	21.88/3.34	K.VVDLDGKVTVWEAPFTVGE. K.TPEIDDRDDVLKYEPTTVK.A	126	Calcium ion binding	+ 2,26	S		

Cellular function and sub-cellular localization has been established in accordance with the program Blast2Go.

S = secreted; C = cytoplasmic.

(a) e (b) The two moonlight distinct function of GPDH : ^(a)oxidoreductase activity; acting on the aldehyde or oxo group of donors, NAD or NADP as acceptor NADP binding; NAD binding; ^(b)nucleotide binding

(#) Predicted Tat-associated signal peptide

(P) Access number.

(k) Volume ratio from ImageMaster Platinum 7.0 DIGE interclass report. Protein with significant p-value (p<0,01), obtained by ANOVA test.

Theoretical molecular weights (Mr) and isoelectric points (pI), calculated by the Compute pI/MW tool (ExPASY tools).

Supplementary file 2: List of proteins differentially produced in strain C231, identified by MALDI-TOF-MS/MS

Spot	Databank identified protein	ID (NCBI) ^P C231	Theoretical Mr (kDa)/pI	Observed Mr (kDa)/pI	Sequence of peptide identified	Mascot Score	Cellular Function	^(k) Fold change	Sub-cellular Localization
53	Trehalose corynomycolyl transferase C	ADL11400	70.34/5.61	68.33/5.32	R.GNIYWSPER.G R.TFPSVWALDGLR.A K.LKDNVVAQFER.G R.MTTQTTFVDYAKR.A R.AYWSPATGAHALGGR.V K.NQGTYAGIGLEVISR.M K.SAAMPGNPIQVQVLLAR.D K.TYVSAGSGRDDYQQPGSVAK.N K.GGQVGTVCNNEYDIAGGKAEDFVDGR.A	685	Transferase activity, transferring acyl groups	+ 3,70	S [#]
123	Corynomycolyl transferase	ADL11196	41.80/7.05	45.03/7.75	K.GGVHDWPLFNR.Q K-AAHVAQSIGFPGWR.L K.GVFGISGCYATQEPVGR.I	123	Transferase activity, transferring acyl groups	+ 3,97	S [#]
125	Cytochrome c oxidase subunit 2	ADL10895	40.33/6.03	44.79/6.11	K.VTVDTVTAYQWNWK.F R.DVYNHPEQNKQQ.R K.FGYSDIAADLSPTGAEYK.G K.FGYSDIAADLSPTGAEYKGVDDAR.Q	390	Cytochrome-c oxidase activity	+ 3,47	PSE
138	Surface layer protein A	ADL09734	38.67/5.90	44.22/5.43	R.LQSLNIPADFNLR.N R.NTGTHSWSYWQDDL.R R.GTEVYVSNASGVAGGHDILANPR.F	175	Transferase activity	+ 2,62	S
147	Cytochrome c oxidase subunit 2	ADL10895	40.33/6.03	39.98/5.21	K.VTVDTVTAYQWNWK.F K.SIGEEPYATTTHPFNSER.A	155	Cytochrome-c oxidase activity	+ 2,38	PSE
199	Secreted hydrolase	ADL10025	31.47/9.59	29.89/9.74	R.SVSLQIDQAAQR.T R.RSVSLQIDQAAQR.T	108	Hydrolase activity	+ 2,40	S
204	Hypothetical protein	ADL09626	24.30/9.24	28.56/9.20	K.VAGWNATSQADR.V K.AITLDTTLEYTYTVGV.R.A K.IHSQGGYTEFSELTEFVPSVGR.L	309	Unknown function	+ 3,35	S
240	Metalloendopeptidase	ADL10125	24.83/7.23	13.98/7,68	K.IVVHTPAMGTLTSPYGM.R.W	64	Metalloendopeptidase activity	+ 2,97	PSE

250	Hypothetical protein	ADL11291	8.97/5.82	8.90/6,75	K.NLATINDFIAR.G K.SVFHFFHQWLTTGSSAPATAPAEK.A	90	Unknown function	+ 5,77	S
-----	----------------------	----------	-----------	-----------	---	----	------------------	--------	---

Cellular function and sub-cellular localization has been established in accordance with the program Blast2Go.

S = secreted; PSE = potentially surface exposed

(#) Predicted Tat-associated signal peptide

(P) Access number.

(k) Volume ratio from ImageMaster Platinum 7.0 DIGE interclass report. Protein with significant *p*-value (*p*<0,01), obtained by ANOVA test.

Theoretical molecular weights (Mr) and isoelectric points (pI), calculated by the Compute pI/MW tool (ExPASY tools).

5. Capítulo 2: Caracterização funcional do genoma de *C. pseudotuberculosis ovis* 1002 em resposta ao estresse utilizando uma abordagem proteômica.

Chapitre 2 : Caractérisation fonctionnelle du génome de *C. pseudotuberculosis* 1002 en réponse au stress nitrosant par une approche protéomique.

5.1 Introdução

Neste capítulo, apresentado em forma de artigo científico, demonstramos uma análise funcional do genoma de *C. pseudotuberculosis ovis* 1002, em resposta ao estresse nitrosativo, em nível proteico. Para lograr este objetivo, nós aplicamos à abordagem proteômica *MudiPit*, associada a quantificação *label-free*, a qual promoveu identificações sensíveis e reproduzibilidade dos dados gerados.

O óxido nítrico (NO), radical livre produzido pela ação da enzima óxido nítrico sintase (iNOS) é uma molécula utilizada pelo sistema imune principalmente por macrófagos no combate à infecção de patógenos, a qual a toxicidade está associada a sua concentração. No caso de baixos níveis de concentração desta molécula, como em escalas nanomolar, pode direcionar a uma função sinalizadora. No entanto, quando expresso em altas concentrações, como em escalas micromolar e milimolar, o NO se apresenta como uma molécula altamente tóxica gerando lesões ao DNA, RNA e proteínas. Assim esta toxicidade confere ao NO uma função bactericida, contra a infecção bacteriana (Nathan & Shiloh, 2000; Schairer et al., 2012).

Assim para resistir à ação do NO durante o processo de infecção *C. pseudotuberculosis*, esta bactéria demanda de uma alteração na expressão gênica para promover a ativação de fatores que favorecem sua resistência e adaptação. Neste contexto, nossa análise proteômica promoveu uma análise global do genoma desta linhagem na presença do estresse nitrosativo, o que permitiu a identificação de vários fatores que podem contribuir para resistência e sobrevivência deste patógeno, durante a exposição ao óxido nítrico.

Introduction

Dans ce chapitre, présenté sous forme d'article scientifique, nous avons mené une analyse fonctionnelle du génome de *C. pseudotuberculosis ovis* 1002, en réponse au stress nitrosant. Pour atteindre cet objectif, nous avons appliqué l'approche protéomique de *MudPit*, associée à une quantification *label-free*, qui est plus sensible que les approches classiques et améliore la reproductibilité des données générées.

C. pseudotuberculosis est confronté au stress nitrosant dans les macrophages. Ce stress est généré par l'oxyde nitrique (NO), un radical libre produit par l'action de l'oxyde nitrique synthase (iNOS). Le NO est une molécule utilisée par le système immunitaire dans la lutte contre l'infection par des agents pathogènes. La toxicité du NO est fonction de sa concentration. Des concentrations faibles de cette molécule (de l'ordre du nanomolaire) peuvent avoir une fonction de signalisation. Par contre, lorsque l'oxyde nitrique est produit à des concentrations plus élevées, (de l'ordre du micromolaire voire millimolaire), il présente une forte toxicité et génère des lésions à l'ADN, à l'ARN et aux protéines. Cette toxicité donne sa fonction bactéricide au NO et constitue un moyen de lutte précoce contre les infections bactériennes (Nathan & Shiloh, 2000; Schairer et al., 2012).

Pour survivre à ce stress, *C. pseudotuberculosis* opère un changement dans l'expression des gènes pour promouvoir l'activation de facteurs qui favorisent résistance et adaptation. Dans ce contexte, notre analyse a abordé de façon globale le protéome de la souche *C. pseudotuberculosis* biovar *ovis* *Cp1002* en présence d'un stress nitrosant. Nous avons adossé cette analyse à celle du génome complet de cette souche ce qui a permis l'identification de plusieurs facteurs qui peuvent contribuer à la résistance et à la survie de cet agent pathogène pendant l'exposition à l'oxyde nitrique.

5.2 Artigo 3: Label-free proteomic analysis to confirm the predicted proteome of *Corynebacterium pseudotuberculosis* under nitrosative stress mediated by nitric oxide. *BMC Genomics.* 4;15:1065. 2014. doi: 10.1186/1471-2164-15-1065.
Silva, W.M., Carvalho, R.D., Soares, S.C., Bastos, I.F., Folador, E.L., Souza, G.H., Le Loir, Y., Miyoshi, A., Silva, A., Azevedo, V.

RESEARCH ARTICLE

Open Access

Label-free proteomic analysis to confirm the predicted proteome of *Corynebacterium pseudotuberculosis* under nitrosative stress mediated by nitric oxide

Wanderson M Silva^{1,4,5}, Rodrigo D Carvalho¹, Siomar C Soares¹, Isabela FS Bastos¹, Edson L Folador¹, Gustavo HMF Souza³, Yves Le Loir^{4,5}, Anderson Miyoshi¹, Artur Silva² and Vasco Azevedo^{1*}

Abstract

Background: *Corynebacterium pseudotuberculosis* biovar *ovis* is a facultative intracellular pathogen, and the etiological agent of caseous lymphadenitis in small ruminants. During the infection process, the bacterium is subjected to several stress conditions, including nitrosative stress, which is caused by nitric oxide (NO). *In silico* analysis of the genome of *C. pseudotuberculosis ovis* 1002 predicted several genes that could influence the resistance of this pathogen to nitrosative stress. Here, we applied high-throughput proteomics using high definition mass spectrometry to characterize the functional genome of *C. pseudotuberculosis ovis* 1002 in the presence of NO-donor Diethylenetriamine/nitric oxide adduct (DETA/NO), with the aim of identifying proteins involved in nitrosative stress resistance.

Results: We characterized 835 proteins, representing approximately 41% of the predicted proteome of *C. pseudotuberculosis ovis* 1002, following exposure to nitrosative stress. In total, 102 proteins were exclusive to the proteome of DETA/NO-induced cells, and a further 58 proteins were differentially regulated between the DETA/NO and control conditions. An interactomic analysis of the differential proteome of *C. pseudotuberculosis* in response to nitrosative stress was also performed. Our proteomic data set suggested the activation of both a general stress response and a specific nitrosative stress response, as well as changes in proteins involved in cellular metabolism, detoxification, transcriptional regulation, and DNA synthesis and repair.

Conclusions: Our proteomic analysis validated previously-determined *in silico* data for *C. pseudotuberculosis ovis* 1002. In addition, proteomic screening performed in the presence of NO enabled the identification of a set of factors that can influence the resistance and survival of *C. pseudotuberculosis* during exposure to nitrosative stress.

Keywords: *Corynebacterium pseudotuberculosis*, Caseous lymphadenitis, Proteomics, Label-free proteomics, Nitrosative stress, Nitric oxide

Background

Corynebacterium pseudotuberculosis is a Gram-positive, facultative, intracellular pathogen belonging to the *Corynebacterium*, *Mycobacterium*, *Nocardia*, or CMN, group. This group belongs to the phylum Actinobacteria. The defining characteristics of the CMN group are a specific cell wall organization, consisting of peptidoglycan, arabinogalactan,

and mycolic acids, and a high chromosomal G + C content [1]. *C. pseudotuberculosis ovis* is the etiological agent of the chronic infectious disease caseous lymphadenitis, which affects small ruminants worldwide. As a result, *C. pseudotuberculosis ovis* is responsible for significant economic losses in the goat and sheep industries, mainly stemming from decreased meat, wool, and milk production, reproductive disorders, and carcass contamination [1,2]. Bacterial factors that contribute to the virulence of *C. pseudotuberculosis* include phospholipase D [3], toxic cell wall lipids [4], and the iron transporter *fagABC* complex [5].

* Correspondence: vasco@icb.ufmg.br

¹Depto de Biologia Geral, Instituto de Ciências Biológicas, Universidade Federal de Minas Gerais, Belo Horizonte, Brazil

Full list of author information is available at the end of the article

In silico analysis of the genome of *C. pseudotuberculosis ovis* 1002 [6], as well as the pan-genome analysis of 15 other strains of *C. pseudotuberculosis* [7], identified genes involved in the response of this pathogen to different types of stress. Recently, the functional genome of *C. pseudotuberculosis ovis* 1002 was evaluated at the transcriptional level following exposure to different types of abiotic stress, including heat, osmotic, and acid stresses [8]. This allowed the characterization of several genes involved in distinct biological processes that favor the survival of the pathogen under the given stress condition.

However, during the infection process, *C. pseudotuberculosis* encounters nitrosative stress, caused by nitric oxide (NO), in the macrophage intracellular environment. A reactive nitrogen species (RNS) found in mammalian systems, NO is produced from L-arginine by NO synthases (NOS), and is present in three isoforms: endothelial NOS, neuronal NOS, involved in blood pressure control and neural signaling, and inducible NOS, associated with host defenses [9,10]. The NO produced during bacterial infection has antimicrobial properties, killing pathogens by causing damage to DNA, RNA, and proteins [11]. However, several pathogens contain pathways that allow bacterial survival under nitrosative stress conditions, including NO-sensitive transcriptional regulators [12], DNA and protein repair systems [13], and antioxidant systems [14].

Currently, little is known about the factors involved in the resistance of *C. pseudotuberculosis* to nitrosative stress. Pacheco et al. [15] showed that the alternative sigma (σ) factor, σ^E , plays a role in the survival of *C. pseudotuberculosis* in the presence of RNS. A σ^E null strain showed increased susceptibility to nitric oxide compared with the wild-type, and, in an *in vivo* assay, was unable to persist in mice. However, in iNOS-deficient mice, the mutant strain maintained its virulence [15]. In the same study, the extracellular proteome of *C. pseudotuberculosis* was analyzed in response to nitrosative stress, allowing the characterization of proteins that contribute to the adaptive processes of the pathogen in this environment [15].

To complement the results obtained in previous studies, and to identify factors involved in the survival of *C. pseudotuberculosis* under nitrosative stress conditions, we applied high-throughput proteomics using an liquid chromatograph high definition mass spectrometry (LC-HDMS^E) (data-independent acquisition, in ion mobility mode) approach to evaluate the global expression of the functional genome of *C. pseudotuberculosis ovis* 1002 at the protein level under nitrosative stress conditions.

Methods

Bacterial strain and growth conditions

C. pseudotuberculosis biovar *ovis* strain 1002, isolated from a goat, was maintained in brain heart infusion broth (BHI; HiMedia Laboratories Pvt. Ltd., Mumbai, India) at

37°C. For stress-resistance assays, strain 1002 was cultivated in a chemically-defined medium (CDM), containing Na₂HPO₄·7H₂O (12.93 g/l), KH₂PO₄ (2.55 g/l), NH₄Cl (1 g/l), MgSO₄·7H₂O (0.20 g/l), CaCl₂ (0.02 g/l), 0.05% (v/v) Tween 80, 4% (v/v) MEM vitamin solution (Invitrogen, Gaithersburg, MD, USA), 1% (v/v) MEM amino acid solution (Invitrogen), 1% (v/v) MEM non-essential amino acid solution (Invitrogen), and 1.2% (w/v) glucose, at 37°C [16].

Nitric oxide assay and preparation of whole bacterial lysates

Diethylenetriamine/nitric oxide adduct (DETA/NO) resistance of *C. pseudotuberculosis* was characterized as previously described [15]. When strain 1002 reached exponential growth phase (OD₆₀₀ = 0.6) in the chemically-defined medium, the culture was divided into two aliquots (control condition, strain 1002_Ct; NO exposure, strain 1002_DETA/NO), and DETA/NO was added to the appropriate aliquot to a final concentration of 0.5 mM. The growth of strain 1002 in the presence of DETA/NO was then evaluated for 10 h. For proteomic analysis, protein was extracted after 1 h of exposure to DETA/NO. Both the control and DETA/NO cultures were centrifuged at 4,000 × g for 10 min at 4°C. The cell pellets were washed in phosphate buffered saline and then resuspended in 1 ml of lysis buffer (7 M urea, 2 M thiourea, 4% (w/v) CHAPS, and 1 M dithiothreitol (DTT)). The cells were then sonicated using five 1-min cycles on ice. The resulting lysates were centrifuged at 14,000 × g for 30 min at 4°C. The extracted proteins were then submitted to centrifugation at 13,000 × g for 10 min using a spin column with a threshold of 10 kDa (Millipore, Billerica, USA). Proteins were denatured with (0.1% (w/v) RapiGEST SF surfactant at 60°C for 15 min (Waters, Milford, CA, USA), reduced using 10 mM DTT for 30 min at 60°C, and alkylated with 10 mM iodoacetamide in a dark chamber at 25°C for 30 min. Next, the proteins were enzymatically digested with 1:50 (w/w) trypsin at 37°C for 16 hours (sequencing grade modified trypsin; Promega, Madison, WI, USA). The digestion process was stopped by adding 10 µl of 5% (v/v) Trifluoroacetic acid (TFA) (Fluka, Buchs, Germany). Glycogen phosphorylase was added to the digests to a final concentration of 20 fmol/µl as an internal standard for normalization prior to each replicate injection. Analysis was carried out using a two-dimensional reversed phase (2D RP-RP) nanoUPLC-MS (Nano Ultra Performance Liquid Chromatography) approach, using multiplexed HDMS^E label-free quantitation as described previously [17].

LC-HDMS^E analysis and data processing

Qualitative and quantitative by 2D nanoUPLC tandem nanoESI-HDMS^E (Nano Electrospray High Definition Mass Spectrometry) experiments were conducted using a 1-h reversed phase (RP) acetonitrile (0.1% v/v formic

acid) gradient (7–40% (v/v)) at 500 nl/min on a nanoACQUITY UPLC 2D RP × RP Technology system [18]. A nanoACQUITY UPLC High Strength Silica (HSS) T3 1.8 μm 75 μm × 15 cm column (pH 3) was used in conjunction with a RP XBridge BEH130 C18 5 μm 300 μm × 50 mm nanoflow column (pH 10). Typical on-column sample loads were 250 ng of the total protein digests for each of the five fractions (250 ng/fraction/load). For all measurements, the mass spectrometer was operated in resolution mode, with a typical effective *m/z* conjoined ion-mobility resolving power of at least 1.5 M FWHM, an ion mobility cell filled with nitrogen gas, and a cross-section resolving power at least $40 \Omega/\Delta\Omega$. All analyses were performed using nano-electrospray ionization in the positive ion mode nanoESI (+), and a NanoLockSpray (Waters) ionization source. The lock mass channel was sampled every 30 s. The mass spectrometer was calibrated with a MS/MS spectrum of [Glu¹]-fibrinopeptide B (Glu-Fib) human solution (100 fmol/μl) delivered through the reference sprayer of the NanoLockSpray source. The double-charged ion ($[M + 2H]^{2+} = 785.8426$) was used for initial single-point calibration, and MS/MS fragment ions of Glu-Fib were used to obtain the final instrument calibration. Multiplexed data-independent scanning with added specificity and selectivity of a non-linear “T-wave” ion mobility (HDMS^E) experiments were performed using a Synapt G2-S HDMS mass spectrometer (Waters). The mass spectrometer was set to switch automatically between standard MS (3 eV) and elevated collision energies HDMS^E (19–45 eV) applied to the transfer “T-wave” collision-induced dissociation cell with argon gas. The trap collision cell was adjusted for 1 eV using a millisecond scan time adjusted based on the linear velocity of the chromatography peak delivered through nanoACQUITY UPLC, to obtain a minimum of 20 scan points for each single peak at both low-energy and high-energy transmission, followed by an orthogonal acceleration time-of-flight from 50–2000 *m/z*. The radio frequency (RF) offset (MS profile) was adjusted so that the nanoUPLC-HDMS^E data were effectively acquired from an *m/z* range of 400–2000, which ensured that any masses observed in the high energy spectra of less than 400 *m/z* arose from dissociations in the collision cell.

Data processing

Protein identification and quantitative data packaging were generated using dedicated algorithms [19,20], and by searching against a *C. pseudotuberculosis* database with default parameters for ion accounting [21]. The databases were reversed “on-the fly” during the database query searches, and appended to the original database to assess the false positive rate of identification. For proper processing of spectra and database searching conditions,

ProteinLynxGlobalServer v.2.5.2 (PLGS) with Identity^E and Expression^E informatics v.2.5.2 (Waters) were used. UniProtKB (release 2013_01) with manually-reviewed annotations was also used, and the search conditions were based on taxonomy (*C. pseudotuberculosis*), maximum missed cleavages by trypsin allowed up to one, and variable carbamidomethyl, acetyl N-terminal, phosphoryl, and oxidation (M) modifications [21,22]. The Identity^E algorithm with Hi3 methodology was used for protein quantitation. The search threshold for accepting each individual spectrum was set to the default value, with a false-positive value of 4%. Biological variability was addressed by analyzing each culture three times. Normalization was performed using the Expression^E tool with a housekeeping protein that showed no significant difference in abundance across all injections. The proteins obtained were organized by the PLGS Expression^E tool algorithm into a statistically significant list corresponding to increased and decreased regulation ratios among the different groups. The quantitation values were averaged over all of the samples, and the quoted standard deviations at $p \leq 0.05$ in the Expression^E software refer to the differences between biological replicates. Only proteins with a differential expression \log_2 ratio between the two conditions greater than or equal to 1.2 were considered [23].

Bioinformatics analysis

The identified proteins were analyzed using the prediction tools SurfG+ v1.0 [24], to predict sub-cellular localization, and Blast2GO, to predict gene ontology functional annotations [25]. The PIPS software predicted proteins present in pathogenicity islands [26]. The protein-protein interaction network was constructed using interolog mapping methodology and metrics according to Rezende et al. [27]. A preview of the interaction network was generated using Cytoscape version 2.8.3 [28], with a spring-embedded layout. CMRegNet was used to predict gene regulatory networks [29].

Results

Effects of nitric oxide on the growth of *C. pseudotuberculosis*

In this study, we examined the exponential growth of *C. pseudotuberculosis* strain 1002 under nitrosative stress. The growth and cell viability of strain 1002 was monitored for 10 h with and without DETA/NO supplementation (Figure 1). The control culture reached stationary phase by 5 h post-inoculation, while the culture containing DETA/NO did not reach stationary phase until approximately 10 h post-inoculation. However, these results showed that although DETA/NO (0.5 mM) affected the growth rate, *C. pseudotuberculosis* likely contains factors that promote survival in the presence of RNS.

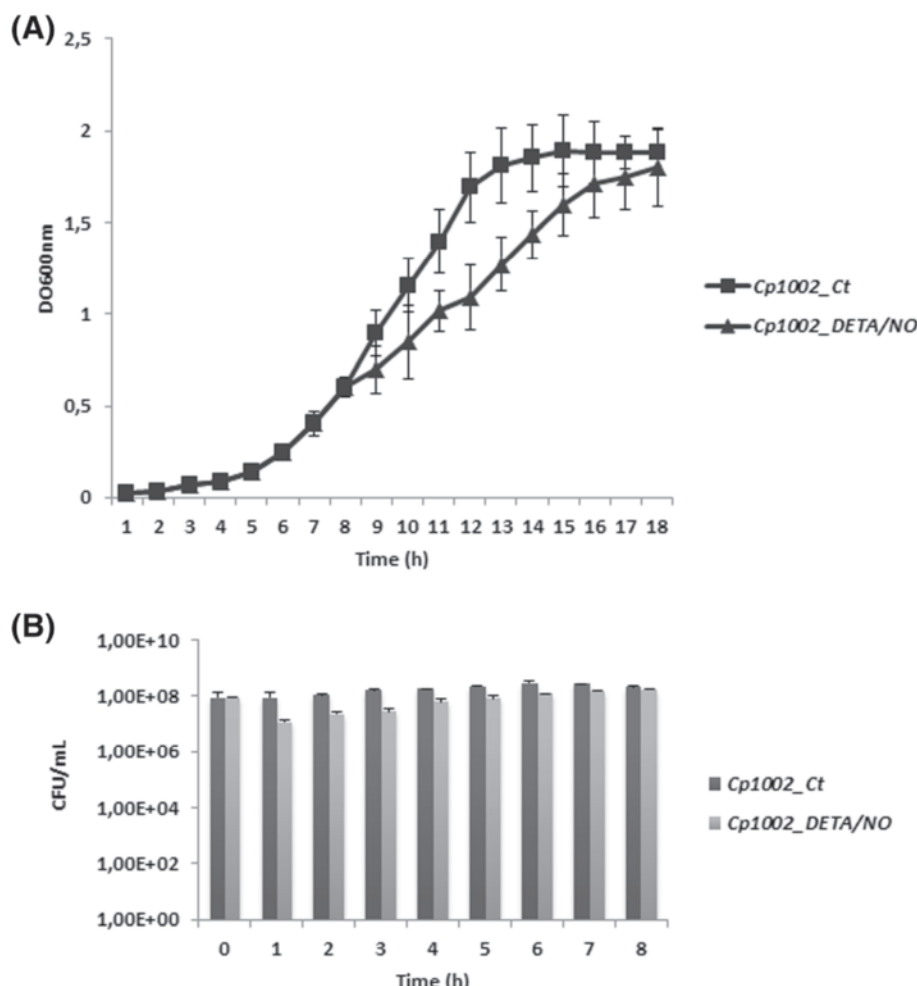


Figure 1 Growth and survival profile of *C. pseudotuberculosis* during NO exposure. **(A)** Growth of *C. pseudotuberculosis* after 10 h exposure to 0.5 mM DETA/NO. **(B)** Survival of *C. pseudotuberculosis* evaluated by colony forming units. The results shown in A and B represent an average of three independent experiments.

Label-free proteomic analysis of *C. pseudotuberculosis* grown under nitrosative stress conditions

Total proteome digests from three biological replicates of each individual condition were subjected to LC/MS^E. In total, we identified more than 31,000 peptides, with a normal distribution of 10 ppm error of the total identified peptides. Peptides as source fragments, peptides with a charge state of at least [M + 2H]²⁺, and the absence of decoys were factors considered to increase data quality. A combined total of 2,063 proteins were present in at least two of the three biological replicates for the two conditions tested, with an average of 15 peptides per protein, and a false discovery rate (FDR) of 0% when decoy detection was set at agreement of two out of three replicates. The proteins referred to as exclusive to one condition or another were only identified in one condition within the detection limits of the experiment (LOD). The dynamic range of the quantified proteins is

about 3 logs, and proteins unique to one condition or another were only observed above the LOD of the experiment, which was determined by the sample normalization prior to injection. Therefore, in our study, all samples were normalized using “scouting runs” taking into account the stoichiometry between the intensity and molarity proportion prior to the replicate runs per condition. The dynamic range was similar for each sample, and the total amount of sample used in fmol was nearly the same. We generate a graph of protein amounts of the identified proteins from all samples against protein ranks (Figure 2A).

After analysis by PLGS v2.5.2 software, the 2,063 proteins originally identified in two out of three replicates were narrowed down to 699 proteins with $p \leq 0.05$. Among these proteins, 44 were up-regulated in the presence of DETA/NO, while 14 proteins were down-regulated (Table 1, Figure 2B and C). The remaining 641 proteins with $p \leq 0.05$ and $\log_2 < 1.2$ that were common to

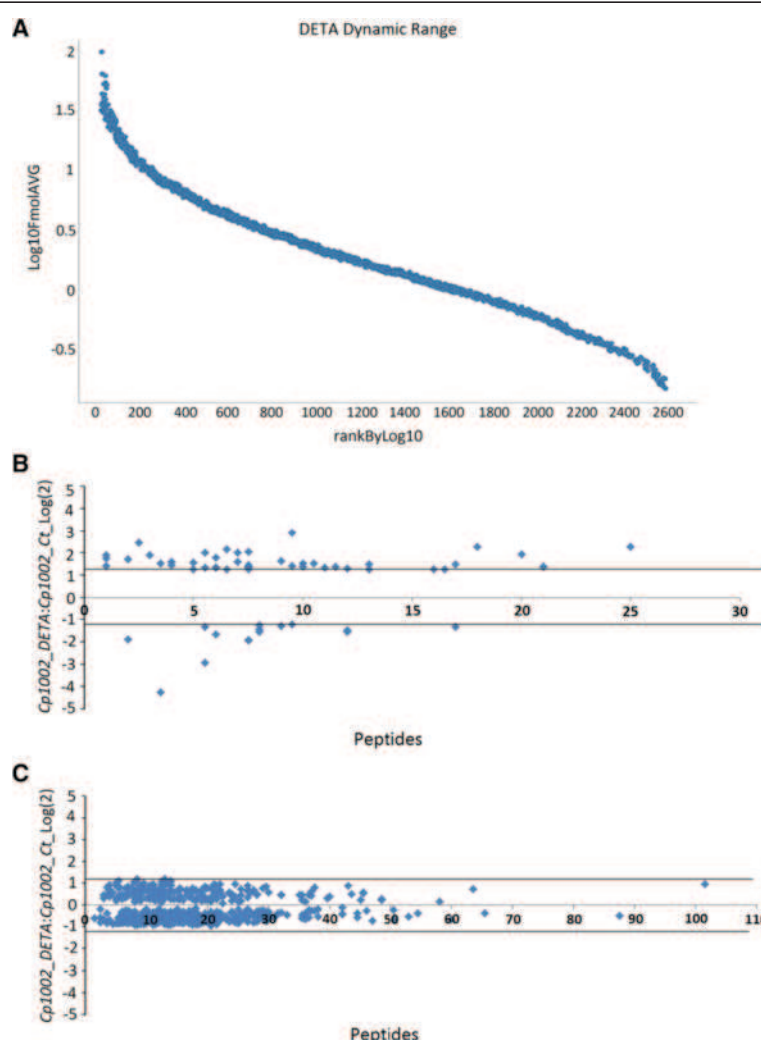


Figure 2 2D nanoUPLC HDMSE analysis showing: (A) Dynamic range of the method based on protein abundance estimates, data points derived from LC-HDMSE analysis. (B and C) Proteins that were significantly differentially-regulated during NO exposure. The distribution of identified proteins with $p < 0.05$, and differentially-regulated proteins with an I:C \log_2 ratio < 1.2 in relation to the number of peptides identified for each protein. (B) Proteins with $p < 0.05$ and an I:C \log_2 ratio < 1.2 . (C) Proteins with $p < 0.05$ and an I:C \log_2 ratio > 1.2 .

the two treatments are summarized in Additional file 1. In addition to the 699 identified proteins that were present under both control and stress conditions, 34 proteins were exclusively expressed under the control conditions, and 102 proteins were exclusively expressed in response to DETA/NO stress (Additional files 2 and 3). Thus, our final list of proteins is composed of 835 proteins from *C. pseudotuberculosis*.

In silico analysis of LC-HDMSE data

The 835 proteins were then analyzed using the SurfG+ tool to predict sub-cellular localization. According with SurfG+, our data set included approximately 41% of the predicted proteome of strain 1002 (Figure 3A). In addition, we characterized proteins belonging to the following cell fractions: cytoplasmic (CYT) (668 proteins), membrane

(MEM) (59 proteins), potentially surface-exposed (PSE) (69 proteins), and secreted (SEC) (39 proteins) (Figure 3B).

To evaluate whether the proteins identified in our proteomic analysis could represent a protein set expressed by *C. pseudotuberculosis* during exposure to nitrosative stress, we correlated our proteomic data with the predicted core-genomes of 15 *C. pseudotuberculosis* strains [7]. Of the open reading frames (ORFs) coding for the differentially-regulated proteins and exclusive proteome of DETA/NO-exposed cells, 86% (50/58 proteins) and 82% (84/102 proteins) were identified, respectively, in the core-genome of *C. pseudotuberculosis* (Figure 3C and D). In addition, of the 835 total proteins identified from the proteome of strain 1002 following exposure to nitrosative stress, 83% (696 proteins) of the ORFs coding for these proteins were present in the core-genome of *C. pseudotuberculosis*,

this result correspond approximately 46% of the predicted core-genome of *C. pseudotuberculosis* (Figure 3E).

Functional classification of the proteome of *C. pseudotuberculosis* expressed under exposure to nitrosative stress

The strain 1002 proteome was functionally classified using the Blast2Go tool [24]. A large proportion of the differentially-regulated proteins and those exclusive to one condition were identified as hypothetical proteins. According to the biological function prediction, 18 biological processes were classified as differentially regulated (Figure 4A). In addition, the analysis of the exclusive proteome of each condition revealed 12 common processes between the control and stress conditions (Figure 4B). However, seven biological processes were identified only in stress-exposed cells. These processes were antibiotic metabolism (six proteins), nucleotide metabolism (five proteins), oxidative phosphorylation (three proteins), translation (three proteins), glycolysis pathways (one protein), iron-sulfur clusters (one protein), and starch and sucrose metabolism (one protein). Among all processes identified, DNA synthesis and repair proteins (14 proteins) were most common. An overview of the *C. pseudotuberculosis* response to nitrosative stress according with the proteins identified is shown in Figure 5.

The proteins that were grouped into of transcriptional process were evaluated by CMRegNet and among regulators identified; we identified the GntR- family regulatory protein (D9Q5B7_CORP1), genes regulated by GntR-type regulators are usually involved in carbohydrate metabolism. The CMRegNet analysis showed that of the four genes under the control of this regulator, the N-acetylglucosamine kinase (D9Q5B6_CORP1) protein was highly expressed by *C. pseudotuberculosis* in response to DETA/NO. We identified other regulator the LexA repressor (D9Q8W2_CORP1) that was down regulated in the DETA/NO condition. According with CMRegNet, two proteins regulated by this repressor were detected in the DETA/NO proteome specific, pyridoxal biosynthesis lyase (PdxS; D9Q5T9_CORP1) and DNA translocase (D9Q8Z6_CORP1). Others proteins under the control of this repressor was detected, however not presented significant differential regulation like RecA protein

Protein-protein interaction network

To investigate the interactions among the proteins identified as exclusive and differentially regulated in cells exposed to DETA/NO, we generated a protein interaction network using Cytoscape. The interactome analysis revealed 67 protein-protein interactions (Figure 6). DnaB/DNA helicase (D9Q578_CORP1), identified in the exclusive proteome for strain 1002_DETA/NO, and PyrE/orotate phosphoribosyltransferase (D9Q4S2_CORP1), which was down-regulated in strain 1002_DETA/NO,

showed the greatest number of interactions with other proteins (eight interactions each). Moreover, both of these proteins interact with proteins that are involved in metabolic processes, DNA processes, antibiotic metabolism, cell cycling, and translation.

Discussion

C. pseudotuberculosis is exposed to different forms of oxidative and nitrosative stress during the infection process. A previous study showed that *C. pseudotuberculosis* resists nitrosative stress generated by the NO-donor DETA/NO, and that a low concentration of DETA/NO (100 μM) induces a change in the extracellular proteome this pathogen [15]. To better understand the physiology of *C. pseudotuberculosis* in response to nitrosative stress, we analyzed the proteome of whole bacterial lysates of *C. pseudotuberculosis* in response to exposure to DETA/NO (0.5 mM).

The strain 1002 proteome under nitrosative stress reveals proteins involved in bacterial defense against DNA damage

Proteomic analysis identified proteins involved in DNA repair systems in both the exclusive proteome of DETA/NO-exposed cells and in the differentially-regulated proteome. We detected the proteins formamidopyrimidine-DNA glycosylase (Fpg) (D9Q598_CORP1), RecB (D9Q8C9_CORP1), and methylated-DNA-protein-cysteine methyltransferase (Ada) (D9Q923_CORP1), the genes for which were previously identified in a transcriptome analysis of strain 1002 in response to different abiotic stresses [8]. Activation of these proteins in response to nitrosative stress confirms that they belong a group of general stress-response proteins in *C. pseudotuberculosis*.

The expression of Fpg was up-regulated in response to acid stress [8]. We also identified endonuclease III (Endo III) (D9Q615_CORP1), which, in addition to Fpg, is involved in the base excision repair (BER) system of various bacteria. This system cleaves N-glycosidic bonds from damaged bases, allowing their excision and replacement. In *Salmonella enterica* serovar Typhimurium, the BER system repairs DNA damaged by exposure to NO. In addition, an *S. Typhimurium* strain defective in Fpg demonstrated reduced virulence in a murine model [30]. Our interactome analysis showed that Endo III had one of the highest numbers of interactions with other proteins, including interactions with proteins involved in DNA replication such zinc metalloprotease (D9Q378_CORP1) and DNA translocase (D9Q8Z6_CORP1), suggesting that this protein could play an important role in the defense pathway against RNS.

The Ada and RecB protein were up-regulated in response to osmotic stress [8]. Ada is involved in the repair of DNA-methylation damage, this protein plays important in the pathway DNA damage [31]. RecB is a component of the RecBC system, which is part of

Table 1 Proteins identified as differentially-expressed following exposure to nitrosative stress

Uniprot access	Proteins	Score	Peptides	$\log_2 \text{DETA:CT}^{(a)}$	p-value ^(a)	Subcellular localization ^(c)	Gene name	Genome ^(b)
Transport								
F9Y2Z3_CORP1	Cell wall channel	5321.88	4	1.42	1	CYT	porH	Shared
Cell division								
D9Q7G2_CORP1	Hypothetical protein	2417.8	21	1.34	1	CYT	Cp1002_0716	Core
DNA synthesis and repair								
D9Q5V6_CORP1	Nucleoid-associated protein	2327.08	5	1.52	1	CYT	ybaB	Core
D9Q923_CORP1	Methylated-DNA-protein-cysteine methyltransferase	6332.83	8	1.22	1	CYT	ada	Core
D9Q4P0_CORP1	7,8-dihydro-8-oxoguanine-triphosphatase	1640.23	8	-1.97	0	CYT	mutT	Core
Transcription								
D9Q8W2_CORP1	LexA repressor	800.31	6	-1.37	0.04	CYT	lexA	Shared
D9Q5L4_CORP1	ECF family sigma factor k	364.82	8	-1.58	0	CYT	sigK	Core
Translation								
D9Q753_CORP1	Fkbp-type peptidyl-prolyl cis-trans isomerase	7113.34	3	2.43	1	CYT	fkbP	Core
D9Q830_CORP1	50S ribosomal protein L35	2271.66	1	1.36	1	CYT	rplml	Core
D9Q7W1_CORP1	Aspartyl glutamyl-tRNA amidotransferase subunit C	3100.8	7	1.24	0.99	CYT	gatC	Core
D9Q582_CORP1	50S ribosomal protein L9	41082.46	10	-1.25	0	CYT	rplll	
D9Q6H6_CORP1	30S ribosomal protein S8	45333.23	9	-1.34	0	CYT	rpsH	Core
Cell communication								
D9Q559_CORP1	Hypothetical protein	1402.27	6	1.99	1	PSE	Cp1002_2005	Core
D9Q5U9_CORP1	Thermosensitive gluconokinase	2068.35	7	1.96	0.99	CYT	gntK	Core
D9Q668_CORP1	Sensory transduction protein RegX3	2540.92	13	1.45	1	CYT	regX3	Core
Detoxification								
D9Q7U6_CORP1	Thioredoxin	1835.7	11	1.50	1	CYT	trxA	Core
D9Q4E5_CORP1	Glutathione peroxidase	1426.27	10	1.47	1	CYT	Cp1002_1731	Core
D9Q5T5_CORP1	Glyoxalase bleomycin resistance protein dihydroxybiphenyl dioxygenase	2417.77	11	1.28	1	CYT	Cp1002_0124	Shared
D9Q5N2_CORP1	NADH dehydrogenase	7030.94	12	1.25	1	CYT	noxC	Shared
D9Q680_CORP1	Glutaredoxin-like domain protein	292.69	2	-1.91	0	CYT	Cp1002_0272	Core
Glycolysis pathways								
D9Q5B6_CORP1	N-Acetylglucosamine kinase	228.69	6	1.74	0.98	CYT	nanK	Core
D9Q4U9_CORP1	Alcohol dehydrogenase	236.02	17	1.22	1	CYT	adhA	Shared
Iron-sulfur clusters								
D9Q7L6_CORP1	Ferredoxin	36927.57	7	2.10	1	CYT	fdxA	Core
Antibiotic resistance								
D9Q827_CORP1	Metallo-beta-lactamase superfamily protein	657.33	6	-2.95	0	CYT	Cp1002_0937	Core

Table 1 Proteins identified as differentially-expressed following exposure to nitrosative stress (Continued)

Amino acid metabolism								
D9Q622_CORP1	Phosphoserine phosphatase	949.15	9	1.58	0.99	PSE	<i>serB</i>	Core
D9Q4N1_CORP1	Carboxylate-amine ligase	205.54	16	1.24	1	CYT	<i>Cp1002_1819</i>	Core
D9Q6H4_CORP1	L-serine dehydratase I	284.11	17	-1.37	0	MEM	<i>sdaA</i>	Core
Lipid metabolism								
D9Q520_CORP1	Glycerophosphoryl diester phosphodiesterase	2417.8	21	1.34	1	PSE	<i>glpQ</i>	Core
Oxidative phosphorylation								
D9Q8I5_CORP1	Cytochrome aa3 controlling protein	676.2	6	1.28	1	MEM	<i>Cp1002_1095</i>	Core
Specific metabolic pathways								
D9Q5M9_CORP1	Inositol-3-phosphate synthase	7473.38	18	2.25	1	CYT	<i>ino1</i>	Core
D9Q721_CORP1	Hypothetical protein	4602.9	17	1.44	1	SEC	<i>Cp1002_0573</i>	Core
D9Q689_CORP1	3-Hydroxyisobutyrate dehydrogenase	2137.24	12	1.34	1	CYT	<i>mmsB</i>	Core
D9Q4X1_CORP1	Urease accessory protein UreG	1532.39	12	-1.6	0	CYT	<i>ureG</i>	Core
Nucleotide metabolism								
D9Q4S2_CORP1	Orotate phosphoribosyltransferase	2618.52	8	-1.26	0	CYT	<i>pyrE</i>	Core
Unknown function								
D9Q6Y9_CORP1	Hypothetical protein	491.89	10	2.87	1	CYT	<i>Cp1002_0540</i>	Core
D9Q6C7_CORP1	Hypothetical protein	689.6	25	2.25	1	PSE	<i>Cp1002_0320</i>	Core
D9Q3P3_CORP1	Hypothetical protein	5703.38	3	1.87	1	CYT	<i>Cp1002_1474</i>	Core
D9Q5V4_CORP1	Hypothetical protein	994.52	1	1.7	1	CYT	<i>Cp1002_0143</i>	Core
D9Q610_CORP1	Hypothetical protein	27217.36	2	1.67	1	CYT	<i>Cp1002_0202</i>	Core
D9Q8D8_CORP1	Hypothetical protein	2324.12	7	1.57	0.98	CYT	<i>Cp1002_1048</i>	Shared
D9Q6W1_CORP1	Hypothetical protein	9303.91	4	1.54	1	CYT	<i>Cp1002_0512</i>	Core
D9Q6V5_CORP1	Hypothetical protein	1346.2	4	1.5	0.99	CYT	<i>Cp1002_0506</i>	Core
D9Q5R7_CORP1	Hypothetical protein	2090.7	8	1.42	1	CYT	<i>Cp1002_0105</i>	Core
D9Q917_CORP1	Hypothetical protein	555.89	10	1.37	1	PSE	<i>Cp1002_1281</i>	Core
D9Q3P5_CORP1	Hypothetical protein	1121.7	6	1.29	1	SEC	<i>Cp1002_1476</i>	Core
D9Q7U5_CORP1	Hypothetical protein	517.06	8	1.28	1	CYT	<i>Cp1002_0852</i>	Core
D9Q7L1_CORP1	Hypothetical protein	15693.97	6	1.28	1	SEC	<i>Cp1002_0766</i>	Core
D9Q3P6_CORP1	Hypothetical protein	1729.59	5	1.22	1	CYT	<i>Cp1002_1477</i>	Core
D9Q6Z7_CORP1	Hypothetical protein	1835.7	13	1.22	1	CYT	<i>Cp1002_0548</i>	Core
D9Q8V8_CORP1	Hypothetical protein	293.23	8	-1.48	0		<i>Cp1002_1221</i>	Core
D9Q6C8_CORP1	Hypothetical protein	413.31	12	-1.52	0	PSE	<i>Cp1002_0321</i>	Core
D9Q5H0_CORP1	Hypothetical protein	12376.2	6	-1.71	0	CYT	<i>Cp1002_0007</i>	Core
D9Q4D5_CORP1	Hypothetical protein	10161.64	4	-4.29	0	CYT	<i>Cp1002_1721</i>	Shared
Others								
D9Q5N5_CORP1	Iron-regulated MEM protein	992.54	8	2.01	0	PSE	<i>piuB</i>	Core
D9Q922_CORP1	CobW/HypB/UreG, nucleotide-binding	1771.22	20	1.88	1	CYT	<i>Cp1002_1286</i>	Core

Table 1 Proteins identified as differentially-expressed following exposure to nitrosative stress (Continued)

D9Q8C4_CORP1	Prokaryotic ubiquitin-like protein Pup	2194.86	1	1.84	1	CYT	pup	Core
D9Q7B8_CORP1	Ribosomal-protein-alanine n-acetyltransferase	2791.1	10	1.34	1	CYT	rimJ	Shared
D9Q7K9_CORP1	Arsenate reductase	5147.54	8	1.32	1	CYT	arsC	Core

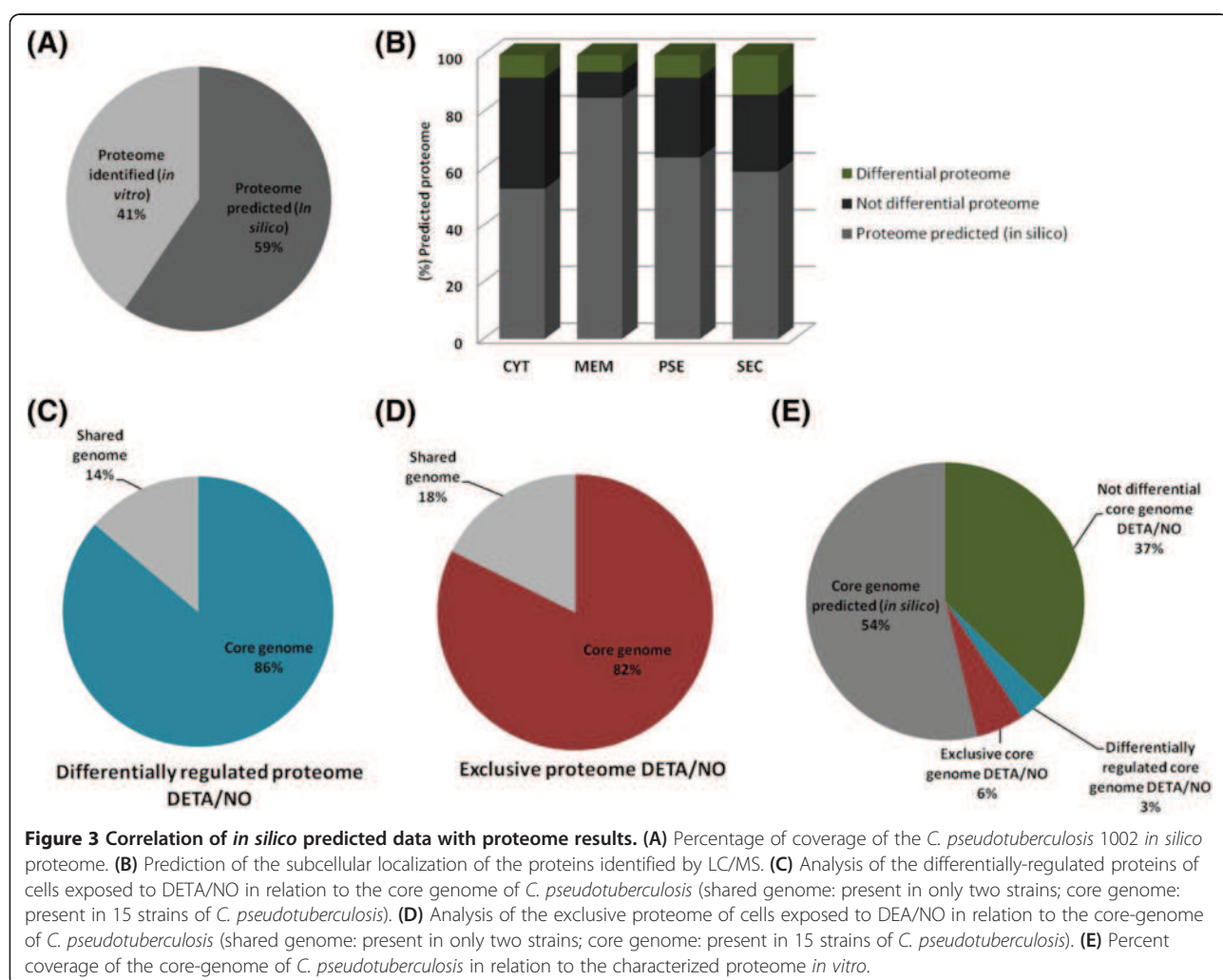
(a) Ratio values to: strain 1002_DETA/NO:strain 1002_Ct, Log(2) Ratio > 1.5, $p > 0.95$ = up-regulation, $p < 0.05$ = down-regulation.

(b) Core-genome analysis of 15 strains of *C. pseudotuberculosis*: shared = present in two or more strains; core = present in 15 strains of *C. pseudotuberculosis*.

(c) CYT =cytoplasmic, MEM = membrane, PSE = potentially surface-exposed, SEC = secreted.

the SOS response the more regulatory network encoded by prokaryotic involved in DNA repair [32]. The RecBC system acts in the recombination or degradative repair of arrested DNA replication forks. Studies in *S. Typhimurium* showed that *recBC* mutant strains are more attenuated than *recA* mutants in a murine model of infection [33]. In addition, unlike *recA* mutants, *recBC* mutants were susceptible to RNS [34], indicating that RecBC is highly important in the bacterial response to nitrosative stress. The LexA repressor (D9Q8W2_CORP1),

which forms part of the general SOS system along with RecA [35], was down-regulated in *C. pseudotuberculosis* cells exposed to DETA/NO. We also detected the RecA protein (D9Q8Y3_CORP1); however, despite having a *p*-value <0.05, the fold-change of -0.50 showed that this protein was not activated under the experimental conditions. Studies performed in *Mycobacterium tuberculosis* showed that *recA* was not induced until cells had been exposed to DETA/NO (0.5 mM) for 4 h, but that hydrogen peroxide induced the immediate expression of *recA* [36], suggesting



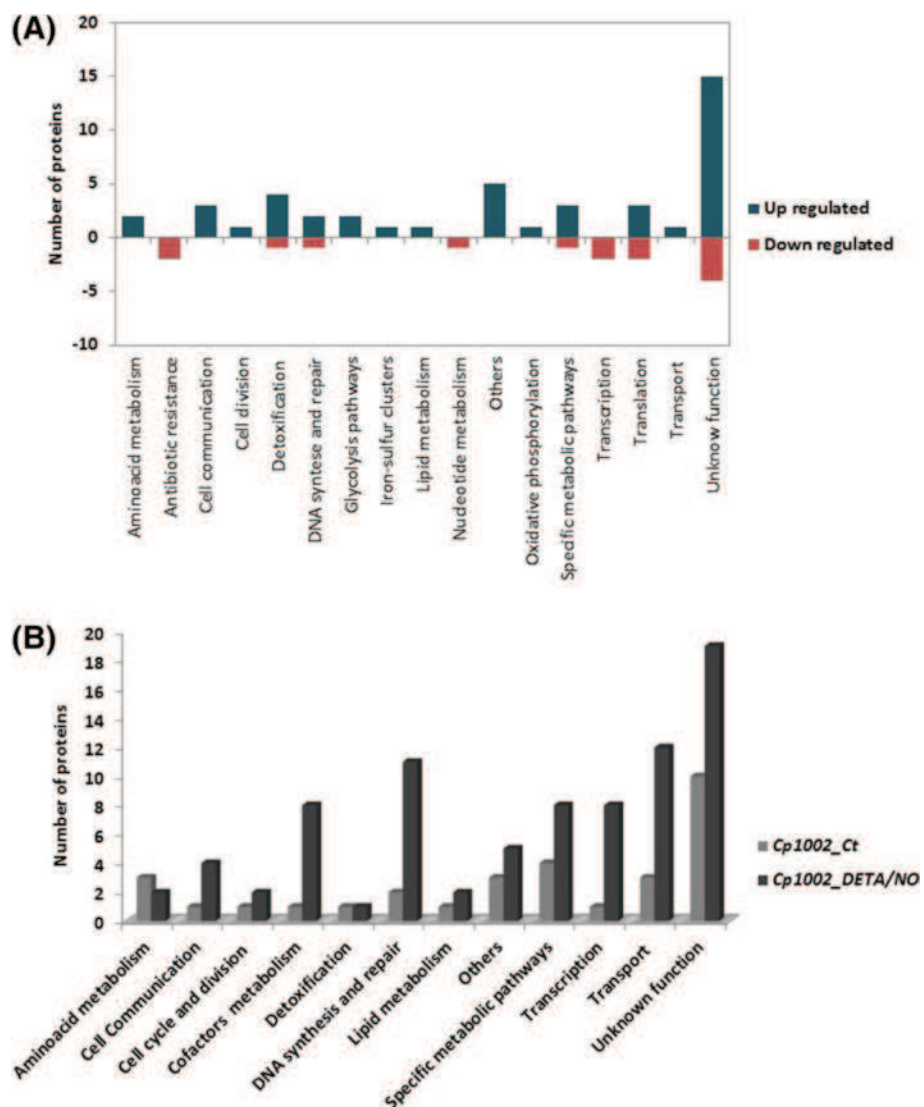


Figure 4 Comparison of biological processes between control and DETA/NO conditions. A representation of the biological processes in relation to a set list of proteins identified as (A) differentially-regulated in DETA/NO-stressed cells and (B) comparison of exclusive biological process between the two test conditions.

that RecA is involved in the later stages of the nitrosative stress response. Nevertheless, CMRegNet analysis identified other proteins that are regulated by LexA in the DETA/NO-specific proteome, including pyridoxal biosynthesis lyase (PdxS; D9Q5T9_CORP1) and DNA translocase (D9Q8Z6_CORP1).

NO-sensitive transcriptional regulators are activated in the presence of NO

To activate these DNA repair systems, it is essential that bacteria can detect ROS and RNS, and concomitantly activate the transcriptional regulators needed for the expression of genes involved in protection against these compounds. In the DETA/NO-specific proteome, we detected the transcription factor WhiB (D9Q6Y2_CORP1). The WhiB

transcriptional family is composed of iron-sulfur (Fe-S) cluster proteins. These proteins are O₂- and NO-sensitive, and allow the sensing of both external environmental signals and the redox state for intracellular bacteria [37,38]. In *M. tuberculosis*, the reaction of the iron-sulfur cluster of WhiB3 with NO generates a dinitrosyl iron complex (DNIC), which activates a sensing mechanism in response to the NO, consequently activating a system of defense against nitrosative stress [12]. In addition, other *in vivo* and *in vitro* studies have also demonstrated that WhiB regulators play a role in the adaptation and survival of *M. tuberculosis* during exposure to redox environments [12,39-41].

We identified other regulators that are activated in response to environmental stimuli, such as a MerR-family transcriptional regulator (D9Q889_CORP1) and a LysR-

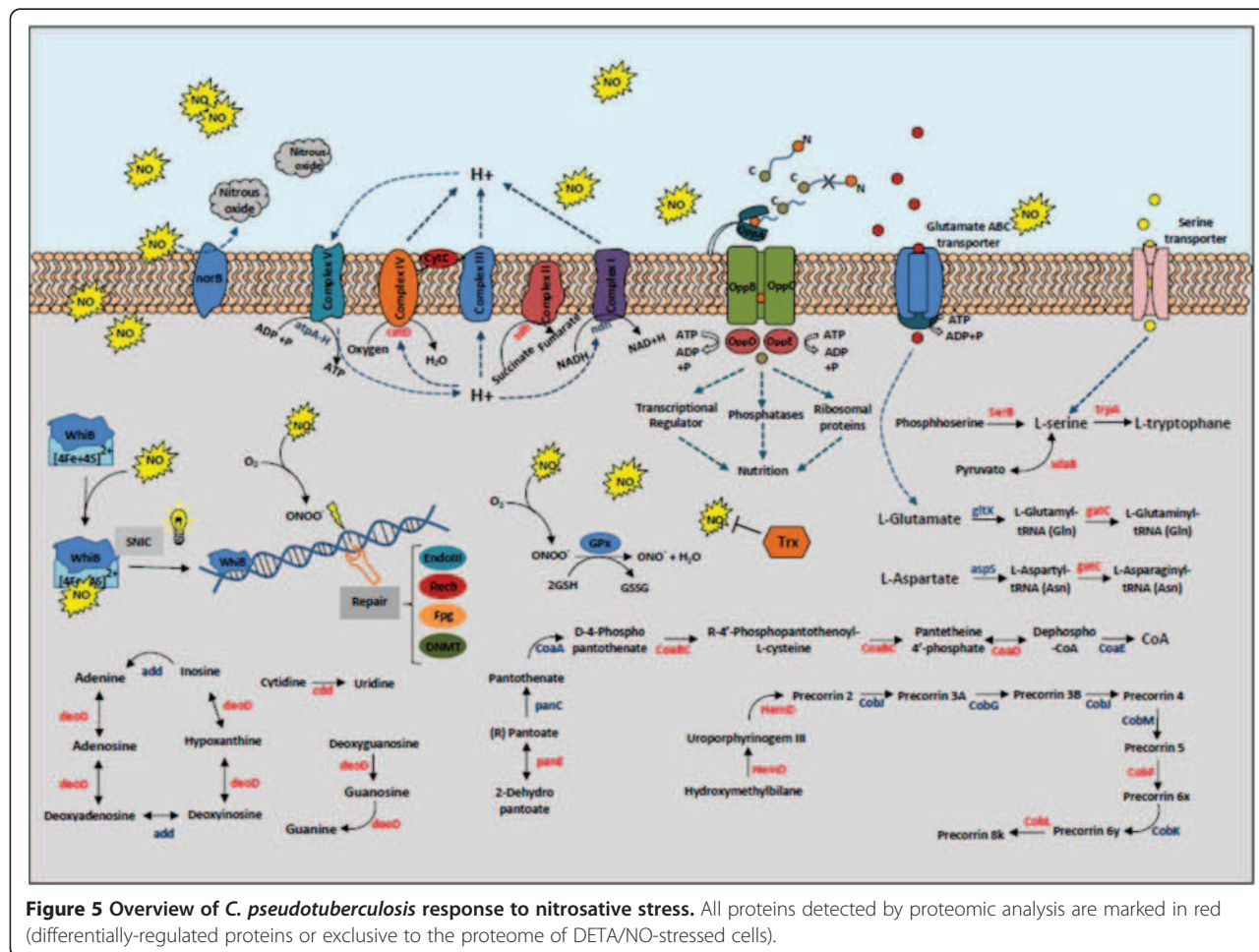


Figure 5 Overview of *C. pseudotuberculosis* response to nitrosative stress. All proteins detected by proteomic analysis are marked in red (differentially-regulated proteins or exclusive to the proteome of DETA/NO-stressed cells).

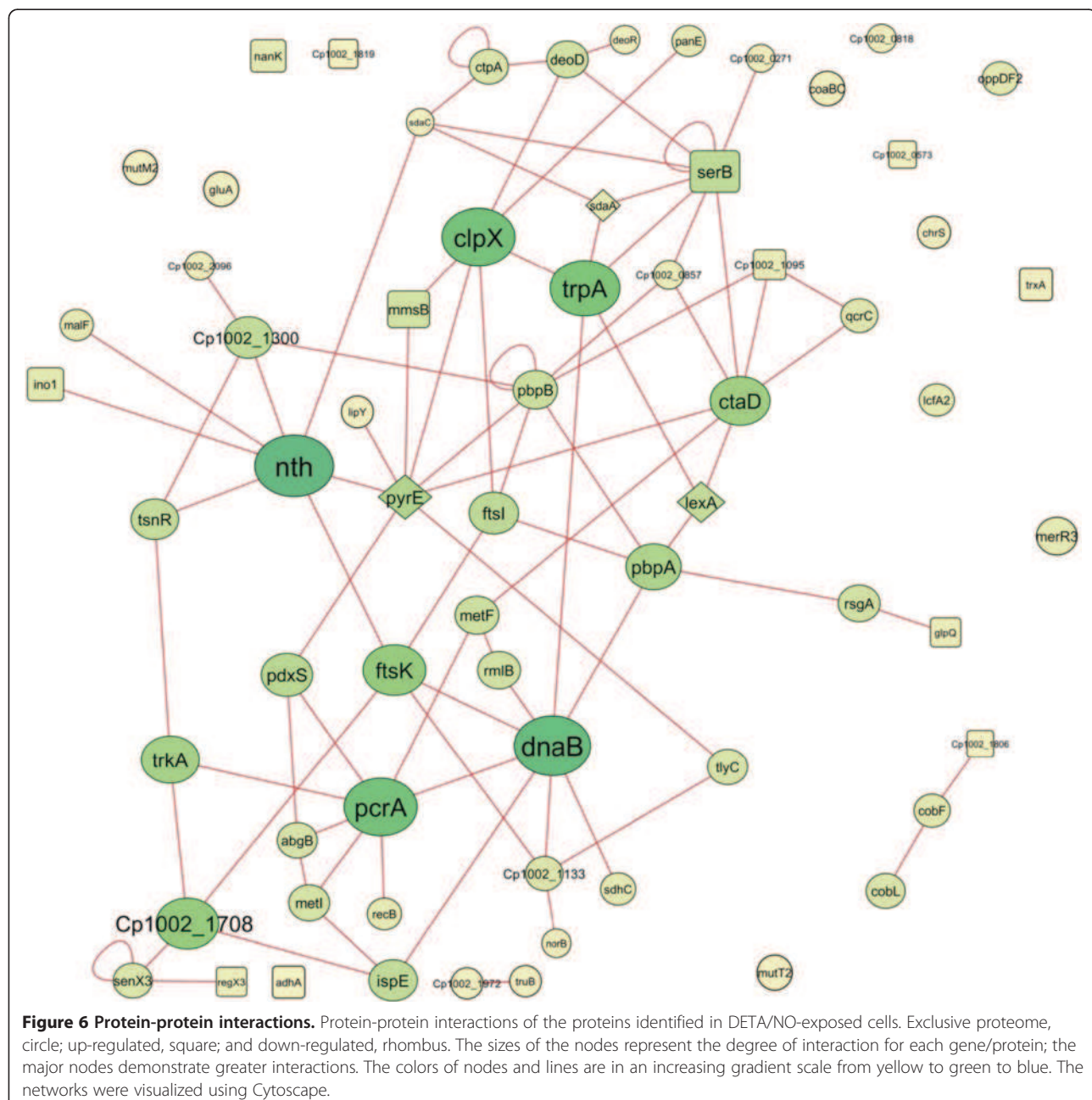
type transcriptional regulator (LTTR) (D9Q7H8_CORP1). This regulator was also highly expressed in the transcriptional response of *C. pseudotuberculosis* 1002 to acid stress [8]. MerR-type regulators have been described in the detoxification of toxic metal in several pathogenic and non-pathogenic bacteria [42]. Other studies have shown that this class of regulator plays a role in bacterial resistance to oxidative and nitrosative stress [43,44]. LTTRs are associated with the regulation of several biological processes, as well as in the adaptive response of bacteria to different types of stress [45]. In *Vibrio cholerae*, LTTRs are associated with efflux pump regulation, which contribute to antimicrobial resistance, and are involved in colonization of the human host [46]. In pathogens like *E. coli* [47], *Enterococcus faecalis* [48], *S. enterica* [49], and *Pseudomonas aeruginosa* [50], LTTRs are involved in resistance to oxidative stress.

The detoxification pathways of *C. pseudotuberculosis* following NO exposure

Our proteomic analysis identified proteins specifically expressed by cells exposed to DETA/NO that are involved

in the detoxification process. Two of these proteins were thioredoxin (*trxA*) (D9Q7U6_CORP1) and glutathione peroxidase (D9Q4E5_CORP1). The thioredoxin and glutathione systems play major roles in thiol and disulfide balance, respectively [14]. In pathogens such as *Helicobacter pylori*, *Streptococcus pyogenes*, and *M. tuberculosis*, this system is of great importance in combating the presence of ROS/RNS [36,51,52]. A glyoxalase/dioxygenase (D9Q5T5_CORP1) was identified in the differential proteome of cells exposed to DETA/NO. This protein was previously detected in the proteome of *C. pseudotuberculosis* strain 1002 in response to 0.1 mM DETA/NO [15]. The presence of this protein suggests that glyoxalase/dioxygenase plays a role in the resistance of this pathogen to nitrosative stress.

Nevertheless, unlike *P. aeruginosa*, which contains a complete denitrification pathway [53], the predicted genome of *C. pseudotuberculosis ovis* 1002 revealed a truncated denitrification pathway. However, we detected the nitric-oxide reductase cytochrome b (NorB) (D9Q5T6_CORP1) in the exclusive proteome of DETA/NO-stressed cells. *norB*, which codes for this nitric-oxide reductase, is organized into the *norCBQDEF* operon in *Paracoccus*



denitrificans [54], and into the *norCBD* operon in *P. aeruginosa* [55]. The *C. pseudotuberculosis* genome was predicted to only contain *norB*. Moreover, *norB* is located in the *Cp1002PiCp12* pathogenicity island, suggesting horizontal acquisition of the gene by this pathogen. Nitric-oxide reductase is an important protein in the denitrification process of some bacteria [56]. In *P. aeruginosa*, NorB plays a role in both the growth of the pathogen in the presence of NO, and in its survival in macrophages [55]. The flavohemoglobin Hmp is involved in the NO detoxification pathway in *S. Typhimurium*, and levels of Hmp are increased approximately two-fold in

macrophages [57]. Interestingly, in *N. meningitidis*, NorB levels are increased ten-fold in macrophages [58], demonstrating the great power of this protein in the detoxification process.

Metabolic profile of *C. pseudotuberculosis* in response to nitrosative stress

In addition to the presence of proteins involved in bacterial defense and detoxification pathways, strain 1002 needs to undergo metabolic adaptation to favor bacterial survival. We observed a metabolic readjustment in this pathogen in the proteomic analysis. Of the proteins

involved in central carbohydrate metabolism, we detected only phosphoglycerate mutase (D9Q533_CORP1) and N-acetylglucosamine kinase (D9Q5B6_CORP1) in the proteome of DETA/NO-exposed cells. Other essential proteins involved in glycolysis (the Embden-Meyerhof pathway), the pentose phosphate pathway, and the citric acid cycle were not detected. Similar results were found in a metabolomic study of *V. cholerae* in response to nitrosative stress [59].

However, we hypothesized that *C. pseudotuberculosis* uses oxidative phosphorylation to obtain energy. This is supported by the presence of cytochrome C oxidase polypeptide I (D9Q486_CORP1), succinate dehydrogenase cytochrome b556 subunit (D9Q650_CORP1), and ubiquinol-cytochrome C reductase cytochrome C subunit (D9Q3J7_CORP1) in the exclusive proteome of DETA/NO-stressed cells, and by the up-regulation of the cytochrome oxidase assembly protein (D9Q8I5_CORP1) under the same conditions. However, this oxidative phosphorylation may be associated with the bacterial culture conditions used in this work, in which *C. pseudotuberculosis* was cultivated in the presence of DETA/NO under aerobic conditions. Studies have shown that growing *M. tuberculosis* in a low concentration of NO with low levels of O₂ can induce anaerobic respiration as a result of the inhibition of the respiratory proteins cytochrome c oxidase and NADH reductase by irreversible ligation of NO. The ligation of NO to the respiratory proteins is an effect that may be both short-term reversible and long-term irreversible [60]. Thus, we suggest that activation of the oxidative phosphorylation system may be a more effective pathway for this pathogen to obtain energy [61].

Another metabolic adjustment was observed in relation to amino acid biosynthesis. Transporters and enzymes involved in the synthesis of methionine, tryptophan, and serine were identified. However, the presence of these proteins can be associated with the bioavailability of these amino acids during exposure to NO. In addition, we detected two oligopeptide transport ATP-binding proteins (OppD) (D9Q6G5_CORP1/D9Q3X0_CORP1) that compose the oligopeptide permease system (Opp). This complex is associated with the internalization of peptides from the extracellular environment to be used as a source of carbon and nitrogen in bacterial nutrition [62]. We also identified proteins that are cofactors of metabolism, such as CoaBC (D9Q8L2_CORP1), phosphopantetheine adenylyltransferase (D9Q809_CORP1), and 2-dehydropantoate 2-reductase (D9Q7J9_CORP1). The presence of these proteins demonstrates activity in pantothenic acid metabolism and the biosynthesis of coenzyme A (CoA). Studies performed in species such as *Corynebacterium diphtheriae* [63], *Streptococcus haemolyticus* [64], and *M. tuberculosis* [65] showed that pantothenic

acid and CoA could have an important role in the growth and viability of these pathogens.

Conclusions

In this work, we applied high-throughput proteomics to characterize the proteome of *C. pseudotuberculosis ovis* 1002 following exposure to NO. Our proteomic analysis generated two profiles, which together validated findings from previous *in silico* analyses of *C. pseudotuberculosis ovis* 1002. The proteomic profile generated after the addition of the NO-donor, DETA/NO (0.5 mM), revealed a set of proteins that are involved in distinct biological process. We detected proteins related to both the general stress response and to a more specific nitrosative stress response, which together form a network of factors that promote the survival of this pathogen under stress conditions. However, more detailed studies are needed to assess the true role of these proteins in response to nitrosative stress in *C. pseudotuberculosis*. In conclusion, this functional analysis of the genome of *C. pseudotuberculosis* shows the versatility of this pathogen in the presence of NO. Moreover, the results presented in this study provide insights into the processes of resistance of *C. pseudotuberculosis* during exposure to nitrosative stress.

Additional files

Additional file 1: Table S1. Complete list of proteins identified as significantly altered ($p < 0.05$).

Additional file 2: Table S2. Unique proteins identified in strain 1002_DETA/NO.

Additional file 3: Table S3. Unique proteins identified in strain 1002 control condition.

Abbreviations

G: Guanine; C: Citosine; NO: Nitric oxide; RNS: Reactive nitrogen species; NOS: Nitric oxide synthases; LC-HDMS^E: Liquid chromatograph high definition mass spectrometry; LC/MS: Liquid chromatograph mass spectrometry; CDM: Chemically-defined medium; DETA/NO: Diethylenetriamine/nitric oxide adduct; DTT: Dithiothreitol; 2D-RP: Two-dimensional reversed phase; nanoUPLC: Nano Ultra performance liquid chromatography; nanoESI-HDMS: Nano electrospray high definition mass spectrometry; HSS: High strength silica; PLGS: Protein lynx global server; FDR: False discovery rate.

Competing interests

The authors declare that they have no competing interests.

Authors' contributions

WMS, RDC, and IFSB performed microbiological analyses and sample preparation for proteomic analysis. GHMFS and WMS conducted the proteomic analysis. SCS and ELF performed bioinformatics analysis of the data. YLL and AM contributed substantially to data interpretation and revisions. VA and AS participated in all steps of the project as coordinators, and critically reviewed the manuscript. All authors read and approved the final manuscript.

Acknowledgements

This work was supported by the Genomics and Proteomics Network of the State of Pará of the Federal University of Pará, the Amazon Research Foundation (FAPESPA), the National Council for Scientific and Technological

Development (CNPq), the Brazilian Federal Agency for the Support and Evaluation of Graduate Education (CAPES), the Minas Gerais Research Foundation (FAPEMIG), and Waters Corporation, Brazil. Yves Le Loir is the recipient of a PVE grant (71/2013) from Programa Ciências sem Fronteiras.

Author details

¹Depto de Biologia Geral, Instituto de Ciências Biológicas, Universidade Federal de Minas Gerais, Belo Horizonte, Brazil. ²Instituto de Ciências Biológicas, Universidade Federal do Pará, Belém, Pará, Brazil. ³Waters Corporation, MS Applications and Development Laboratory, São Paulo, Brazil. ⁴Institut National de la Recherche Agronomique - INRA, UMR1253 STLO, Rennes 35042, France. ⁵Agrocampus Ouest, UMR1253 STLO, Rennes 35042, France.

Received: 4 September 2014 Accepted: 24 November 2014

Published: 4 December 2014

References

- Dorella FA, Pacheco LG, Oliveira SC, Miyoshi A, Azevedo V: *Corynebacterium pseudotuberculosis*: microbiology, biochemical properties, pathogenesis and molecular studies of virulence. *Vet Res* 2006, 37:201–218.
- Baird GJ, Fontaine MC: *Corynebacterium pseudotuberculosis* and its role in ovine caseous lymphadenitis. *J Comp Pathol* 2007, 137:179–210.
- Hodgson AL, Bird P, Nisbet JT: Cloning, nucleotide sequence, and expression in *Escherichia coli* of the phospholipase D gene from *Corynebacterium pseudotuberculosis*. *J Bacteriol* 1990, 172:1256–1261.
- Hard GC: Comparative toxic effect of the surface lipid of *Corynebacterium ovis* on peritoneal macrophages. *Infect Immun* 1975, 12:1439–1449.
- Billington SJ, Esmay PA, Songer JG, Jost BH: Identification and role in virulence of putative iron acquisition genes from *Corynebacterium pseudotuberculosis*. *J Bacteriol* 2002, 180:3233–3236.
- Ruiz JC, D'Afonseca V, Silva A, Ali A, Pinto AC, Santos AR, Rocha AA, Lopes DO, Dorella FA, Pacheco LG, Costa MP, Turk MZ, Seyffert N, Moraes PM, Soares SC, Almeida SS, Castro TL, Abreu VA, Trost E, Baumbach J, Tauch A, Schneider MP, McCulloch J, Cerdeira LT, Ramos RT, Zerlotini A, Dominitini A, Resende DM, Coser EM, Oliveira LM, et al: Evidence for reductive genome evolution and lateral acquisition of virulence functions in two *Corynebacterium pseudotuberculosis* strains. *PLoS One* 2011, 6:e21851.
- Soares SC, Silva A, Trost E, Blom J, Ramos R, Carneiro A, Ali A, Santos AR, Pinto AC, Diniz C, Barbosa EG, Dorella FA, Aburjaile F, Rocha FS, Nascimento KK, Guimarães LC, Almeida S, Hassan SS, Bakhtiar SM, Pereira UP, Abreu VA, Schneider MP, Miyoshi A, Tauch A, Azevedo V: The pan-genome of the animal pathogen *Corynebacterium pseudotuberculosis* reveals differences in genome plasticity between the biovar *ovis* and *equi* strains. *PLoS One* 2013, 8:e53818.
- Pinto AC, de Sá PH, Ramos RT, Barbosa S, Barbosa HP, Ribeiro AC, Silva WM, Rocha FS, Santana MP, de Paula Castro TL, Miyoshi A, Schneider MP, Silva A, Azevedo V: Differential transcriptional profile of *Corynebacterium pseudotuberculosis* in response to abiotic stresses. *BMC Genomics* 2014, 15:914.
- Marletta MA: Nitric oxide synthase: aspects concerning structure and catalysis. *Cell* 1994, 77:927–930.
- Griffith OW, Stueh DJ: Nitric oxide synthases: properties and catalytic mechanism. *Annu Rev Physiol* 1995, 57:707–736.
- Nathan C, Shihol MU: Reactive oxygen and nitrogen intermediates in the relationship between mammalian hosts and microbial pathogens. *Proc Natl Acad Sci USA* 2000, 97:8841–8848.
- Singh A, Guidry L, Narasimhulu KV, Mai D, Trombley J, Redding KE, Giles GL, Lancaster JR Jr, Steyn AJ: *Mycobacterium tuberculosis* WhiB3 responds to O₂ and nitric oxide via its [4Fe–4S] cluster and is essential for nutrient starvation survival. *Proc Natl Acad Sci USA* 2007, 104:11562–11567.
- Ehrt S, Schnappinger D: Mycobacterial survival strategies in the phagosome: defence against host stresses. *Cell Microbiol* 2009, 11:1170–1178.
- Lu J, Holmgren A: The thioredoxin antioxidant system. *Free Radic Biol Med* 2013, 103:75–87.
- Pacheco LG, Castro TL, Carvalho RD, Moraes PM, Dorella FA, Carvalho NB, Slade SE, Scrivens JH, Feelisch M, Meyer R, Miyoshi A, Oliveira SC, Dowson CG, Azevedo V: A role for sigma factor σ^F in *Corynebacterium pseudotuberculosis* resistance to nitric oxide/peroxide stress. *Front Microbiol* 2012, 3:126.
- Moura-Costa LF, Paule BJA, Freire SM, Nascimento I, Schaer R, Regis LF, Vale VLC, Matos DP, Bahia RC, Carminati R, Meyer R: Chemically defined synthetic medium for *Corynebacterium pseudotuberculosis* culture. *Rev Bras Saude Publica* 2002, 36:1–9.
- Silva JC, Gorenstein MV, Li GZ, Vissers JP, Geromanos SJ: Absolute quantification of proteins by LC/MS⁵: a virtue of parallel MS acquisition. *Mol Cell Proteomics* 2006, 5:144–156.
- Gilar M, Olivova P, Daly AE, Gebler JC: Two-dimensional separation of peptides using RP-RP-HPLC system with different pH in first and second separation dimensions. *J Sep Sci* 2005, 28:1694–1703.
- Silva JC, Denny R, Dorschel CA, Gorenstein M, Kass IJ, Li GZ, McKenna T, Nold MJ, Richardson K, Young P, Geromanos S: Quantitative proteomic analysis by accurate mass retention time pairs. *Anal Chem* 2005, 77:2187–2000.
- Geromanos SJ, Vissers JP, Silva JC, Dorschel CA, Li GZ, Gorenstein MV, Bateman RH, Langridge JL: The detection, correlation, and comparison of peptide precursor and product ions from data independent LC-MS with data dependent LC-MS/MS. *Proteomics* 2009, 9:1683–1695.
- Li GZ, Vissers JP, Silva JC, Golick D, Gorenstein MV, Geromanos SJ: Database searching and accounting of multiplexed precursor and product ion spectra from the data independent analysis of simple and complex peptide mixtures. *Proteomics* 2009, 9:1696–1719.
- Curty N, Kubitschek-Barreira PH, Neves GW, Gomes D, Pizzatti L, Abdelhay E, Souza GH, Lopes-Bezerra LM: Discovering the infectome of human endothelial cells challenged with *Aspergillus fumigatus* applying a mass spectrometry label-free approach. *J Proteomics* 2014, 31:126–140.
- Levin Y, Hadetzyk E, Bahn S: Quantification of proteins using data-independent analysis (MSE) in simple and complex samples: a systematic evaluation. *Proteomics* 2011, 11:3273–3287.
- Barinov A, Loux V, Hammani A, Nicolas P, Langella P, Ehrlich D, Maguin E, van de Gucht M: Prediction of surface exposed proteins in *Streptococcus pyogenes*, with a potential application to other Gram-positive bacteria. *Proteomics* 2009, 9:61–73.
- Conesa A, Gotz S, García-Gómez JM, Terol J, Talón M, Robles M: Blast2GO: a universal tool for annotation, visualization and analysis in functional genomics research. *Bioinformatics* 2005, 21:3674–3676.
- Soares SC, Abreu VA, Ramos RT, Cerdeira L, Silva A, Baumbach J, Trost E, Tauch A, Hirata R Jr, Mattos-Guaraldi AL, Miyoshi A, Azevedo V: PIPs: pathogenicity island prediction software. *PLoS One* 2012, 7:e30848.
- Rezende AM, Folador EL, Resende Dde M, Ruiz JC: Computational prediction of protein-protein interactions in *Leishmania* predicted proteomes. *PLoS One* 2012, 7:e51304.
- Shannon P, Markiel A, Ozier O, Baliga NS, Wang JT, Ramage D, Amin N, Schwikowski B, Ideker T: Cytoscape: a software environment for integrated models of biomolecular interaction networks. *Genome Res* 2003, 13:2498–2504.
- Pauling J, Röttger R, Tauch A, Azevedo V, Baumbach J: CoryneRegNet 6.0 -Updated database content, new analysis methods and novel features focusing on community demands. *Nucleic Acids Res* 2012, 40:D610–D614.
- Richardson AR, Soliven KC, Castor ME, Barnes PD, Libby SJ, Fang FC: The base excision repair system of *Salmonella enterica* serovar *typhimurium* counteracts DNA damage by host nitric oxide. *PLoS Pathog* 2009, 5:e1000451.
- Sedgwick B: Repairing DNA-methylation damage. *Nat Rev Mol Cell Biol* 2004, 5:148–157.
- Baharoglu Z, Mazel D: SOS, the formidable strategy of bacteria against aggressions. *FEMS Microbiol Rev* 2014, 38:1126–1145.
- Cano DA, Pucciarelli MG, García-del Portillo F, Casadesús J: Role of the recBCD recombination pathway in *Salmonella* virulence. *J Bacteriol* 2002, 184:592–595.
- Koskinen M, Andersson Di: Translesion DNA polymerases are required for spontaneous deletion formation in *Salmonella typhimurium*. *Proc Natl Acad Sci U S A* 2009, 106:10248–10253.
- Butala M, Zgur-Bertok D, Busby SJ: The bacterial LexA transcriptional repressor. *Cell Mol Life Sci* 2009, 66:82–93.
- Voskuil MI, Bartek IL, Visconti K, Schoolnik GK: The response of *Mycobacterium tuberculosis* to reactive oxygen and nitrogen species. *Front Microbiol* 2011, 2:105.
- Green J, Paget MS: Bacterial redox sensors. *Nat Rev Microbiol* 2004, 2:954–966.
- Green J, Rolfe MD, Smith LJ: Transcriptional regulation of bacterial virulence gene expression by molecular oxygen and nitric oxide. *Virulence* 2014, 5:4(4).
- Singh A, Crossman DK, Mai D, Guidry L, Voskuil MI, Renfrow MB, Steyn AJ: *Mycobacterium tuberculosis* WhiB3 maintains redox homeostasis by regulating virulence lipid anabolism to modulate macrophage response. *PLoS Pathog* 2009, 5:e1000545.
- Chawla M, Parikh P, Saxena A, Munshi M, Mehta M, Mai D, Srivastava AK, Narasimhulu KV, Redding KE, Vashi N, Kumar D, Steyn AJ, Singh A:

- Mycobacterium tuberculosis* WhiB4 regulates oxidative stress response to modulate survival and dissemination *in vivo*. *Mol Microbiol* 2012, 85:1148–1165.
41. Larsson C, Luna B, Ammerman NC, Maiga M, Agarwal N, Bishai WR: Gene expression of *Mycobacterium tuberculosis* putative transcription factors WhiB1-7 in redox environments. *PLoS One* 2012, 7:e37516.
 42. Hobman JL: MerR family transcription activators: similar designs, different specificities. *Mol Microbiol* 2007, 63:1275–1278.
 43. McEwan AG, Djoko KY, Chen NH, Couffago RL, Kidd SP, Potter AJ, Jennings MP: Novel bacterial MerR-like regulators their role in the response to carbonyl and nitrosative stress. *Adv Microb Physiol* 2011, 58:1–22.
 44. Brown NL, Stoyanov JV, Kidd SP, Hobman JL: The MerR family of transcriptional regulators. *FEMS Microbiol Rev* 2003, 27:145–163.
 45. Maddocks SE, Oyston PC: Structure and function of the LysR-type transcriptional regulator (LTTR) family proteins. *Microbiology* 2008, 154:3609–3623.
 46. Chen S, Wang H, Katziyaner DS, Zhong Z, Zhu J: LysR family activator-regulated major facilitator superfamily transporters are involved in *Vibrio cholerae* antimicrobial compound resistance and intestinal colonisation. *Int J Antimicrob Agents* 2013, 41:188–192.
 47. Gonzalez-Flecha B, Demple B: Role for the oxyS gene in regulation of intracellular hydrogen peroxide in *Escherichia coli*. *J Bacteriol* 1999, 181:3833–3836.
 48. Verneuil N, Rincé A, Sanguinetti M, Posteraro B, Fadda G, Auffray Y, Hartke A, Giard JC: Contribution of a PerR-like regulator to the oxidative-stress response and virulence of *Enterococcus faecalis*. *Microbiology* 2005, 151:3997–4004.
 49. Lahiri A, Das P, Chakravortty D: The LysR-type transcriptional regulator Hrg counteracts phagocyte oxidative burst and imparts survival advantage to *Salmonella enterica* serovar Typhimurium. *Microbiology* 2008, 154:2837–2846.
 50. Reen FJ, Haynes JM, Mooij MJ, O'Gara F: A non-classical LysR-type transcriptional regulator PA2206 is required for an effective oxidative stress response in *Pseudomonas aeruginosa*. *PLoS One* 2013, 8:e54479.
 51. Comtois SL, Gidley MD, Kelly DJ: Role of the thioredoxin system and the thiol-peroxidases Tpx and Bcp in mediating resistance to oxidative and nitrosative stress in *Helicobacter pylori*. *Microbiology* 2003, 149:121–129.
 52. Brenot A, King KY, Janowiak B, Griffith O, Caparon MG: Contribution of glutathione peroxidase to the virulence of *Streptococcus pyogenes*. *Infect Immun* 2004, 72:408–413.
 53. Kalkowski I, Conrad R: Metabolism of nitric oxide in denitrifying *Pseudomonas aeruginosa* and nitrate-respiring *Bacillus cereus*. *FEMS Microbiol Lett* 1991, 15:107–111.
 54. de Boer AP, van der Oost J, Reijnders WN, Westerhoff HV, Stouthamer AH, van Spanning RJ: Mutational analysis of the nor gene cluster which encodes nitric-oxide reductase from *Paracoccus denitrificans*. *Eur J Biochem* 1996, 15:592–600.
 55. Kakishima K, Shiratsuchi A, Taoka A, Nakanishi Y, Fukumori Y: Participation of nitric oxide reductase in survival of *Pseudomonas aeruginosa* in LPS-activated macrophages. *Biochem Biophys Res Commun* 2007, 6:587–591.
 56. Hendriks J, Oubrie A, Castresana J, Urbani A, Gemeinhart S, Saraste M: Nitric oxide reductases in bacteria. *Biochim Biophys Acta* 2000, 15:266–273.
 57. Stevanin TM, Poole RK, Demoncheaux EA, Read RC: Flavohemoglobin Hmp protects *Salmonella enterica* serovar Typhimurium from nitric oxide-related killing by human macrophages. *Infect Immun* 2002, 70:4399–4405.
 58. Stevanin TM, Moir JW, Read RC: Nitric oxide detoxification systems enhance survival of *Neisseria meningitidis* in human macrophages and in nasopharyngeal mucosa. *Infect Immun* 2005, 73:3322–3329.
 59. Stern AM, Liu B, Bakken LR, Shapleigh JP, Zhu J: A novel protein protects bacterial iron-dependent metabolism from nitric oxide. *J Bacteriol* 2013, 195:4702–4708.
 60. Brown GC: Regulation of mitochondrial respiration by nitric oxide inhibition of cytochrome C oxidase. *Biochim Biophys Acta* 2001, 1:46–57.
 61. Kadenbach B: Intrinsic and extrinsic uncoupling of oxidative phosphorylation. *Biochim Biophys Acta* 2003, 5:77–94.
 62. Payne JW, Smith MW: Peptide transport by micro-organisms. *Adv Microb Physiol* 1994, 36:1–80.
 63. Mueller JH, Klotz AW: Pantothenic acid as a growth factor for the diphtheria bacillus. *J Am Chem Soc* 1938, 60:3086–3087.
 64. McLwain H: Pantothenic acid and the growth of *Streptococcus haemolyticus*. *Br J Exp Pathol* 1939, 20:330–333.
 65. Sassetti CM, Boyd DH, Rubin EJ: Genes required for mycobacterial growth defined by high density mutagenesis. *Mol Microbiol* 2003, 48:77–84.

doi:10.1186/1471-2164-15-1065

Cite this article as: Silva et al.: Label-free proteomic analysis to confirm the predicted proteome of *Corynebacterium pseudotuberculosis* under nitrosative stress mediated by nitric oxide. *BMC Genomics* 2014 15:1065.

Submit your next manuscript to BioMed Central and take full advantage of:

- Convenient online submission
- Thorough peer review
- No space constraints or color figure charges
- Immediate publication on acceptance
- Inclusion in PubMed, CAS, Scopus and Google Scholar
- Research which is freely available for redistribution

Submit your manuscript at
www.biomedcentral.com/submit



5.2.1 Supplementary file:

Table S.1 (see, Annex 2 – pag. 240)

Table S.2: Unique proteins identified in strain 1002_DETA/NO

Accession Uniprot	Description	Score	Peptides	Average (%)	Subcellular localization ^(c)	Gene name	Genome ^(b)
Antibiotic resistance							
D9Q376_CORP1	SEC penicillin-binding protein	203,84	20	26.59	SEC	<i>pbpA</i>	Core
D9Q7R4_CORP1	Multiple antibiotic resistance protein marR	3778,88	10	38.81	CYT	<i>marR</i>	Shared
D9Q8Q1_CORP1	Metallo-beta-lactamase superfamily protein	6020,12	9	56.13	CYT	<i>glob1</i>	Core
D9Q3H2_CORP1	Penicillin-binding protein	315,05	20	29.82	PSE	<i>ftsl</i>	Core
D9Q5J8_CORP1	Penicillin-binding protein A	296,31	7	14.19	SEC	<i>pbpB</i>	Core
D9Q642_CORP1	dTDP-glucose 4-6-dehydratase	182,08	17	58.08	CYT	<i>rmlB</i>	Core
Transport and binding proteins							
D9Q4N8_CORP1	ABC transporter	1053,23	4	12.65	MEM	<i>Cp1002_1826</i>	Core
D9Q8R0_CORP1	Preprotein translocase subunit YajC	10072,04	4	57.66	MEM	<i>yajC</i>	Core
D9Q6G5_CORP1	Oligopeptide transport ATP-binding protein	392,02	24	28.93	CYT	<i>oppD1</i>	Core
D9Q3X0_CORP1	Oligopeptide transport ATP-binding protein	212,32	24	43.60	CYT	<i>oppDF2</i>	Core
D9Q6I4_CORP1	Maltose transport system permease protein	1034,89	11	18.27	MEM	<i>malF</i>	Shared
D9Q6N7_CORP1	Methionine import system permease protein metI	1135,08	2	13.33	MEM	<i>metI</i>	Core
D9Q6H3_CORP1	Serine transporter	160,62	8	14.33	MEM	<i>sdaC</i>	Core
D9Q575_CORP1	Cation transport protein	9374,4	4	95.52	CYT	<i>Cp1002_2021</i>	Core
D9Q7R2_CORP1	ATP-binding protein	263,4	30	26.43	CYT	<i>Cp1002_0818</i>	Core
D9Q686_CORP1	Cation-transporting P-type ATPase A	96,84	27	24.37	MEM	<i>ctpA</i>	Core
D9Q4F0_CORP1	Trk system potassium uptake protein trkA	928,08	7	30.05	CYT	<i>trkA</i>	Core
D9Q795_CORP1	Glutamate ABC transporter	313,06	12	46.16	CYT	<i>gluA</i>	Core
Cell cycle and							

division								
D9Q3G4_CORP1	Cell division protein FtsQ		158,25	11	56.19	SEC	<i>ftsQ</i>	Shared
D9Q8Z6_CORP1	DNA translocase		308,68	30	33.90	PSE	<i>ftsK</i>	Shared
Glycolysis pathways								
D9Q533_CORP1	Phosphoglycerate mutase		724,72	8	36.2	CYT	<i>pgmB</i>	Core
Lipid metabolism								
D9Q4L5_CORP1	Secretory lipase		251,43	8	23.49	SEC	<i>lipY</i>	Core
D9Q7S7_CORP1	Long-chain-fatty-acid-CoA ligase		247,87	18	31.94	CYT	<i>lcfA2</i>	Core
Aminoacid metabolism								
D9Q481_CORP1	Phosphoserine phosphatase		272,46	18	39.93	CYT	<i>serB1</i>	Core
D9Q5E1_CORP1	Tryptophan synthase alpha chain		826,65	10	61.82	CYT	<i>trpA</i>	Core
Specific metabolic pathways								
D9Q527_CORP1	HAD-family hydrolase		298,03	6	12.23	CYT	<i>Cp1002_1972</i>	Core
D9Q6S1_CORP1	Aminobenzoyl-glutamate utilization protein B		319,12	11	29.77	CYT	<i>abgB</i>	Core
D9Q5C7_CORP1	Hypothetical protein		1177,82	8	26.57	CYT	<i>Cp1002_2073</i>	Core
D9Q4N5_CORP1	Acetyltransferase		1406,55	12	45.15	CYT	<i>Cp1002_1823</i>	Core
D9Q4A4_CORP1	DoxX family MEM protein		840,73	5	36.60	MEM	<i>Cp1002_1689</i>	Shared
D9Q515_CORP1	MEM-associated phospholipid phosphatase		703,28	9	59.52	MEM	<i>Cp1002_1960</i>	Shared
D9Q7D1_CORP1	4-diphosphocytidyl-2-C-methyl-D-erythritol kinase		256,05	15	68.33	CYT	<i>ispE</i>	
D9Q8M3_CORP1	Epimerase family protein		297,46	29	48.00	CYT	<i>Cp1002_1133</i>	Shared
Cofactors metabolism								
D9Q8B5_CORP1	Precorrin-6Y C5 15-methyltransferase		304,34	16	60.54	CYT	<i>cobL</i>	Core
D9Q8L2_CORP1	Coenzyme A biosynthesis bifunctional protein coaBC		197,56	18	56.11	PSE	<i>coaBC</i>	Core
D9Q777_CORP1	Precorrin-6A synthase		263,07	8	41.7	CYT	<i>cobF</i>	Core

D9Q5T9_CORP1	Pyridoxal biosynthesis lyase PdxS	4647,71	9	23.07	CYT	<i>pdxS</i>	Core
D9Q683_CORP1	Uroporphyrinogen-III synthase	271,86	27	37.81	CYT	<i>hemD</i>	Core
D9Q3I0_CORP1	Methylenetetrahydrofolate reductase	298,44	14	29.33	CYT	<i>metF</i>	Shared
D9Q7J9_CORP1	2-dehydropantoate 2-reductase	214,63	9	30.84	CYT	<i>panE</i>	Shared
D9Q809_CORP1	Phosphopantetheine adenylyltransferase	10627,4	11	76.85	CYT	<i>coaD</i>	
Starch and sucrose metabolism							
D9Q4G7_CORP1	Trehalose-phosphate phosphatase	1711,48	15	69.50	CYT	<i>otsB</i>	Shared
Nucleotide metabolism							
D9Q543_CORP1	Cytidine deaminase	1546,79	5	25.32	CYT	<i>cdd</i>	Core
D9Q5W9_CORP1	Purine nucleoside phosphorylase DeoD-type	2107,88	6	22.05	CYT	<i>deoD</i>	Core
D9Q6W3_CORP1	Thymidylate kinase	2939,09	9	29.12	CYT	<i>tmK</i>	Core
D9Q5E9_CORP1	MutT/NUDIX family protein	197,7	11	26.77	CYT	<i>Cp1002_2096</i>	Core
D9Q7V0_CORP1	NUDIX hydrolase	46,36	13	48.13	CYT	<i>Cp1002_0857</i>	Core
Oxidative phosphorylation							
D9Q486_CORP1	Cytochrome C oxidase polypeptide I	254,49	8	16.75	MEM	<i>ctaD</i>	Core
D9Q650_CORP1	Succinate dehydrogenase cytochrome b556 subunit	113,35	4	24.21	MEM	<i>sdhC</i>	Shared
D9Q3J7_CORP1	Ubiquinol-cytochrome C reductase cytochrome C subunit	180,85	11	24.83	PSE	<i>qcrC</i>	Shared
Iron-sulfur clusters							
D9Q8H6_CORP1	NifU		7	49.66	CYT	<i>nifU</i>	Core
DNA Synthesis and repair							
D9Q615_CORP1	Endonuclease III	391,57	13	31.53	CYT	<i>ntH</i>	Core
D9Q578_CORP1	Replicative DNA helicase	268,38	21	36.89	CYT	<i>dnaB</i>	Core
D9Q790_CORP1	ATP-dependent DNA helicase pcrA	277,41	26	25.94	CYT	<i>pcrA</i>	Shared

D9Q598_CORP1	Formamidopyrimidine-DNA glycosylase	870,74	10	20.64	CYT	<i>mutM2</i>	Core
D9Q8T4_CORP1	Ribonuclease D	1005,54	13	25.43	CYT	<i>rndD</i>	Core
D9Q8C9_CORP1	RecB family nuclease	2042,19	18	34.81	CYT	<i>recB</i>	Core
D9Q5W8_CORP1	Deoxyribonucleoside regulator	231,78	17	56.41	CYT	<i>deoR</i>	Core
D9Q7M7_CORP1	Glycosyl transferase group 2	729,98	9	32.99	CYT	<i>Cp1002_0782</i>	Core
D9Q679_CORP1	Haloacid dehalogenase-like hydrolase	745,79	13	36.6	CYT	<i>Cp1002_0271</i>	Core
D9Q7Z9_CORP1	7,8-dihydro-8-oxoguanine-triphosphatase	2831,62	15	41.34	CYT	<i>mutT2</i>	Core
D9Q378_CORP1	Zinc metalloprotease	169,5	11	19.18	MEM	<i>Cp1002_1300</i>	Core
Transcription							
D9Q7H8_CORP1	Transcriptional regulator LysR family	7765	10	50.21	CYT	<i>lysR</i>	Core
D9Q889_CORP1	MerR family transcriptional regulator	306,74	6	39.46	CYT	<i>merR</i>	Core
D9Q5B7_CORP1	GntR family regulatory protein	316,21	13	46.51	CYT	<i>Cp1002_2063</i>	Core
D9Q464_CORP1	Two component transcriptional regulator	831,79	10	42.30	CYT	<i>tcsR5</i>	Core
D9Q833_CORP1	rRNA methyltransferase	1425,23	9	41.40	CYT	<i>tsnR</i>	Core
D9Q6Y2_CORP1	Transcription factor WhiB	8629,19	2	34.88	CYT	<i>whiB</i>	Core
D9Q4C3_CORP1	tRNA-dihydrouridine synthase	1299,51	21	57.94	CYT	<i>Cp1002_1708</i>	Core
D9Q3I3_CORP1	Transcription regulator	5081,79	4	27.06	CYT	<i>Cp1002_1408</i>	Core
Translation							
D9Q414_CORP1	ATP-dependent Clp protease ATP-binding subunit	265,59	18	37.85	CYT	<i>clpX</i>	Core
D9Q480_CORP1	Ribosomal-protein-alanine acetyltransferase		10	40.91	CYT	<i>Cp1002_1664</i>	Core
D9Q907_CORP1	tRNA pseudouridine synthase B		9	23.76	CYT	<i>truB</i>	Core
Cell Communication							
D9Q5B0_CORP1	Two-component system histidine kinase ChrS	204,06	14	23.94	PSE	<i>chrS</i>	Core
D9Q667_CORP1	Signal-transduction histidine kinase senX3	322,78	18	38.83	PSE	<i>senX3</i>	Core
D9Q3R0_CORP1	Low molecular weight protein-tyrosine-phosphatase	5787,31	7	61.96	CYT	<i>ptpA</i>	Core
D9Q7Y7_CORP1	Signal-transduction protein containing cAMP-binding	241,47	19	23.39	CYT	<i>Cp1002_0896</i>	Shared
Detoxification							

D9Q5T6_CORP1	Nitric-oxide reductase cytochrome b-containing subunit I	647,29	14	18.52	PSE	<i>norB</i>	Shared
Unknown function							
D9Q3F4_CORP1	Hypothetical protein	4172,88	5	32.95	PSE	<i>Cp1002_1379</i>	Core
D9Q420_CORP1	Hypothetical protein	8126,81	6	72.29	CYT	<i>Cp1002_1603</i>	Core
D9Q476_CORP1	Hypothetical protein	3051,72	7	62.36	CYT	<i>Cp1002_1660</i>	Core
D9Q4D8_CORP1	Hypothetical protein	1832,3	6	49.23	CYT	<i>Cp1002_1724</i>	Core
D9Q4I5_CORP1	Hypothetical protein	2502,86	3	48.21	SEC	<i>Cp1002_1772</i>	Core
D9Q4N2_CORP1	Hypothetical protein	2396,27	5	26.77	SEC	<i>Cp1002_1820</i>	Core
D9Q7J8_CORP1	Hypothetical protein	2659,4	7	22.73	MEM	<i>Cp1002_0752</i>	Core
D9Q746_CORP1	Hypothetical protein	1017,75	14	55.32	CYT	<i>Cp1002_0598</i>	Shared
D9Q5M4_CORP1	Hypothetical protein	4875,82	4	57.74	CYT	<i>Cp1002_0061</i>	Core
D9Q8R7_CORP1	Hypothetical protein	647,49	9	18.63	MEM	<i>Cp1002_1178</i>	Core
D9Q7L0_CORP1	Hypothetical protein	4931,36	4	30.50	CYT	<i>Cp1002_0765</i>	Core
D9Q888_CORP1	Hypothetical protein	4291,71	5	38.61	CYT	<i>Cp1002_0998</i>	Core
D9Q8K1_CORP1	Hypothetical protein	451,3	6	36.97	MEM	<i>Cp1002_1111</i>	Core
D9Q8Q4_CORP1	Hypothetical protein	1402,43	2	27.87	MEM	<i>Cp1002_1165</i>	Core
D9Q614_CORP1	Hypothetical protein	487,44	4	36.27	MEM	<i>Cp1002_0206</i>	Shared
D9Q6M6_CORP1	Hypothetical protein	2215,15	7	17.58	PSE	<i>Cp1002_0422</i>	Core
D9Q6Y5_CORP1	Hypothetical protein	1152,17	12	26.6	SEC	<i>Cp1002_0536</i>	Core
D9Q5K2_CORP1	Hypothetical protein	182,58	9	40.38	CYT	<i>Cp1002_0536</i>	Core
D9Q7B9_CORP1	Hypothetical protein	707,2	8	16.10	MEM	<i>Cp1002_0671</i>	Core
Others							
D9Q4V8_CORP1	Predicted permease	1703,58	7	22.91	MEM	<i>Cp1002_1902</i>	Shared
D9Q561_CORP1	Sortase-like protein	704,98	5	18.53	MEM	<i>srtB</i>	Core
D9Q6X5_CORP1	Ribosome biogenesis GTPase RsgA	1071,38	12	40.08	CYT	<i>rsgA</i>	Core
D9Q3Q1_CORP1	Chad domain-containing protein	313,06	26	48.00	CYT	<i>Cp1002_1482</i>	Core
D9Q893_CORP1	Hemolysin-related protein	102,78	16	21.31	MEM	<i>tlyC</i>	Core

(b) Core-genome analysis of 15 strains of *C. pseudotuberculosis*: shared = present in two or more strains; core = present in 15 strains of *C. pseudotuberculosis*

(c) CYT = cytoplasmique; MEM = membrane; PSE = potentially surface-exposed; SEC = secreted

Table S.3: Unique proteins identified in strain 1002 control condition.

Accession Uniprot	Description	Score	Peptides	Average (%)	Subcellular localization ^(c)	Gene name
Transport and binding proteins						
D9Q5Q5_CORP1	Glycerol uptake facilitator protein	833,04	4	12.06	MEM	<i>glpF</i>
D9Q885_CORP1	Protein translocase subunit SecA2	324,42	34	30.59	CYT	<i>secA2</i>
D9Q8E7_CORP1	Fructose-specific phosphotransferase enzyme IIA component	1146,12	5	35.81	CYT	<i>dhaM</i>
Detoxification						
D9Q778_CORP1	Glutaredoxin	1408,91	5	51.19	CYT	<i>Cp1002_0630</i>
Copper resistance						
D9Q8S8_CORP1	Copper resistance protein CopC	486,77	4	36.84	PSE	<i>copC</i>
Cell cycle and division						
D9Q3G9_CORP1	Phospho-N-acetylmuramoyl-pentapeptide-transferase	439,72	4	7.1	MEM	<i>mraY</i>
Cell Communication						
D9Q805_CORP1	Dihydroxyacetone kinase 2	343,76	15	26.27	CYT	<i>daK3</i>
DNA synthesis and repair						
D9Q6Z1_CORP1	DNA helicase UvrD/REP type	325,47	46	33.61	CYT	<i>uvrD</i>
D9Q8N7_CORP1	Uncharacterized AAA domain-containing protein	437,4	20	30	CYT	<i>Cp1002_1148</i>
Transcription						
D9Q4T7_CORP1	Hypothetical protein	706,04	7	16.36	PSE	<i>Cp1002_1878</i>
Specific metabolic pathways						
D9Q3C7_CORP1	Inositol monophosphate phosphatase	667,14	7	34.03	CYT	<i>impA</i>
D9Q807_CORP1	Biotin/lipoyl attachment protein	3891,13	5	81.76	CYT	<i>pca</i>

D9Q4H2_CORP1	2-C-methyl-D-erythritol 2 4-cyclodiphosphate synthase	922,78	3	23.58	CYT	<i>ispF</i>
D9Q4P5_CORP1	Acetyltransferase	631,34	8	36.86	CYT	<i>Cp1002_1834</i>
Fructose and mannose metabolism						
D9Q396_CORP1	PTS system fructose-specific IIABC component	381,92	19	31.68	PSE	<i>manP</i>
Galactose metabolism						
D9Q7Q3_CORP1	Galactokinase	353,55	17	28.38	CYT	<i>galK</i>
Lipid metabolism						
D9Q541_CORP1	Glycerophosphoryl diester phosphodiesterase	337,13	9	48.95	CYT	<i>glpQ</i>
Aminoacid metabolism						
D9Q5W7_CORP1	2-isopropylmalate synthase	522,9	28	40.37	CYT	<i>leuA</i>
D9Q789_CORP1	Chorismate mutase	854,12	4	44.5	CYT	<i>csm</i>
D9Q6T6_CORP1	Propionyl-CoA carboxylase beta chain 2	446,2	17	31.4	CYT	<i>pccB2</i>
Cofactors metabolism						
D9Q5S8_CORP1	Cysteine desulfurase	380,52	13	40.80	CYT	<i>csd</i>
Unknown function						
D9Q4G6_CORP1	Hypothetical protein	856,15	7	39.62	PSE	<i>Cp1002_1753</i>
D9Q4Q0_CORP1	Hypothetical protein	591,25	5	65.05	CYT	<i>Cp1002_1840</i>
D9Q509_CORP1	Hypothetical protein	420,14	6	40.85	PSE	<i>Cp1002_1954</i>
D9Q517_CORP1	Hypothetical protein	497,01	18	34.03	PSE	<i>Cp1002_1962</i>
D9Q5Q8_CORP1	Hypothetical protein	1024,86	6	38.33	SEC	<i>Cp1002_0096</i>
D9Q763_CORP1	Hypothetical protein	423	6	26.32	SEC	<i>Cp1002_0615</i>
D9Q7Q5_CORP1	Hypothetical protein	924,1	7	41.72	PSE	<i>Cp1002_0810</i>
D9Q8Y0_CORP1	Hypothetical protein	324,02	6	17.48	MEM	<i>Cp1002_1244</i>
D9Q7G5_CORP1	Hypothetical protein	1582,56	3	19.41	MEM	<i>Cp1002_0719</i>
D9Q8P3_CORP1	Hypothetical protein	436,66	10	32.59	CYT	<i>Cp1002_1154</i>

Others

D9Q3A0_CORP1	Cupin domain-containing protein	462,04	9	28.24	CYT	<i>Cp1002_1323</i>
D9Q8C2_CORP1	Protein pafB	584,23	16	59.12	CYT	<i>pafB</i>
D9Q8G4_CORP1	1-deoxy-D-xylulose-5-phosphate synthase	787,36	4	25.38	PSE	<i>dxs</i>

(c) CYT = CYT; MEM = MEM; PSE = potentially surface-exposed; SEC = SEC

6. Capítulo 3: Alteração do potencial de virulência de *C. pseudotuberculosis* demonstrado por análise proteômica

**Chapitre 3 : Modification du potentiel de virulence de
C. pseudotuberculosis révélée par analyse protéomique**

6.1 Introdução

Este capítulo será apresentado em forma de artigo científico. Neste estudo, nós combinamos um ensaio de infecção experimental em um modelo de infecção murino, associado à análise proteômica, como uma estratégia para identificar fatores que possam estar envolvidos na virulência e patogênese de *C. pseudotuberculosis*. Uma vez que as enfermidades causadas por *C. pseudotuberculosis* são caracterizadas como crônicas, na maioria dos casos de infecções, os animais são diagnosticados em estágios avançados. Outro ponto a ser observado, a respeito da infecção por *C. pseudotuberculosis*, é o fator hospedeiro, onde os biovariares *ovis* e *equi* infectam diferentes hospedeiros, além disso, lesões viscerais são menos comum no biovar *equi*. Assim, torna-se extremamente difícil realizar estudos para medir os fatores expressos por *C. pseudotuberculosis* durante as fases iniciais da infecção. Além disso, infecções experimentais conduta nestes animais (ovelhas ou cavalos) envolve custos elevados.

Neste contexto, a utilização de um modelo de infecção experimental murino no presente trabalho, nos propiciou avaliar pela primeira vez, o comportamento de *C. pseudotuberculosis* durante os estágios iniciais da infecção, bem como o potencial de virulência de linhagens *ovis* e *equi*, durante a infecção em um hospedeiro comum. Além disso, o processo de passagem serial das linhagens 1002_*ovis* e 258_*equi* neste modelo de infecção, associado à análise proteômica, permitiu a identificação de fatores que podem desempenhar um papel importante durante o confronto entre *C. pseudotuberculosis* e a rede de fatores do hospedeiro. Assim, os resultados gerados neste estudo permitiram a descrição de um *set* de proteínas que podem estar diretamente envolvidas na patogênese e virulência de *C. pseudotuberculosis*. Além disso, pela primeira vez foi demonstrado um estudo funcional em *C. pseudotuberculosis equi*.

Introduction

Ce chapitre est présenté sous forme d'article scientifique. Dans cette étude, nous combinons un essai d'infection expérimentale sur modèle murin à une analyse protéomique comme stratégie pour identifier les facteurs qui peuvent être impliqués dans la virulence et la pathogenèse de *C. pseudotuberculosis*. Les infections causées par *C. pseudotuberculosis* sont chroniques dans la plupart des cas et les animaux sont le plus souvent diagnostiqués à un stade avancé. Un autre point à noter concernant l'infection à *C. pseudotuberculosis* est la spécificité d'hôte qui définit deux biovars au sein de l'espèce : les biovars *ovis* et *equi* qui infectent différents hôtes, respectivement ovins et équins. Les lésions viscérales sont moins fréquentes chez les animaux infectés par le biovar *equi*. Il est extrêmement difficile de mener des études qui permettent de mesurer les facteurs exprimés par *C. pseudotuberculosis* durant les premiers stades de l'infection. En outre, mener des infections expérimentales sur ces animaux (ovins ou équins) implique des coûts élevés.

Dans ce contexte, l'utilisation d'un modèle d'infection expérimentale murin nous a fourni une première évaluation du comportement de *C. pseudotuberculosis* durant les premiers stades de l'infection. Ce modèle a aussi permis d'établir le potentiel de virulence des souches *equi* et *ovis*, lors d'une infection dans un hôte commun. En outre, le processus de passage en série des souches 1002_*ovis* et 258_*equi* dans ce modèle d'infection nous a permis d'observer les changements dans le potentiel de virulence de ces souches. La combinaison de ces passages *in vivo* avec l'analyse protéomique des souches avant et après passage a permis l'identification de facteurs qui peuvent jouer un rôle important lors de la confrontation entre *C. pseudotuberculosis* et l'hôte. Les résultats obtenus dans cette étude ont permis la description d'un ensemble de protéines qui peuvent être

directement impliquées dans la pathogenèse et la virulence de *C. pseudotuberculosis*. Ce travail constitue le premier travail d'étude fonctionnelle de *C. pseudotuberculosis equi*.

6.2 Artigo 4: A shift in the virulence potential of *Corynebacterium pseudotuberculosis* biovars *ovis* and *equi* after passage in a murine host demonstrated through comparative proteomics. (Submitted for publication in the journal: *Journal of Proteomics* - Online ISSN: 1874-3919).

Wanderson M. Silva, Fernanda A. Dorella, Siomar C. Soares, Gustavo H. M. F. Souza, Agenor V. Santos, Adriano M. Pimenta, Yves Le Loir, Anderson Miyoshi, Artur Silva, Vasco Azevedo.

Abstract

Corynebacterium pseudotuberculosis is a pathogen subdivided into two biovars: *C. pseudotuberculosis ovis*, etiologic agent of caseous lymphadenitis in small ruminants, and *C. pseudotuberculosis equi*, which causes ulcerative lymphangitis in equines. For insight into biovar differences and to identify proteins that favor the virulence of this pathogen, we applied an experimental passage process using a murine model and high-throughput proteomics to evaluate the functional genome of the strains 1002_*ovis* and 258_*equi*. The experimental infection assays revealed that strain 258_*equi* exhibits higher virulence than strain 1002_*ovis*. However, recovering these strains from infected mice spleens induced a dramatic change in the strain 1002_*ovis* virulence potential, which became as virulent as strain 258_*equi* in a new infection challenge. The proteomic screening performed from the culture supernatant of these recovered strains, revealed 118 proteins differentially regulated in the strain 1002_*ovis* and 140 proteins differentially regulated in the strain 258_*equi*. In addition, this proteomic analysis revealed that strain 1002_*ovis* and strain 258_*equi* produce different classes of proteins involved in detoxification process, pathogenesis and export pathways. The results indicate that the stains 1002_*ovis* and 258_*equi* use distinct mechanisms during infection. Moreover, this study enhances our understanding of the factors that may influence pathogenesis of *C. pseudotuberculosis*.

6.2.1 Introduction

Corynebacterium pseudotuberculosis is a Gram-positive facultative intracellular pathogen that is subdivided into two biovars: *C. pseudotuberculosis ovis*, which is the etiologic agent of caseous lymphadenitis in small ruminants, and *C. pseudotuberculosis equi*, which causes ulcerative lymphangitis in equines. The human infection caused by *C. pseudotuberculosis*, this associated to occupational exposure. These diseases are characterized by abscess formation in lymph nodes and internal organs [1,2]. In caseous lymphadenitis, progression of these abscesses generates different size nodes that contain a caseous mass [2]; whereas, in ulcerative lymphangitis, this progression ruptures the nodular lesion-forming abscesses and ulcers of irregular shapes and sizes [3]. Both diseases are globally distributed and cause large economic losses to goat, sheep, horse and cattle farmers [4,5]. These two biovars can be distinguished by a simple *in vitro* test; *ovis* produces a negative nitrate reduction phenotype, whereas *equi* produces a positive nitrate reduction phenotype [2].

The pathogenic process of *C. pseudotuberculosis* in host is separated into two phases: (i) initial colonization and replication in lymph nodes that drain the site of infection, which is associated with pyogranuloma formation, and (ii) a secondary cycle of replication and dissemination via the lymphatic or circulatory systems. This dissemination is promoted by the action of phospholipase D (PLD) exotoxin, which allows this pathogen to contaminate visceral organs and lymph nodes, where it ultimately induces lesion formation [6-8]. Moreover, during this pathogenic process, in contrast to other intracellular microorganisms, *C. pseudotuberculosis* shows a capacity to survive in macrophages [9]. Studies suggest that this process is mediated by lipids at the *C. pseudotuberculosis* cell surface [10] and action by the PLD exotoxin [8]. In addition, other factors, such as the iron uptake complex *fagABCD* [11] and extracytoplasmatic

(ECF) sigma factor σ^E , which play key roles in bacterial resistance to nitrosative stress [12], contribute to the *C. pseudotuberculosis* infection process.

Recently a comparative genomic study was performed on 15 *C. pseudotuberculosis* strains of the biovars *ovis* and *equi*, revealed several genes that can be involved in the pathogenesis of each biovar. In addition, 16 pathogenicity islands were detected in the genome of all 15 strains, containing several genes that can play a role in the virulence of *C. pseudotuberculosis* [13]. Thus, to validate previous *in silico* data and identify factors that could influence in the pathogenic process of *C. pseudotuberculosis*, several strategies were applied to evaluate the functional genome this pathogen.

Studies show that proteins exported by pathogenic bacteria favor the infection process, this class of proteins are involved in the adhesion and invasion to host cell, nutrient acquisition, exportation of toxins and mainly in the defense against immune system [14,15]. Thus, certain strategies have been used to identify exported *C. pseudotuberculosis ovis* proteins [16]. Furthermore, comparative proteomic strategies also allowed for characterization of the extracellular proteome of *C. pseudotuberculosis ovis*, as well the extracellular imunoproteome (strains C231_*ovis* and 1002_*ovis*) [17-20]. In these studies, with respect to strain 1002_*ovis*, certain proteins related to bacterial virulence were not detected in this strain, which suggests that this strain can present low virulence. Recently the surface proteome of *C. pseudotuberculosis ovis* was characterized, from bacterial strains isolated of naturally infected sheep lymph nodes. This proteomic analysis, allow the identification of proteins of this pathogen that favor the chronic phase of caseous lymphadenitis, that is, when the infection is already established [21].

During the infection process *C. pseudotuberculosis* is exposed to different stress condition, thus transcriptomic and proteomic studies of the functional genome of *C.*

pseudotuberculosis ovis, after the exposure to different stress condition were performed [12, 22, 23]. The results obtained in these *in vitro* studies, promoted the characterization of several factors that have influence in the adaptation and resistance of *C. pseudotuberculosis* to different stress conditions. Regarding the *C. pseudotuberculosis equi*, functional genomic studies have not been conducted between the *equi* strains or *ovis* and *equi* strains.

Thus, in this study, we sought to better understand the differences among *C. pseudotuberculosis ovis* and *equi* during infection of a common host, as well complement previous studies in the research by factors that can influence in the virulence of *C. pseudotuberculosis*. We adopted an *in vivo* assay, where the strains 1002_*ovis* and 258_*equi* were experimentally inoculated in a murine model followed by analysis high-throughput proteomics. The utilization of an *in vivo* model enables us to generate a confrontation that occurs, between the pathogen and the dynamics network of host factors, like the immune system. Thus, after the experimental passage process in murine model, we conducted a screening of the functional genome of the 1002_*ovis* and 258_*equi*, through of the comparison of proteins released in the culture supernatant of these two strains, which represent the biovars *ovis* and *equi* of *C. pseudotuberculosis*, respectively.

6.2.2 Materials and Methods

Bacterial strains and growth conditions

The *C. pseudotuberculosis* biovar *ovis* strain 1002 was isolated from a goat in Brazil, and the *C. pseudotuberculosis* biovar *equi* strain 258 was isolated from an equine in Belgium; these strains were cultivated under routine conditions in brain-heart infusion broth (BHI-HiMedia Laboratories Pvt. Ltd., India) at 37°C. When necessary, 1.5% of agar was added to the medium for a solid culture. For extracellular proteomic analyses, *Cp1002_ovis* and *Cp258_equi*

were grown in a chemically defined medium (CDM) [(Na₂HPO₄·7H₂O (12.93 g/L), KH₂PO₄ (2.55 g/L), NH₄Cl (1 g/L), MgSO₄·7H₂O (0.20 g/L), CaCl₂ (0.02 g/L) and 0.05% (v/v) Tween 80], 4% (v/v) MEM Vitamins Solution (Invitrogen, Gaithersburg, MD, USA), 1% (v/v) MEM Amino Acids Solution (Invitrogen), 1% (v/v) MEM Non-Essential Amino Acids Solution (Invitrogen), and 1.2% (w/v) glucose at 37°C [24].

Experimental infection of strain 1002_*ovis* and strain 258_*equi* in a murine model (*in vivo* assay)

Female BALB/c mice between six and eight weeks old were used for all experiments; they were provided by the Animal Care Facility of the Biological Sciences Institute from the Federal University of Minas Gerais and were handled in accordance with the guidelines of the UFMG Ethics Committee on Animal Testing (Permit Number: CETEA 103/2011). For the bacterial passage assay using the murine model, two groups of three mice each were infected via intraperitoneal injection with 10⁶ colony forming units (CFU) of strain 1002_*ovis* and strain 258_*equi*. Thirty-six hours after infection, the animals were sacrificed, and their spleens were removed to recover the bacterial strains. The recovered bacterial strains are referred to as *Cp1002Rc_ovis* and *Cp258Rc_equi*. For the bacterial virulence assay, we used the recovered bacteria and bacteria that did not contact the host as a control, which are referred to as *Cp1002Ct_ovis* and *Cp258Ct_equi*. Thus, groups of five mice each were infected with *Cp1002Ct_ovis*, *Cp1002Rc_ovis*, *Cp258Ct_equi* or *Cp258Rc_equi*, via intraperitoneal injection of a suspension containing 10⁶ CFU or 10⁵ CFU. The animals' survival rates were calculated and represented in GraphPad Prism v.5.0 (GraphPad Software, San Diego, CA, USA) using the Kaplan-Meier survival function.

Preparation of proteins from culture filtrates for proteome analysis

The non-recovered and recovered strain 1002_*ovis* and strain 258_*equi* obtained from the infected mice spleens were grown in CDM (three independent experiments) to OD₆₀₀=0.8. The cultures were then centrifuged for 20 min at 2,700 x g. The supernatants were then filtered using 0.22-μm filters, 30% (w/v) ammonium sulfate was added to the samples, and the pH of the mixtures was adjusted to 4.0. Next, 20 mL/L N-butanol was added to each sample. The samples were centrifuged for 10 min at 1,350 x g and 4 °C. The interfacial precipitate was collected and re-suspended in 1 mL of 20 mM Tris-HCl pH 7.2 [25]. To label-free proteomic analysis the protein extract was concentrated using a spin column with a 10 kDa threshold (Millipore, Billerica, MA, USA). The protein was denatured (0.1% *RapiGEST* SF at 60 °C for 15 min) (Waters, Milford, CA, USA), reduced (10 mM DTT), alkylated (10 mM iodoacetamide) and enzymatically digested with trypsin (Promega, Sequencing Grade Modified Trypsin, Madison, WI, USA). The digestion process was stopped by adding 10 μL of 5% TFA (Fluka, Buchs, Germany), and glycogen phosphorilase (P00489) was added to the digested samples at 20 fmol.uL⁻¹ as an internal standard for normalization prior to each replicate injection using a two-dimensional reversed phase (2D RPxRP) nanoUPLC-MS (Nano Ultra Performance Liquid Chromatography Mass Spectrometry) approach with multiplexed high definition mass spectrometry (HDMS^E) label-free quantitation [26].

2D nanoUPLC-HDMS^E data acquisition

Qualitative and quantitative nanoUPLC tandem nanoESI-HDMS^E (Nano Electrospray High Definition Mass Spectrometry) experiments were performed using both a 1 h reversed phase gradient from 7% to 40% (v/v) acetonitrile (0.1% v/v formic acid) at 500 nL·min⁻¹ using a nanoACQUITY UPLC 2D RPxRP Technology system [27]. A nanoACQUITY UPLC HSS T3 1.8 μm, 75 μm × 15 cm column (pH 3) was used with a RP XBridge BEH130 C18 5 μm 300 μm

x 50 mm nanoflow column (pH 10). Typical on-column sample loads were 250 ng of the total protein digests for each of the 5 fractions (250 ng/fraction/load). For all measurements, the mass spectrometer was operated in the resolution mode with a typical effective m/z with an ion-mobility resolving power of at least 1.5M FWHM, an ion mobility cell filled with nitrogen gas and a cross-section resolving power of at least 40 $\Omega/\Delta\Omega$. All analyses were performed using nano-electrospray ionization in the positive ion mode nanoESI (+) and a NanoLockSpray (Waters, Manchester, UK) ionization source. The lock mass channel was sampled every 30 s. The mass spectrometer was calibrated using a MS/MS spectrum of [Glu¹]-Fibrinopeptide B human (Glu-Fib) solution (100 fmol.uL⁻¹) delivered through the NanoLockSpray source reference sprayer. The doubly charged ion ($[M + 2H]^{2+} = 785.8426$) was used for initial single-point calibration, and Glu-Fib MS/MS fragment ions were used for the final instrument calibration. Multiplexed data-independent (DIA) scanning with additional specificity and selectivity for non-linear ‘T-wave’ ion mobility (HDMS^E) experiments were performed using a Synapt G2-S HDMS mass spectrometer (Waters, Manchester, UK), which was constructed to automatically switch between standard MS (3 eV) and elevated collision energies HDMS^E (19–45 eV) applied to the transfer ‘T-wave’ CID (collision-induced dissociation) cell with argon gas. The trap collision cell was adjusted for 1 eV using a millisecond scan time, which was previously adjusted based on the linear velocity of the chromatography peak that was delivered using a nanoACQUITY UPLC to yield a minimum of 20 scan points for each single peak both through low-energy and high-energy transmissions followed by orthogonal acceleration time-of-flight (*oa*-TOF) from m/z 50 to 2000. The RF offset (MS profile) was adjusted such that nanoUPLC-HDMS^E data were effectively acquired from m/z 400 to 2000, which ensured that masses observed in the high-energy spectra at less than m/z 400 arose from dissociation in the collision cell.

Data processing

The proteins were identified, and the quantitative data were packaged using dedicated algorithms [28,29] and searching against a database with default parameters to account for ions[30]. The databases used were reversed “on-the fly” during the database queries and appended to the original database to assess the false positive rate during identification. For proper spectra processing and database searching conditions, the ProteinLynxGlobalServer v.2.5.2 (PLGS) with Identity^E and Expression^E informatics v.2.5.2 (Waters, Manchester, UK) was used. UniProtKB (release 2013_01) with manually reviewed annotations was used, and the search conditions were based on taxonomy (*Corynebacterium pseudotuberculosis*). The maximum allowed missed cleavages by trypsin were up to 1, and various modifications by carbamidomethyl (C), acetyl N-terminal, phosphoryl (STY) and oxidation (M) were allowed [31]. Normalization was performed using the Expression^E tool with a housekeeping protein that exhibited no significant difference in abundance throughout all injections. The proteins collected were organized by the PLGS Expression^E tool algorithm into a statistically significant list that corresponded to higher or lower regulation ratios between the different groups.

Bioinformatics analysis

The proteins identified from strain 1002_*ovis* and strain 258_*equi* under both conditions were analyzed using bioinformatics through the following prediction tools: the SecretomeP 2.0 server to predict proteins exported from non-classical systems (positive prediction score greater than to 0.5) [32] and the PIPs software to predict proteins in the pathogenicity islands [33]. Gene ontology (GO) functional annotations were generated using the Blast2GO tool [34].

6.2.3 Results

The virulence of the *Cp1002_ovis* and *Cp258_equi* strains was altered after passage in the murine host

Our first objective in this study was to evaluate the virulence of the strains *1002_ovis* and *258_equi* in a murine model; thus, we performed an *in vivo* survival assay with BALB/c mice infected by 10^6 CFU of each strain (**Figure 1a**). We observed that all the animals infected with strain *258_equi* died within 48 h of infection. In contrast, the group of animals infected with strain *1002_ovis* survived over the evaluated period (6 days). These results reveal a statistically significant difference ($P = 0.0011$) and demonstrate that the strain *258_equi* was more virulent than the strain *1002_ovis* in the murine model; in addition, this result confirms the low virulence of strain *1002_ovis*, which was suggested in a previous study on the extracellular proteome for this strain.

Next, after the bacterial recovery of the mice spleen, the strains *1002_ovis* and *258_equi* were analyzed using a second round of the survival assay in BALB/c mice infected with 10^6 CFU; however, the recovered (Rc) and non-recovered (Ct) samples were used to determine the infection kinetics. In this assay, all the animals infected with *Cp1002Rc_ovis*, *Cp258Ct_equi* or *Cp258Rc* died within 48 h after infection (**Figure 1b**). A comparison between the control and recovered conditions for each strain only showed a significantly different survival curve between *Cp1002Ct_ovis* and *Cp1002Rc_ovis* ($P = 0.0015$). This results shows that the strain *1002_ovis* passage process in a murine host modifies its virulence potential. However, in relation to strain *258_equi*, which was demonstrated as virulent in the first assay, and based on the kinetics using a 10^6 CFU dose, this strain did not show altered virulence.

On the other hand, using a new survival assay and 10^5 CFU (**Figure 1c**), we observed altered virulence in strain 258_*equi*, for which the mortality of mice infected with *Cp258Rc_equi* reached 100% after 3 weeks and began the first week post infection (40% drop in the survival rate). In *Cp258Ct_equi*, although mortality begins during the first weeks of infection, this early stage only yields 20% mortality, and the mortality reached 100% four weeks post infection. However, despite this reported difference between the strain 258_*equi* control and recovered conditions survival curves, pairwise comparisons were not statistically significant.

With respect to the group of mice infected with *Cp1002Rc_ovis* using 10^5 CFU, mortality was observed at week 2 post infection, and 100% mortality was observed four weeks post infection. In addition, we observed a significant difference ($P = 0.0015$) between strain 1002_*ovis* control and recovered (**Figure 1c**). Finally, regarding the clinical indicates, in the assays using 10^5 CFU, we detected caseous lesions in all animals infected with strain 1002_*ovis* recovered, and 258_*equi* control or recovered (data not shown). Together, these results show that passage in a murine host dramatically affects the virulence potential of strain 1002_*ovis* and, moderately affects strain 258_*equi*.

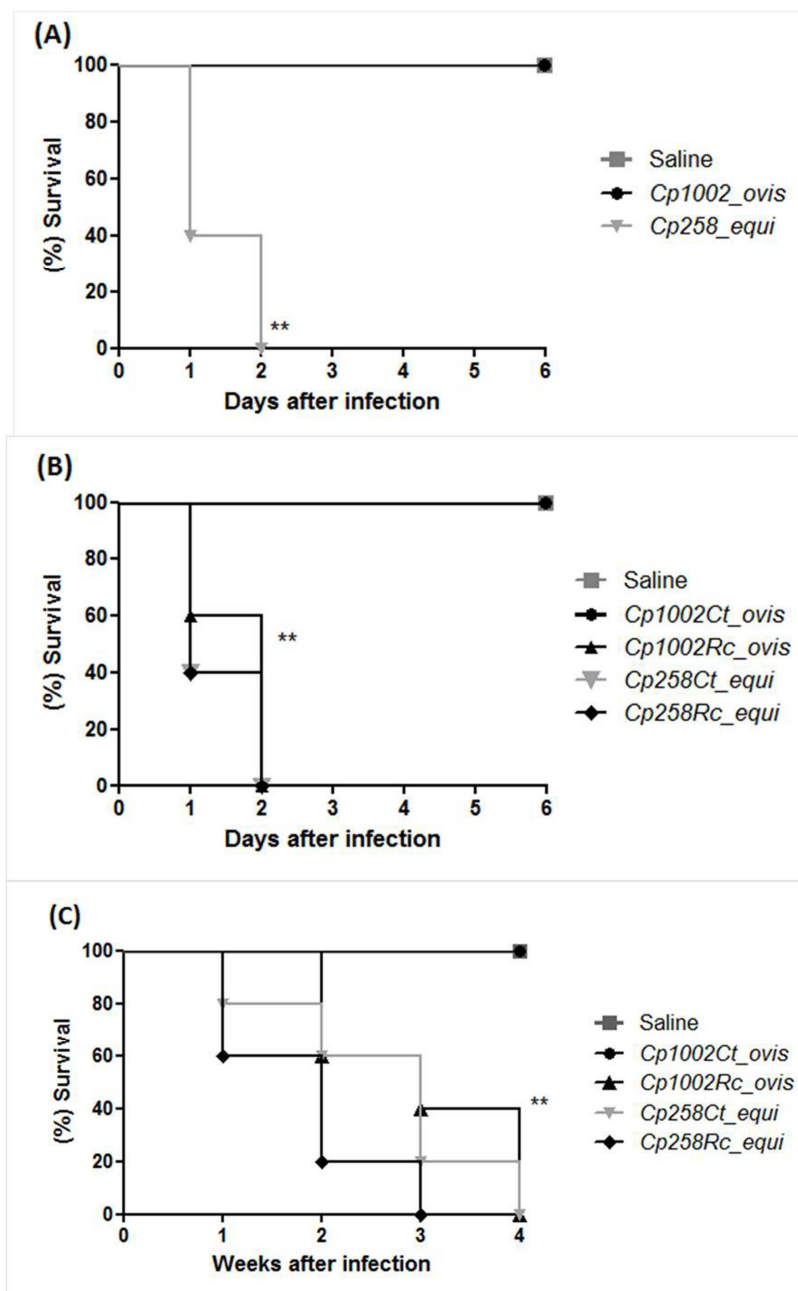


Figure 1: Survival of Balb/C mice infected with strain 1002_{ovis} or strain 258_{equi}. (A) The survival rate was measured to determine the virulence profile of the strains 1002_{ovis} and 258_{equi} in mice infected with 10⁶ CFU of bacteria. (B) Ct = control condition, Rc recovered condition. Survival rates of mice infected with 10⁶ CFU of Cp1002Ct_{ovis}, Cp1002Rc_{ovis}, Cp258Ct_{equi} or Cp258Rc_{equi}. (C) Survival rates of mice infected with 10⁵ CFU of Cp1002Ct_{ovis}, Cp1002Rc_{ovis}, Cp258Ct_{equi} or Cp258Rc_{equi}. The mortality rates were measured daily. Results A, B and C represent three independent experiments. The P values were calculated using the log rank test. **, P < 0.01.

Characterization of the proteome in the strains1002_*ovis* and 258_*equi* culture supernatant after bacterial strain passage in a murine host

After passage of the strains in BALB/c mice, we detected change in the virulence potential of the strains 1002_*ovis* and 258_*equi*. We hypothesized that such a phenotypic change should be visible at the proteome level because *C. pseudotuberculosis* virulence relies on proteinous virulence factor production. To corroborate the results obtained in the *in vivo* survival assay, we analyzed the control and recovered isolates from the two strains at the protein level. Considering the importance of extracellular proteins in bacterial virulence, the analysis was conducted on the extracellular proteome of strain 1002_*ovis* and strain 258_*equi* recovered from the infected mice spleens using high-throughput proteomics and compared with the control strains (see materials and methods for details). Collectively, approximately 46,570 peptides were identified within a 10 ppm error among 97.5% of the total identified peptides. Peptides used as source fragments, peptides with a charge state of at least $[M + 2H]^{2+}$, and no decoys were considered to enhance the data quality assessment. A total of 20,633 peptides in the sample *Cp258Ct_equi*, 12,194 peptides in the *Cp258Rc_equi*, 6,807 peptides for *Cp1002Ct_ovis*, and 6,936 for *Cp1002Rc_ovis* were identified under the experimental conditions. We detected 3,449 proteins that were identified across all conditions with 82% identified in at least 2 out of 3 biological replicates with an average of 16 peptides per protein. Among these samples, 51 proteins were exclusive to *Cp258Ct_equi*, 1 was assigned to *Cp258Rc_equi*, 48 were assigned to *Cp1002Ct_ovis*, and 32 proteins were exclusive to *Cp1002Rc_ovis* (**Supplementary File 1 and 2**).

Only proteins with differential expression of the *Cp258Rc_equi*: *Cp258Ct_equi* and *Cp1002Rc_ovis* and *Cp1002Rc_ovis* log₂ ratios equal or greater than a factor of 1.2 were

considered, as described previously [36]. For protein quantitation, we used the PLGS v2.5.2 software with the Identity^E algorithm using the Hi3 methodology. The search threshold to accept each spectrum was the default value in the program such that the false positive value was 4%. Biological variability was addressed by analyzing each culture three times. The quantitation values were averaged over all the samples, and the standard deviations at $p < 0.05$, which were determined using the Expression^E software, refer to the differences between biological replicates. Based on these parameters, only proteins that presented $p < 0.05$, $\log(2) > 1.2$, and in 2/3 replicates were considered. In accordance with these criteria, our final list of proteins differentially regulated in strain 258_equi was composed by 118 proteins up-regulated and 22 proteins down-regulated compared with *Cp258Rc_equi*. With respect to strain 1002_ovis, 88 proteins were considered up-regulated, and 30 proteins were considered down-regulated compared with *Cp1002Rc_ovis* and *Cp1002Ct_ovis* (**Supplementary File 3 and 4**). The quantitation values were averaged over all samples, and the standard deviations at $p < 0.05$, which were determined using the Expression^E software, refer to the differences between biological replicates (**Figure 2**). The proteins identified in both strains were analyzed by SecretomeP [32] to predict non-classical secretion systems. Of the 192 total proteins identified in strain 258_equi and 197 total proteins identified in strain 1002_ovis, 53% (102 proteins) and 28% (55 proteins) generated positive predictions for a non-classical secretion system, respectively (**Supplementary File 1,2,3 and 4**).

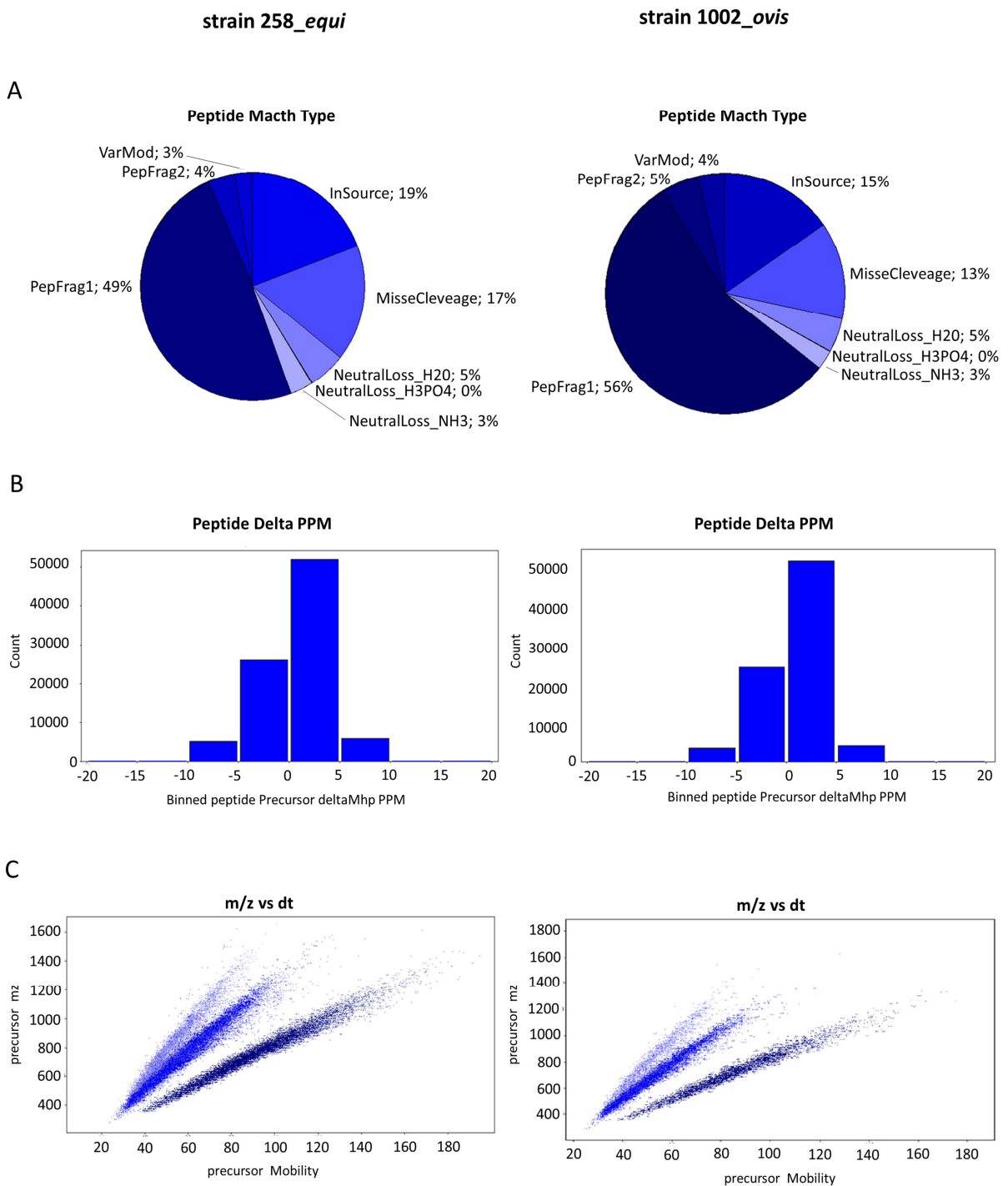


Figure 2: 2D nanoUPLC HDMS^E analysis showing MS/MS data (A) the peptide match distribution to ascertain the quality of fragmentation and digestion; (B) the distribution of fragment masses and exact mass accuracy for 90% of the precursor ions with a 10 ppm maximum error; and (C) DT vs *m/z* plot produced by LCMS/E from strain 1002_ovis and strain 258_equi.

Identification of proteins in pathogenicity islands

As the available genomes of various *C. pseudotuberculosis* strains exhibit great variability, we analyzed the gene content of genomic islands that may explain the experimentally observed differences among strain 1002_*ovis* and strain 258_*equi* in our *in vivo* assay. Thus, the genome sequences of both strains were analyzed using the PIPS tool to identify putative pathogenicity islands and, subsequently, predict whether the genes that encode the proteins identified herein are included in predicted pathogenicity islands [33]. Using the PIPS tool, we identified 16 proteins in strain 258_*equi* and 17 proteins in strain 1002_*ovis* that were encoded by genes located in a predicted pathogenicity island (**Supplementary File 5**). In 258_*equi*, the genes that code these proteins are involved different biological process such as: detoxification, DNA process, lipid metabolism, nucleotide metabolism, pathogenesis, translation, transport and unknow function. In 1002_*ovis*, these genes are involved in the process: oxido-reduction, stress general response, transcription, carbohydrate metabolism, pathogenesis, translation, transport and unknow function.

Functions of the proteins that are differentially expressed in strain 1002_*ovis* after passage in the murine host

The proteins identified in the control and recovered conditions from strain 1002_*ovis* after label-free proteomic analysis were classified into functional groups using the Blast2Go tool [34]. The differentially expressed proteins were classified into 17 biological processes (**Figure 3**). Among these processes, we identified proteins that are differentially regulated between the condition control and recovered and included in processes that can be directly involved in bacterial pathogenesis, such as: transport (8 proteins), pathogenesis (8 proteins), detoxification (6 proteins), general stress response (2 proteins) and cell adhesion (1 protein) (**Table 1**).

Additionally, a comparative analysis of the list of exclusive proteins in 1002_*ovis* control and recovered condition (**Supplementary File 1**) revealed the presence of PLD exotoxin (D9Q5J0_CORP1) major virulence factor of *C. pseudotuberculosis*. This results show that passage in a murine host induces expression of the strain 1002_*ovis* PLD encoding gene.

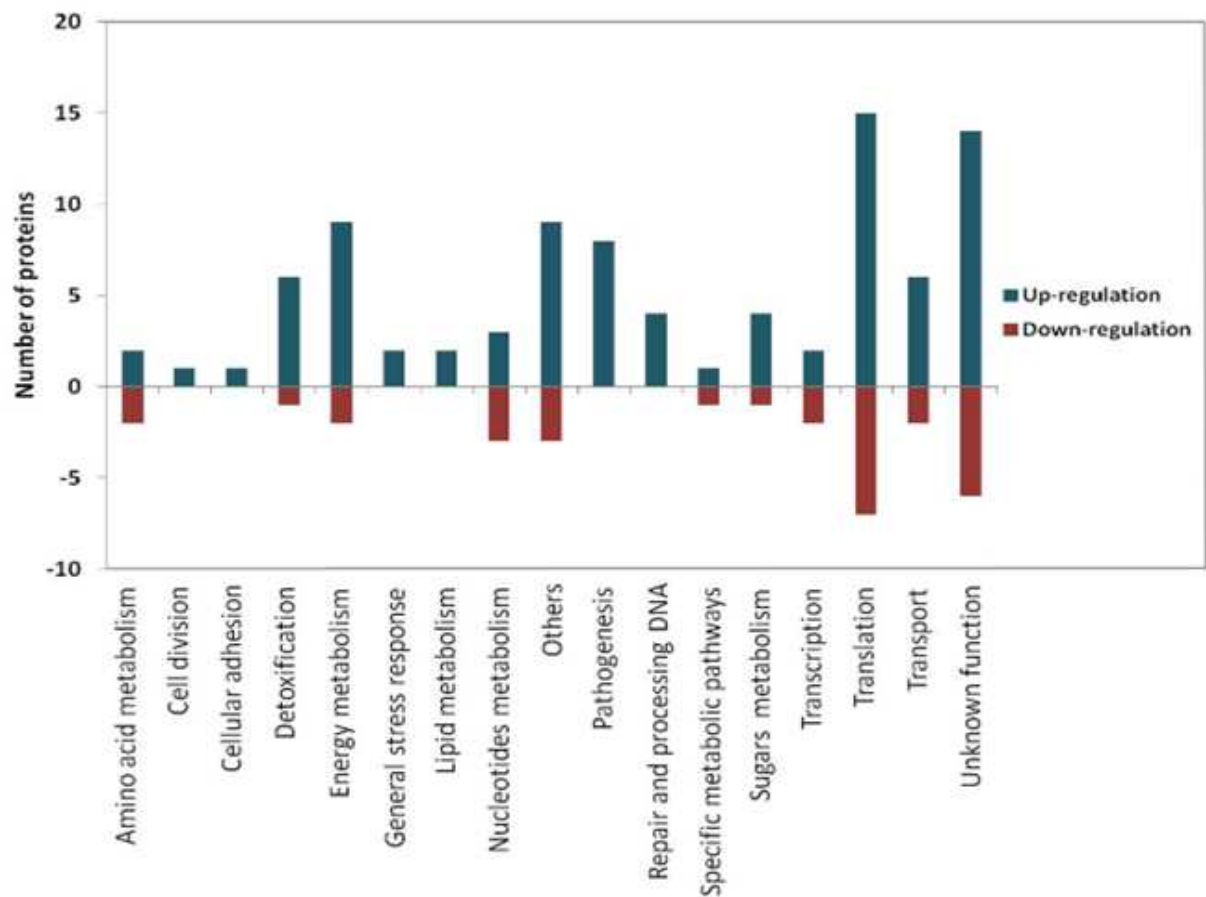


Figure 3: Biological processes differentially regulated in strain 1002_*ovis* after passage in mice.
Analysis of the differentially regulated proteins grouped into biological processes for strain 1002_*ovis* after passage in mice.

Table 1: Proteins differentially produced between the recovered and control conditions for strain 1002_*ovis*.

Accession	Description	Score	Log(2)Ratio ^(a)	p-value ^(a)
Transport				
D9Q5H9_CORP1	Periplasmic binding protein LacI transc	5601,78	3,26	1
D9Q6G4_CORP1	Oligopeptide binding protein oppA	4120,1	3,00	1
D9Q4T5_CORP1	ABC transporter domain containing ATP	1264,05	2,57	1
D9Q7K5_CORP1	Oligopeptide binding protein oppA	33697,17	2,11	1
D9Q5B8_CORP1	Oligopeptide binding protein oppA	852,88	1,88	1
D9Q6C3_CORP1	ABC type metal ion transport system permease	650,43	1,59	1
D9Q796_CORP1	Glutamate binding protein GluB	6254,68	-1,46	0
D9Q7W9_CORP1	Iron 3 hydroxamate binding protein fh	2774,62	-1,62	0,05
General stress response				
D9Q566_CORP1	Universal stress protein A	2498,69	1,70	1
D9Q824_CORP1	Stress related protein	2467,24	1,54	1
Cell adhesion				
D9Q5H7_CORP1	Hypothetical protein	115906,3	1,51	1
Detoxification				
D9Q4Q8_CORP1	Cytochrome c nitrate reductase small	1118,33	2,68	1
D9Q929_CORP1	Mycothione glutathione reductase	490,36	2,67	1
D9Q5T5_CORP1	Glyoxalase Bleomycin resistance protein	8420,32	2,21	1
D9Q424_CORP1	DSBA oxidoreductase	12179,8	2,09	1
D9Q4P4_CORP1	Ferredoxin ferredoxin NADP reductase	1086,71	1,69	1
D9Q692_CORP1	Thiol disulfide isomerase thioredoxin	3721,88	-2,25	0
Pathogenesis				
D9Q8M7_CORP1	Metallopeptidase family M24	3213,83	5,55	1
D9Q608_CORP1	Penicillin binding protein transpeptidase	1215,32	3,68	1
D9Q827_CORP1	Metallo beta lactamase superfamily protein	629,38	2,64	1
D9Q721_CORP1	Hypothetical protein	112025	2,24	1
D9Q7K8_CORP1	Trypsin like serine protease	35041,27	1,96	1
D9Q416_CORP1	ATP dependent Clp protease proteolytic	2467,24	1,77	1
D9Q639_CORP1	Secreted hydrolase	22798,13	1,75	1
D9Q588_CORP1	Penicillin binding protein	9951,61	1,26	1
D9Q407_CORP1	Ornithine cyclodeaminase	2566,18	-2,58	0

(a) Ratio values to: Cp1002Rc:Cp1002Ct_Log(2)Ratio>1.5 - p>0.95 up-regulation, p<0.05 down-regulation

Functions of the proteins differentially expressed in strain 258_equi after passage in a murine host

The proteins identified under the strain 258_equi control and recovered conditions after label-free proteomic analysis were also classified into functional groups using the Blast2Go tool [34]. The proteins differentially regulated between 258_equi control and recovered conditions were divided into 17 biological processes (**Figure 4**). We identified many hypothetical proteins (37 proteins) among these processes. Showed a great number of proteins that can be involved in the pathogenesis of strain 258_equi, thus more study are necessary to evaluated the verily play role this proteins in the virulence of this strain. Moreover, as in strain 1002_ovis, we also identified processes that can be directly involved in bacterial pathogenesis, such as transport (18 proteins), pathogenesis (12 proteins), detoxification (8 proteins), general stress response (3 proteins) and cell adhesion (1 protein) (**Table 2**). However, in strain 258_equi, with regard to the PLD exotoxin that was detected under both conditions (control and recovered), we did not detect significantly different expression levels ($\log(2)$ ratio=<1.2), therefore not been included in our final list of proteins.

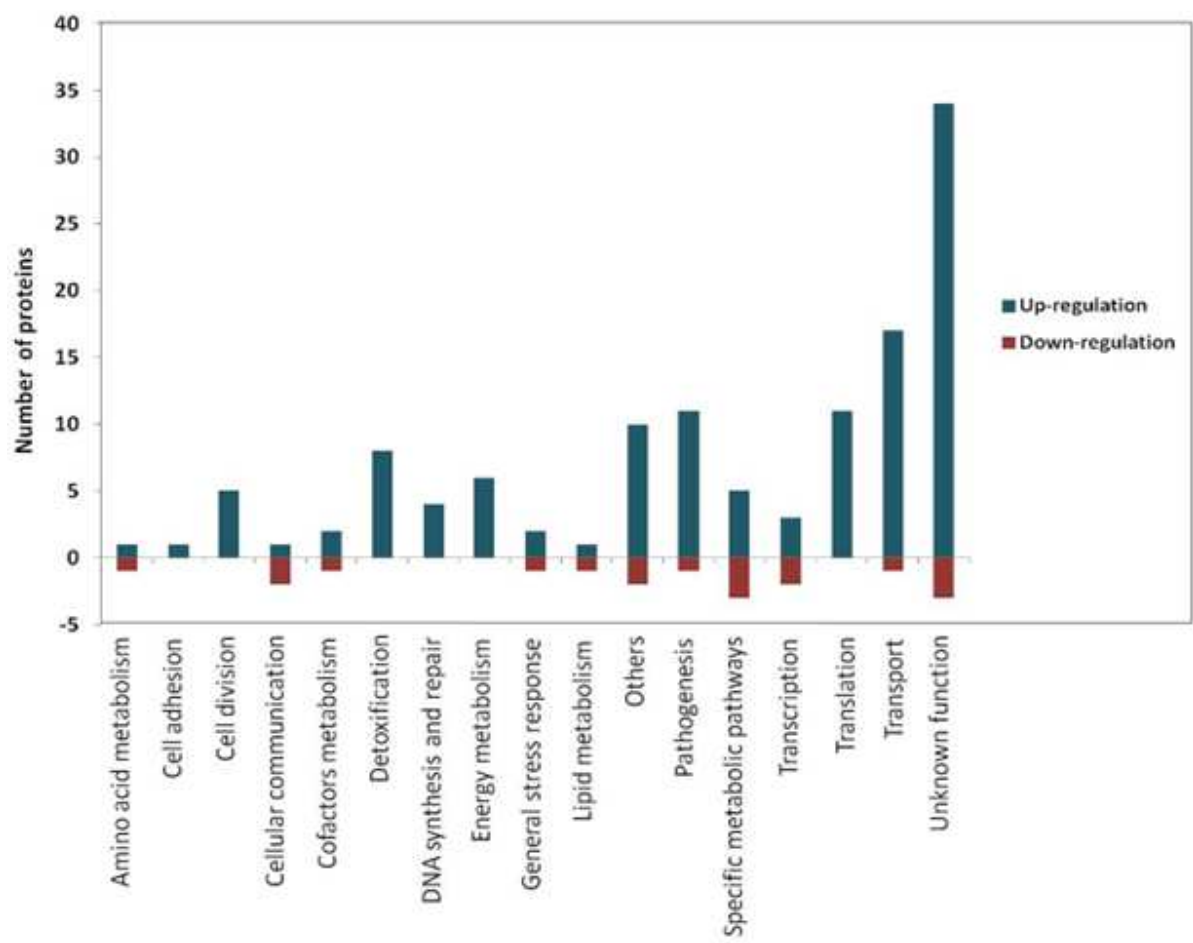


Figure 4: Biological processes differentially regulated in strain 258_equi after passage in mice.
 Analysis of the differentially regulated proteins grouped into biological processes in strain 258_equi after passage in mice.

Table 2: Proteins differentially produced between the recovered and control conditions for strain 258_equi.

Accession	Description	Score	Log(2)Ratio ^(a)	p-value ^(a)
Transport				
I3QZ34_CORPS	ABC transporter ATP binding protein	20158,7	3,00	1
I3QWP4_CORPS	Oligopeptide transport OppD	6266,77	2,77	1
I3QVU7_CORPS	Uncharacterized protein cter	14835,01	2,39	1
I3QVT3_CORPS	Manganese ABC transporter substrate binding	16263,86	2,31	1
I3QVU3_CORPS	Cell surface hemin receptor	11874,87	2,22	1
I3QW10_CORPS	Protein translocase subunit SecA	7923,5	1,89	1
I3QUW4_CORPS	ABC type metal ion transport system permease	1016,6	1,75	1
I3QXV8_CORPS	Protein translocase subunit SecF	1729,78	1,66	1
I3QWD2_CORPS	Glutamate binding protein GluB ryn	8414,45	1,54	1
I3R0D7_CORPS	Oligopeptide binding protein oppA	3469,47	1,50	1
I3QVU4_CORPS	Hemin binding periplasmic protein hmuT	14010	1,47	1
I3QUV4_CORPS	Glycine betaine binding protein	4096,23	1,43	1
I3QWP1_CORPS	Oligopeptide binding protein oppA	41781,98	1,38	1
I3QVC7_CORPS	ABC type transporter m	11220,09	1,36	1
I3QZC0_CORPS	ABC type antimicrobial peptide transport	1159,51	1,34	1
I3QXV9_CORPS	Protein translocase subunit SecD	2879,45	1,24	1
I3QX10_CORPS	Iron 3 hydroxamate binding protein fh	13922,33	1,21	1
I3QUW5_CORPS	Manganese zinc iron transport system ATP	391,52	-1,38	0
General stress response				
I3R095_CORPS	Phage shock protein A	29691,47	3,10	1
I3QX77_CORPS	Stress related protein	36248,9	2,65	1
I3QYV1_CORPS	Heat inducible transcription repressor	177,37	-1,88	0
Cell adhesion				
I3QZX5_CORPS	Fimbrial associated sortase like protein	13261,7	1,28	1
Detoxification				
I3QZG0_CORPS	Glutathione peroxidase	46259,61	4,82	1
I3QW94_CORPS	Superoxide dismutase Cu-Zn	8883,72	4,26	1
I3QYL8_CORPS	Iron sulfur cluster insertion protein	27250,26	3,59	1
I3QZV3_CORPS	Oxidoreductase	4356,68	3,52	1
I3QZ61_CORPS	Oxidoreductase	3324,33	1,85	1
I3QV23_CORPS	Catalase	15172,47	1,73	1
I3R0H6_CORPS	Thioredoxin reductase	19119,71	1,64	1
I3R0G3_CORPS	Iron sulfur protein	5690,8	1,53	1
I3QY82_CORPS	Mycothione glutathione reductase	5838,24	1,53	1
Pathogenesis				

I3QV43_CORPS	Penicillin binding protein transpeptidase	18512,68	1,80	1
I3QWE6_CORPS	Serine protease	9952,11	1,75	1
I3QYI9_CORPS	Penicillin binding protein	11772,81	1,70	1
I3QXC5_CORPS	Iron ABC transporter substrate binding	12242,99	1,64	1
I3QY03_CORPS	Diphtheria toxin repressor	45534,1	1,60	1
I3R059_CORPS	O acetyltransferase OatA	2935,54	1,47	1
I3QZM5_CORPS	D alanyl D alanine carboxypeptidase	2988,16	1,46	1
I3QW38_CORPS	Lon protease	6439,26	1,34	1
I3QXC3_CORPS	Esterase	496,62	1,30	1
I3QZ50_CORPS	Peptidase S8A Subtilisin family protein	40174,72	1,23	1
I3QW24_CORPS	Hydrolase domain containing protein	17234,12	-1,26	0
I3QYP5_CORPS	MutT NUDIX family protein	5870,55	-1,38	0

(a) Ratio values to: $Cp258Rc:Cp258Ct$ _Log(2)Ratio>1.2 - p>0.95 up-regulation, p<0.05 down-regulation

Comparative proteomics analysis between the recovered condition of strain 1002_*ovis* and strain 258_*equi*

To evaluate the differences among strains 1002_*ovis* and 258_*equi*, we compared the biological processes differential identified in the recovered condition for each strain. Fourteen biological processes were common among the two strains; however, two processes were exclusive to each strain; cellular communication and cofactor metabolism were identified only in strain 258_*equi*, and sugar as well as nucleotide metabolism were exclusive to strain 1002_*ovis*. We compared the following processes between strain 258_*equi* recovered and strain 1002_*ovis* recovered: transport, pathogenesis, detoxification, general stress response and cell adhesion. The general stress response and adhesion process exhibited the same number of proteins in both strains; yet the transport, pathogenesis, detoxification process present more number of proteins in *Cp258Rc_equi* than *Cp1002Rc_ovis* (**Figure 5**).

According to the data predicted genome for strain 1002_*ovis* [36] and strain 258_*equi* [37]. The comparative analysis for 1002_*ovis* and 258_*equi* enabled identification of potential proteins that

are specific to each strain. In strain *1002_ovis*, 4 proteins were detected: the copper resistance protein CopC (D9Q8S8_CORP1), a hypothetical protein (D9Q4T0_CORP1), the 50S ribosomal protein L21 (D9Q402_CORP1), and a serine-aspartate repeat-containing protein (D9Q5X4_CORP1). In strain *258_equi*, 2 proteins were identified: an ABC-type metal ion transport system protein (I3QUW4_CORPS) and a disulfide bond formation protein in the DsbB family (I3QZR6_CORPS).

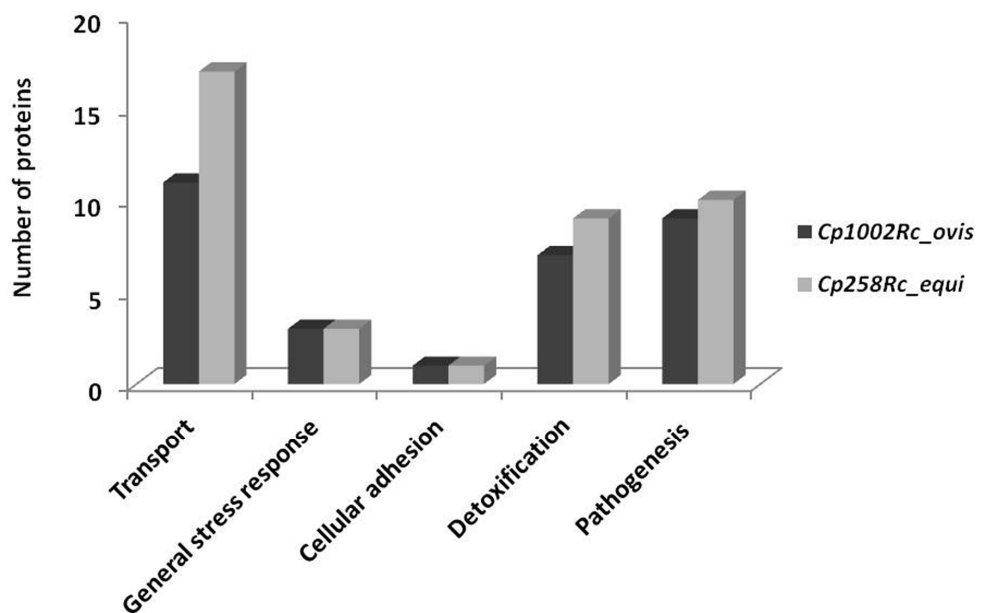


Figure 5: Comparison of biological processes in the strains *1002_ovis* and *258_equi*. Comparative analysis of the biovars *ovis* and *equi* reveals the biological processes shared by strain *1002_ovis* recovered (*Cp1002Rc_ovis*) and strain *258_equi* (*Cp258Rc_equi*).

6.2.4 Discussion

To investigate the protein factors that could influence the adaptive processes of the *C. pseudotuberculosis* biovars *ovis* and *equi*, during the infection process, we combined a unique

bacterial passage experiment in a murine host with proteomic analyses of strain 1002_*ovis* and strain 258_*equi* culture supernatant collected before and after passage. In the first analysis, the 1002_*ovis* and 258_*equi* strains virulence were evaluated via experimental infection of Balb/C mice; strain 258_*equi* exhibited greater virulence than strain 1002_*ovis*. This result is consistent with reports that indicate strain 258_*equi* is a highly virulent strain, which was recently isolated from equine [35]. On the other hand, 1002_*ovis* is a strain that was naturally isolated from caprine and exhibits less virulence [38,39]. Although a recent *in silico* analysis of the strain 1002_*ovis* genome revealed various genes involved in virulence [36], a study examining the 1002_*ovis* exoproteome after growth under laboratory conditions did not detect these virulence-associated proteins [17-19]. This finding correlates with lower virulence in stain 1002_*ovis* and was confirmed here through experimental infection of Balb/C mice. After isolation, strain 1002_*ovis* was maintained under laboratory conditions (with extensive passages on culture medium), which may alter gene expression, especially for genes involved in bacterial virulence, and subsequently lower virulence. This phenomenon has also been reported in other pathogens, such as *Helicobacter pylori*, *Staphylococcus aureus*, and *Listeria monocytogenes*, where extensive *in vitro* passages on culture medium alter both bacterial physiology and virulence profile [40-42].

However, we showed that the bacterial passage process in a murine model changed the virulence of the strains 1002_*ovis* and 258_*equi*. Previous reports on experimental serial passages showed that pathogens such as *H. pylori*, *Escherichia coli*, *Xenorhabdus nematophila*, *Arcobacter butzleri* and *Salmonella enterica* also exhibited altered virulence profiles after *in vivo* passage in a host and identified factors that enable bacterial adaptation during the infection process [43-47]. This altered physiology and virulence in both strain 1002_*ovis* and strain

258_ *equi* is supported by the proteomics analyses. Several proteins involved in distinct processes that favor infection and adaptation of *C. pseudotuberculosis* were differentially regulated after passage in mice.

Cytoplasmic proteins were detected in the proteomics analyses. Their presence in the extracellular milieu is related by several proteomic studies [17,21,32,48]; in addition, it can result from cell lysis and, therefore, be considered artifacts. However, the presence of cytoplasmic proteins in the culture supernatant can also be associated with several processes, including export via a non-classical export pathway or *moonlighting proteins* [17,32,49]. An analysis of the strain 1002_ *ovis* and strain 258_ *equi* exoproteomes in recovered condition revealed proteins that are differentially regulated and described as *moonlighting proteins*. This class of proteins can be detected in different subcellular locations (membranes, cell surface and extracellular locations) and exhibit distinct functional behavior depending on the cell type and cell localization [49].

When exported by Gram-positive and Gram-negative bacteria, the proteins peptidyl prolyl cis trans isomerase B (I3QXV3_CORPS) and DnaK (I3QZX2_CORPS) detected in strain 258_ *equi* recovered; 6-phosphogluconate dehydrogenase (D9Q895_CORP1) detected in strain 1002_ *ovis* recovered; and enolase (D9Q7G0_CORP1/ I3QWJ6_CORPS) detected in both strains played a role in host cell adhesion through its plasminogen-binding capacity, which favors bacteria colonization [50,51]. Moreover, in the pathogen *Streptococcus pneumonia*, enolase contributes to evasion of the complement system during infection [49]. In the previous proteomic study performed with strain of *C. psedotuberculosis ovis* isolated directly from naturally infected sheep lymph nodes, show the presence of enolase and DnaK in the surface proteome of this strains [21], suggesting that these proteins can play a role important in the virulence of *C. pseudotuberculosis*. In addition, we detected others proteins that can be involved in the cell

adhesion like fimbrial associated sortase-like protein (I3QZX5_CORPS) in strain 258_*equi* recovered and a hypothetical protein (D9Q5H7_CORP1) in strain 1002_*ovis* recovered that according with Blast2Go classified into group of proteins associated with cell adhesion. Nevertheless, in *C. pseudotuberculosis*, currently no study has confirmed the role of enolase or of these other proteins in bacterial adhesion; however, these proteins may develop a similar function in this pathogen.

In our study, we detected several proteases induced by strain 1002_*ovis* and strain 258_*equi* after bacterial passage in a murine model. Proteases degrade tissue barriers formed by extracellular matrices and basement membranes, structurally damage the host cell, and allow bacterial invasion [52]. In addition to contributing to the bacterial invasion process, studies show that proteases such as Lon (I3QW38_CORPS) and Clp (D9Q416_CORP1) detected in strain 258_*equi* and strain 1002_*ovis* recovered, respectively, play a role in expression of several factors that contribute to bacterial pathogenesis [53]. Studies using the Lon mutant strains on pathogens, such as *Salmonella enterica* [54, 55] and *Pseudomonas aeruginosa* [56], and that also generate Clp mutant in *S. aureus* [57] and *L. monocytogenes* [58] showed that the proteins Lon and Clp plays an important role in the bacterial pathogenesis due these strains reduced virulence during infection in both in vivo and/or in vitro models.

During the infection, *C. pseudotuberculosis* is exposed to various stress conditions as well as reactive oxygen species and reactive nitrogen species production [8,12]. Our proteomics analyses showed that, after passage of strain 1002_*ovis* and strain 258_*equi* in a murine host, several proteins that belong to antioxidant systems were activated in each strain compared with the control condition. The presence of mycothione/glutathione reductase (D9Q929_CORP1/I3QY82_CORPS), in the recovered condition of 1002_*ovis* and strain 258_*equi*, Glutaredoxin

like protein nrdH (D9Q493_CORP1) in 1002_*ovis* and glutathione peroxidase (I3QZG0_CORPS) in strain 258_*equi*, show the induction of components of glutathione system (GSH-system) and mycothiol system. In the pathogen *Mycobacterium tuberculosis* that show lack of GSH system, using the mycothiol system such as an alternative form to GSH system [59,60]. According with *in silico* genome analysis of strain 1002_*ovis* and strain 258_*equi* both strains presented genes involved in GSH-system well as in mycothiol system. The glutaredoxin like protein nrdH is proteins present in bacteria that show absent of GSH system, however despite of the similarity with glutaredoxin and micoredoxin, this protein show thioredoxin-like activity [61,62]. Nevertheless, the presence of glutathione peroxidase in strain 258_*equi* recovered; show a presence of a component of GSH-system. Thus these results suggest that *C. pseudotuberculosis* could present an incomplete GHS-system and micothiol system, however, at the same time being complementary, and may be of great importance during the infection process.

In strain 258_*equi* recovered our also detected catalase (I3QV23_CORPS), superoxide dismutase [Cu/Zn] (I3QW94_CORPS), study show that this proteins plays an important role in the resistance to ROS and RNS as well in the virulence of pathogens like *Mycobacterium tuberculosis* [63,64] and *Campylobacter jejuni* [65]. In addition thioredoxin reductase (I3R0H6_CORPS) component of the thioredoxin system was identified in 258_*equi* recovered; this is the major antioxidant system in prokaryotic [61]. In strain 1002_*ovis* recovered was observed the induction of Copper resistance protein CopC (D9Q8S8_CORP1), the *Open reading frame* ORF that codify this proteins is absent in strain 258_*equi*. During the infection process the host immune system utilize the cooper as a defense mechanism against bacterial infection. In *M. tuberculosis* was showed that proteins involved in resistance to cooper are essential to virulence of this pathogen [66,67].

We identified several differentially expressed proteins involved in transport pathways in both *Cp1002Rc_ovis* and *Cp258Rc_equi*. The following proteins were identified: OppA, OppC and OppD, which are components of the oligopeptide permease system (Opp) in both recovered conditions to strains *1002_ovis* and *258_equi*; this system facilitates uptake of extracellular peptides used as carbon and nitrogen sources in bacterial nutrition. In addition, in *Bacillus subtilis*, the Opp system is involved in uptake of signaling molecules that favor quorum sensing and regulate biofilm formation [68]. Whether such properties are involved or not in *C. pseudotuberculosis* pathogenesis has not been determined.

Efflux pump proteins, such as in the ABC-type antimicrobial peptide transport system (D9Q4A8_CORP1) and the multidrug resistance protein (I3QWA4_CORPS), were identified in the strain *258_equi* (in both control and recovered samples) and strain *1002_ovis* (recovered condition) samples, which suggests that the corresponding genes were induced due to passage in the mice. Similarly, proteins for resistance to antimicrobial agents, such as penicillin-binding proteins (D9Q588_CORP1/ I3QYI9_CORPS), metallo-beta-lactamase (D9Q827_CORP1) and penicillin binding protein transpeptidase (D9Q608_CORP1/I3QV43_CORPS), were also identified only after passage in the host for the strain *1002_ovis* recovered samples. These data are consistent with previous *in vitro* studies, which show that *C. pseudotuberculosis* presents resistance to various classes of antimicrobial agents [69], and activation of these defense pathways against antimicrobial agents might favor *C. pseudotuberculosis* survival.

Several proteins involved in iron metabolism were identified herein. The Ciua protein (I3QXC5_CORPS), which is a component of the siderophore-based CiuaABCD iron acquisition complex, was identified as highly up-regulated only in the *Cp258Rc_equi* proteome. Study performed with strain *ciua* mutant show virulence reduced, moreover, this strain was able of

protect the immunized mice upon challenge with a virulent strain as well [70], demonstrating the role of this protein in the virulence of *C. pseudotuberculosis*. The cell-surface hemin receptor (I3QVU3_CORPS/I3QYP0_CORPS/D9Q6Q5_CORP1) was up-regulated in strain 258_equi recovered and exclusively detected in the strain 1002_ovis recovered proteome. Together, these results indicate that, similar to other pathogens, iron acquisition likely plays a crucial role in virulence, and this strain uses distinct iron acquisition systems during infection. This ability to acquire iron may contribute to the virulence increase observed in strain 258_equi and 1002_ovis.

Components of the major secretion systems in *C. pseudotuberculosis*, namely SecA (I3QW10_CORPS), SecD (I3QXV9_CORPS) and SecF (I3QXV8_CORPS), were also up-regulated in the recovered condition of strain 258_equi. Together with the higher number of secreted virulence-associated proteins in the strain 258_equi proteome, this up-regulation may also account for the higher virulence potential observed in strain 258_equi compared with strain 1002_ovis. The presence of these proteins confirms that secretion and secreted proteins are key elements in *C. pseudotuberculosis* virulence and adaptation, as suggested by previous reports that identified several secreted proteins as potential virulence factors in *C. pseudotuberculosis* [17-19].

6.2.5 Conclusion

Herein, we show changes in the virulence and proteomic profiles of the strains 1002_ovis and 258_equi after recovery from the murine host spleens. The proteomic screening performed showed an overview of the functional genome of *C. pseudotuberculosis*, during the infection process, that allowed the identification of several proteins involved in the virulence bacterial. In addition, this proteomic analysis showed that strain 1002_ovis and strain 258_equi present a set of different proteins grouped into the same biological process, and the associated *in*

vivo results suggest that *C. pseudotuberculosis* developed several strategies for pathogenesis depending on the biovar, which might also reflect adaptation to different hosts. However, more specific study will be required to determine the role specific of each protein in the virulence of *C. pseudotuberculosis*. Altogether, our results show that *C. pseudotuberculosis* passage in a murine model induces important changes in the extracellular proteome that account for pathogenesis and increased virulence in this pathogen.

Competing interests

The authors have declared no conflict of interest.

Acknowledgment

This work involved the collaboration of various institutions, including the Genomics and Proteomics Network of the State of Pará of the Federal University of Pará, the Amazon Research Foundation (FAPESPA), the National Council for Scientific and Technological Development (CNPq), the Brazilian Federal Agency for the Support and Evaluation of Graduate Education (CAPES), the Minas Gerais Research Foundation (FAPEMIG) and the Waters Corporation, Brazil. Yves Le Loir is the recipient of a PVE grant (71/2013) from Programa Ciências sem Fronteiras.

6.2.6 References

- [1] Pratt SM, Spier SJ, Carroll SP, Vaughan B, Whitcomb MB, Wilson WD. Evaluation of clinical characteristics, diagnostic test results, and outcome in horses with internal infection caused by *Corynebacterium pseudotuberculosis*: 30 cases (1995–2003). J Am Vet Med Assoc 2005;1:441-448.
- [2] Dorella FA, Pacheco LG, Oliveira SC, Miyoshi A, Azevedo V. *Corynebacterium pseudotuberculosis*: microbiology, biochemical properties, pathogenesis and molecular studies of virulence. Vet. Res 2006;37:201–218.
- [3] Aleman M, Spier SJ, Wilson WD, Doherr M. *Corynebacterium pseudotuberculosis* infection in horses: 538 cases (1982-1993). J Am Vet Med Assoc 1996;15:804-809.
- [4] Paton MW, Walker SB, Rose IR, Watt GF. Prevalence of caseous lymphadenitis and usage of caseous lymphadenitis vaccines in sheep flocks. Aust Vet J 2002;81:91-95.
- [5] Foley JE, Spier SJ, Mihalyi J, Drazenovich N, Leutenegger CM. Molecular epidemiologic features of *Corynebacterium pseudotuberculosis* isolated from horses. Am J Vet Res 2004;65:1734-1737.
- [6] Batey RG. Pathogenesis of caseous lymphadenitis in sheep and goats. Aust Vet J 1986;63:269-272.
- [7] Pépin M, Pittet JC, Olivier M, Gohin I. Cellular composition of *Corynebacterium pseudotuberculosis* pyogranulomas in sheep. J Leukoc Biol 1994;56:666-670.
- [8] McKean SC, Davies JK, Moore RJ. Expression of phospholipase D, the major virulence factor of *Corynebacterium pseudotuberculosis*, is regulated by multiple environmental factors and plays a role in macrophage death. Microbiology 2007;153:2203-2211.
- [9] Stefańska I, Gieryńska M, Rzewuska M, Binek M. Survival of *Corynebacterium pseudotuberculosis* within macrophages and induction of phagocytes death. Pol J Vet Sci 2010;13:143-149.
- [10] Hard GC. Comparative Toxic Effect of the Surface Lipid of *Corynebacterium ovis* on Peritoneal Macrophages. Infect. Immun 1975;12:1439-1449.
- [11] Billington SJ, Esmay PA, Songer JG, Jost BH. Identification and role in virulence of putative iron acquisition genes from *Corynebacterium pseudotuberculosis*. FEMS Microbiol Lett 2002;208:41–45.

- [12] Pacheco LG, Castro TL, Carvalho RD, Moraes PM, Dorella FA, Carvalho NB, Slade SE, Scrivens JH, Feelisch M, Meyer R, Miyoshi A, Oliveira SC, Dowson CG, Azevedo V. A Role for Sigma Factor σ(E) in *Corynebacterium pseudotuberculosis* Resistance to Nitric Oxide/Peroxide Stress. *Front Microbiol* 2012;3:126.
- [13] Soares SC, Silva A, Trost E, Blom J, Ramos R, Carneiro A, Ali A, Santos AR, Pinto AC, Diniz C, Barbosa EG, Dorella FA, Aburjaile F, Rocha FS, Nascimento KK, Guimarães LC, Almeida S, Hassan SS, Bakhtiar SM, Pereira UP, Abreu VA, Schneider MP, Miyoshi A, Tauch A, Azevedo V. The pan-genome of the animal pathogen *Corynebacterium pseudotuberculosis* reveals differences in genome plasticity between the biovar *ovis* and *equi* strains. *PLoS One* 2013;8:e53818.
- [14] Cassat JE, Hammer, N.D., Campbell, J.P., Benson, M.A. Perrien DS, Mrak LN, Smeltzer MS, Torres VJ, Skaar EP. A secreted bacterial protease tailors the *Staphylococcus aureus* virulence repertoire to modulate bone remodeling during osteomyelitis. *Cell Host Microbe* 2013;13:759-772.
- [15] Pflughoeft KJ, Swick MC, Engler DA, Yeo HJ, Koehler TM. Modulation of the *Bacillus anthracis* secretome by the immune inhibitor A1 protease. *J Bacteriol* 2014;196:424-435.
- [16] Dorella FA, Estevam EM, Pacheco LG, Guimarães CT, Lana UG, Gomes EA, Barsante MM, Oliveira SC, Meyer R, Miyoshi A, Azevedo V. *In vivo* insertional mutagenesis in *Corynebacterium pseudotuberculosis*: an efficient means to identify DNA sequences encoding exported proteins. *Appl Environ Microbiol* 2006;72:7368-7372.
- [17] Pacheco LG, Slade SE, Seyffert N, Santos AR, Castro TL, Silva WM, Santos AV, Santos SG, Farias LM, Carvalho MA, Pimenta AM, Meyer R, Silva A, Scrivens JH, Oliveira SC, Miyoshi A, Dowson CG, Azevedo V. A combined approach for comparative exoproteome analysis of *Corynebacterium pseudotuberculosis*. *BMC Microbiol* 2011;17:12.
- [18] Silva WM, Seyffert N, Santos AV, Castro TL, Pacheco LG, Santos AR, Ciprandi A, Dorella FA, Andrade HM, Barh D, Pimenta AM, Silva A, Miyoshi A, Azevedo V. Identification of 11 new exoproteins in *Corynebacterium pseudotuberculosis* by comparative analysis of the exoproteome. *Microb Pathog* 2013;16:37-42.
- [19] Silva WM, Seyffert N, Ciprandi A, Santos AV, Castro TL, Pacheco LG, Barh D, Le Loir Y, Pimenta AM, Miyoshi A, Silva A, Azevedo V. Differential Exoproteome analysis of two *Corynebacterium pseudotuberculosis* biovar *ovis* strains isolated from goat (1002) and sheep (C231). *Curr Microbiol* 2013;67:460-465.

- [20] Seyffert N, Silva RF, Jardin J, Silva WM, de Paula Castro TL, Tartaglia NR, de Oliveira Santana KT, Portela RW, Silva A, Miyoshi A, Le Loir Y, Azevedo V. Serological proteome analysis of *Corynebacterium pseudotuberculosis* isolated from different hosts reveals novel candidates for prophylactics to control caseous lymphadenitis. *Vet Microbiol* 2014;174:255-260.
- [21] Rees MA, Kleifeld O, Crellin PK, Ho B, Stinear TP, Smith AI, Coppel RL. Proteomic Characterization of a Natural Host-Pathogen Interaction: Repertoire of *in vivo* Expressed Bacterial and Host Surface-Associated Proteins. *J Proteome Res*, 2014.
- [22] Pinto AC, de Sá PH, Ramos RT, Barbosa S, Barbosa HP, Ribeiro AC, Silva WM, Rocha FS, Santana MP, de Paula Castro TL, Miyoshi A, Schneider MP, Silva A, Azevedo V. Differential transcriptional profile of *Corynebacterium pseudotuberculosis* in response to abiotic stresses. *BMC Genomics* 2014;15:14.
- [23] Silva WM, Carvalho RD, Soares SC, Bastos IF, Folador EL, Souza GH, Le Loir Y, Miyoshi A, Silva A, Azevedo V. Label-free proteomic analysis to confirm the predicted proteome of *Corynebacterium pseudotuberculosis* under nitrosative stress mediated by nitric oxide. *BMC Genomics*. 2014;15:1065.
- [24] Moura-Costa LF, Paule BJA, Freire SM, Nascimento I, Schaer R, Regis LF, Vale VLC, Matos DP, Bahia RC, Carminati R, Meyer R. Chemically defined synthetic medium for *Corynebacterium pseudotuberculosis* culture. *Rev Bras Saúde Prod An* 2002;3:1-9.
- [25] Paule BJ, Meyer R, Moura-Costa LF, Bahia RC, Carminati R, Regis LF, Vale VL, Freire SM, Nascimento I, Schaer R, Azevedo V. Three-phase partitioning as an efficient method for extraction/concentration of immunoreactive excreted-secreted proteins of *Corynebacterium pseudotuberculosis*. *Protein Expr Purif* 2004;34:311-166.
- [26] Silva JC, Gorenstein, MV, Li GZ, Vissers JP. Geromanos, S.J. Absolute quantification of proteins by LCMS^E: a virtue of parallel MS acquisition. *Mol Cell Proteomics* 2006;5:144-156.
- [27] Gilar M, Olivova P, Daly AE, Gebler JC. Two-dimensional separation of peptides using RP-RP-HPLC system with different pH in first and second separation dimensions. *J Sep Sci*. 2005;28:1694-1703.
- [28] Silva JC, Denny R, Dorschel CA, Gorenstein M, Kass IJ, Li GZ, McKenna T, Nold MJ, Richardson K, Young P, Geromanos S. Quantitative proteomic analysis by accurate mass retention time pairs. *Anal Chem* 2005;1:2187-2000.

- [29] Geromanos SJ, Vissers JP, Silva JC, Dorschel CA, Li GZ, Gorenstein MV, Bateman RH, Langridge JI. The detection, correlation, and comparison of peptide precursor and products from data independent LC-MS with data dependant LC-MS/MS. *Proteomics* 2009;9:1683-1695.
- [30] Li GZ, Vissers JP, Silva JC, Golick D, Gorenstein MV, Geromanos SJ. Database searching and accounting of multiplexed precursor and product ion spectra from the data independent analysis of simple and complex peptide mixtures. *Proteomics* 2009;9:1696-719.
- [31] Curty N, Kubitschek-Barreira PH, Neves GW1, Gomes D, Pizzatti L, Abdelhay E, Souza GH, Lopes-Bezerra LM. Discovering the infectome of human endothelial cells challenged with *Aspergillus fumigatus* applying a mass spectrometry label-free approach. *J Proteomics* 2014;31:126-140.
- [32] Bendtsen JD, Kiemer L, Fausboll A, Brunak S. Non-classical protein secretion in bacteria. *BMC Microbiol* 2005;5,58.
- [33] Soares SC, Abreu VA, Ramos RT, Cerdeira L et al. Soares SC, Abreu VA, Ramos RT, Cerdeira L, Silva A, Baumbach J, Trost E, Tauch A, Hirata R Jr, Mattos-Guaraldi AL, Miyoshi A, Azevedo V. PIPS: pathogenicity island prediction software. *PLoS One* 2012;7:e30848.
- [34] Conesa A, Gotz S, García-Gómez JM, Terol J, Talón M, Robles M. Blast2GO: a universal tool for annotation, visualization and analysis in functional genomics research. *Bioinformatics* 2005;15:3674-3676.
- [35] Levin Y, Hradetzky E, Bahn S. Quantification of proteins using data-independent analysis (MSE) in simple and complex samples: a systematic evaluation. *Proteomics* 2011;11:3273–3287.
- [36] Ruiz JC, D'Afonseca V, Silva A, Ali A, Pinto AC, Santos AR, Rocha AA, Lopes DO, Dorella FA, Pacheco LG, Costa MP, Turk MZ, Seyffert N, Moraes PM, Soares SC, Almeida SS, Castro TL, Abreu VA, Trost E, Baumbach J, Tauch A, Schneider MP, McCulloch J, Cerdeira LT, Ramos RT, Zerlotini A, Dominitini A, Resende DM, Coser EM, Oliveira LM, Pedrosa AL, Vieira CU, Guimarães CT, Bartholomeu DC, Oliveira DM, Santos FR, Rabelo ÉM, Lobo FP, Franco GR, Costa AF, Castro IM, Dias SR, Ferro JA, Ortega JM, Paiva LV, Goulart LR, Almeida JF, Ferro MI, Carneiro NP, Falcão PR, Grynberg P, Teixeira SM, Brommonschenkel S, Oliveira SC, Meyer R, Moore RJ, Miyoshi A, Oliveira GC, Azevedo

- V. Evidence for reductive genome evolution and lateral acquisition of virulence functions in two *Corynebacterium pseudotuberculosis* strains. PLoS One 2012;18: e18551.
- [37] Soares SC, Trost E, Ramos RT, Carneiro AR, Santos AR, Pinto AC, Barbosa E, Aburjaile F, Ali A, Diniz CA, Hassan SS, Fiaux K, Guimarães LC, Bakhtiar SM, Pereira U, Almeida SS, Abreu VA, Rocha FS, Dorella FA, Miyoshi A, Silva A, Azevedo V, Tauch A. Genome sequence of *Corynebacterium pseudotuberculosis* biovar *equi* strain 258 and prediction of antigenic targets to improve biotechnological vaccine production. J Biotechnol 2013;20:135-141.
- [38] Ribeiro OC, Silva JAH, Oliveira SC, Meyer R, Fernandes GB. Preliminary results on a living vaccine against caseous lymphadenitis. Pesq Agrop Brasileira 1991;26:461-465.
- [39] Meyer R, Carminati R, Cerqueira RB, Vale V, Viegas S, Martinez T, Nascimento I, Schaer R, Silva JAH, Ribeiro M, Regis L, Paule B, Freire SM. Evaluation of the goats humoral immune response induced by the *Corynebacterium pseudotuberculosis* lyophilized live vaccine. Rev Cienc Méd Biol 2002;1:42-48.
- [40] Hopkins RJ, Morris JG Jr, Papadimitriou JC, Drachenberg C, Smoot DT, James SP, Panigrahi P. Loss of *Helicobacter pylori* hemagglutination with serial laboratory passage and correlation of hemagglutination with gastric epithelial cell adherence. Pathobiology 1996;64:247-254.
- [41] Somerville GA, Beres SB, Fitzgerald JR, DeLeo FR, Cole RL, Hoff JS, Musser JM. *In Vitro* Serial Passage of *Staphylococcus aureus*: Changes in Physiology, Virulence Factor Production, and *agr* Nucleotide Sequence. J Bacteriol 2002;184:1430-1437.
- [42] Asakura H, Kawamoto K, Okada Y, Kasuga F, Makino S, Yamamoto S, Igimi S. Intrahost passage alters SigB-dependent acid resistance and host cell-associated kinetics of *Listeria monocytogenes*. Infect Genet Evol 2012;12:94-101.
- [43] Bleich A, Kohn I, Glage S, Beil W, Wagner S, Mahler M. Multiple *in vivo* passages enhance the ability of a clinical *Helicobacter pylori* isolate to colonize the stomach of *Mongolian gerbils* and to induce gastritis. Lab Anim 2005;39:221-229.
- [44] Chapuis É, Pagès S, Emelianoff V, Givauda, Ferdy JB. Virulence and pathogen multiplication: a serial passage experiment in the hypervirulent bacterial insect-pathogen *Xenorhabdus nematophila*. PLoS One 2011 ;31:e15872.
- [45] Fernandez-Brando RJ, Miliwebsky E, Mejías MP, Baschkier A, Panek CA, Abrey-Recalde MJ, Cabrera G, Ramos MV, Rivas M, Palermo MS. Shiga toxin-producing *Escherichia coli*

- O157: H7 shows an increased pathogenicity in mice after the passage through the gastrointestinal tract of the same host. *J Med Microbiol* 2012;61: 852-859.
- [46] Fernández H, Flores SP, Villanueva M, Medina G, Carrizo M. Enhancing adherence of *Arcobacter butzleri* after serial intraperitoneal passages in mice. *Rev Argent Microbiol* 2013;45:75-79.
- [47] Koskineni S, Gibbons HS, Sandegren L, Anwar N, Ouellette G, Broomall S, Karavis M, McGregor P, Liem A, Fochler E, McNew L, Rosenzweig CN, Rhen M, Skowronski EW, Andersson DI. Pathoadaptive mutations in *Salmonella enterica* isolated after serial passage in mice. *PLoS One* 2013;25:e70147.
- [48] Muthukrishnan G, Quinn GA, Lamers RP, Diaz C, Cole AL, Chen S, Cole AM. Exoproteome of *Staphylococcus aureus* reveals putative determinants of nasal carriage. *J Proteome Res* 2011;1:2064-2078.
- [49] Henderson B, Martin A. Bacterial virulence in the moonlight: multitasking bacterial moonlighting proteins are virulence determinants in infectious disease. *Infect Immun* 2011;79: 3476-3491.
- [50] Peng Z, Krey V, Wei H, Tan Q, Vogelmann R, Ehrmann MA, Vogel RF. Impact of actin on adhesion and translocation of *Enterococcus faecalis*. *Arch Microbiol* 2014;196:109-117.
- [51] Agarwal V, Hammerschmidt S, Malm S, Bergmann S, Riesbeck K, Blom AM. Enolase of *Streptococcus pneumoniae* binds human complement inhibitor C4b-binding protein and contributes to complement evasion. *J Immunol* 2012;1:3575-3584.
- [52] Bhattacharya S, Ploplis VA, Castellino FJ. Bacterial plasminogen receptors utilize host plasminogen system for effective invasion and dissemination. *J Biomed Biotechnol* 2012; 482096.
- [53] Ingmer H, Brondsted L. Proteases in bacterial pathogenesis. *Res Microbiol* 2009;160:704-710.
- [54] Takaya A, Suzuki M, Matsui H, Tomoyasu T, Sashinami H, Nakane A, Yamamoto T. Lon, a stress-induced ATP-dependent protease, is critically important for systemic *Salmonella enterica* serovar *typhimurium* infection of mice. *Infect Immun* 2003;71:690-696.
- [55] Boddicker JD, Jones BD. Lon protease activity causes down-regulation of *Salmonella* pathogenicity island 1 invasion gene expression after infection of epithelial cells. *Infect Immun*. 2004;72:2002–2013.

- [56] Breidenstein EB, Janot L, Strehmel J, Fernandez L, Taylor PK, Kukavica-Ibrulj I, Gellatly SL, Levesque RC, Overhage J, Hancock RE. The Lon protease is essential for full virulence in *Pseudomonas aeruginosa*. PLoS One 2012 ;7: e49123.
- [57] Frees D, Qazi SN, Hill PJ, Ingmer H. Alternative roles of ClpX and ClpP in *Staphylococcus aureus* stress tolerance and virulence. Mol Microbiol 2003;48:1565-1578.
- [58] Gaillot O, Pellegrini E, Bregenholt S, Nair S, Berche P. The ClpP serine protease is essential for the intracellular parasitism and virulence of *Listeria monocytogenes*. Mol Microbiol 2000;35:1286-1294.
- [59] Lu J, Holmgren A. The thioredoxin antioxidant system. Free Radic Biol Med 2014;8:75-87.
- [60] Newton GL, Arnold K, Price MS, Sherrill C, Delcardayre SB, Aharonowitz Y, Cohen G, Davies J, Fahey RC, Davis C. Distribution of thiols in microorganisms: mycothiol is a major thiol in most actinomycetes. J Bacteriol 1996;178:1990-1995.
- [61] Jordan A, Aslund F, Pontis E, Reichard P, Holmgren A. Characterization of *Escherichia coli* NrdH. A glutaredoxin-like protein with a thioredoxin-like activity profile. J Biol Chem 1997;18:18044-18050.
- [62] Van Laer K, Dziewulska AM, Fislage M, Wahni K, Hbeddou A, Collet JF, Versées W, Mateos LM, Tamu Dufe V, Messens J. NrdH-redoxin of *Mycobacterium tuberculosis* and *Corynebacterium glutamicum* dimerizes at high protein concentration and exclusively receives electrons from thioredoxin reductase. J Biol Chem 2013;15:7942-7955.
- [63] Piddington DL, Fang FC, Laessig T, Cooper AM, Orme IM, Buchmeier NA. Cu,Zn superoxide dismutase of *Mycobacterium tuberculosis* contributes to survival in activated macrophages that are generating an oxidative burst. Infect Immun 2001;69:4980-4987.
- [64] Ng VH, Cox JS, Sousa AO, MacMicking JD, McKinney JD. Role of KatG catalase-peroxidase in mycobacterial pathogenesis: countering the phagocyte oxidative burst. Mol Microbiol 2004;52:1291-1302.
- [65] Day WA Jr, Sajecki JL, Pitts TM, Joens LA. Role of catalase in *Campylobacter jejuni* intracellular survival. Infect Immun 2000;68:6337-6345.
- [66] Wolschendorf F, Ackart D, Shrestha TB, Hascall-Dove L, Nolan S, Lamichhane G, Wang Y, Bossmann SH, Basaraba RJ, Niederweis M. Copper resistance is essential for virulence of *Mycobacterium tuberculosis*. Proc Natl Acad Sci U S A 2011;25:1621-1626.
- [67] Rowland JL, Niederweis M. A multicopper oxidase is required for copper resistance in *Mycobacterium tuberculosis*. J Bacteriol 2013;195:3724-3733.

- [68] Lazazzera BA, Solomon JM, Grossman AD. An exported peptide functions intracellularly to contribute to cell density signaling in *B. subtilis*. *Cell* 1997;13:917-925.
- [69] Judson R, Songer JG. *Corynebacterium pseudotuberculosis: in vitro* susceptibility to 39 antimicrobial agents. *Vet Microbiol* 1991;27:145-150.
- [70] Ribeiro D, Rocha Fde S, Leite KM, Soares Sde C, Silva A, Portela RW, Meyer R, Miyoshi A, Oliveira SC, Azevedo V, Dorella FA. An iron-acquisition-deficient mutant of *Corynebacterium pseudotuberculosis* efficiently protects mice against challenge. *Vet Res* 2014;45:28.

6.2.7 Supplementary data

Supplementary file 1: Table S.1: List of proteins identified in the exclusive proteome of *Cp1002_ovis*

Accession	Description	Score	Strain Condition ^(a)	SecretomeP	Biological process
D9Q8D5_CORP1	Phosphoribosyl ATP pyrophosphatase	614,73	<i>Cp1002Ct_ovis</i>	0.046269	Amino acid metabolism
D9Q7P6_CORP1	Shikimate 5 dehydrogenase	433,39	<i>Cp1002Ct_ovis</i>	0.048080	Amino acid metabolism
D9Q663_CORP1	UDP N acetylglucosamine	287,39	<i>Cp1002Ct_ovis</i>	0.036816	Cell division
D9Q5F5_CORP1	N Acetylmuramyl L Alanine Amidase	361,27	<i>Cp1002Ct_ovis</i>	0.071526	Cell wall organization
D9Q8B1_CORP1	Precorrin 8X methyl mutase	1462,24	<i>Cp1002Ct_ovis</i>	0.032623	Co factor metabolism
D9Q8K4_CORP1	Riboflavin synthase alpha chain	781,81	<i>Cp1002Ct_ovis</i>	0.055386	Co factor metabolism
D9Q778_CORP1	Glutaredoxin	2995,27	<i>Cp1002Ct_ovis</i>	0.901365	Detoxification
D9Q7U6_CORP1	Thioredoxin TrxA	554,29	<i>Cp1002Ct_ovis</i>	0.041210	Detoxification
D9Q3E0_CORP1	DNA polymerase III PolC	291,64	<i>Cp1002Ct_ovis</i>	0.248958	DNA process
D9Q914_CORP1	Predicted nucleic acid binding protein	282,83	<i>Cp1002Ct_ovis</i>	0.062597	DNA process
D9Q6U0_CORP1	N5 carboxyaminoimidazole ribonucleotide	522,81	<i>Cp1002Ct_ovis</i>	0.028255	Nucleotide metabolism
D9Q7I1_CORP1	Phosphinothricin acetyltransferase YwnH	260,31	<i>Cp1002Ct_ovis</i>	0.103816	Nucleotide metabolism
D9Q5Q2_CORP1	Antigen Cfp30B	522,45	<i>Cp1002Ct_ovis</i>	0.096113	Pathogenesis
D9Q3K2_CORP1	Iron sulfur cluster insertion protein	2853,68	<i>Cp1002Ct_ovis</i>	0.510849	Detoxification
D9Q6T7_CORP1	Biotin Acetyl CoA carboxylase ligase	411,62	<i>Cp1002Ct_ovis</i>	0.050761	Specific metabolic pathways
D9Q4I2_CORP1	Carbonic anhydrase	332,51	<i>Cp1002Ct_ovis</i>	0.048372	Specific metabolic pathways
D9Q8S4_CORP1	Hit Histidine triad family protein	498,51	<i>Cp1002Ct_ovis</i>	0.084869	Specific metabolic pathways
D9Q720_CORP1	Methylmalonyl CoA carboxyltransferase	610,14	<i>Cp1002Ct_ovis</i>	0.035262	Specific metabolic pathways
D9Q850_CORP1	Probable inorganic polyphosphate ATP NA	246,27	<i>Cp1002Ct_ovis</i>	0.043190	Specific metabolic pathways
D9Q4X1_CORP1	Urease accessory protein UreG	1619,84	<i>Cp1002Ct_ovis</i>	0.053554	Specific metabolic pathways
D9Q6P6_CORP1	DtxR family transcriptional regulator	476,35	<i>Cp1002Ct_ovis</i>	0.061484	Transcription
D9Q8R4_CORP1	Probable transcriptional regulatory	1207,31	<i>Cp1002Ct_ovis</i>	0.060539	Transcription
D9Q8V4_CORP1	Proteasome assembly chaperones 2 PAC2	82,89	<i>Cp1002Ct_ovis</i>	0.157143	Transcription
D9Q413_CORP1	TetR family regulatory protein	476,91	<i>Cp1002Ct_ovis</i>	0.043968	Transcription

D9Q8V7_CORP1	Transcriptional activator protein lysR	509,17	<i>Cp1002Ct_ovis</i>	0.060577	Transcription
D9Q6J6_CORP1	30S ribosomal protein S11	1208,02	<i>Cp1002Ct_ovis</i>	0.552473	Translation
D9Q6J9_CORP1	50S ribosomal protein L17	315,11	<i>Cp1002Ct_ovis</i>	0.095106	Translation
D9Q394_CORP1	50S ribosomal protein L19	2549,53	<i>Cp1002Ct_ovis</i>	0.047140	Translation
D9Q831_CORP1	50S ribosomal protein L20	4751,49	<i>Cp1002Ct_ovis</i>	0.034064	Translation
D9Q402_CORP1	50S ribosomal protein L21	1697,91	<i>Cp1002Ct_ovis</i>	0.530435	Translation
D9Q6I0_CORP1	50S ribosomal protein L30	4941,83	<i>Cp1002Ct_ovis</i>	0.201221	Translation
D9Q7A4_CORP1	50S ribosomal protein L33	3619,64	<i>Cp1002Ct_ovis</i>	0.626709	Translation
D9Q7W1_CORP1	Aspartyl glutamyl tRNA	1952,62	<i>Cp1002Ct_ovis</i>	0.045227	Translation
D9Q4V4_CORP1	Protein GrpE	2269,98	<i>Cp1002Ct_ovis</i>	0.071334	Translation
D9Q5F9_CORP1	Ribosomal RNA small subunit methyltransferase G	355,11	<i>Cp1002Ct_ovis</i>	0.045879	Translation
D9Q8D3_CORP1	Anaerobic C4 dicarboxylate transporter	196,94	<i>Cp1002Ct_ovis</i>	0.955392	Transport
D9Q7T5_CORP1	ATP synthase subunit C	375,91	<i>Cp1002Ct_ovis</i>	0.927537	Transport
D9Q381_CORP1	Hyphotetical protein	1137,01	<i>Cp1002Ct_ovis</i>	0.953098	Unknow function
D9Q4D5_CORP1	Hyphotetical protein	6896,58	<i>Cp1002Ct_ovis</i>	0.916450	Unknow function
D9Q8U6_CORP1	Hyphotetical protein	2159,14	<i>Cp1002Ct_ovis</i>	0.895819	Unknow function
D9Q5K2_CORP1	Hyphotetical protein	426,06	<i>Cp1002Ct_ovis</i>	0.891997	Unknow function
D9Q6I0_CORP1	Hyphotetical protein	3030,99	<i>Cp1002Ct_ovis</i>	0.845293	Unknow function
D9Q8T3_CORP1	Hyphotetical protein	697,39	<i>Cp1002Ct_ovis</i>	0.503971	Unknow function
D9Q919_CORP1	Hyphotetical protein	291,41	<i>Cp1002Ct_ovis</i>	0.471479	Unknow function
D9Q6Y7_CORP1	Hyphotetical protein	11801,47	<i>Cp1002Ct_ovis</i>	0.316462	Unknow function
D9Q5E4_CORP1	Hyphotetical protein	355,77	<i>Cp1002Ct_ovis</i>	0.170139	Unknow function
D9Q3P6_CORP1	Hyphotetical protein	1275,28	<i>Cp1002Ct_ovis</i>	0.054071	Unknow function
F9Y300_CORP1	Hyphotetical protein	515,11	<i>Cp1002Ct_ovis</i>	0.034427	Unknow function
D9Q481_CORP1	Phosphoserine phosphatase	307,3	<i>Cp1002Rc_ovis</i>	0.035351	Amino acid metabolism
D9Q474_CORP1	Glutamate racemase	343,98	<i>Cp1002Rc_ovis</i>	0.040278	Cell wall organization
D9Q4C9_CORP1	Mycothiol acetyltransferase	207,95	<i>Cp1002Rc_ovis</i>	0.107996	Cell wall organization
D9Q8S8_CORP1	Copper resistance protein CopC	4315,26	<i>Cp1002Rc_ovis</i>	0.964015	Detoxification
D9Q493_CORP1	Glutaredoxin like protein nrdH	725,98	<i>Cp1002Rc_ovis</i>	0.033036	Detoxification
D9Q7N5_CORP1	O-methyltransferase	619,11	<i>Cp1002Rc_ovis</i>	0.032455	DNA process
D9Q578_CORP1	Replicative DNA helicase	221,71	<i>Cp1002Rc_ovis</i>	0.079212	DNA process

D9Q598_CORP1	Formamidopyrimidine DNA glycosylase	365,17	<i>Cp1002Rc_ovis</i>	0.079073	General stress response
D9Q5N3_CORP1	Gamma type carbonic anhydratase	577,75	<i>Cp1002Rc_ovis</i>	0.035357	Others
D9Q5J0_CORP1	Phospholipase D	40,25	<i>Cp1002Rc_ovis</i>	0.409585	Pathogenesis
D9Q599_CORP1	Carbohydrate kinase	166,88	<i>Cp1002Rc_ovis</i>	0.039737	Specific metabolic pathways
D9Q8M3_CORP1	Epimerase family protein yfcH	72,07	<i>Cp1002Rc_ovis</i>	0.150238	Specific metabolic pathways
D9Q4X0_CORP1	Urease accessory protein UreD	414,1	<i>Cp1002Rc_ovis</i>	0.055896	Specific metabolic pathways
D9Q5B3_CORP1	Glucosamine 6 phosphate deaminase	524,55	<i>Cp1002Rc_ovis</i>	0.079507	Sugars metabolism
D9Q6Y6_CORP1	ATP dependent RNA helicase rhIE	1438,25	<i>Cp1002Rc_ovis</i>	0.060627	Transcription
D9Q889_CORP1	MerR family transcriptional regulator	358,64	<i>Cp1002Rc_ovis</i>	0.327138	Transcription
D9Q5N4_CORP1	Transcription factor Rok	321,64	<i>Cp1002Rc_ovis</i>	0.061937	Transcription
D9Q4M0_CORP1	Cell wall channel	4008,59	<i>Cp1002Rc_ovis</i>	0.025882	Transport
D9Q6Q5_CORP1	Hemin import ATP-binding protein	388,4	<i>Cp1002Rc_ovis</i>	0.035446	Transport
D9Q4V9_CORP1	Oligopeptide ABC transporter	558,79	<i>Cp1002Rc_ovis</i>	0.047328	Transport
D9Q3X0_CORP1	Oligopeptide transport	90,42	<i>Cp1002Rc_ovis</i>	0.035905	Transport
D9Q4C6_CORP1	Phosphate import ATP binding protein	316,23	<i>Cp1002Rc_ovis</i>	0.092471	Transport
D9Q6V9_CORP1	Hyphotetical protein	1278,45	<i>Cp1002Rc_ovis</i>	0.953803	Unknow function
D9Q6A8_CORP1	Hyphotetical protein	326,47	<i>Cp1002Rc_ovis</i>	0.918886	Unknow function
D9Q485_CORP1	Hyphotetical protein	2795,11	<i>Cp1002Rc_ovis</i>	0.890081	Unknow function
D9Q4N2_CORP1	Hyphotetical protein	708,75	<i>Cp1002Rc_ovis</i>	0.857050	Unknow function
D9Q538_CORP1	Hyphotetical protein	81,51	<i>Cp1002Rc_ovis</i>	0.822424	Unknow function
D9Q559_CORP1	Hyphotetical protein	475,62	<i>Cp1002Rc_ovis</i>	0.472378	Unknow function
D9Q4D0_CORP1	Hyphotetical protein	177,57	<i>Cp1002Rc_ovis</i>	0.292552	Unknow function
D9Q4G6_CORP1	Hyphotetical protein	204,55	<i>Cp1002Rc_ovis</i>	0.094884	Unknow function
D9Q4L8_CORP1	Hyphotetical protein	5324,08	<i>Cp1002Rc_ovis</i>	0.038893	Unknow function
D9Q4T0_CORP1	Hyphotetical protein	732,37	<i>Cp1002Rc_ovis</i>	0.037132	Unknow function

(a) *Cp1002Ct_ovis* = control condition - *Cp1002Rc_ovis* = recovered condition

Supplementary file 2: Table S.2: List of proteins identified in the exclusive proteome of strain 258_equi

Accession	Description	Score	Strain Condition ^(a)	SecretomeP	Biological process
I3QXJ4_CORPS	Hyphotetical protein	625,28	<i>Cp258Ct_equi</i>	0.973196	Unknow function
I3QUU9_CORPS	Glycerol uptake facilitator protein	1634,27	<i>Cp258Ct_equi</i>	0.971079	Transport
I3QXZ6_CORPS	Hyphotetical protein	1129,85	<i>Cp258Ct_equi</i>	0.971021	Unknow function
I3QY62_CORPS	Multidrug resistance protein norM	487,65	<i>Cp258Ct_equi</i>	0.969447	Pathogenesis
I3QZB5_CORPS	DoxX family membrane protein	1563,44	<i>Cp258Ct_equi</i>	0.967799	Specific metabolic pathway
I3QWA4_CORPS	Multidrug resistance protein norM	561,85	<i>Cp258Ct_equi</i>	0.967740	Pathogenesis
I3QXN4_CORPS	Cytochrome oxidase assembly protein	893,51	<i>Cp258Ct_equi</i>	0.963873	Oxidative phosphorylation
I3QV37_CORPS	Na H antiporter subunit C	1895,12	<i>Cp258Ct_equi</i>	0.952578	Transport
I3QY94_CORPS	Hyphotetical protein	13369,39	<i>Cp258Ct_equi</i>	0.946713	Unknow function
I3QVD0_CORPS	Hyphotetical protein	836,52	<i>Cp258Ct_equi</i>	0.946202	Unknow function
I3QVU2_CORPS	Cell surface hemin receptor	1012,97	<i>Cp258Ct_equi</i>	0.944615	Transport
I3QXZ1_CORPS	Hyphotetical protein	1357,98	<i>Cp258Ct_equi</i>	0.940925	Unknow function
I3QZX6_CORPS	Putative permease	2142,56	<i>Cp258Ct_equi</i>	0.939130	Pathogenesis
I3QY34_CORPS	Hyphotetical protein	595,58	<i>Cp258Ct_equi</i>	0.939063	Unknow function
I3QWP3_CORPS	Oligopeptide transport system permease	799,58	<i>Cp258Ct_equi</i>	0.936468	Transport
I3QWM5_CORPS	Hyphotetical protein	538,56	<i>Cp258Ct_equi</i>	0.912515	Unknow function
I3QVD1_CORPS	Hyphotetical protein	1817,98	<i>Cp258Ct_equi</i>	0.909554	Unknow function
I3QV55_CORPS	Hyphotetical protein	338	<i>Cp258Ct_equi</i>	0.900477	Unknow function
I3QWR5_CORPS	Hyphotetical protein	1286,94	<i>Cp258Ct_equi</i>	0.760648	Unknow function
I3QZI2_CORPS	Hyphotetical protein	1218,63	<i>Cp258Ct_equi</i>	0.683346	Unknow function
I3QW43_CORPS	Hyphotetical protein	2549,35	<i>Cp258Ct_equi</i>	0.649127	Unknow function
I3QV51_CORPS	Thioredoxin related protein	259,85	<i>Cp258Ct_equi</i>	0.596727	Detoxification
I3QWD9_CORPS	30S ribosomal protein S14	2898,68	<i>Cp258Ct_equi</i>	0.519183	Translation
I3QWN0_CORPS	Phosphonoacetate hydrolase	510,88	<i>Cp258Ct_equi</i>	0.488603	Pathogenesis
I3QVQ7_CORPS	Hyphotetical protein	3502,56	<i>Cp258Ct_equi</i>	0.487451	Unknow function
I3QW42_CORPS	Hyphotetical protein	1727,65	<i>Cp258Ct_equi</i>	0.444079	Unknow function
I3QV77_CORPS	Peptidase family M1 containing protein	479,38	<i>Cp258Ct_equi</i>	0.282710	Pathogenesis
I3QZ69_CORPS	Hyphotetical protein	2426,64	<i>Cp258Ct_equi</i>	0.240903	Unknow function

I3QZ19_CORPS	Hypothetical protein	993,7	<i>Cp258Ct_equi</i>	0.206547	Unknow function
I3QXI8_CORPS	Hypothetical protein	1788,22	<i>Cp258Ct_equi</i>	0.192808	Unknow function
I3R0G5_CORPS	Hypothetical protein	13524,08	<i>Cp258Ct_equi</i>	0.153840	Unknow function
I3QZ86_CORPS	Ribosomal protein alanine acetyltransferase	970,9	<i>Cp258Ct_equi</i>	0.117920	Translation
I3QW17_CORPS	3-Phosphoshikimate 1-carboxyvinyltransferase	1106,2	<i>Cp258Ct_equi</i>	0.096154	Amino acid metabolism
I3QWK8_CORPS	Hypothetical protein	548,56	<i>Cp258Ct_equi</i>	0.087259	Unknow function
I3R019_CORPS	Hypothetical protein	703,49	<i>Cp258Ct_equi</i>	0.081506	Unknow function
I3QXF7_CORPS	Precorrin 3B synthase	527,47	<i>Cp258Ct_equi</i>	0.080371	Cofactor metabolism
I3QWC1_CORPS	G U mismatch specific DNA glycosylase	278,39	<i>Cp258Ct_equi</i>	0.077252	DNA process
I3QYS0_CORPS	Acyl carrier protein	841,21	<i>Cp258Ct_equi</i>	0.062111	Others
I3QXD7_CORPS	Hypothetical protein	579,17	<i>Cp258Ct_equi</i>	0.058854	Unknow function
I3QYF3_CORPS	TetR family transcriptional regulator	1667,81	<i>Cp258Ct_equi</i>	0.050249	Transcription
I3QYA3_CORPS	Hypothetical protein	6414,88	<i>Cp258Ct_equi</i>	0.042842	Unknow function
I3QZM7_CORPS	Rhodanese related sulfurtransferase	1553,18	<i>Cp258Ct_equi</i>	0.040820	Specific metabolic pathway
I3QZG2_CORPS	Hypothetical protein	3885,47	<i>Cp258Ct_equi</i>	0.039155	Unknow function
I3QW55_CORPS	Hypothetical protein	2560,11	<i>Cp258Ct_equi</i>	0.038971	Unknow function
I3QYA9_CORPS	Hypothetical protein	1092,72	<i>Cp258Ct_equi</i>	0.038753	Unknow function
I3QZN5_CORPS	Cell wall channel	27525,38	<i>Cp258Ct_equi</i>	0.037132	Transport
I3QXU8_CORPS	Hypothetical protein	1329,61	<i>Cp258Ct_equi</i>	0.035266	Unknow function
I3QYN8_CORPS	Hypothetical protein	4416,59	<i>Cp258Ct_equi</i>	0.033503	Unknow function
I3QVA5_CORPS	DNA binding Excisionase protein	2176,67	<i>Cp258Ct_equi</i>	0.031201	DNA process
I3QV14_CORPS	Deoxyribose phosphate aldolase	1064,78	<i>Cp258Ct_equi</i>	0.026562	Carbohydrate metabolism
I3QX53_CORPS	Biotin lipoyl attachment protein	1978,17	<i>Cp258Ct_equi</i>	0.025928	Others
I3QZS6_CORPS	Cytochrome c nitrate reductase small	1035,81	<i>Cp258Rc_equi</i>	0.901105	Nitrogen metabolism

(a) *Cp258Ct_equi* = control condition - *Cp258Rc_equi* = recovered condition

Supplementary file 3: Table S.3: Complet list of proteins differentially produced among the recovered and control condition of strain 1002_*ovis*.

Accession	Description	Score	Cp1002Rc:Cp1002Ct_Ratio	Cp1002Rc:Cp1002Ct_Log(2)Ratio ^(a)	Cp1002Rc:Cp1002Ct_Log(e)Ratio	Cp1002Rc:Cp1002Ct_Log(e)StdDev	Cp1002Rc:Cp1002Ct_P ^(a)	secretomeP
Transport								
D9Q5H9_CORP1	Periplasmic binding protein LacI	5601,78	9,583089075	3,26	2,26	0,11	1	0.530178
D9Q6G4_CORP1	Oligopeptide binding protein oppA	4120,1	8,004468304	3,00	2,08	0,08	1	0.884444
D9Q4T5_CORP1	ABC transporter domain containing ATP	1264,05	5,929856249	2,57	1,78	0,31	1	0.068463
D9Q7K5_CORP1	Oligopeptide binding protein oppA	33697,17	4,305959693	2,11	1,46	0,1	1	0.873687
D9Q5B8_CORP1	Oligopeptide binding protein oppA	852,88	3,669296493	1,88	1,3	0,13	1	0.849217
D9Q6C3_CORP1	ABC type metal ion transport system permease	650,43	3,004166096	1,59	1,1	0,03	1	0.078043
D9Q796_CORP1	Glutamate binding protein GluB	6254,68	0,364218983	-1,46	-1,01	0,25	0	0.840325
D9Q7W9_CORP1	Iron 3 hydroxamate binding protein	2774,62	0,326279793	-1,62	-1,12	1,02	0,05	0.824030
Cell division								
D9Q7G1_CORP1	Septum formation initiator protein	2071,46	2,611696417	1,38	0,96	0,11	1	0.551153
Cell adhesion								
D9Q5H7_CORP1	Hypothetical protein	115906,3	2,857650982	1,51	1,05	0,22	1	0.840443

DNA synthesis and repair

D9Q7J1_CORP1	GTP binding protein YchF	3487,98	6,423736863	2,68	1,86	0,07	1	0.042575
D9Q5F7_CORP1	Chromosome partitioning protein ParB	2467,24	5,419481015	2,44	1,69	0,16	1	0.052395
D9Q5G6_CORP1	DNA polymerase III subunit beta	1907,74	3,490342957	1,80	1,25	0,22	1	0.071008
D9Q5V6_CORP1	Nucleoid associated protein	68097,59	3,004166096	1,59	1,1	0,1	1	0.070074

Transcription

D9Q6J8_CORP1	DNA directed RNA polymerase subunit	29671,46	2,611696417	1,38	0,96	0,1	1	0.094910
D9Q748_CORP1	tRNA rRNA methyltransferase	2467,24	2,410899695	1,27	0,88	0,36	1	0.060356
D9Q8L3_CORP1	DNA directed RNA polymerase subunit omega	3784,13	0,431710535	-1,21	-0,84	0,13	0	0.700214
D9Q6D1_CORP1	DNA directed RNA polymerase subunit beta	2611,89	0,414782914	-1,27	-0,88	0,48	0	0.067182
D9Q8A5_CORP1	RNA polymerase-binding protein RbpA	10787,51	0,298197268	-1,75	-1,21	0,23	0	0.103548

Translation

D9Q584_CORP1	30S ribosomal protein S6	20750,74	28,21912428	4,82	3,34	0,66	1	0.047667
D9Q6E4_CORP1	Elongation factor G	16882,71	9,487735836	3,25	2,25	0,17	1	0.082321
D9Q5I3_CORP1	Peptidyl prolyl cis trans isomerase	61648,39	7,53832479	2,91	2,02	0,27	1	0.142641
D9Q835_CORP1	Phenylalanine tRNA ligase beta subunit	1269,7	6,685894283	2,74	1,9	0,15	1	0.064869
D9Q6L0_CORP1	50S ribosomal protein L13	5689,37	6,233886926	2,64	1,83	0,15	1	0.101816
D9Q6H2_CORP1	50S ribosomal protein L5	3269,32	4,349235265	2,12	1,47	0,04	1	0.076250
D9Q918_CORP1	Proline tRNA ligase	932,79	4,349235265	2,12	1,47	0,47	1	0.072151
D9Q6C0_CORP1	50S ribosomal protein L10	27143,51	3,632786417	1,86	1,29	0,08	1	0.031374
D9Q6F6_CORP1	50S ribosomal protein L23	6947,79	3,596639623	1,85	1,28	0,07	1	0.060878
D9Q6H1_CORP1	50S ribosomal protein L24	27887,33	3,35348478	1,75	1,21	0,32	1	0.078408
F9Y2W9_CORP1	Hypothetical protein	3152,39	3,35348478	1,75	1,21	0,13	1	0.591013
D9Q6H6_CORP1	30S ribosomal protein S8	4941,19	2,944679677	1,56	1,08	0,15	1	0.088407
D9Q6F3_CORP1	30S ribosomal protein S10	25117,55	2,915379653	1,54	1,07	0,09	1	0.048124
D9Q6G2_CORP1	50S ribosomal protein L29	2467,24	2,718281828	1,44	1	0,59	1	0.050948
D9Q401_CORP1	50S ribosomal protein L27	2467,24	2,611696417	1,38	0,96	0,53	1	0.081399
D9Q7E8_CORP1	50S ribosomal protein L25	1358,05	0,410655759	-1,28	-0,89	0,2	0	0.037225

D9Q6H8_CORP1	50S ribosomal protein L18	8920,94	0,402524213	-1,31	-0,91	0,15	0	0,049024
D9Q7S4_CORP1	Homoserine dehydrogenase	698,17	0,379083027	-1,40	-0,97	0,23	0	0,035138
D9Q6F7_CORP1	50S ribosomal protein L2	3079,3	0,323033258	-1,63	-1,13	0,87	0	0,633387
D9Q4T4_CORP1	ATP dependent chaperone protein ClpB	1883,16	0,286504797	-1,80	-1,25	0,46	0	0,045308
D9Q8N9_CORP1	Aspartate tRNA ligase	1004,33	0,22090998	-2,18	-1,51	0,17	0	0,092415
D9Q7S2_CORP1	Arginine tRNA ligase	2679,11	0,184519513	-2,44	-1,69	0,15	0	0,051908

Pathogenesis

D9Q8M7_CORP1	Metallopeptidase family M24	3213,83	46,99305875	5,55	3,85	0,33	1	0,050024
D9Q608_CORP1	Penicillin binding protein transpeptidase	1215,32	12,80710317	3,68	2,55	0,24	1	0,859830
D9Q827_CORP1	Metallo beta lactamase superfamily protein	629,38	6,233886926	2,64	1,83	0,33	1	0,144158
D9Q721_CORP1	Hypothetical protein	112025	4,711469958	2,24	1,55	0,11	1	0,260801
D9Q7K8_CORP1	Trypsin like serine protease	35041,27	3,896193358	1,96	1,36	0,14	1	0,648370
D9Q416_CORP1	ATP dependent Clp protease proteolytic	2467,24	3,421229602	1,77	1,23	0,07	1	0,087255
D9Q639_CORP1	Secreted hydrolase	22798,13	3,35348478	1,75	1,21	0,28	1	0,072385
D9Q588_CORP1	Penicillin binding protein	9951,61	2,386910865	1,26	0,87	0,41	1	0,916125

Energy metabolism

Pyruvate metabolism

D9Q4P2_CORP1	Acetate kinase	10828,79	3,896193358	1,96	1,36	0,94	1	0,063340
D9Q4Z7_CORP1	Phosphoenolpyruvate carboxykinase GTP	8764,35	3,158192834	1,66	1,15	0,11	1	0,147167

TCA Cycle

D9Q651_CORP1	Succinate dehydrogenase flavoprotein	797,48	4,05519987	2,02	1,4	0,09	1	0,159059
D9Q8G5_CORP1	Aconitate hydratase	4250,81	3,596639623	1,85	1,28	0,22	1	0,217637
D9Q648_CORP1	Dihydrolipoyl dehydrogenase	4110,08	2,974274172	1,57	1,09	0,29	1	0,047180
D9Q752_CORP1	Citrate synthase	6299,21	0,431710535	-1,21	-0,84	0,2	0	0,116042

Main glycolytic pathways

D9Q787_CORP1	Glucose 6 phosphate isomerase	1025,89	22,64637705	4,50	3,12	0,41	1	0,058841
D9Q7G0_CORP1	Enolase	53290,95	4,526730751	2,18	1,51	0,09	1	0,068928

D9Q7X0_CORP1	6 phosphofructokinase	1806,65	3,034358438	1,60	1,11	0,75	0,99	0.052885
Pentose phosphate pathway								
D9Q895_CORP1	6-Phosphogluconate dehydrogenase	4246,26	0,269820072	-1,89	-1,31	0,41	0	0.050906
Oxidative phosphorylation								
D9Q7T8_CORP1	ATP synthase subunit alpha	2467,24	2,801065755	1,49	1,03	0,13	1	0.070875
Lipid metabolism								
D9Q520_CORP1	Glycerophosphoryl diester phosphodiester	2494,25	16,28101918	4,03	2,79	0,07	1	0.802154
D9Q718_CORP1	Methylmalonyl CoA carboxyltransferase 1	2467,24	4,48168907	2,16	1,5	0,18	1	0.049504
Amino acid metabolism								
D9Q5X8_CORP1	Aspartokinase	1944,81	7,242743123	2,86	1,98	0,34	1	0.043575
D9Q4C2_CORP1	Succinyl CoA Coenzyme A transferase	10894,63	3,095656485	1,63	1,13	0,08	1	0.061344
D9Q3L8_CORP1	Glutamine synthetase	320,71	0,427414922	-1,23	-0,85	0,18	0	0.263700
D9Q8H7_CORP1	Cysteine desulfurase	1689,36	0,307278755	-1,70	-1,18	0,22	0	0.067087
General stress response								
D9Q566_CORP1	Universal stress protein A	2498,69	3,254374032	1,70	1,18	0,45	1	0.034684
D9Q824_CORP1	Stress related protein	2467,24	2,915379653	1,54	1,07	0,14	1	0.035291
Metabolism of nucleotides and nucleic acids								
D9Q4Y6_CORP1	Deoxycytidine triphosphate deaminase	887,26	5,259310669	2,39	1,66	0,18	1	0.216897
D9Q6J1_CORP1	Adenylate kinase	15629,86	4,61817669	2,21	1,53	0,08	1	0.059568
D9Q8L4_CORP1	Guanylate kinase	2467,24	2,534509196	1,34	0,93	0,12	1	0.050095
D9Q6T2_CORP1	Ribokinase	890,09	0,427414922	-1,23	-0,85	0,32	0	0.032324
D9Q4E9_CORP1	Adenylosuccinate lyase	1441,99	0,343008499	-1,54	-1,07	0,09	0	0.035597
D9Q6P0_CORP1	D methionine binding lipoprotein metQ	11519,67	0,26184566	-1,93	-1,34	0,52	0	0.817217
Specific metabolic pathways								

D9Q7W0_CORP1	Hypothetical protein	2467,24	2,386910865	1,26	0,87	0,31	1	0.039678
D9Q7W3_CORP1	Mycothiol acetyltransferase	947,33	0,232236266	-2,11	-1,46	0,22	0	0.214833

Sugars metabolism

D9Q8V2_CORP1	UDP glucose 4 epimerase	2001,76	8,758284709	3,13	2,17	0,29	1	0.094403
D9Q6V6_CORP1	Phosphomannomutase ManB	1730,63	4,137120263	2,05	1,42	0,18	1	0.053146
D9Q659_CORP1	Formate acetyltransferase	5456,95	2,915379653	1,54	1,07	0,12	1	0.539548
D9Q423_CORP1	Ribose 5 phosphate isomerase B	2467,24	2,611696417	1,38	0,96	0,26	1	0.064467
D9Q6V1_CORP1	Mannose 1 phosphate guanylyltransferase	1612,45	0,431710535	-1,21	-0,84	0,15	0	0.068085

Detoxification

D9Q929_CORP1	Mycothione glutathione reductase	490,36	6,359819674	2,67	1,85	0,18	1	0.085017
D9Q5T5_CORP1	Glyoxalase Bleomycin resistance protein	8420,32	4,61817669	2,21	1,53	0,13	1	0.226764
D9Q424_CORP1	DSBA oxidoreductase	12179,8	4,263114718	2,09	1,45	0,28	1	0.061566
D9Q4P4_CORP1	Ferredoxin ferredoxin NADP reductase	1086,71	3,2219925	1,69	1,17	0,36	1	0.083585
D9Q692_CORP1	Thiol disulfide isomerase thioredoxin	3721,88	0,210136083	-2,25	-1,56	0,21	0	0.438415

Nitrogen metabolism

D9Q4Q8_CORP1	Cytochrome c nitrate reductase small	1118,33	6,423736863	2,68	1,86	0,23	1	0.901856
--------------	--------------------------------------	---------	-------------	------	------	------	---	----------

Unknow function

D9Q6T0_CORP1	Hypothetical protein	2277,6	12,30492994	3,62	2,51	0,1	1	0.050552
D9Q744_CORP1	Hypothetical protein	442,07	10,17567363	3,35	2,32	0,09	1	0.866986
D9Q6N1_CORP1	Hypothetical protein	561,84	8,08491447	3,02	2,09	0,11	1	0.062141
D9Q8Q4_CORP1	Hypothetical protein	72711,5	7,767900736	2,96	2,05	0,46	1	0.974016
D9Q832_CORP1	Hypothetical protein	1774,59	7,463317276	2,90	2,01	0,3	1	0.752478
D9Q3S8_CORP1	Hypothetical protein	837,6	6,88950988	2,78	1,93	0,38	1	0.231421
D9Q7M9_CORP1	Hypothetical protein	3246,28	6,049647176	2,60	1,8	0,08	1	0.147602
D9Q7I6_CORP1	Hypothetical protein	3751,96	5,36555569	2,42	1,68	0,22	1	0.707595
D9Q739_CORP1	Hypothetical protein	2845,77	4,85495602	2,28	1,58	0,08	1	0.836229
D9Q4C5_CORP1	Hypothetical protein	1339,3	3,560852494	1,83	1,27	0,14	1	0.023133

D9Q5C3_CORP1	Hypothetical protein	111234,6	2,801065755	1,49	1,03	0,16	1	0.946918
D9Q700_CORP1	Hypothetical protein	2467,24	2,801065755	1,49	1,03	0,08	1	0.072810
D9Q657_CORP1	Hypothetical protein	1172,66	2,664456293	1,41	0,98	1,17	0,96	0.830926
D9Q6F2_CORP1	Hypothetical protein	2467,24	2,534509196	1,34	0,93	0,03	1	0.061860
D9Q7X5_CORP1	Hypothetical protein	38716,45	0,431710535	-1,21	-0,84	0,21	0	0.825761
D9Q4T9_CORP1	Hypothetical protein	553,76	0,410655759	-1,28	-0,89	0,21	0	0.934591
D9Q6R6_CORP1	Hypothetical protein	1457,62	0,379083027	-1,40	-0,97	0,28	0	0.206908
D9Q890_CORP1	Hypothetical protein	1948,52	0,349937766	-1,51	-1,05	0,14	0	0.847549
D9Q6M6_CORP1	Hypothetical protein	1935,68	0,267135288	-1,90	-1,32	0,11	0	0.823541

Others

D9Q6I3_CORP1	Maltotriose binding protein	5210,9	37,33756355	5,22	3,62	0,39	1	0.864851
D9Q4A3_CORP1	DsbG protein	3101,13	4,178698973	2,06	1,43	0,12	1	0.814366
D9Q6N9_CORP1	D methionine binding lipoprotein metQ	2665,58	3,455613498	1,79	1,24	0,16	1	0.764416
D9Q732_CORP1	Carbonic anhydrase	689,15	3,158192834	1,66	1,15	0,18	1	0.130559
D9Q6W6_CORP1	Lipoprotein LpqB	1484,31	3,095656485	1,63	1,13	0,05	1	0.670057
D9Q556_CORP1	LSR2 like protein	2714,21	2,801065755	1,49	1,03	0,15	1	0.096802
D9Q5Q0_CORP1	UPF0145 protein	2467,24	2,585709628	1,37	0,95	0,16	1	0.025009
D9Q701_CORP1	UPF0182 protein	1682,98	2,386910865	1,26	0,87	0,47	1	0.869411
D9Q8A3_CORP1	Protein ycel	16885,01	2,316366916	1,21	0,84	0,11	1	0.901679
D9Q5X4_CORP1	Serine aspartate repeat containing protein	528,36	0,283654029	-1,82	-1,26	0,22	0	0.892317
D9Q826_CORP1	DoxX family protein	697,26	0,236927745	-2,08	-1,44	0,72	0	0.614317
D9Q407_CORP1	Ornithine cyclodeaminase	2566,18	0,166960176	-2,58	-1,79	0,47	0	0.048247

(a) Ratio values to: Cp1002Rc:Cp1002Ct_Log(2)Ratio \geq 1.5 - p>0.95 up-regulation, p<0.05 down-regulation

Supplementary file 4: Table S.4: Functional classification of the total proteins differentially produced between the recovered and control conditions of *strain 258_equi*.

Accession	Description	Score	Cp258Rc:Cp258Ct_Log(2)Ratio	Cp258Rc:Cp258Ct_Log(e)Ratio ^(a)	Cp258Rc:Cp258Ct_Log(e)StdDev	Cp258Rc:Cp258Ct_P ^(a)	SecretomeP
Transport							
I3QZ34_CORPS	ABC transporter ATP binding protein	20158,7	0,124930222	3,000805575	2,08	0,1	1 0.121002
I3QWP4_CORPS	Oligopeptide transport OppD	6266,77	0,146606968	2,769974417	1,92	0,15	1 0.056002
I3QVU7_CORPS	hypothetical protein	14835,01	0,190138986	2,39487372	1,66	0,13	1 0.919607
I3QVT3_CORPS	Manganese ABC transporter substrate binding	16263,86	0,201896513	2,3083121	1,6	0,11	1 0.744046
I3QVU3_CORPS	Cell surface hemin receptor	11874,87	0,21438111	2,221750308	1,54	0,12	1 0.940714
I3QW10_CORPS	Protein translocase subunit SecA	7923,5	0,269820072	1,889930421	1,31	0,11	1 0.066620
I3QUW4_CORPS	ABC type metal ion transport system permease	1016,6	0,298197268	1,745661055	1,21	0,29	1 0.783828
I3QXV8_CORPS	Protein translocase subunit SecF	1729,78	0,316636777	1,659099263	1,15	0,14	1 0.924484
I3QWD2_CORPS	Glutamate binding protein GluB yn	8414,45	0,343008499	1,543683769	1,07	0,14	1 0.842669
I3R0D7_CORPS	Oligopeptide binding protein oppA	3469,47	0,353454695	1,500402787	1,04	0,24	1 0.846561
I3QVU4_CORPS	Hemin binding periplasmic protein hmuT	14010	0,360594947	1,471548914	1,02	0,14	1 0.070076
I3QUV4_CORPS	Glycine betaine binding protein	4096,23	0,371576687	1,428268104	0,99	0,22	1 0.680214
I3QWP1_CORPS	Oligopeptide binding protein oppA	41781,98	0,382892894	1,384987208	0,96	0,06	1 0.871277
I3QVC7_CORPS	ABC type transporter	11220,09	0,390627836	1,356133335	0,94	0,07	1 0.311901
I3QZC0_CORPS	ABC type antimicrobial peptide transport	1159,51	0,394553708	1,341706398	0,93	0,13	1 0.674852

I3QXV9_CORPS	Protein translocase subunit SecD	2879,45	0,423162076	1,240717756	0,86	0,09	1	0.871060
I3QX10_CORPS	Iron 3 hydroxamate binding protein fh	13922,33	0,431710535	1,211863797	0,84	0,11	1	0.827145
I3QUW5_CORPS	Manganese zinc iron transport system ATP	391,52	2,611696417	-1,384987208	-0,96	0,29	0	0.035018
Cell division								
I3QYH6_CORPS	Cell division protein sepF	54755,19	0,034735263	4,847455186	3,36	0,34	1	0.116970
I3R031_CORPS	Trehalose corynomycolyl transferase B	112067,8	0,116484147	3,101794475	2,15	0,07	1	0.177019
I3QW64_CORPS	Cell division protein ftsX	2967,84	0,272531806	1,875503484	1,3	0,15	1	0.814468
I3QYB7_CORPS	Signal recognition particle receptor Ft	3214,53	0,295230158	1,760087991	1,22	0,17	1	0.076709
I3QYI0_CORPS	Cell division protein FtsQ	4225,31	0,423162076	1,240717756	0,86	0,15	1	0.186066
Cell adhesion								
I3QZX5_CORPS	Fimbrial associated sortase like protein	13261,7	0,410655759	1,283998566	0,89	0,12	1	0.503426
DNA synthesis and repair								
I3QXW2_CORPS	Holliday junction ATP dependent DNA	2827,61	0,11883728	3,072940602	2,13	0,52	1	0.039364
I3QWU4_CORPS	hypothetical protein	3242,55	0,267135288	1,90435753	1,32	0,22	1	0.659226
I3QVV1_CORPS	Endonuclease Exonuclease phosphatase	16088,91	0,301194198	1,731234118	1,2	0,13	1	0.650379
I3R0A4_CORPS	Single stranded DNA binding protein	7273,43	0,418951547	1,255144692	0,87	0,13	1	0.780518
Transcription								
I3QZY6_CORPS	Transcriptional regulatory protein	2190,63	0,158817421	2,654558923	1,84	0,24	1	0.068301
I3R000_CORPS	Lysine tRNA ligase	1520,14	0,295230158	1,760087991	1,22	0,23	1	0.450158
I3QWK3_CORPS	Transcription elongation factor GreA	63144,89	0,343008499	1,543683769	1,07	0,07	1	0.715029
I3QV02_CORPS	Galactonate operon transcriptional	586,51	4,392945765	-2,135188688	-1,48	0,63	0	0.042736
I3QZA9_CORPS	HTH type transcriptional regulator CmtR	734,34	10,91349509	-3,448041299	-2,39	1,58	0	0.050448
Translation								
I3QVL3_CORPS	50S ribosomal protein L6	33564,54	0,162025742	2,62570505	1,82	0,08	1	0.075646
I3QXS6_CORPS	Elongation factor P	126499,7	0,208045171	2,26503129	1,57	0,07	1	0.706707
I3QXV3_CORPS	Peptidyl prolyl cis trans isomerase B	3638,31	0,216535674	2,207323371	1,53	0,27	1	0.941581

I3QZR6_CORPS	Disulfide bond formation protein DsbB	5386,2	0,234570277	2,091907878	1,45	0,17	1	0.732982
I3QZN6_CORPS	60 kDa chaperonin	87750,49	0,234570277	2,091907878	1,45	0,04	1	0.034984
I3QVK3_CORPS	50S ribosomal protein L5	51229,82	0,267135288	1,90435753	1,32	0,09	1	0.075957
I3QVN3_CORPS	30S ribosomal protein S11	23582,5	0,275270794	1,861076548	1,29	0,1	1	0.543184
I3QZU6_CORPS	ATP dependent chaperone protein ClpB	5524,23	0,286504797	1,803368801	1,25	0,18	1	0.045370
I3QVI8_CORPS	50S ribosomal protein L2	17137,85	0,292292572	1,774514928	1,23	0,09	1	0.646682
I3QZX2_CORPS	Chaperone protein DnaK	88814,63	0,329558956	1,601391516	1,11	0,04	1	0.125700
I3QVJ4_CORPS	30S ribosomal protein S17	55278,48	0,418951547	1,255144692	0,87	0,07	1	0.725334

Pathogenesis

I3QV43_CORPS	Penicillin binding protein transpeptidase	18512,68	0,286504797	1,803368801	1,25	0,06	1	0.866080
I3QWE6_CORPS	Serine protease	9952,11	0,298197268	1,745661055	1,21	0,14	1	0.847369
I3QYI9_CORPS	Penicillin binding protein	11772,81	0,307278755	1,702380073	1,18	0,12	1	0.398995
I3QXC5_CORPS	Iron ABC transporter substrate binding	12242,99	0,319819026	1,644672326	1,14	0,07	1	0.937660
I3QY03_CORPS	Diphtheria toxin repressor	45534,1	0,329558956	1,601391516	1,11	0,1	1	0.040516
I3R059_CORPS	O acetyltransferase OatA	2935,54	0,360594947	1,471548914	1,02	0,1	1	0.946859
I3QZM5_CORPS	D alanyl D alanine carboxypeptidase	2988,16	0,364218983	1,457121978	1,01	0,13	1	0.158234
I3QW38_CORPS	Lon protease	6439,26	0,394553708	1,341706398	0,93	0,15	1	0.453022
I3QXC3_CORPS	Esterase	496,62	0,406569669	1,298425502	0,9	0,28	1	0.858380
I3QZ50_CORPS	Peptidase S8A Subtilisin family protein	40174,72	0,427414922	1,226290819	0,85	0,07	1	0.483486
I3QW24_CORPS	Hydrolase domain containing protein	17234,12	2,386910865	-1,255144692	-0,87	0,06	0	0.404443
I3QYP5_CORPS	MutT NUDIX family protein	5870,55	2,611696417	-1,384987208	-0,96	0,32	0	0.067993

Cellular communication

I3QX73_CORPS	Phosphotransferase system II Component	32053,52	0,22090998	2,178469498	1,51	0,06	1	0.926114
I3R080_CORPS	Hypothetical protein	2564,2	6,233886926	-2,640131987	-1,83	0,27	0	0.465419
I3QVG4_CORPS	Response regulator	484,78	7,242743123	-2,856536208	-1,98	0,35	0	0.038592

Energy metabolism

Oxidative phosphorylation

I3QYL2_CORPS	Ubiquinol cytochrome c reductase iron	3300,67	0,113041523	3,145075285	2,18	0,75	1	0.824410
--------------	---------------------------------------	---------	-------------	-------------	------	------	---	----------

I3QYL3_CORPS	Ubiquinol cytochrome C reductase	3477,1	0,227637684	2,135188688	1,48	0,93	1	0.729101
Electron transport								
I3QXE7_CORPS	NADH dehydrogenase p	6117,37	0,22090998	2,178469498	1,51	0,14	1	0.145985
Pentose phosphate pathway								
I3QXN8_CORPS	Glucose 6 phosphate 1 dehydrogenase	3823,39	0,241714027	2,048626896	1,42	0,13	1	0.143037
Main glycolytic pathways								
I3QWJ6_CORPS	Enolase	54266,63	0,301194198	1,731234118	1,2	0,07	1	0.067111
I3QX11_CORPS	6-Phosphofructokinase	4219,85	0,323033258	1,630245389	1,13	0,15	1	0.052818
Lipid metabolism								
I3QYV5_CORPS	Long chain fatty acid CoA ligase	2395,48	0,249075308	2,005346086	1,39	0,19	1	0.075961
I3QX04_CORPS	Mycothiol acetyltransferase	5934,73	24,53253137	-4,6166242	-3,2	0,37	0	0.233457
Cofactors metabolism								
I3QXA7_CORPS	Thiamin pyrophosphokinase catalytic	4400,58	0,254106958	1,976492213	1,37	0,16	1	0.115323
I3QVB7_CORPS	Uroporphyrinogen decarboxylase	3376,83	0,269820072	1,889930421	1,31	0,29	1	0.079400
I3QWN5_CORPS	2 dehydropantoate 2 reductase	854,95	3,095656485	-1,630245389	-1,13	0,36	0	0.035677
Amino acid metabolism								
I3QWW3_CORPS	Diaminopimelate decarboxylase	600,78	2,410899695	-1,269571629	-0,88	0,32	0	0.044701
I3QY54_CORPS	Dihydrodipicolinate reductase	1212,64	3,18993317	-1,673526199	-1,16	0,26	0	0.042288
Specific metabolic pathways								
I3QZU1_CORPS	Glycerol 3 phosphate dehydrogenase	6827,79	0,114177608	3,130648349	2,17	0,14	1	0.044286
I3QZB7_CORPS	Phosphoglucomutase	4079,06	0,166960176	2,582424068	1,79	0,19	1	0.296123
I3QW69_CORPS	Carbonic anhydrase	4725,92	0,188247074	2,409300656	1,67	0,13	1	0.120871
I3QVZ1_CORPS	Hypothetical protein	2256,66	2,435129616	-1,283998566	-0,89	0,36	0	0.043791
I3QW96_CORPS	Enoyl CoA hydratase echA6	611,75	2,637944535	-1,399414231	-0,97	0,22	0	0.028978

I3QXH4_CORPS	AAA ATPase forming ring shaped complexe	206,2	2,829216906	-1,500402787	-1,04	0,26	0	0.060990
I3QXT1_CORPS	Chorismate synthase	614,35	2,915379653	-1,543683769	-1,07	0,4	0	0.054386
I3R0F7_CORPS	Anthranilate synthase component II	382,53	3,095656485	-1,630245389	-1,13	0,47	0	0.047168
Detoxification								
I3QZG0_CORPS	Glutathione peroxidase	46259,61	0,035436961	4,818601313	3,34	0,22	1	0.157902
I3QW94_CORPS	Superoxide dismutase Cu Zn	8883,72	0,052339703	4,255950439	2,95	0,2	1	0.783532
I3QYL8_CORPS	Iron sulfur cluster insertion protein	27250,26	0,082909966	3,592310666	2,49	0,13	1	0.549416
I3QZV3_CORPS	Oxidoreductase	4356,68	0,087160846	3,520175982	2,44	0,29	1	0.147757
I3QZ61_CORPS	Oxidoreductase	3324,33	0,278037308	1,846649611	1,28	0,19	1	0.053385
I3QV23_CORPS	Catalase	15172,47	0,301194198	1,731234118	1,2	0,15	1	0.688884
I3R0H6_CORPS	Thioredoxin reductase	19119,71	0,319819026	1,644672326	1,14	0,11	1	0.050399
I3R0G3_CORPS	Iron sulfur protein	5690,8	0,34645583	1,529256661	1,06	0,3	1	0.832641
I3QY82_CORPS	Mycothione glutathione reductase	5838,24	0,34645583	1,529256661	1,06	0,13	1	0.084368
General stress response								
I3R095_CORPS	Phage shock protein A	29691,47	0,116484147	3,101794475	2,15	0,21	1	0.738405
I3QX77_CORPS	Stress related protein	36248,9	0,158817421	2,654558923	1,84	0,18	1	0.035033
I3QYV1_CORPS	Heat inducible transcription repressor	177,37	3,669296493	-1,875503484	-1,3	0,44	0	0.040916
Unknow function								
I3QYG9_CORPS	Hypothetical protein	48351,61	0,025476468	5,29469091	3,67	0,43	1	0.761607
I3QUL2_CORPS	Hypothetical protein	144705	0,072802871	3,779860842	2,62	0,12	1	0.843663
I3QZP8_CORPS	Hypothetical protein	14676,76	0,131335525	2,928670892	2,03	0,21	1	0.855820
I3QV45_CORPS	Hypothetical protein	55280,53	0,148080392	2,75554748	1,91	0,15	1	0.841023
I3R0E2_CORPS	Hypothetical protein	141172,41	0,165298896	2,596851005	1,8	0,05	1	0.945639
I3QW83_CORPS	Hypothetical protein	1589,85	0,190138986	2,39487372	1,66	0,23	1	0.875922
I3QYP3_CORPS	Hypothetical protein	44252,51	0,190138986	2,39487372	1,66	0,14	1	0.773934
I3QZY5_CORPS	Hypothetical protein	7128,02	0,195929575	2,35159291	1,63	0,3	1	0.769233
I3QWP8_CORPS	Hypothetical protein	54353,63	0,203925605	2,293885163	1,59	0,07	1	0.634600
I3QXD9_CORPS	Hypothetical protein	6296,71	0,212247984	2,236177245	1,55	0,24	1	0.839411

I3QW99_CORPS	Hypothetical protein	2338,97	0,21438111	2,221750308	1,54	0,23	1	0.776200
I3R049_CORPS	Hypothetical protein	2318,32	0,232236266	2,106334815	1,46	0,15	1	0.912729
I3QY71_CORPS	Hypothetical protein	6074,68	0,232236266	2,106334815	1,46	0,23	1	0.501111
I3QV39_CORPS	Hypothetical protein	2019,95	0,236927745	2,077480941	1,44	0,1	1	0.787028
I3QZX4_CORPS	Hypothetical protein	25206,64	0,267135288	1,90435753	1,32	0,12	1	0.961461
I3QYT4_CORPS	Hypothetical protein	3551,34	0,269820072	1,889930421	1,31	0,13	1	0.175378
I3QUN9_CORPS	Hypothetical protein	9403,28	0,269820072	1,889930421	1,31	0,1	1	0.894266
I3QYK9_CORPS	Hypothetical protein	40473,31	0,272531806	1,875503484	1,3	0,19	1	0.935468
I3QYJ0_CORPS	Hypothetical protein	2357,66	0,275270794	1,861076548	1,29	0,54	1	0.954441
I3QUT5_CORPS	Hypothetical protein	17863,35	0,289384215	1,788941864	1,24	0,09	1	0.802914
I3QVS4_CORPS	Hypothetical protein	41289,1	0,301194198	1,731234118	1,2	0,09	1	0.837490
I3QW79_CORPS	Hypothetical protein	19885,47	0,301194198	1,731234118	1,2	0,17	1	0.911052
I3QZ21_CORPS	Hypothetical protein	20851,47	0,307278755	1,702380073	1,18	0,17	1	0.546694
I3QXU0_CORPS	Hypothetical protein	2075,26	0,313486191	1,673526199	1,16	0,25	1	0.674418
I3QX85_CORPS	Hypothetical protein	10890,95	0,319819026	1,644672326	1,14	0,12	1	0.749362
I3R032_CORPS	Hypothetical protein	2184	0,326279793	1,615818453	1,12	0,16	1	0.924949
I3QYD0_CORPS	Hypothetical protein	15201,74	0,326279793	1,615818453	1,12	0,13	1	0.624419
I3QZF0_CORPS	Hypothetical protein	19038,35	0,336216482	1,572537643	1,09	0,12	1	0.917276
I3QZK0_CORPS	Hypothetical protein	1030,59	0,386741028	1,370560272	0,95	0,46	1	0.931367
I3QV90_CORPS	Hypothetical protein	12638,51	0,394553708	1,341706398	0,93	0,16	1	0.865032
I3QW88_CORPS	Hypothetical protein	3483	0,410655759	1,283998566	0,89	0,08	1	0.561287
I3R0H2_CORPS	Hypothetical protein	1173,47	0,418951547	1,255144692	0,87	0,16	1	0.681717
I3QVF9_CORPS	hypothetical protein	49161,19	0,418951547	1,255144692	0,87	0,05	1	0.922133
I3QZX3_CORPS	Hypothetical protein	10648,72	0,423162076	1,240717756	0,86	0,07	1	0.886361
I3QYV3_CORPS	Hypothetical protein	141,46	2,886370824	-1,529256661	-1,06	0,28	0	0.030697
I3QV42_CORPS	Hypothetical protein	23153,72	2,974274172	-1,572537643	-1,09	0,48	0	0.033011
I3QWK1_CORPS	Hypothetical protein	221,77	4,05519987	-2,019773023	-1,4	0,43	0	0.967645
Others								
I3QZJ3_CORPS	Lipoprotein LpqE	44732,01	0,075020047	3,736580032	2,59	0,12	1	0.873355
I3QXX7_CORPS	Lipoprotein	36815,57	0,08126824	3,621164539	2,51	0,12	1	0.193552

I3QVZ0_CORPS	Maltose maltodextrin transport system	8729,23	0,158817421	2,654558923	1,84	0,15	1	0.852112
I3R060_CORPS	SEC C domain containing protein y	2461,62	0,229925479	2,120761751	1,47	0,38	1	0.091071
I3QVM0_CORPS	Maltotriose binding protein	21621,59	0,254106958	1,976492213	1,37	0,07	1	0.867672
I3QUS8_CORPS	Putative iron regulated membrane	7389,79	0,278037308	1,846649611	1,28	0,19	1	0.851148
I3QXT3_CORPS	Amino deoxychorismate lyase	4162,99	0,339595511	1,558110706	1,08	0,12	1	0.363600
I3QUL3_CORPS	Periplasmic binding protein LacI	10698,25	0,353454695	1,500402787	1,04	0,09	1	0.529965
I3QVS8_CORPS	D methionine binding lipoprotein metQ	7471,36	0,386741028	1,370560272	0,95	0,15	1	0.794259
I3QW71_CORPS	Periplasmic binding protein	11884,29	0,431710535	1,211863797	0,84	0,11	1	0.659522
I3QXJ1_CORPS	Prolipoprotein LppL	2671,28	10,38123567	-3,375906272	-2,34	0,15	0	0.625365
I3QZA3_CORPS	Protein NrdI	7211,97	26,04953689	-4,70318582	-3,26	0,22	0	0.056271

(a) Ratio values to: $Cp258Rc:Cp258Ct$:Log(2)Ratio>1.2 - p>0.95 up-regulation, p<0.05 down-regulation

Supplementary file 5: Table S.5 : Proteins identified in the pathogenicity island.

Accession	Protein name	Island number
Strain 258_equi		
I3QXC5_CORPS	Iron ABC transporter substrate binding ^(P)	>Cp258PiCp04
I3QZY6_CORPS	Transcriptional regulatory protein ^(P)	>Cp258PiCp07
I3QWK3_CORPS	Transcription elongation factor GreA ^(P)	>Cp258PiCp07
I3QV14_CORPS	Deoxyribose phosphate aldolase ^(#)	>Cp258PiCp08
I3QW42_CORPS	Hypothetical protein ^(#)	>Cp258PiCp09
I3QW43_CORPS	Hypothetical protein ^(#)	>Cp258PiCp09
I3QW55_CORPS	Hypothetical protein ^(#)	>Cp258PiCp09
I3QZ50_CORPS	Peptidase S8A Subtilisin family protein ^(P)	>Cp258PiCp10
I3QZB5_CORPS	DoxX family membrane protein ^(#)	>Cp258PiCp14
I3QZC0_CORPS	ABC type antimicrobial peptide transport ^(P)	>Cp258PiCp14
I3QZB7_CORPS	Phosphoglucomutase ^(P)	>Cp258PiCp14
I3QZA9_CORPS	HTH type transcriptional regulator CmtR ^(S)	>Cp258PiCp14
I3QZU6_CORPS	ATP dependent chaperone protein ClpB ^(P)	>Cp258PiCp15
I3QZV3_CORPS	Oxidoreductase ^(P)	>Cp258PiCp15
I3QZU1_CORPS	Glycerol 3 phosphate dehydrogenase ^(P)	>Cp258PiCp15
I3R095_CORPS	Phage shock protein A ^(P)	>Cp258PiCp16
Strain 1002_ovis		
D9Q5J0_CORP1	Phospholipase D ^(#)	>Cp1002PiCp01
D9Q4Y6_CORP1	Deoxycytidine triphosphate deaminase ^(P)	>Cp1002PiCp07
D9Q4V9_CORP1	Oligopeptide ABC transporter ^(#)	>Cp1002PiCp07
D9Q4X0_CORP1	Urease accessory protein UreD ^(#)	>Cp1002PiCp07
D9Q4X1_CORP1	Urease accessory protein UreG ^(#)	>Cp1002PiCp07
D9Q5X4_CORP1	Serine aspartate repeat containing protein ^(S)	>Cp1002PiCp08
D9Q718_CORP1	Methylmalonyl CoA carboxyltransferase ^(P)	>Cp1002PiCp09
D9Q721_CORP1	Hypothetical protein ^(P)	>Cp1002PiCp09
D9Q720_CORP1	Methylmalonyl CoA carboxyltransferase ^(#)	>Cp1002PiCp09
D9Q5C3_CORP1	Hypothetical protein ^(P)	>Cp1002PiCp11
D9Q5T5_CORP1	Glyoxalase Bleomycin resistance protein ^(P)	>Cp1002PiCp12
D9Q4A3_CORP1	DsbG protein ^(P)	>Cp1002PiCp14
D9Q4T5_CORP1	ABC transporter domain containing ATP ^(P)	>Cp1002PiCp15
D9Q4T9_CORP1	Hypothetical protein ^(S)	>Cp1002PiCp15
D9Q4T4_CORP1	ATP dependent chaperone protein ClpB ^(S)	>Cp1002PiCp15

D9Q4T0_CORP1	Hypothetical protein ^(#)	>Cp1002PiCp15
D9Q578_CORP1	Replicative DNA helicase ^(#)	>Cp1002PiCp16

(P) Up-regulation

(\\$) Down-regulation

(#) Exclusive

7. Discussão geral

Neste presente trabalho, foram aplicadas diferentes abordagens e estratégias proteômicas para caracterizar o proteoma das linhagens 1002_*ovis* e 258_*equi* de *C. pseudotuberculosis*. A combinação de diferentes técnicas demonstra uma estratégia eficaz na caracterização de um proteoma (Trost et al., 2005; Mao et al., 2011; Sun et al., 2011). Por exemplo, quando utilizado a 2-DE, nós identificamos a presença de isoformas nos mapas proteicos das linhagens 1002_*ovis* e C231_*ovis*, o que não foi possível observar na LC-MS/MS. Entretanto, a utilização da LC-MS/MS, nós permitiu a identificação de proteínas de caráter hidrofóbico que é uma das limitações da 2-DE. Outro fator a ser considerado nesta complementaridade, são os tipos de soluções utilizadas por cada técnica para solubilizar o extrato proteico. Pois dependendo da característica intrínseca de cada proteína, as mesmas podem ou não serem solubilizadas e consequentemente influenciar na sua detecção (Mao et al., 2011).

Uma vez que o fator ambiente influencia na expressão gênica, a utilização de diferentes condições de cultivo bacteriano, como: composições de meios de cultura, presença ou ausência de estresse, diferentes pontos do crescimento bacteriano, contato com o hospedeiro, proporcionou uma ampla avaliação do *status* funcional do genoma de *C. pseudotuberculosis*. Assim, a compilação dos resultados obtidos neste trabalho de Tese, associado a prévios estudos proteômicos de *C. pseudotuberculosis ovis* 1002 (Pacheco et al., 2011; Pacheco et al., 2012), resultou na caracterização de aproximadamente de 45% do proteoma predito desta linhagem. A respeito de *C. pseudotuberculosis equi* 258, representante do biovar *equi*, foi demonstrado pela primeira vez uma análise funcional do seu genoma em nível proteico. Os resultados provenientes deste estudo promoveram a validação de aproximadamente 9% do genoma desta linhagem.

Além da validação do genoma das linhagens 1002_*ovis* e 258_*equi*, esta análise proteômica permitiu validar aproximadamente 55% do core-genoma predito *in silico* de *C. pseudotuberculosis*. A busca por genes que compreendem um core-genoma bacteriano fornece

informações importantes, a cerca de um conjunto mínimo de genes essenciais, necessários para a realização de funções básicas que permitam a sobrevivência bacteriana (Gil et al., 2004). Assim, estas proteínas detectadas podem representar um *set* de fatores requeridos por *C. pseudotuberculosis* para as condições utilizadas neste trabalho.

Nós detectamos a *Glyoxalase/dioxygenase* (D9Q5T5_CORP1) estudos demonstram que esta proteína está envolvida em processos de detoxificação de óxido nítrico (Mitsumoto et al., 1999). Entretanto, o interessante foi à detecção desta proteína altamente regulada na análise proteômica de 1002_*ovis* em resposta ao estresse nitrosativo, e no proteoma de 1002_*ovis* após ser recuperada do baço de camundongos. Além disso, esta proteína também foi detectada no exoproteoma exclusivo de 1002_*ovis*, em resposta ao estresse nitrosativo (Pacheco et al., 2012). Assim, três experimentos proteômicos independentes foram feitos e com isto pode ser sugerido que a *Glyoxalase/dioxygenase* possa ser uma proteína importante tanto no mecanismo de defesa contra o óxido nítrico, quanto no processo de patogênese de 1002_*ovis*.

Outras 17 proteínas foram identificadas, tanto no proteoma de 1002_*ovis* em resposta ao óxido nítrico, quanto no proteoma de 1002_*ovis* após passagem em camundongos (**Anexo 1**). A proteína *Formamidopyrimidine DNA glycosylase* (D9Q598_CORP1), que está envolvida no mecanismo de reparo de DNA e o regulador transcricional MerR (D9Q889_CORP1) envolvido na resposta a diferentes tipos de estresse, também foram detectadas nestes dois estudos. Além disso, os genes que codificam estas proteínas foram altamente regulados na análise transcricional de 1002_*ovis*, em resposta ao estresse ácido (Pinto et al., 2014). Assim, estas proteínas podem estar envolvidas no mecanismo de resposta geral de estresse de *C. pseudotuberculosis*.

Quatro proteínas preditas como hipotéticas, também foram detectadas nestes dois estudos proteômicos, entretanto, apenas a *hypothetical protein* (D9Q721_CORP1) teve função

predita como atividade catalítica pela ferramenta Blast2Go (Conesa et al., 2005). Contudo, estudos mais precisos devem ser realizados para avaliar o verdadeiro papel desempenhado por estas proteínas na patogênese de *C. pseudotuberculosis*.

No presente trabalho, a utilização de um modelo murino de infecção experimental possibilitou avaliar pela primeira vez o potencial de virulência de linhagens *ovis* e *equi* em um mesmo modelo de infecção. Além disso, ao contrário do prévio estudo realizado por Rees et al. (2014) que ao caracterizar o proteoma de linhagens de *C. pseudotuberculosis ovis* isoladas diretamente de nódulos de ovinos infectados, identificou proteínas que favorecem a sobrevivência deste patógeno no estágio crônico da linfadenite caseosa, ou seja, quando a enfermidade já está estabelecida. O modelo murino de infecção utilizado, favoreceu a identificação de proteínas que podem estar associadas a estágios iniciais de infecção por *C. pseudotuberculosis*, que não foram identificadas por Rees et al. (2014).

A detecção de adesinas e proteases em 1002_*ovis* e 258_*equi*, após o processo de passagem demonstram ativação de proteínas que favorecem um dos primeiros passos para o processo de infecção, principalmente para patógenos intracelulares que é a capacidade de aderir e invadir a célula hospedeira (Ribet, 2015). Nós identificamos proteínas envolvidas em mecanismos de captação de ferro em 1002_*ovis* e 258_*equi*, a aquisição de ferro é um processo altamente requerido para o estabelecimento da infecção bacteriana (Weinberg, 2009). Estudos *in vivo* realizados com *Escherichia coli* (Chouikha et al., 2008), *Bordetella pertussis* (Brickman et al., 2008) e *Staphylococcus aureus* (Szafranska et al., 2014) demonstram a ativação de sistemas de ferro durante estágios iniciais de infecção. Além disso, um estudo *in vitro* realizado com uma linhagem de *Pseudomonas aeruginosa* isolada durante a fase aguda de infecção, também demonstrou a ativação de sistemas de aquisição de ferro (Hare et al., 2012).

A ativação de proteínas que participam de diferentes mecanismos de detoxificação demonstra ativação de um sistema defensivo das linhagens 1002_*ovis* e 258_*equi*, contra a ação de espécies reativas de oxigênio e nitrogênio. Estes sistemas são de extrema importância para a resistência e *C. pseudotuberculosis*, contra a ação do sistema imune, principalmente nos estágios iniciais da infecção dentro do ambiente intracelular de macrófagos. Assim, a associação com os dados obtidos no estudo do estresse nitrosativo, possibilitou ampliar a identificação de mecanismos envolvidos em sistemas detoxificação.

Outro fator importante que precede os estágios crônicos da infecção por *C. pseudotuberculosis* é a capacidade deste patógeno em disseminar dentro do hospedeiro e consequentemente a instalação do patógeno em órgãos viscerais (Batey, 1986; Mckean et al., 2007). Este processo é mediado pela ação da exotoxina PLD, que também foi detectada no nosso estudo. Assim, esta estratégia utilizada, permitiu detectar um conjunto de proteínas que podem desempenhar papel importante nos estágios iniciais das infecções causadas por *C. pseudotuberculosis ovis* e *equi*. Além disso, vale ressaltar que estas proteínas não foram detectadas no trabalho realizado por Ree et al. (2014).

Os resultados obtidos a partir destes diferentes estudos possibilitou a identificação de vários fatores que podem contribuir para o processo de virulência e patogenicidade de *C. pseudotuberculosis*.

Discussion générale

Dans ce travail, nous avons appliqué différentes approches et stratégies protéomiques pour caractériser le protéome des souches de *C. pseudotuberculosis* 1002_*ovis* et 258_*equi*. La combinaison de différentes techniques s'est révélée une stratégie efficace pour la caractérisation de protéomes (Trost et al., 2005; Mao et al., 2011; Sun et al., 2011). Par exemple, lorsque nous avons utilisé le 2-DE, nous avons identifié la présence d'isoformes de certaines protéines des souches 1002_*ovis* et C231_*ovis*, ce qui n'avait pas été observé en LC-MS / MS. Cependant, l'utilisation de la LC-MS / MS, on a permis l'identification de protéines hydrophobes, ce qui est une des limites de la 2-DE. Les types de solutions utilisées par chaque technique pour solubiliser l'extrait protéique constituent un autre facteur à prendre en considération dans cette complémentarité. En fonction des caractéristiques intrinsèques de chacune des protéines, ils peuvent ou peuvent ne pas les solubiliser et par conséquent influencer la détection (Mao et al., 2011).

Puisque les facteurs environnementaux influencent l'expression des gènes, l'utilisation de différentes conditions de culture (telles que des compositions de milieux différentes, la présence ou l'absence de stress, différentes phases de croissance bactérienne, le contact avec l'hôte) nous a permis une évaluation très large de l'état fonctionnel du génome de *C. pseudotuberculosis*. Ainsi, la compilation des résultats obtenus dans ce travail de thèse associée à des études protéomiques précédentes de *C. pseudotuberculosis ovis* 1002 (Pacheco et al., 2011; Pacheco et al., 2012), a permis la caractérisation d'environ 45% du protéome prédit de cette souche. En ce qui concerne la souche *C. pseudotuberculosis equi* 258, représentative du biovar *equi*, il s'agit de la première

analyse de son génome au niveau protéomique. Les résultats de cette étude ont permis la validation d'environ 9% du génome de cette souche.

En plus de la validation du génome des souches 1002_*ovis* et 258_*equi*, cette analyse protéomique a permis de valider environ 55% du *core*-génome (ou génome central) prédit *in silico* de *C. pseudotuberculosis*. La recherche des gènes qui composent le *core*-génome bactérien fournit des informations importantes sur un ensemble minimal de gènes essentiels requis pour exécuter des fonctions de base qui permettent la survie des bactéries (Gil et al., 2004). Ainsi, les protéines détectées peuvent représenter un ensemble de facteurs nécessaires à *C. pseudotuberculosis* dans les conditions expérimentales utilisées lors de l'étude.

Nous avons ainsi détecté une *glyoxalase/dioxygenase* (D9Q5T5_CORP1) qui a été décrite comme impliquée dans les processus de détoxification de l'oxyde nitrique (Mitsumoto et al., 1999). De façon surprenante, nous avons montré ici que cette protéine était étroitement régulée d'après l'analyse protéomique de 1002_*ovis* et produite en réponse au stress nitrosant, d'une part, et après infection et récupération à partir de rate de souris infectée, d'autre part. En outre, cette protéine a également été détectée uniquement dans l'exoproteome de 1002_*ovis* en réponse à un stress nitrosant (Pacheco et al., 2012). Ainsi, trois expériences protéomiques indépendantes suggèrent que la *glyoxalase / dioxygénase* est une protéine importante à la fois dans le mécanisme de défense contre l'oxyde nitrique, et dans la pathogénèse de 1002_*ovis*.

Dix-sept autres protéines ont été identifiées à la fois dans le protéome de 1002_*ovis* en réponse à l'oxyde nitrique et dans le protéome de 1002_*ovis* après le passage dans la souris (**Annexe 1**). La protéine de l'ADN glycosylase formamidopyrimidine, qui est impliquée dans le mécanisme de réparation d'ADN, et le régulateur transcriptionnel Merr, impliquée dans la réponse à différents types de stress, ont également été détectés dans ces deux études. En outre, des gènes codant ces protéines se sont révélés être fortement régulés dans 1002_*ovis*, d'après

l'analyse du transcriptome de cette souche en réponse à un stress acide (Pinto et al., 2014). Ainsi, ces protéines pourraient être impliquées dans un mécanisme de réponse générale au stress chez *C. pseudotuberculosis*. Quatre protéines prédictes hypothétiques ont également été détectées dans ces deux études protéomiques. Cependant, seule la protéine hypothétique (D9Q721_CORP1) présentait une fonction d'activité catalytique prédictée par Blast2Go (Conesa et al., 2005). Des études plus précises seront nécessaires pour évaluer le vrai rôle de ces protéines dans la pathogenèse de *C. pseudotuberculosis*.

Dans cette étude, l'utilisation d'un modèle murin d'infection expérimentale nous a permis d'évaluer pour la première fois le potentiel de virulence des souches *equi* et *ovis* dans le même modèle d'infection. Une précédente étude de Rees et al. (2014) a caractérisé le protéome des souches de *C. pseudotuberculosis ovis*, isolées directement à partir de nodules de moutons infectés. Rees et al. ont ainsi identifié des protéines qui favorisent la survie du pathogène dans la phase chronique de la lymphadénite caséuse, ou lorsque la maladie est déjà établie. Le modèle murin d'infection utilisé dans ce travail favorise, quant à lui, l'identification de protéines qui peuvent être associées aux premiers stades de l'infection de *C. pseudotuberculosis* et qui, de fait, n'ont pas été identifiées par Rees et al. (2014).

La détection d'adhésine et de protéase dans 1002_*ovis* et 258_*equi*, après le processus de passage dans l'hôte murin, montre l'activation de protéines impliquées dans les premières étapes du processus d'infection, en particulier pour des agents pathogènes intracellulaires qui ont besoin d'adhérer et d'envahir la cellule hôte (Ribet, 2015). Des protéines impliquées dans les mécanismes d'acquisition du fer ont aussi été identifiées dans les souches 1002_*ovis* et 258_*equi*. L'acquisition du fer est un élément très important pour établir l'infection bactérienne (Weinberg, 2009). Des études *in vivo* effectuées avec *Escherichia coli* (Chouikha et al., 2008), *Bordetella*

pertussis (Brickman et al., 2008) et *Staphylococcus aureus* (Szafranska et al., 2014) ont démontré l'activation des systèmes d'acquisition du fer pendant les stades initiaux de l'infection. En outre, une étude *in vitro* effectuée avec une souche de *Pseudomonas aeruginosa* dans la phase aiguë de l'infection, a également montré l'activation des systèmes d'acquisition de fer (Hare et al., 2012).

L'activation des protéines qui participent à des mécanismes de détoxification différents chez les souches *1002_ovis* et *258_equi* reflète l'activation de systèmes de défense contre l'action des espèces réactives de l'oxygène et de l'azote. Ces systèmes sont extrêmement importants pour la survie de *C. pseudotuberculosis* face à l'action du système immunitaire, en particulier dans les premiers stades de l'infection dans l'environnement intracellulaire des macrophages. Ainsi, l'association avec les données obtenues dans l'étude du stress nitrosant, a permis d'étendre nos connaissances sur les mécanismes impliqués dans les systèmes de détoxification.

Un autre facteur important qui précède les stades chroniques de l'infection par *C. pseudotuberculosis* est sa capacité à se propager à l'intérieur de l'hôte et à coloniser les organes viscéraux (Batey, 1986; McKean et al., 2007). Ce processus est médié par l'action du PLD, une exotoxine qui a également été identifiée dans notre étude.

Ainsi, les approches utilisées ont permis d'identifier plusieurs protéines pouvant jouer un rôle dans les phases initiales des infections causées par *C. pseudotuberculosis equi* et *ovis*. En outre, il est à noter que ces protéines n'ont pas été détectées dans les travaux précédents portant sur les phases plus avancées de l'infection (Ree et al., 2014).

Les résultats obtenus à partir de ces différentes études contribuent ainsi à une meilleure connaissance de la virulence et de la pathogénicité de *C. pseudotuberculosis*.

8. Conclusão/Conclusion

Conclusão

Neste presente trabalho de Tese, nós demonstramos que a utilização de diferentes estratégias e abordagens proteômicas, foi capaz de promover a mais completa análise funcional do genoma de *C. pseudotuberculosis*, em nível proteico. No qual esta análise descritiva, além de validar dados de prévios estudos *in silico*, identificou vários genes envolvidos em diferentes processos biológicos, que podem favorecer o processo patogênico de *C. pseudotuberculosis*. Além disso, estes resultados forneceram informações importantes a cerca da biologia deste patógeno.

Conclusion

Dans ce travail de thèse, nous avons démontré que l'utilisation de différentes stratégies et approches protéomiques était en mesure de compléter l'analyse fonctionnelle du génome de *C. pseudotuberculosis* au niveau protéomique. En plus de valider les analyses génomiques *in silico* antérieures, ce travail a permis d'identifier un certain nombre de gènes impliqués dans différents processus biologiques et susceptibles de favoriser le processus infectieux de *C. pseudotuberculosis*. En outre, ces résultats fournissent des informations importantes sur la biologie de cette espèce.

9. Perspectivas/Perspectives

Os resultados obtidos neste trabalho abrem perspectivas para:

- Concluir a análise comparativa entre o proteoma do lisado total das linhagens 1002_*ovis* e 258_*equi*, em condições laboratoriais.
- Averiguar o papel das principais proteínas diferencialmente reguladas na virulência de *C. pseudotuberculosis*, através de estudos com linhagens defectivas para os genes que codificam estas proteínas.
- Utilizar a estratégia adotada neste trabalho como base, para avaliar o proteoma de *C. pseudotuberculosis* em resposta a outros tipos de estresse.
- Avaliar o potencial imunogênico de proteínas relacionadas a fatores de virulência, com o intuito de empregá-las na produção de vacinas e métodos de diagnóstico.

Les résultats obtenus dans cette étude ouvrent des perspectives pour :

- Compléter l'analyse comparative du protéome du lysat total des souches 1002_*ovis* et 258_*equi* dans des conditions de laboratoire.
- Étudier le rôle des principales protéines différemment régulées dans la virulence de *C. pseudotuberculosis*, par des études de souches défectueuses pour les gènes codant pour ces protéines (mutagenèse dirigée).
- Utiliser la stratégie adoptée dans ce travail comme base pour évaluer le protéome de *C. pseudotuberculosis* en réponse à d'autres stress.
- Évaluer le potentiel immunogène des protéines liées à la virulence, afin de les utiliser dans la production de vaccins et de méthodes de diagnostic.

10. Referências/Reference

As seguintes referências bibliográficas são referentes aos tópicos:

1.2 Introdução geral, **2** Revisão da literatura e **7** Discussão geral.

Les références suivantes sont liés aux sujets:

1.2 Introduction générale, **2** Révision de la littérature et **7** Discussion générale

Adamson, P.J., Wilson, W.D., Hirsh, D.C. et al. Susceptibility of equine bacterial isolates to antimicrobial agents. *Am J Vet Res.* v. 46, p. 447-450. 1985.

Aleman, M., Spier, S.J., Wilson, W.D. et al. *Corynebacterium pseudotuberculosis* infection in horses: 538 cases (1982-1993). *J Am Vet Med Assoc.* v. 209, p. 804-809. 1996.

Altelaar AF, Munoz J, Heck AJ. Next-generation proteomics: towards an integrative view of proteome dynamics. *Nat Rev Genet.* v. 14, p.35-48. 2013.

Alves, F.S.F., Pinheiro, R.R., Pires, P.C. Linfadenite caseosa: patogenia-diagnóstico-controle. Artigo Técnico. Documento n° 27, Sobral: CE, Embrapa. 1997.

Arrey, T.N., Rietschel, B., Papasotiriou, D.G. et al. Approaching the complexity of elastase-digested membrane proteomes using off-gel IEF/nLC-MALDI-MS/MS. *Anal Chem.* v. 1, p. 2145-2149. 2010.

Baird, G.J., Fontaine, M.C. *Corynebacterium pseudotuberculosis* and its role in ovine caseous lymphadenitis. *J Comp Pathol.* v. 137, p. 179-210. 2007.

Barreiro, C., González-Lavado, E., Brand, S. et al. Heat shock proteome analysis of wild-type *Corynebacterium glutamicum* ATCC 13032 and a spontaneous mutant lacking GroEL1, a dispensable chaperone. *J Bacteriol.* v. 187, p. 884-889. 2005.

Barriuso-Iglesias, M., Schluesener, D., Barreiro, C. et al. Response of the cytoplasmic and membrane proteome of *Corynebacterium glutamicum* ATCC 13032 to pH changes. *BMC Microbiol.* v. 17, 8:225. 2008.

Batey, R.G. Pathogenesis of caseous lymphadenitis in sheep and goats. *Aust Vet J.* v. 63, p. 269-272. 1986.

Beckers, G., Strosser, J., Hildebrandt, U. et al., Regulation of AmtR-controlled gene expression in *Corynebacterium glutamicum*: mechanism and characterization of the AmtR regulon. *Mol. Microbiol.* v. 58, p. 580–595. 2005.

Billington, S.J., Esmay, P.A., Songer, J.G. et al. Identification and role in virulence of putative iron acquisition genes from *Corynebacterium pseudotuberculosis*. *FEMS Microbiol. Lett.* v. 208, p. 41–45. 2002.

Brickman, T.J., Hanawa, T., Anderson, M.T. et al. Differential expression of *Bordetella pertussis* iron transport system genes during infection. *Mol Microbiol.* v. 70, p. 3-14. 2008.

Brogden, K.A., Chedid, L., Cutlip, R.C., et al. Effect of muramyl dipeptide on immunogenicity of *Corynebacterium pseudotuberculosis* whole-cell vaccines in mice and lambs. *Am. J. Vet. Res.* v. 51, p. 200-202. 1990.

Bumann, D. Pathogen proteomes during infection: A basis for infection research and novel control strategies. *J Proteomics.* v. 73, p. 2267–2276. 2010.

Cassat, J.E., Skaar, E.P. Iron in infection and immunity. *Cell Host Microbe.* v. 15, p. 509-519. 2013.

Cerdeira, L.T., Pinto, A.C., Schneider, M.P.C. et al. Whole-genome sequence of *Corynebacterium pseudotuberculosis* PAT10 strain isolated from sheep in Patagonia, Argentina. *J Bacteriol.* 2011; 193:6420–6421a.

Cerdeira, L.T., Schneider, M.P.C., Pinto, A.C. et al. Complete genome sequence of *Corynebacterium pseudotuberculosis* strain CIP 52.97, isolated from a horse in Kenya. *J Bacteriol.* 2011; 193: 7025–7026b.

Chang, J.H., Desveaux, D., Creason, A.L. The ABCs and 123s of bacterial secretion systems in plant pathogenesis. *Annu Rev Phytopathol.* v. 52, p. 317-345. 2014.

- Chi, B.K., Busche, T., Van Laer, K. et al. Protein S-mycothiolation functions as redox-switch and thiol protection mechanism in *Corynebacterium glutamicum* under hypochlorite stress. *Antioxid Redox Signal.* v. 1, p. 589-605. 2014.
- Chouikha, I., Bree, A., Moulin-Schouleur, M. et al. Differential expression of *iutA* and *ibeA* in the early stages of infection by extra-intestinal pathogenic *E. coli*. *Microbes Infect.* v. 10, p. 432-438. 2008.
- Claes, W. A., P. uhler, A., Kalinowski, J. Identification of two *prpDBC* gene clusters in *Corynebacterium glutamicum* and their involvement in propionate degradation via the 2-methylcitrate cycle. *J. Bacteriol.* v. 184, p. 2728-2739. 2002.
- Conesa, A., Götz, S., García-Gómez, JM. et al. Blast2GO: a universal tool for annotation, visualization and analysis in functional genomics research. *Bioinformatics*. v. 15, p. 3674-3676. 2005.
- Doherr, M.G., Carpenter, T.E., Wilson, W.D. et al. Application and evaluation of a mailed questionnaire for an epidemiologic study of *Corynebacterium pseudotuberculosis* infection in horses. *Prev Vet Med.* v. 30, p. 241-53. 1998.
- Dorella, F.A., Pacheco, L.G., Oliveira, S.C. et al. *Corynebacterium pseudotuberculosis*: microbiology, biochemical properties, pathogenesis and molecular studies of virulence. *Vet. Res.* v. 37, p. 201-218. 2006.
- Dorella FA, Pacheco, LGC, Coelho KS, Rocha C, Lobo FP, Franco GR, Meyer R, Myoshi A, Azevedo V. Seqüenciamento do genoma de *Corynebacterium pseudotuberculosis* pela rede genoma de Minas Gerais: impactos esperados na ovina e caprinocultura nacional. In: Biotecnologia e Saúde Animal. Viçosa: Editora Folha de Viçosa, 2007, p. 111-150.
- Eggleton, D.G., Middleton, H.D., Doidge, C.V. et al. Immunisation against ovine caseous lymphadenitis: comparison of *Corynebacterium pseudotuberculosis* vaccines with and without bacterial cells. *Aust. Vet. J.* v. 68, p. 317-319. 1991.
- Ellis, J.A. Antigen specificity of antibody responses to *Corynebacterium pseudotuberculosis* in naturally infected sheep with caseous lymphadenitis. *Vet. Immunol. Immunopathol.* v. 28, p. 289-301. 1991.

- Fanous, A., Weiss, W., Görg, A. et al. A proteome analysis of the cadmium and mercury response in *Corynebacterium glutamicum*. *Proteomics*. v. 8, p. 4976-4986. 2008.
- Fanous, A., Hecker, M., Gorg, A., et al. *Corynebacterium glutamicum* as an indicator for environmental cobalt and silver stress – a proteome analysis. *J. Environ. Sci. Health B*. v. 45, p. 666–675. 2010.
- Fischer, F., Wolters, D., Rögner, M. et al. Toward the complete membrane proteome: high coverage of integral membrane proteins through transmembrane peptide detection. *Mol Cell Proteomics*. v. 5, p. 444-453. 2006.
- Foley, J.E., Spier, S.J., Mihalyi, J., et al. Molecular epidemiologic features of *Corynebacterium pseudotuberculosis* isolated from horses. *Am J Vet Res*. v. 65, p. 1734-1737. 2004.
- Follmann, M., Ochrombel, I., Krämer, R. et al. Functional genomics of pH homeostasis in *Corynebacterium glutamicum* revealed novel links between pH response, oxidative stress, iron homeostasis and methionine synthesis. *BMC Genomics*. v. 21, 10:621. 2009.
- Fränzel, B., Fischer, F., Trötschel, C. et al. The two-phase partitioning system--a powerful technique to purify integral membrane proteins of *Corynebacterium glutamicum* for quantitative shotgun analysis. *Proteomics*. v. 9, p. 2263-2272. 2009.
- Fränzel, B., Poetsch, A., Trötschel, C. et al. Quantitative proteomic overview on the *Corynebacterium glutamicum*-lysine producing strain DM1730. *J Proteomics*. v. 10, p. 2336-2353. 2010.
- Funke, G., von Graevenitz, A., Clarridge, J.E. 3rd, et al. Clinical microbiology of coryneform bacteria. *Clin Microbiol Rev*. v. 10, p. 125-159. 1997.
- Gstaiger, M & Aebersold R. Applying mass spectrometry-based proteomics to genetics, genomics and network biology. *Nat Rev Genet*. v. 10, p. 617-627. 2009.
- Gil, R., Silva, F.J., Peretó, J. et al. Determination of the core of a minimal bacterial gene set. *Microbiol Mol Biol Rev*. v. 68, p. 518-537. 2004.

Guimarães, A. S., Seyffert, N., Bastos, B.L. et al. Caseous lymphadenitis in sheep flocks of the state of Minas Gerais, Brazil: Prevalence and management surveys. *Small Rumin Res.* v. 87, p. 86–91. 2009.

Hansmeier, N., Chao, T.C., Pühler, A et al. The cytosolic, cell surface and extracellular proteomes of the biotechnologically important soil bacterium *Corynebacterium efficiens* YS-314 in comparison to those of *Corynebacterium glutamicum* ATCC 13032. *Proteomics.* v. 6, p. 233-250. 2006a.

Hansmeier, N., Chao, T.C., Kalinowski, J. et al. Mapping and comprehensive analysis of the extracellular and cell surface proteome of the human pathogen *Corynebacterium diphtheriae*. *Proteomics.* v. 6, p. 2465-2476. 2006b.

Hansmeier, N., Chao, T.C., Daschkey, S. et al. A comprehensive proteome map of the lipid-requiring nosocomial pathogen *Corynebacterium jeikeium* K411. *Proteomics.* v. 7, p. 1076-1096. 2007.

Hard, G.C. Comparative Toxic Effect of the Surface Lipid of *Corynebacterium ovis* on Peritoneal Macrophages. *Infect. Immun.* v. 12, p. 1439-1449. 1975.

Hare, N.J., Soe, C.Z., Rose, B. et al. Proteomics of *Pseudomonas aeruginosa* Australian epidemic strain 1 (AES-1) cultured under conditions mimicking the cystic fibrosis lung reveals increased iron acquisition via the siderophore pyochelin. *J Proteome Res.* v. 3, p. 776-795. 2012.

Hassan, S.S., Schneider, M.P.C., Ramos, R.T.J et al. Whole-Genome Sequence of *Corynebacterium pseudotuberculosis* Strain Cp162, Isolated from Camel. *J Bacteriol.* v. 194, p. 5718–5719. 2012.

Haussmann, U., Qi, S.W., Wolters, D. et al. Physiological adaptation of *Corynebacterium glutamicum* to benzoate as alternative carbon source - a membrane proteome-centric view. *Proteomics.* v. 9, p. 3635-3651. 2009.

Haussmann, U. & Poetsch, A. Global proteome survey of protocatechuate- and glucose-grown *Corynebacterium glutamicum* reveals multiple physiological differences. *J Proteomics.* v. 17, p. 2649-2659. 2012.

Havelsrud, O.E., Sorum, H., Gaustad, P. Genome Sequences of *Corynebacterium pseudotuberculosis* Strains 48252 (Human, Pneumonia), CS_10 (Lab Strain), Ft_2193/67 (Goat, Pus), and CCUG 27541. *Genome Announc.* v. 4. pii: e00869-14. 2014.

Hermann, T., Wersch, G., Uhlemann, E.M. et al. Mapping and identification of *Corynebacterium glutamicum* proteins by two-dimensional gel electrophoresis and microsequencing. *Electrophoresis.* v. 19, p. 3217-3221. 1998.

Hermann, T., Finkemeier, M., Pfefferle, W. et al. Two-dimensional electrophoretic analysis of *Corynebacterium glutamicum* membrane fraction and surface proteins. *Electrophoresis.* v. 21, p. 654-659. 2000.

Hermann, T., Pfefferle, W., Baumann, C. Proteome analysis of *Corynebacterium glutamicum*. *Electrophoresis.* v. 22, p.1712–1723. 2001.

Hermann T. Industrial production of amino acids by coryneform bacteria. *J Biotechnol.* v. 4, p. 155-172. 2003.

Hilbi H & Haas A. Secretive bacterial pathogens and the secretory pathway. *Traffic.* 2012 v. 13, p. 1187-1197. 2012.

Hodgson, A.L., Krywult, J., Corner, L.A. et al. Rational attenuation of *Corynebacterium pseudotuberculosis*: potential cheesy gland vaccine and live delivery vehicle. *Infect. Immun.*, v. 60, p.2900–2905, 1992.

Hueck CJ. Type III Protein Secretion Systems in Bacterial Pathogens of Animals and Plants. *Microb mol biolog reviews.* v. 62, p. 379–433. 1998.

Jolly, R.D. Some observations on surface lipids of virulent and attenuated strains of *Corynebacterium ovis*. *J. Appl. Bacteriol.* v. 29, p. 189-1966. 1966.

Judson, R., Songer JG. *Corynebacterium pseudotuberculosis*: *in vitro* susceptibility to 39 antimicrobial agents. *Vet Microbiol.* v. 27, p. 145-150. 1991.

Kalinowski J, Bathe B, Bartels D. et al. The complete *Corynebacterium glutamicum* ATCC 13032 genome sequence and its impact on the production of L-aspartate-derived amino acids and vitamins. *J Biotechnol.* v. 4, p. 5-25. 2003.

- Koch-Koerfges, A., Kabus, A., Ochrombel, I. Physiology and global gene expression of a *Corynebacterium glutamicum* $\Delta F(1)F(O)$ -ATP synthase mutant devoid of oxidative phosphorylation. *Biochim Biophys Acta.* v. 1817, p. 370-380. 2012.
- Kilcoyne, I., Spier, S.J., Carter, C.N. et al. Frequency of *Corynebacterium pseudotuberculosis* infection in horses across the United States during a 10-year period. *J Am Vet Med Assoc.* v. 1, p. 309-314. 2014.
- LeaMaster, B.R., Shen, D.T., Gorham, J.R. et al. Efficacy of *Corynebacterium pseudotuberculosis* bacterin for the immunologic protection of sheep against development of caseous lymphadenitis. *Am. J. Vet. Res.* v. 48, p. 869-872. 1987.
- Lee, S.M., Lee, J.Y., Park, K.J. et al. The regulator RamA influences cmytA transcription and cell morphology of *Corynebacterium ammoniagenes*. *Curr Microbiol.* v. 61, p. 92-100. 2010.
- Li, L., Wada, M., Yokota, A. Cytoplasmic proteome reference map for a glutamic acid-producing *Corynebacterium glutamicum* ATCC 14067. *Proteomics.* v. 7, p. 4317-22. 2007.
- Lopes, T., Silva, A., Thiago, R. et al. Complete genome sequence of *Corynebacterium pseudotuberculosis* strain Cp267, isolated from a llama. *J Bacteriol.* v. 194, p. 3567-3568. 2012.
- Mao, S., Luo, Y., Bao, G. et al. Comparative analysis on the membrane proteome of *Clostridium acetobutylicum* wild type strain and its butanol-tolerant mutant. *Mol Biosyst.* v. 7, p. 1660-1677. 2011.
- McKean, S.C., Davies, J.K., Moore, R.J. Identification of macrophage induced genes of *Corynebacterium pseudotuberculosis* by differential fluorescence induction. *Microbes Infect.* v. 7, p. 1352-1363. 2005.
- McKean, S.C., Davies, J.K., Moore, R.J. Expression of phospholipase D, the major virulence factor of *Corynebacterium pseudotuberculosis*, is regulated by multiple environmental factors and plays a role in macrophage death. *Microbiology.* v. 153, p. 2203–2211. 2007.
- Mills, A.E., Mitchell, R.D., Lim, E.K. *Corynebacterium pseudotuberculosis* is a cause of human necrotising granulomatous lymphadenitis. *Patholog.* v. 29, p. 231-233, 1997.

- Mitsumoto, A., Kim, K.R., Oshima, G. et al. Glyoxalase I is a novel nitric-oxide-responsive protein. *Biochem J.* v. 15, p. 837-844. 1999.
- Moraes, P.M., Seyffert, N., Silva, W.M. et al. Characterization of the Opp peptide transporter of *Corynebacterium pseudotuberculosis* and its role in virulence and pathogenicity. *Biomed Res Int.* v. 2014, p. 1-7. 2014.
- Muckle, C.A., Gyles, C.L. Characterization of strains of *Corynebacterium pseudotuberculosis*, *Can. J. Comp. Med.*, v. 46, p. 206–208. 1982.
- Nathan, C. & Shiloh, M.U. Reactive oxygen and nitrogen intermediates in the relationship between mammalian hosts and microbial pathogens. *Proc Natl Acad Sci USA.* v. 1, p. 8841-8848. 2000.
- Nishio, Y., Nakamura, Y., Kawarabayasi, Y. et al. Comparative complete genome sequence analysis of the amino acid replacements responsible for the thermostability of *Corynebacterium efficiens*. *Genome Res.* v. 13, p. 1572-1579. 2003.
- Ohl, M.E.; Miller S.I. Salmonella: A Model for Bacterial Pathogenesis. *Ann Rev Med.* v. 52, p. 259-274. 2001.
- Osman, K.M., Ali, M.M., Radwan, M.I. et al. Comparative proteomic analysis on *Salmonella Gallinarum* and *Salmonella Enteritidis* exploring proteins that may incorporate host adaptation in poultry. *J Proteomics.* v. 72, p. 815-821. 2009.
- Ott, L., Höller, M., Gerlach, R.G. et al. *Corynebacterium diphtheriae* invasion-associated protein (DIP1281) is involved in cell surface organization, adhesion and internalization in epithelial cells. *BMC Microbiol.* v. 5, p. 10:2. 2010.
- Otto, A., Bernhardt, J., Hecker, M. et al. Global relative and absolute quantitation in microbial proteomics *Curr Opin Microbiol.* v.15, p. 364-372. 2012
- Otto, A., Becher, D., Schmidt, F. Quantitative proteomics in the field of microbiology. *Proteomics.* v. 14, p. 547-565. 2014.

Pacheco, L.G., Pena, R.R., Castro, T.L. et al. Multiplex PCR assay for identification of *Corynebacterium pseudotuberculosis* from pure cultures and for rapid detection of this pathogen in clinical samples. *J Med Microbiol.* v. 56, 480-486. 2007.

Pacheco, L.G., Castro, T.L., Carvalho, R.D. et al. A Role for Sigma Factor σ(E) in *Corynebacterium pseudotuberculosis* Resistance to Nitric Oxide/Peroxide Stress. *Front Microbiol.* 3:126. 2012.

Pan, S., Aebersold, R., Chen, R. et al. Mass spectrometry based targeted protein quantification: methods and applications. *J Proteome Res.* v. 8, p. 787-797. 2009.

Pandey, A. & Mann, M. Proteomics to study genes and genomes. *Nature.* v. 15, p. 837-846. 2000.

Paton, M.W., Walker, S.B., Rose, I.R. et al. Prevalence of caseous lymphadenitis and usage of caseous lymphadenitis vaccines in sheep flocks. *Aust Vet J.* v. 81, p. 91-95. 1994.

Peel, M.M., Palmer, G.G., Stacpoole, A.M et al. Human lymphadenitis due to *Corynebacterium pseudotuberculosis*: report of ten cases from Australia and review. *Clin. Infect. Dis.* v. 24, p. 185–191. 1997.

Pethick, F.E., Lainson, A.F., Yaga, R. et al. Complete genome sequences of *Corynebacterium pseudotuberculosis* strains 3/99-5 and 42/02-A, isolated from sheep in Scotland and Australia, respectively. *J Bacteriol.* v. 194, p :4736-4737. 2012a.

Pethick, F.E., Lainson, A.F., Yaga, R. et al. Complete genome sequence of *Corynebacterium pseudotuberculosis* strain 1/06-A, isolated from a horse in North America. *J Bacteriol.* v. 194, p.4476. 2012b.

Pinto, A.C., de Sá PH., Ramos, R.T. et al. Differential transcriptional profile of *Corynebacterium pseudotuberculosis* in response to abiotic stresses. *BMC Genomics.* 9;15:14. 2014

Pocsfalvi, G., Cacace, G., Cuccurullo, M. et al. Proteomic analysis of exoproteins expressed by enterotoxigenic *Staphylococcus aureus* strains. *Proteomics.* v. 8, p. 2462-76. 2008.

Polen, T., Schluesener, D., Poetsch, A. et al. Characterization of citrate utilization in *Corynebacterium glutamicum* by transcriptome and proteome analysis. *FEMS Microbiol. Lett.* v. 273, p. 109–119. 2007.

Qi, S. W., Chaudhry, M. T., Zhang, Y. et al., Comparative proteomes of *Corynebacterium glutamicum* grown on aromatic compounds revealed novel proteins involved in aromatic degradation and a clear link between aromatic catabolism and gluconeogenesis via fructose- 1,6-bisphosphatase. *Proteomics.* v. 7, p. 3775–3787. 2007.

Ramos, R.T.J., Silva, A., Carneiro, A.R. et al. Genome Sequence of the *Corynebacterium pseudotuberculosis* Cp316 Strain, Isolated from the Abscess of a Californian Horse. *J Bacteriol.* v. 194, p. 6620–6621. 2012.

Ramos, R.T.J., Carneiro, A.R., Soares, S.C., Santos, A.R. et al.. Tips and tricks for the assembly a *Corynebacterium pseudotuberculosis* genome using a semiconductor sequencer. *Microbiol Biotechnol.* v. 6, p. 150-156. 2013.

Rees MA, Kleifeld O, Crellin PK, Ho B, Stinear TP, Smith AI, Coppel RL. Proteomic Characterization of a Natural Host-Pathogen Interaction: Repertoire of in Vivo Expressed Bacterial and Host Surface-Associated Proteins. *J Proteome Res.* v. 30. P. 120-132. 2014.

Renzone, G., D'Ambrosio, C., Arena, S. et al. Differential proteomic analysis in the study of prokaryotes stress resistance. *Ann Ist Super Sanita.* v. 41, p. 459-468. 2005.

Ribeiro, M.G.; Junior, J.G.D.; Paes, A.C. et al. Punção aspirativa com agulha fina no diagnóstico de *Corynebacterium pseudotuberculosis* na linfadenite caseosa caprina. *Arq. Inst. Biol.*, v. 68, p. 23-28. 2001.

Ribeiro, D., Rocha, FS., Leite, K.M., et al. An iron-acquisition-deficient mutant of *Corynebacterium pseudotuberculosis* efficiently protects mice against challenge. *Vet Res.* v. 6 :45:28. 2014.

Riegel P. Bacteriological and clinical aspects of corynebacterium. *Ann Biol Clin (Paris).* v. 56, p. 285-296.1998.

- Rietschel, B., Arrey, T.N., Meyer, B. et al. Elastase digests: new ammunition for shotgun membrane proteomics. *Mol Cell Proteomics*. v. 8, p. 1029-1043. 2009.
- Ribet D, Cossart P. How bacterial pathogens colonize their hosts and invade deeper tissues. *Microbes Infect*. v. 29, pii: S1286-4579(15)00017-9. 2015.
- Rogers EA, Das A, Ton-That H. Adhesion by pathogenic corynebacteria. *Adv Exp Med Biol*. 2011, 715:91-103.
- Ruiz, J.C., D'Afonseca, V., Silva, A., et al. Evidence for reductive genome evolution and lateral acquisition of virulence functions in two *Corynebacterium pseudotuberculosis* strains. *PLoS One*. 6:e18551. 2011.
- Sangal V, Burkovski A, Hunt AC, Edwards B, Blom J, Hoskisson PA. A lack of genetic basis for biovar differentiation in clinically important *Corynebacterium diphtheriae* from whole genome sequencing. *Infect Genet Evol*. 2014, 21:54-57.
- Schairer, D.O., Chouake, J.S., Nosanchuk, J.D. et al. The potential of nitric oxide releasing therapies as antimicrobial agents. *Virulence*. v. 1, p. 271-279. 2012.
- Schirmer, E.C., Yates, J.R. e Gerace, L. MudPIT: A powerful proteomics tool for discovery, limited primarily by our imagination. *Discovery Medicine*. v. 3, p. 38-39. 2003.
- Schluesener, D., Fischer, F., Kruip, J. et al. Mapping the membrane proteome of *Corynebacterium glutamicum*. *Proteomics*. v. 5, p. 1317-1330. 2005.
- Schneewind, O. & Missiakas, D.M. Protein secretion and surface display in Gram-positive bacteria. *Philos Trans R Soc Lond B Biol Sci*. v. 19, p. 1123-1139. 2012.
- Schreuder, B.E., Ter LaaK, E.A., de Gee, A.L. *Corynebacterium pseudotuberculosis* in milk of CL affected goats. *Vet Rec*. v. 13, p. 387. 1990.
- Sengupta, N.; Alam, S.Y. *In Vivo* Studies of *Clostridium perfringens* in Mouse Gas Gangrene Model. *Curr Microbiol*. v. 62, p. 999–1008. 2011.

- Seyffert, N., Guimarães, A.S., Pacheco, L.G. et al. High seroprevalence of caseous lymphadenitis in Brazilian goat herds revealed by *Corynebacterium pseudotuberculosis* secreted proteins-based ELISA. *Res Vet Sci.* v. 88, p. 50-55. 2010.
- Shi, L., Adkins, J.N., Coleman, J.R. et al. Proteomic Analysis of *Salmonella enterica* Serovar Typhimurium Isolated from RAW 264.7 Macrophages. *J Biol Chem.* v. 281, p. 29131–29140. 2006.
- Silberbach, M., Schäfer, M., Häuser, A. T., Kalinowski, J. et al., Adaptation of *Corynebacterium glutamicum* to ammonium limitation: a global analysis using transcriptome and proteome techniques. *Appl Environ Microbiol.* v. 71, p. 2391–2402. 2005.
- Silva, A., Schneider, M.P.C., Cerdeira, L., et al. Complete genome sequence of *Corynebacterium pseudotuberculosis* I19, a strain isolated from a cow in Israel with bovine mastitis. *J Bacteriol.* 2011; 193:323–324.
- Silva, A., Ramos, R.T.J., Ribeiro A, Cybelle, A. et al. Complete Genome Sequence of *Corynebacterium pseudotuberculosis* Cp31, Isolated from an Egyptian Buffalo. *J Bacteriol.* v. 194, p. 6663–6664. 2012.
- Soares, S.C., Trost, E., Ramos, R.T.J., et al.. Genome sequence of *Corynebacterium pseudotuberculosis* biovar *equi* strain 258 and prediction of antigenic targets to improve biotechnological vaccine production. *J Biotechnol.* v. 20, p. 135-141. 2012.
- Soares, S.C., Silva, A., Trost, E. et al. The pan-genome of the animal pathogen *Corynebacterium pseudotuberculosis* reveals differences in genome plasticity between the biovar ovis and equi strains. *PLoS One.* v. 8, e53818. 2013.
- Songer, J. G. Bacterial phospholipases and their role in virulence. *Trends Microbiol.* v. 5, p. 156-160. 1997.
- Szafranska, A.K., Oxley, A.P., Chaves-Moreno, D. et al. High-Resolution Transcriptomic Analysis of the Adaptive Response of *Staphylococcus aureus* during Acute and Chronic Phases of Osteomyelitis. *MBio.* v. 23, pii: e01775-14. 2014.

Stefańska, I., Gieryńska, M., Rzewuska, M., et al. Survival of *Corynebacterium pseudotuberculosis* within macrophages and induction of phagocytes death. *Pol J Vet Sci.* v. 13, p. 143-149. 2010.

Sun, X., Yang, X.Y., Yin, X.F. et al. Proteomic analysis of membrane proteins from *Streptococcus pneumoniae* with multiple separation methods plus high accuracy mass spectrometry. *OMICS.* v. 15, p. 683-694. 2011.

Surmann, K., Michalik, S., Hildebrandt, P. et al. Comparative proteome analysis reveals conserved and specific adaptation patterns of *Staphylococcus aureus* after internalization by different types of human non-professional phagocytic host cells. *Front Microbiol.* v. 5, p. 1-14. 2014.

Tauch, A., Kaiser, O., Hain, T. et al. Complete genome sequence and analysis of the multiresistant nosocomial pathogen *Corynebacterium jeikeium* K411, a lipid-requiring bacterium of the human skin flora. *J Bacteriol.* v. 187, p. 4671-4682. 2005.

Trost, E., Ott, L., Schneider, J., Schröder, J. et al. The complete genome sequence of *Corynebacterium pseudotuberculosis* FRC41 isolated from a 12-year-old girl with necrotizing lymphadenitis reveals insights into gene-regulatory networks contributing to virulence. *BMC Genomics.* 11:728. 2010.

Trost, E., Blom, J., Soares, S.C. et al. Pangenomic study of *Corynebacterium diphtheriae* that provides insights into the genomic diversity of pathogenic isolates from cases of classical diphtheria, endocarditis, and pneumonia. *J Bacteriol.* v. 194, p. 3199-3215. 2012.

Trost, M., Wehmöhner, D., Kärst, U. et al. Comparative proteome analysis of secretory proteins from pathogenic and nonpathogenic *Listeria* species. *Proteomics.* v. 5, p. 1544-1557. 2005.

Van Oudenhove, L & Devreese, B. A review on recent developments in mass spectrometry instrumentation and quantitative tools advancing bacterial proteomics. *Appl Microbiol Biotechnol.* v. 97, p. 4749-4762. 2013.

Voges, R. & Noack, S. Quantification of proteome dynamics in *Corynebacterium glutamicum* by ^{(15)N}-labeling and selected reaction monitoring. *J Proteomics.* v. 17, p. 2660-2669.

Xam, X., Aslanian, A., Yates, J.R. Mass spectrometry for proteomics. *Curr Opin Chem Biol.* v. 12, p. 483-490. 2008.

Ziebuhr, W. et al. Evolution of bacterial pathogenesis. *CMLS, Cell. Mol. Life Sci.* v. 56, p. 719–728. 1999.

Washburn, M.P. Utilisation of proteomics datasets generated via multidimensional protein identification technology (MudPIT). *Brief Funct Genomic Proteomic.* v. 3, p. 280-286. 2004.

Weinberg, E.D. Iron availability and infection. *Biochim Biophys Acta.* v. 1790, p. 600-605. 2009

Williamson, L.H. Caseous lymphadenitis in small ruminants. *Vet Clin N Amer Food An Pract.* v. 17, p. 359–371. 2001.

Wu, H.J., Wang, A.H., Jennings, M.P. Discovery of virulence factors of pathogenic bacteria. *Curr Opin Chem Biol.* v. 12, p. 93-101. 2008.

11. Anexos/Annexe

Anexo 1: Proteínas diferencias presentes em mais de um experimento proteômico em que foi aplicado estresse.

Annexe 1: Protéines différentiellement produites dans au moins deux études au cours desquelles une condition de stress a été appliquée.

Proteínas diferenciais que foram detectadas em mais de um experimento

Acesso	Proteína	A	B	C
D9Q5T5_CORP1	Glyoxalase Bleomycin resistance protein	X	X	X
D9Q827_CORP1	Metallo beta lactamase superfamily protein	X	X	
D9Q578_CORP1	Replicative DNA helicase	X	X	
D9Q598_CORP1	Formamidopyrimidine DNA glycosylase	X	X	
D9Q5V6_CORP1	Nucleoid associated protein	X	X	
D9Q481_CORP1	Phosphoserine phosphatase	X	X	
D9Q8M3_CORP1	Epimerase family protein yfcH	X	X	
D9Q520_CORP1	Glycerophosphoryl diester phosphodiester	X	X	
D9Q721_CORP1	Hypothetical protein	X	X	
D9Q889_CORP1	MerR family transcriptional regulator	X	X	
D9Q6H6_CORP1	30S ribosomal protein S8	X	X	
D9Q3X0_CORP1	Oligopeptide transport	X	X	
D9Q4N2_CORP1	Hypothetical protein	X	X	
D9Q6M6_CORP1	Hypothetical protein	X	X	
D9Q8Q4_CORP1	Hypothetical protein	X	X	
D9Q559_CORP1	Hypothetical protein	X	X	
D9Q6C3_CORP1	ABC-type metal ion transport		X	X
D9Q5J8_CORP1	Penicillin-binding protein A	X		X

(A) Presente neste trabalho de Tese - análise do proteoma total de 1002_*ovis* em resposta ao óxido nítrico.

Présent dans ce travail de Thèse - analyse du protéome total de 1002_*ovis* en réponse à l'oxyde nitrique.

(B) Presente neste trabalho de Tese - análise do proteoma de 1002_*ovis*, após passagem em modelo murino.

Présent dans ce travail de Thèse - analyse du protéome de 1002_*ovis* après le passage chez la souris.

(C) Estudo do exoproteoma de 1002_*ovis* em resposta ao óxido nítrico (Pacheco et al., 2012).

Étude d'exoproteome de 1002_*ovis* en réponse à l'oxyde nitrique (Pacheco et al., 2012).

Anexo/Annexe 2: Supplementary data (Paper 3; Table S.1)

Table S.1: Complete list of proteins identified as significantly altered ($p \leq 0.05$)

Accession	Description	Score	Peptides	DETACT:SNOX_Ratio	DETACT:SNOX_Log(2)Ratio	DETACT:SNOX_Log(e)Ratio	DETACT:SNOX_Log(e)StdDev	CTDETA_Rel Profile	CTDETA_Rel Profile SD	SNOX_Rel Profile	SNOX_Rel Profile SD	DETACT:SNOX_P	SurfG Prediction (c)	Core genome (b)
D9Q375_CORP1	Methionine aminopeptidase	4047,09	10	0,5599	-0,84	-0,58	0,14	1,28	0,07	0,72	0,07	0	CYT	Core
D9Q377_CORP1	4 hydroxy 3 methylbut 2 en 1 yl diphosp	4629,38	22	0,6313	-0,66	-0,46	0,11	1,23	0,05	0,77	0,05	0	CYT	Core
D9Q381_CORP1	Putative uncharacterized protein	10227,34	4	0,625	-0,68	-0,47	0,17	1,23	0,08	0,77	0,08	0	MEM	Core
D9Q383_CORP1	Ribosome recycling factor	31636,81	13	2,2034	1,14	0,79	0,13	0,63	0,06	1,37	0,06	1	CYT	Core
D9Q385_CORP1	Elongation factor Ts erium	62946,71	24	1,3634	0,45	0,31	0,06	0,85	0,03	1,15	0,03	1	CYT	Core
D9Q386_CORP1	30S ribosomal protein S2 e	72923,45	20	1,786	0,84	0,58	0,07	0,72	0,03	1,28	0,03	1	CYT	Core
D9Q391_CORP1	Putative uncharacterized protein	6857,03	6	0,5769	-0,79	-0,55	0,2	1,27	0,09	0,73	0,09	0	CYT	Core
D9Q393_CORP1	Signal peptidase I	635,92	12	1,5373	0,62	0,43	0,34	0,79	0,16	1,21	0,16	0,98	MEM	Shared
D9Q394_CORP1	50S ribosomal protein L19	10454,94	8	1,477	0,56	0,39	0,16	0,81	0,08	1,19	0,08	1	CYT	Core
D9Q398_CORP1	tRNA guanine N 1 methyltransferase	951,3	17	0,7047	-0,50	-0,35	0,22	1,17	0,11	0,83	0,11	0	CYT	Core
D9Q399_CORP1	Ribosome maturation factor RimM y	1078,46	10	0,644	-0,63	-0,44	0,2	1,21	0,09	0,79	0,09	0	CYT	Core
D9Q3A1_CORP1	30S ribosomal protein S16	55491,64	9	0,5434	-0,88	-0,61	0,09	1,29	0,04	0,71	0,04	0	CYT	Core
D9Q3A2_CORP1	Signal recognition particle protein OS	4563,34	30	0,8106	-0,30	-0,21	0,11	1,1	0,06	0,9	0,06	0	CYT	Core
D9Q3A4_CORP1	Nitrogen regulatory protein P II	10551,54	5	0,5543	-0,85	-0,59	0,18	1,29	0,08	0,71	0,08	0	CYT	Core
D9Q3A5_CORP1	Signal recognition particle receptor Ft	4192,94	21	0,6637	-0,59	-0,41	0,14	1,2	0,07	0,8	0,07	0	PSE	Core
D9Q3A8_CORP1	Na alanine symporter family	1958,2	11	0,7408	-0,43	-0,3	0,18	1,15	0,09	0,85	0,09	0	MEM	Core
D9Q3B2_CORP1	Putative uncharacterized protein	13963,88	17	0,5655	-0,82	-0,57	0,12	1,28	0,05	0,72	0,05	0	CYT	Core

D9Q3B4_CORP1	Glutamate dehydrogenase er	11866,74	25	0,5599	-0,84	-0,58	0,09	1,28	0,04	0,72	0,04	0	CYT	Shared
D9Q3B5_CORP1	Glycerate kinase se	822,99	7	0,5543	-0,85	-0,59	0,24	1,29	0,11	0,71	0,11	0	CYT	Core
D9Q3B9_CORP1	Phosphorylase seudo	4712,91	45	1,1735	0,23	0,16	0,11	0,92	0,05	1,08	0,05	1	CYT	Core
D9Q3C0_CORP1	Putative uncharacterized protein	1647,38	6	0,6005	-0,74	-0,51	0,22	1,25	0,1	0,75	0,1	0	SEC	Shared
D9Q3C1_CORP1	Pyruvate kinase seu	27634,23	26	1,1503	0,20	0,14	0,07	0,93	0,03	1,07	0,03	1	CYT	Core
D9Q3C8_CORP1	1 5 phosphoribosyl 5 5 phosphoribos	2371,93	13	2,2933	1,20	0,83	0,29	0,61	0,12	1,39	0,12	1	CYT	Core
D9Q3D3_CORP1	Histidinol phosphate aminotransferase O	1297,45	16	0,7408	-0,43	-0,3	0,24	1,15	0,11	0,85	0,11	0,01	CYT	Core
D9Q3D7_CORP1	Putative uncharacterized protein	9610,35	6	0,8187	-0,29	-0,2	0,13	1,1	0,07	0,9	0,07	0	PSE	Core
D9Q3D9_CORP1	Glycogen debranching protein	1762,46	36	0,7711	-0,38	-0,26	0,18	1,13	0,09	0,87	0,09	0	CYT	Core
D9Q3E0_CORP1	DNA polymerase III PolC er	744,73	12	0,5827	-0,78	-0,54	0,22	1,26	0,1	0,74	0,1	0	CYT	Core
D9Q3E2_CORP1	RelA SpoT domain containing protein OS	590,13	15	0,7866	-0,35	-0,24	0,28	1,12	0,13	0,88	0,13	0,05	CYT	Core
D9Q3E7_CORP1	Threonine dehydratase eriu	1389,2	22	0,657	-0,61	-0,42	0,19	1,21	0,09	0,79	0,09	0,01	CYT	Shared
D9Q3E8_CORP1	DNA polymerase III subunit alpha	363,37	58	1,1275	0,17	0,12	0,1	0,94	0,05	1,06	0,05	0,98	CYT	Core
D9Q3F3_CORP1	Putative uncharacterized protein	1161,52	10	0,4771	-1,07	-0,74	0,18	1,35	0,08	0,65	0,08	0	SEC	Core
D9Q3F9_CORP1	Antigen 84 b	26297,81	21	1,5527	0,63	0,44	0,08	0,78	0,04	1,22	0,04	1	CYT	Core
D9Q3G1_CORP1	Cell division protein sepF ac	8038,91	12	0,4916	-1,02	-0,71	0,16	1,34	0,07	0,66	0,07	0	CYT	Core
D9Q3G3_CORP1	Cell division protein FtsZ ac	37385,29	23	0,6977	-0,52	-0,36	0,06	1,18	0,03	0,82	0,03	0	CYT	Core
D9Q3G6_CORP1	UDP N acetylglucosamine N acetylmuramy	1791,74	16	1,1735	0,23	0,16	0,18	0,92	0,09	1,08	0,09	0,96	CYT	Core
D9Q3H0_CORP1	UDP N acetyl muramoyl tripeptide D alan	377,64	17	1,391	0,48	0,33	0,24	0,84	0,12	1,16	0,12	1	CYT	Core
D9Q3H1_CORP1	UDP N acetyl muramoyl L alanyl D glutama	3120,38	18	0,7189	-0,48	-0,33	0,16	1,16	0,08	0,84	0,08	0	CYT	Core
D9Q3I5_CORP1	Phospho 2 dehydro 3 deoxyheptonate aldo	2166,16	27	0,8106	-0,30	-0,21	0,17	1,1	0,09	0,9	0,09	0	CYT	Shared
D9Q3I8_CORP1	1 acyl sn glycerol 3 phosphate acyltran	8078,4	17	1,4623	0,55	0,38	0,15	0,81	0,07	1,19	0,07	1	CYT	Shared
D9Q3I9_CORP1	Glucose kinase seud	619,66	9	0,6065	-0,72	-0,5	0,38	1,24	0,18	0,76	0,18	0	CYT	Core
D9Q3J1_CORP1	Cell wall peptidase NlpC P60 protein OS	1654,89	12	0,4771	-1,07	-0,74	0,15	1,35	0,07	0,65	0,07	0	SEC	Core
D9Q3J5_CORP1	Ubiquinol cytochrome C reductase cytoch	5819,09	18	1,2337	0,30	0,21	0,18	0,9	0,09	1,1	0,09	0,99	MEM	Core
D9Q3K0_CORP1	Cytochrome c oxidase subunit II y	9032,85	9	0,6839	-0,55	-0,38	0,12	1,19	0,06	0,81	0,06	0	PSE	Core
D9Q3K2_CORP1	Iron sulfur cluster insertion protein e	4436,95	7	0,5827	-0,78	-0,54	0,25	1,26	0,11	0,74	0,11	0	CYT	Core
D9Q3K3_CORP1	Putative uncharacterized protein	4454,27	8	0,644	-0,63	-0,44	0,19	1,21	0,09	0,79	0,09	0	MEM	Core
D9Q3K8_CORP1	Probable cytosol aminopeptidase y	31107,81	24	0,7866	-0,35	-0,24	0,05	1,12	0,03	0,88	0,03	0	CYT	Core
D9Q3L0_CORP1	Glycine cleavage system P protein	10820,58	38	1,7683	0,82	0,57	0,09	0,72	0,04	1,28	0,04	1	CYT	Core
D9Q3L1_CORP1	Aminomethyltransferase eri	20774,03	22	0,5488	-0,87	-0,6	0,08	1,29	0,04	0,71	0,04	0	CYT	Core

D9Q3L2_CORP1	Glycine cleavage system H protein	75485,59	4	1,3634	0,45	0,31	0,08	0,85	0,04	1,15	0,04	1	CYT	Core
D9Q3L5_CORP1	Lipoyl synthase seu	2719,27	16	0,5655	-0,82	-0,57	0,16	1,28	0,07	0,72	0,07	0	CYT	Core
D9Q3L6_CORP1	Putative uncharacterized protein	2979,3	12	1,31	0,39	0,27	0,15	0,87	0,07	1,13	0,07	1	MEM	Shared
D9Q3L8_CORP1	Glutamine synthetase erium	7915,94	25	0,6065	-0,72	-0,5	0,07	1,25	0,03	0,75	0,03	0	CYT	Shared
D9Q3N8_CORP1	Inosine 5 monophosphate dehydrogenase O	1181,49	19	0,5599	-0,84	-0,58	0,26	1,28	0,12	0,72	0,12	0	CYT	Core
D9Q3P0_CORP1	Putative uncharacterized protein	25209,15	3	1,3771	0,46	0,32	0,17	0,84	0,08	1,16	0,08	1	CYT	Core
D9Q3P4_CORP1	Threonine synthase	6600,34	29	0,7945	-0,33	-0,23	0,12	1,11	0,06	0,89	0,06	0	CYT	Core
D9Q3P9_CORP1	Glutamine synthetase II er	2139,1	16	0,6637	-0,59	-0,41	0,24	1,2	0,12	0,8	0,12	0	CYT	Core
D9Q3Q3_CORP1	Galactokinase seudo	503,38	10	1,9937	1,00	0,69	0,4	0,67	0,18	1,33	0,18	1	CYT	Core
D9Q3Q5_CORP1	Bifunctional RNase H acid phosphatase O	512,33	22	0,6703	-0,58	-0,4	0,33	1,2	0,16	0,8	0,16	0	CYT	Core
D9Q3Q6_CORP1	Zn ribbon protein s	3217,07	18	0,5379	-0,89	-0,62	0,14	1,3	0,06	0,7	0,06	0	CYT	Core
D9Q3Q7_CORP1	NIF3 NGG1p interacting factor 3	4090,53	18	0,5117	-0,97	-0,67	0,14	1,32	0,06	0,68	0,06	0	CYT	Core
D9Q3R4_CORP1	Putative uncharacterized protein	5948,68	7	0,8353	-0,26	-0,18	0,16	1,09	0,08	0,91	0,08	0,02	CYT	Core
D9Q3R5_CORP1	Pyruvate dehydrogenase E1 component OS	19152,76	55	0,7788	-0,36	-0,25	0,08	1,13	0,04	0,87	0,04	0	CYT	Core
D9Q3S0_CORP1	Putative uncharacterized protein	15446,78	5	1,5068	0,59	0,41	0,3	0,8	0,14	1,2	0,14	1	CYT	Core
D9Q3S3_CORP1	Glutamine fructose 6 phosphate aminotransferase	5688	28	0,6505	-0,62	-0,43	0,11	1,21	0,05	0,79	0,05	0	CYT	Core
D9Q3S8_CORP1	Putative uncharacterized protein	1454,52	30	0,7261	-0,46	-0,32	0,18	1,16	0,09	0,84	0,09	0	PSE	Core
D9Q3T1_CORP1	Glycine tRNA ligase erium	16280,62	27	0,7711	-0,38	-0,26	0,1	1,13	0,05	0,87	0,05	0	CYT	Core
D9Q3T3_CORP1	HTH type transcriptional regulator	2461,81	8	1,4477	0,53	0,37	0,34	0,82	0,16	1,18	0,16	0,99	CYT	Shared
D9Q3T4_CORP1	Ferric uptake regulatory protein	7666,99	9	1,1972	0,26	0,18	0,14	0,91	0,07	1,09	0,07	1	CYT	Core
D9Q3U2_CORP1	Phosphate starvation inducible protein	2845,73	21	0,6313	-0,66	-0,46	0,09	1,23	0,04	0,77	0,04	0	CYT	Core
D9Q3U4_CORP1	Chaperone protein DnaJ eri	3102,56	16	0,7408	-0,43	-0,3	0,19	1,15	0,09	0,85	0,09	0	CYT	Core
D9Q3U8_CORP1	Long chain fatty acid CoA ligase	6982,26	36	1,3771	0,46	0,32	0,1	0,84	0,05	1,16	0,05	1	CYT	Shared
D9Q3V2_CORP1	Peptidyl dipeptidase erium	3563,02	26	0,6703	-0,58	-0,4	0,1	1,2	0,05	0,8	0,05	0	CYT	Shared
D9Q3X3_CORP1	Pyridoxal phosphate enzyme YggS family	1490,92	12	0,625	-0,68	-0,47	0,23	1,23	0,11	0,77	0,11	0	CYT	Shared
D9Q3Y3_CORP1	Elongation factor 4 erium	2739,51	28	0,5827	-0,78	-0,54	0,13	1,26	0,06	0,74	0,06	0	CYT	Core
D9Q3Z3_CORP1	Protein yqeL seudot	2488,19	7	0,4404	-1,18	-0,82	0,23	1,39	0,1	0,61	0,1	0	CYT	Core
D9Q3Z5_CORP1	Gamma glutamyl phosphate reductase	814,23	14	0,7634	-0,39	-0,27	0,3	1,13	0,15	0,87	0,15	0,03	CYT	Core
D9Q400_CORP1	GTPase obg b	2019,61	20	0,6977	-0,52	-0,36	0,17	1,18	0,08	0,82	0,08	0	CYT	Core
D9Q401_CORP1	50S ribosomal protein L27	45244,93	7	1,6323	0,71	0,49	0,14	0,76	0,07	1,24	0,07	1	CYT	Core
D9Q402_CORP1	50S ribosomal protein L21	27355,07	7	1,6989	0,76	0,53	0,29	0,74	0,14	1,26	0,14	1	CYT	Shared

D9Q403_CORP1	Ribonuclease E G family er	6490,78	60	0,5886	-0,76	-0,53	0,1	1,26	0,04	0,74	0,04	0	CYT	Shared
D9Q406_CORP1	Nucleoside diphosphate kinase yne	14461,18	8	0,4677	-1,10	-0,76	0,12	1,36	0,05	0,64	0,05	0	CYT	Core
D9Q407_CORP1	Ornithine cyclodeaminase e	12219,18	17	0,7118	-0,49	-0,34	0,08	1,17	0,04	0,83	0,04	0	CYT	Core
D9Q409_CORP1	Bifunctional protein folC	1502,08	24	0,5886	-0,76	-0,53	0,18	1,26	0,08	0,74	0,08	0	CYT	Core
D9Q410_CORP1	Valine tRNA ligase erium	3133,04	43	1,8404	0,88	0,61	0,11	0,7	0,05	1,3	0,05	1	CYT	Core
D9Q411_CORP1	Malate dehydrogenase erium	20873,87	17	0,7261	-0,46	-0,32	0,09	1,16	0,04	0,84	0,04	0	CYT	Core
D9Q413_CORP1	TetR family regulatory protein yn	5165,93	12	1,682	0,75	0,52	0,32	0,75	0,15	1,25	0,15	1	CYT	Core
D9Q416_CORP1	ATP dependent Clp protease proteolytic	15885,59	9	0,657	-0,61	-0,42	0,12	1,21	0,06	0,79	0,06	0	CYT	Core
D9Q417_CORP1	ATP dependent Clp protease proteolytic	26383,46	12	0,6188	-0,69	-0,48	0,11	1,24	0,05	0,76	0,05	0	CYT	Core
D9Q418_CORP1	Trigger factor seud	21008,9	18	0,7558	-0,40	-0,28	0,08	1,14	0,04	0,86	0,04	0	CYT	Core
D9Q421_CORP1	Putative uncharacterized protein	3510,48	7	0,7118	-0,49	-0,34	0,15	1,17	0,07	0,83	0,07	0	PSE	Core
D9Q422_CORP1	Pirin C terminal domain containing prot	864,01	7	0,6376	-0,65	-0,45	0,28	1,22	0,13	0,78	0,13	0	CYT	Core
D9Q423_CORP1	Ribose 5 phosphate isomerase B yn	4146,88	11	0,5326	-0,91	-0,63	0,2	1,31	0,09	0,69	0,09	0	CYT	Core
D9Q424_CORP1	DSBA oxidoreductase erium	6515,89	12	0,6977	-0,52	-0,36	0,2	1,18	0,1	0,82	0,1	0	CYT	Core
D9Q430_CORP1	Thioesterase seudot	2710,9	6	0,6771	-0,56	-0,39	0,19	1,19	0,09	0,81	0,09	0	CYT	Core
D9Q431_CORP1	ABC transporter ATP binding protein OS	2586,9	28	0,4819	-1,05	-0,73	0,12	1,35	0,05	0,65	0,05	0	CYT	Shared
D9Q449_CORP1	Mycocerosic acid synthase	1677,38	13	0,7261	-0,46	-0,32	0,29	1,16	0,14	0,84	0,14	0,02	CYT	Shared
D9Q450_CORP1	Short chain dehydrogenase	12239,6	18	0,8187	-0,29	-0,2	0,21	1,1	0,1	0,9	0,1	0,05	CYT	Core
D9Q451_CORP1	Oligoribonuclease s	550,31	12	0,6977	-0,52	-0,36	0,21	1,18	0,1	0,82	0,1	0	CYT	Core
D9Q452_CORP1	Dihydrodipicolinate synthase	606,05	13	0,5488	-0,87	-0,6	0,39	1,29	0,18	0,71	0,18	0	CYT	Core
D9Q454_CORP1	Oxidoreductase seud	3091,59	15	0,625	-0,68	-0,47	0,19	1,23	0,09	0,77	0,09	0	CYT	Core
D9Q457_CORP1	Putative uncharacterized protein	17409,68	7	1,3499	0,43	0,3	0,13	0,85	0,06	1,15	0,06	1	MEM	Core
D9Q458_CORP1	Bacterioferritin comigratory protein OS	5618,1	10	1,6	0,68	0,47	0,16	0,77	0,07	1,23	0,07	1	CYT	Core
D9Q461_CORP1	Fatty acid synthase erium	2629,12	102	1,9348	0,95	0,66	0,07	0,68	0,03	1,32	0,03	1	CYT	Shared
D9Q471_CORP1	Non canonical purine NTP pyrophosphatas	933,72	8	0,657	-0,61	-0,42	0,29	1,2	0,14	0,8	0,14	0,01	CYT	Core
D9Q472_CORP1	Ribonuclease PH seu	4912,41	12	1,284	0,36	0,25	0,21	0,88	0,1	1,12	0,1	0,99	CYT	Core
D9Q488_CORP1	Ribonucleoside diphosphate reductase su	10301,76	20	0,6313	-0,66	-0,46	0,07	1,23	0,03	0,77	0,03	0	CYT	Core
D9Q490_CORP1	Ferritin like protein eriu	1350,94	13	1,3364	0,42	0,29	0,11	0,85	0,06	1,15	0,06	1	CYT	Core
D9Q491_CORP1	Ribonucleoside diphosphate reductase OS	8150,3	38	0,8353	-0,26	-0,18	0,08	1,09	0,04	0,91	0,04	0	CYT	Core
D9Q495_CORP1	NH 3 dependent NAD synthetase	2273,98	10	0,7408	-0,43	-0,3	0,16	1,15	0,08	0,85	0,08	0	CYT	Core
D9Q4A3_CORP1	DsbG protein seudot	4077,54	13	0,8106	-0,30	-0,21	0,19	1,1	0,1	0,9	0,1	0,02	SEC	Shared

D9Q4A5_CORP1	Phosphoglucomutase	506,7	19	0,6771	-0,56	-0,39	0,29	1,19	0,14	0,81	0,14	0	CYT	Shared
D9Q4A8_CORP1	ABC type antimicrobial peptide transpor	2739,51	32	1,391	0,48	0,33	0,1	0,84	0,05	1,16	0,05	1	PSE	Shared
D9Q4A9_CORP1	ABC superfamily ATP binding cassette tr	13076,21	13	1,4918	0,58	0,4	0,18	0,8	0,08	1,2	0,08	1	CYT	Shared
D9Q4B0_CORP1	UDP N acetylglucosamine 1 carboxyvinylt	3457,53	18	0,6839	-0,55	-0,38	0,11	1,19	0,05	0,81	0,05	0	CYT	Core
D9Q4B2_CORP1	Transcriptional regulator LuxR family	28534,79	14	1,31	0,39	0,27	0,08	0,86	0,04	1,14	0,04	1	CYT	Core
D9Q4B4_CORP1	Cysteine synthase s	47106,28	18	1,5373	0,62	0,43	0,1	0,79	0,05	1,21	0,05	1	CYT	Core
D9Q4B6_CORP1	Acetyltransferase s	10563,89	9	1,3499	0,43	0,3	0,17	0,85	0,08	1,15	0,08	0,99	CYT	Core
D9Q4C2_CORP1	Succinyl CoA Coenzyme A transferase OS	55515,49	30	1,8221	0,87	0,6	0,08	0,71	0,04	1,29	0,04	1	CYT	Core
D9Q4C4_CORP1	Phosphate uptake regulator ac	551,05	15	0,7945	-0,33	-0,23	0,27	1,11	0,13	0,89	0,13	0,04	CYT	Core
D9Q4C8_CORP1	Phosphate ABC transporter phosphate bi	1572,74	11	0,644	-0,63	-0,44	0,17	1,22	0,08	0,78	0,08	0	PSE	Core
D9Q4D2_CORP1	UPF0678 fatty acid binding protein like	8639,18	11	0,5543	-0,85	-0,59	0,12	1,29	0,06	0,71	0,06	0	CYT	Core
D9Q4D6_CORP1	Phosphoribosylformylglycinamide cyclo	4865,9	16	0,5827	-0,78	-0,54	0,12	1,26	0,06	0,74	0,06	0	CYT	Core
D9Q4D7_CORP1	Amidophosphoribosyltransferase yn	1431,28	16	0,6637	-0,59	-0,41	0,16	1,2	0,08	0,8	0,08	0	CYT	Core
D9Q4E2_CORP1	Phosphoribosylformylglycinamide synth	1022,92	24	0,4966	-1,01	-0,7	0,13	1,34	0,06	0,66	0,06	0	CYT	Core
D9Q4E3_CORP1	Phosphoribosylformylglycinamide synth	2299,57	10	0,6505	-0,62	-0,43	0,25	1,21	0,12	0,79	0,12	0	CYT	Core
D9Q4E6_CORP1	Protease II	3043,52	26	0,7558	-0,40	-0,28	0,2	1,14	0,1	0,86	0,1	0,01	CYT	Core
D9Q4E8_CORP1	Phosphoribosylaminoimidazole succinocar	4978,16	20	1,2712	0,35	0,24	0,21	0,88	0,11	1,12	0,11	0,98	CYT	Core
D9Q4E9_CORP1	Adenylosuccinate lyase eri	10977,34	27	0,6907	-0,53	-0,37	0,06	1,18	0,03	0,82	0,03	0	CYT	Core
D9Q4F2_CORP1	Phosphoribosylamine glycine ligase OS	14066,24	19	0,6977	-0,52	-0,36	0,09	1,18	0,04	0,82	0,04	0	CYT	Core
D9Q4F3_CORP1	HIT family protein	2935,88	7	0,4966	-1,01	-0,7	0,32	1,33	0,14	0,67	0,14	0	CYT	Core
D9Q4F8_CORP1	Corynomycolyl transferase	767,45	15	0,6703	-0,58	-0,4	0,23	1,2	0,11	0,8	0,11	0	SEC	Core
D9Q4G1_CORP1	Acetolactate synthase large subunit llv	1993,32	21	0,6771	-0,56	-0,39	0,18	1,19	0,09	0,81	0,09	0	CYT	Core
D9Q4G4_CORP1	Putative uncharacterized protein	3158,54	4	1,477	0,56	0,39	0,2	0,81	0,1	1,19	0,1	1	CYT	Core
D9Q4H0_CORP1	SpoU rRNA Methylase family protein	3824,87	19	1,3771	0,46	0,32	0,2	0,84	0,1	1,16	0,1	0,99	CYT	Core
D9Q4H4_CORP1	Transcriptional regulator	3171,47	11	0,6703	-0,58	-0,4	0,15	1,2	0,07	0,8	0,07	0	CYT	Core
D9Q4H6_CORP1	Lipoprotein LpqE se	22357,24	4	1,9155	0,94	0,65	0,15	0,69	0,07	1,31	0,07	1	SEC	Core
D9Q4I1_CORP1	Putative uncharacterized protein	2305,04	11	1,2969	0,38	0,26	0,24	0,87	0,12	1,13	0,12	0,98	PSE	Core
D9Q4I6_CORP1	ATP dependent Clp protease ATP binding	12555,31	42	0,9231	-0,12	-0,08	0,07	1,04	0,04	0,96	0,04	0,01	CYT	Core
D9Q4I9_CORP1	Inosine uridine preferring nucleoside h	1748,43	12	0,5488	-0,87	-0,6	0,2	1,29	0,09	0,71	0,09	0	CYT	Core
D9Q4J0_CORP1	Hydrolase alpha beta fold family	1615,56	10	0,6376	-0,65	-0,45	0,24	1,22	0,11	0,78	0,11	0	CYT	Shared
D9Q4J6_CORP1	Betaine aldehyde dehydrogenase yn	9610,88	18	1,716	0,78	0,54	0,18	0,74	0,08	1,26	0,08	1	CYT	Core

D9Q4J8_CORP1	Choline dehydrogenase eriu	2829,03	35	1,391	0,48	0,33	0,15	0,84	0,07	1,16	0,07	1	CYT	Core
D9Q4K7_CORP1	ATP dependent zinc metalloprotease FtsH	5274,4	31	0,6907	-0,53	-0,37	0,12	1,18	0,06	0,82	0,06	0	PSE	Core
D9Q4K8_CORP1	Hypoxanthine guanine phosphoribosyltran	6541,73	10	0,6005	-0,74	-0,51	0,19	1,25	0,09	0,75	0,09	0	CYT	Core
D9Q4L0_CORP1	D alanyl D alanine carboxypeptidase OS	687,18	13	1,5841	0,66	0,46	0,38	0,78	0,18	1,22	0,18	1	SEC	Core
D9Q4L6_CORP1	Multiple antibiotic resistance protein	1691,72	9	0,5326	-0,91	-0,63	0,17	1,3	0,08	0,7	0,08	0	CYT	Core
D9Q4M1_CORP1	60 kDa chaperonin s	88468,93	37	1,3634	0,45	0,31	0,03	0,85	0,02	1,15	0,02	1	CYT	Core
D9Q4M2_CORP1	Thiol dipeptidase s	15501,16	15	0,5543	-0,85	-0,59	0,09	1,29	0,04	0,71	0,04	0	CYT	Core
D9Q4N6_CORP1	Exodeoxyribonuclease III e	414,98	14	2,1598	1,11	0,77	0,35	0,64	0,15	1,36	0,15	1	CYT	Core
D9Q4N9_CORP1	ABC superfamily ATP binding cassette tr	2141,02	16	0,7408	-0,43	-0,3	0,17	1,15	0,08	0,85	0,08	0	CYT	Core
D9Q4P2_CORP1	Acetate kinase seud	55935,54	23	1,3364	0,42	0,29	0,09	0,85	0,04	1,15	0,04	1	CYT	Core
D9Q4P3_CORP1	Phosphotransacetylase eriu	24882,77	23	0,644	-0,63	-0,44	0,09	1,22	0,04	0,78	0,04	0	CYT	Core
D9Q4P4_CORP1	Ferredoxin ferredoxin NADP reductase OS	8861,18	29	0,6907	-0,53	-0,37	0,09	1,18	0,05	0,82	0,05	0	CYT	Core
D9Q4P7_CORP1	Phosphoribosyl glycinate formyltransf	2142,2	16	0,6771	-0,56	-0,39	0,23	1,19	0,11	0,81	0,11	0	CYT	Core
D9Q4Q9_CORP1	Adenylosuccinate synthetase a	3636,98	20	0,7408	-0,43	-0,3	0,1	1,15	0,05	0,85	0,05	0	CYT	Core
D9Q4R6_CORP1	Putative uncharacterized protein	2490,66	9	2,2933	1,20	0,83	0,39	0,61	0,16	1,39	0,16	1	CYT	Shared
D9Q4R9_CORP1	Fructose bisphosphate aldolase class 2	28576,08	21	1,9542	0,97	0,67	0,09	0,68	0,04	1,32	0,04	1	CYT	Core
D9Q4S0_CORP1	Glycoside hydrolase family 76 protein O	2920,32	17	0,6839	-0,55	-0,38	0,22	1,19	0,1	0,81	0,1	0	CYT	Core
D9Q4S5_CORP1	Glycerol 3 phosphate dehydrogenase	9116,55	28	1,3771	0,46	0,32	0,08	0,84	0,04	1,16	0,04	1	CYT	Core
D9Q4T4_CORP1	ATP dependent chaperone protein ClpB OS	8721,09	47	0,6065	-0,72	-0,5	0,1	1,25	0,05	0,75	0,05	0	CYT	Shared
D9Q4T5_CORP1	ABC transporter domain containing ATP b	32711,08	13	0,7788	-0,36	-0,25	0,11	1,12	0,05	0,88	0,05	0	CYT	Core
D9Q4T8_CORP1	Sodium glutamate symporter ac	591,89	6	1,3499	0,43	0,3	0,22	0,85	0,11	1,15	0,11	1	MEM	Core
D9Q4U1_CORP1	Oxidoreductase seud	2389,41	18	0,7334	-0,45	-0,31	0,25	1,15	0,12	0,85	0,12	0,01	CYT	Core
D9Q4U5_CORP1	Secretion protein HlyD eri	9392,81	26	0,7261	-0,46	-0,32	0,13	1,16	0,07	0,84	0,07	0	PSE	Shared
D9Q4V4_CORP1	Protein GrpE seudot	3220,13	10	0,5886	-0,76	-0,53	0,2	1,26	0,09	0,74	0,09	0	CYT	Core
D9Q4V5_CORP1	Chaperone protein DnaK eri	88642,89	46	1,5068	0,59	0,41	0,06	0,8	0,03	1,2	0,03	1	CYT	Core
D9Q4W5_CORP1	Putative uncharacterized protein	3999,63	12	1,1618	0,22	0,15	0,16	0,92	0,08	1,08	0,08	0,96	PSE	Core
D9Q4X3_CORP1	Urease accessory protein UreE yne	4552,59	14	0,4819	-1,05	-0,73	0,18	1,35	0,08	0,65	0,08	0	CYT	Core
D9Q4X4_CORP1	Urease subunit alpha erium	1962,68	21	0,7634	-0,39	-0,27	0,22	1,13	0,11	0,87	0,11	0	CYT	Core
D9Q4Y1_CORP1	Lysyl tRNA synthetase eriu	1922,37	40	1,2586	0,33	0,23	0,17	0,88	0,08	1,12	0,08	1	PSE	Core
D9Q4Y6_CORP1	Deoxycytidine triphosphate deaminase OS	2209,23	7	0,5599	-0,84	-0,58	0,18	1,28	0,08	0,72	0,08	0	CYT	Core
D9Q506_CORP1	Phthiocerol synthesis polyketide syntha	4024,35	51	0,8607	-0,22	-0,15	0,15	1,08	0,08	0,92	0,08	0,05	CYT	Core

D9Q507_CORP1	Long chain fatty acid AMP ligase FadD3	29427,22	32	1,3771	0,46	0,32	0,08	0,84	0,04	1,16	0,04	1	CYT	Core
D9Q508_CORP1	Cutinase ber	2572,9	12	0,5117	-0,97	-0,67	0,16	1,32	0,07	0,68	0,07	0	PSE	Shared
D9Q510_CORP1	Trehalose corynomycolyl transferase C O	31307,3	36	1,1163	0,16	0,11	0,07	0,95	0,03	1,05	0,03	1	SEC	Core
D9Q512_CORP1	Trehalose corynomycolyl transferase B O	41956,45	13	0,7945	-0,33	-0,23	0,11	1,11	0,05	0,89	0,05	0	SEC	Core
D9Q516_CORP1	Glycosyltransferase erium	3415,8	33	0,7261	-0,46	-0,32	0,1	1,16	0,05	0,84	0,05	0	CYT	Core
D9Q521_CORP1	Glycerol 3 phosphate transporter	589,61	10	0,5655	-0,82	-0,57	0,28	1,28	0,12	0,72	0,12	0	MEM	Shared
D9Q522_CORP1	UDP galactopyranose mutase ac	14078,63	17	0,7334	-0,45	-0,31	0,12	1,16	0,06	0,84	0,06	0	CYT	Core
D9Q526_CORP1	Peptidoglycan recognition protein	4191,41	18	0,7408	-0,43	-0,3	0,18	1,15	0,09	0,85	0,09	0	SEC	Core
D9Q528_CORP1	Acyltransferase family protein yn	1489,08	12	1,5841	0,66	0,46	0,23	0,78	0,11	1,22	0,11	1	CYT	Core
D9Q529_CORP1	Serine tRNA ligase erium	9711,01	24	0,7634	-0,39	-0,27	0,11	1,13	0,05	0,87	0,05	0	CYT	Core
D9Q530_CORP1	GntR family transcriptional regulator O	1376,45	15	1,5683	0,65	0,45	0,25	0,78	0,12	1,22	0,12	1	CYT	Core
D9Q531_CORP1	Putative uncharacterized protein	1187,74	18	1,6	0,68	0,47	0,45	0,77	0,2	1,23	0,2	0,97	SEC	Shared
D9Q540_CORP1	SEC C domain containing protein y	6131,07	14	0,6637	-0,59	-0,41	0,12	1,2	0,06	0,8	0,06	0	CYT	Core
D9Q544_CORP1	Thymidine phosphorylase er	1903,29	19	0,6505	-0,62	-0,43	0,2	1,21	0,1	0,79	0,1	0	CYT	Core
D9Q545_CORP1	L lactate dehydrogenase er	13330,1	16	1,2092	0,27	0,19	0,11	0,91	0,06	1,09	0,06	1	CYT	Core
D9Q546_CORP1	Peptide methionine sulfoxide reductase	2286,03	11	0,6505	-0,62	-0,43	0,25	1,21	0,12	0,79	0,12	0	CYT	Core
D9Q556_CORP1	LSR2 like protein s	4478,54	6	0,5655	-0,82	-0,57	0,18	1,27	0,08	0,73	0,08	0	CYT	Shared
D9Q557_CORP1	Two component system transcriptional re	4565,54	9	0,6376	-0,65	-0,45	0,22	1,22	0,11	0,78	0,11	0	CYT	Core
D9Q572_CORP1	Putative uncharacterized protein	1990,49	18	0,8106	-0,30	-0,21	0,16	1,1	0,08	0,9	0,08	0	CYT	Core
D9Q574_CORP1	Thioredoxin	7001,85	8	0,7866	-0,35	-0,24	0,18	1,12	0,09	0,88	0,09	0,01	CYT	Core
D9Q583_CORP1	Single stranded DNA binding protein OS	12512,08	7	0,8353	-0,26	-0,18	0,16	1,09	0,08	0,91	0,08	0,02	CYT	Core
D9Q584_CORP1	30S ribosomal protein S6 e	18238,73	7	0,6376	-0,65	-0,45	0,25	1,22	0,12	0,78	0,12	0	CYT	Core
D9Q588_CORP1	Penicillin binding protein ac	1690,08	26	0,7866	-0,35	-0,24	0,18	1,12	0,08	0,88	0,08	0	PSE	Core
D9Q590_CORP1	Multiple antibiotic resistance protein	6202,79	11	0,6005	-0,74	-0,51	0,23	1,25	0,11	0,75	0,11	0	CYT	Core
D9Q591_CORP1	Universal stress protein UspA yne	816,77	20	0,5169	-0,95	-0,66	0,22	1,32	0,1	0,68	0,1	0	CYT	Core
D9Q597_CORP1	DNA protection during starvation protei	5751,7	9	1,1735	0,23	0,16	0,12	0,92	0,06	1,08	0,06	1	CYT	Core
D9Q5A2_CORP1	Leucine tRNA ligase erium	5611,74	45	0,7788	-0,36	-0,25	0,1	1,12	0,05	0,88	0,05	0	CYT	Core
D9Q5B1_CORP1	ChrA CheY winged helix DNA binding dom	702,18	8	0,4868	-1,04	-0,72	0,38	1,34	0,16	0,66	0,16	0	CYT	Core
D9Q5B2_CORP1	Putative uncharacterized protein	14866,76	64	1,6487	0,72	0,5	0,07	0,75	0,03	1,25	0,03	1	PSE	Shared
D9Q5B3_CORP1	Glucosamine 6 phosphate deaminase	2338,6	13	1,6323	0,71	0,49	0,27	0,76	0,12	1,24	0,12	1	CYT	Core
D9Q5B8_CORP1	Oligopeptide binding protein oppA	1049,22	21	1,1972	0,26	0,18	0,2	0,91	0,1	1,09	0,1	0,95	SEC	Core

D9Q5C0_CORP1	Oligopeptide transport ATP binding prot	506,02	24	1,4918	0,58	0,4	0,23	0,8	0,11	1,2	0,11	1	PSE	Core
D9Q5C8_CORP1	UPF0371 protein Cp1002 2074 a	1953,77	25	0,7334	-0,45	-0,31	0,13	1,15	0,07	0,85	0,07	0	CYT	Shared
D9Q5C9_CORP1	Putative uncharacterized protein	12375,18	4	1,6161	0,69	0,48	0,31	0,77	0,14	1,23	0,14	1	CYT	Core
D9Q5E8_CORP1	tRNA nucleotidyltransferase a	635,56	28	0,8025	-0,32	-0,22	0,18	1,11	0,09	0,89	0,09	0,01	CYT	Core
D9Q5F3_CORP1	Thioredoxin reductase eriu	5492,57	15	0,7483	-0,42	-0,29	0,14	1,14	0,07	0,86	0,07	0	CYT	Core
D9Q5F4_CORP1	Thioredoxin	30328,59	7	1,3771	0,46	0,32	0,18	0,84	0,09	1,16	0,09	1	CYT	Core
D9Q5F5_CORP1	N Acetylmuramyl L Alanine Amidase	2205,83	21	0,6907	-0,53	-0,37	0,15	1,18	0,07	0,82	0,07	0	PSE	Core
D9Q5F7_CORP1	Chromosome partitioning protein ParB OS	11456,54	20	0,7634	-0,39	-0,27	0,11	1,13	0,05	0,87	0,05	0	CYT	Core
D9Q5F8_CORP1	Chromosome partitioning protein parA OS	1501,97	9	0,6313	-0,66	-0,46	0,19	1,23	0,09	0,77	0,09	0	CYT	Core
D9Q5G0_CORP1	Inner MEM protein translocase comp	2330,37	11	0,6005	-0,74	-0,51	0,18	1,25	0,08	0,75	0,08	0	MEM	Core
D9Q5G6_CORP1	DNA polymerase III subunit beta y	5534,19	15	0,6188	-0,69	-0,48	0,13	1,23	0,06	0,77	0,06	0	CYT	Core
D9Q5H4_CORP1	DNA gyrase subunit A erium	7018,34	46	1,4477	0,53	0,37	0,09	0,82	0,04	1,18	0,04	1	CYT	Shared
D9Q5I2_CORP1	Putative uncharacterized protein	41840,52	15	1,2214	0,29	0,2	0,11	0,9	0,06	1,1	0,06	1	PSE	Core
D9Q5I3_CORP1	Peptidyl prolyl cis trans isomerase OS	25129,04	9	1,8965	0,92	0,64	0,12	0,69	0,06	1,31	0,06	1	CYT	Core
D9Q5J4_CORP1	Iron siderophore binding protein	13482,74	16	1,6	0,68	0,47	0,18	0,77	0,08	1,23	0,08	1	SEC	Core
D9Q5J5_CORP1	Putative uncharacterized protein	9182,01	2	0,6637	-0,59	-0,41	0,23	1,2	0,11	0,8	0,11	0,02	MEM	Core
D9Q5J6_CORP1	Serine threonine protein kinase y	3021,99	24	0,8106	-0,30	-0,21	0,18	1,1	0,09	0,9	0,09	0	PSE	Core
D9Q5J7_CORP1	Serine threonine protein kinase y	785,87	16	0,5655	-0,82	-0,57	0,22	1,27	0,1	0,73	0,1	0	CYT	Core
D9Q5L0_CORP1	Oligo 1 6 glucosidase 1 er	1431,31	22	0,7866	-0,35	-0,24	0,23	1,12	0,12	0,88	0,12	0,04	CYT	Core
D9Q5M0_CORP1	Choline transport ATP binding protein O	3983,3	19	0,7334	-0,45	-0,31	0,17	1,15	0,08	0,85	0,08	0	CYT	Core
D9Q5M7_CORP1	Putative uncharacterized protein	441,52	19	0,5434	-0,88	-0,61	0,24	1,29	0,11	0,71	0,11	0	PSE	Shared
D9Q5M8_CORP1	Lysozyme M1	4454,14	11	0,4868	-1,04	-0,72	0,12	1,35	0,05	0,65	0,05	0	SEC	Shared
D9Q5N4_CORP1	Transcription factor Rok e	7268,02	11	1,6323	0,71	0,49	0,17	0,76	0,08	1,24	0,08	1	CYT	Core
D9Q5N6_CORP1	Putative uncharacterized protein	766,04	14	0,6637	-0,59	-0,41	0,21	1,2	0,1	0,8	0,1	0	CYT	Shared
D9Q5N7_CORP1	Putative uncharacterized protein	1451,37	27	0,7261	-0,46	-0,32	0,23	1,16	0,11	0,84	0,11	0,01	CYT	Shared
D9Q5P2_CORP1	Putative uncharacterized protein	2765,86	5	1,8589	0,89	0,62	0,3	0,7	0,13	1,3	0,13	1	PSE	Core
D9Q5Q0_CORP1	UPF0145 protein Cp1002 0087 a	3703,26	7	0,7334	-0,45	-0,31	0,24	1,15	0,11	0,85	0,11	0	CYT	Core
D9Q5Q1_CORP1	Uncharacterized protein yaaA	11267,84	10	0,5434	-0,88	-0,61	0,18	1,3	0,08	0,7	0,08	0	CYT	Shared
D9Q5Q7_CORP1	Metalloendopeptidase erium	4220,95	38	0,8781	-0,19	-0,13	0,14	1,06	0,07	0,94	0,07	0,05	CYT	Core
D9Q5R0_CORP1	Glycine betaine binding protein y	672,75	10	0,6505	-0,62	-0,43	0,32	1,21	0,15	0,79	0,15	0,01	PSE	Core
D9Q5R3_CORP1	Decaprenylphosphoryl D 2 keto erythrope	7234,8	9	1,2461	0,32	0,22	0,22	0,89	0,11	1,11	0,11	0,98	CYT	Core

D9Q5S4_CORP1	Periplasmic zinc binding protein troA O	5569,95	16	0,6376	-0,65	-0,45	0,12	1,22	0,06	0,78	0,06	0	SEC	Shared
D9Q5S6_CORP1	O antigen export system ATP binding pr	1135,96	11	0,6005	-0,74	-0,51	0,32	1,25	0,15	0,75	0,15	0	CYT	Shared
D9Q5S9_CORP1	Quinone oxidoreductase 1 e	996,76	10	0,7558	-0,40	-0,28	0,23	1,14	0,11	0,86	0,11	0,02	CYT	Core
D9Q5U2_CORP1	Putative uncharacterized protein	3452,09	6	0,6839	-0,55	-0,38	0,34	1,19	0,17	0,81	0,17	0,04	CYT	Shared
D9Q5U6_CORP1	Queuine tRNA ribosyltransferase y	4994,52	21	0,7047	-0,50	-0,35	0,11	1,17	0,05	0,83	0,05	0	CYT	Core
D9Q5V0_CORP1	Zinc binding alcohol dehydrogenase	1163,74	8	1,7683	0,82	0,57	0,37	0,73	0,17	1,27	0,17	1	CYT	Core
D9Q5V5_CORP1	DNA polymerase III subunit gamma tau OS	1342,02	30	0,7483	-0,42	-0,29	0,18	1,14	0,09	0,86	0,09	0,01	CYT	Shared
D9Q5W4_CORP1	Cobyric acid synthase eriu	3000,69	10	0,6703	-0,58	-0,4	0,29	1,19	0,14	0,81	0,14	0,02	CYT	Core
D9Q5W5_CORP1	UDP N acetylmuramoylalanine D glutamat	2760,44	21	0,7711	-0,38	-0,26	0,2	1,13	0,1	0,87	0,1	0,01	CYT	Core
D9Q5W6_CORP1	DNA polymerase III subunit epsilon	462,32	12	1,4623	0,55	0,38	0,38	0,82	0,18	1,18	0,18	0,95	CYT	Core
D9Q5X1_CORP1	Deoxyribose phosphate aldolase yn	1138,65	9	0,4538	-1,14	-0,79	0,23	1,37	0,1	0,63	0,1	0	CYT	Core
D9Q5X2_CORP1	Phosphoglucosamine mutase	405,38	25	0,5827	-0,78	-0,54	0,24	1,26	0,11	0,74	0,11	0	CYT	Core
D9Q5X8_CORP1	Aspartokinase seudo	9780,94	21	0,6839	-0,55	-0,38	0,11	1,19	0,05	0,81	0,05	0	CYT	Core
D9Q5Y0_CORP1	Aspartate semialdehyde dehydrogenase OS	8540,42	18	1,1853	0,25	0,17	0,14	0,92	0,07	1,08	0,07	0,98	CYT	Core
D9Q5Y2_CORP1	Catalase ber	19263,56	28	0,5169	-0,95	-0,66	0,06	1,32	0,03	0,68	0,03	0	CYT	Core
D9Q601_CORP1	Putative uncharacterized protein	545,93	13	1,2337	0,30	0,21	0,22	0,9	0,11	1,1	0,11	0,97	PSE	Shared
D9Q602_CORP1	Putative uncharacterized protein	11245,36	18	0,6376	-0,65	-0,45	0,11	1,22	0,05	0,78	0,05	0	SEC	Core
D9Q606_CORP1	Uncharacterized metallophosphoesterase	1733,75	14	1,6	0,68	0,47	0,22	0,77	0,11	1,23	0,11	1	SEC	Core
D9Q607_CORP1	Uncharacterized protein yqeY	2060,42	7	1,4191	0,50	0,35	0,3	0,83	0,14	1,17	0,14	1	CYT	Core
D9Q611_CORP1	RutC family protein yabJ e	26539,58	6	0,4819	-1,05	-0,73	0,13	1,35	0,06	0,65	0,06	0	CYT	Core
D9Q613_CORP1	CRP FNR family transcriptional regulato	35521,79	15	0,8437	-0,25	-0,17	0,1	1,09	0,05	0,91	0,05	0	CYT	Core
D9Q632_CORP1	Cold shock protein	12956,59	6	1,7507	0,81	0,56	0,16	0,73	0,07	1,27	0,07	1	CYT	Core
D9Q634_CORP1	OPT family protein	826,01	8	0,7483	-0,42	-0,29	0,34	1,14	0,17	0,86	0,17	0,05	MEM	Core
D9Q638_CORP1	Acetyl coenzyme A synthetase	1729,62	26	1,391	0,48	0,33	0,25	0,84	0,12	1,16	0,12	0,99	CYT	Core
D9Q645_CORP1	Surface layer protein A er	10675,08	20	0,5945	-0,75	-0,52	0,13	1,25	0,06	0,75	0,06	0	SEC	Core
D9Q648_CORP1	Dihydrolipoyl dehydrogenase a	27197,05	27	1,8589	0,89	0,62	0,08	0,7	0,04	1,3	0,04	1	CYT	Core
D9Q649_CORP1	HTH type transcriptional regulator	591,13	21	1,6653	0,74	0,51	0,2	0,75	0,09	1,25	0,09	1	CYT	Core
D9Q651_CORP1	Succinate dehydrogenase flavoprotein su	13400,17	37	0,827	-0,27	-0,19	0,06	1,1	0,03	0,9	0,03	0	CYT	Core
D9Q652_CORP1	Succinate dehydrogenase iron sulfur sub	11006,72	11	0,6977	-0,52	-0,36	0,14	1,18	0,07	0,82	0,07	0	CYT	Core
D9Q653_CORP1	Putative uncharacterized protein	578,12	3	0,5769	-0,79	-0,55	0,3	1,27	0,14	0,73	0,14	0	MEM	Core
D9Q656_CORP1	Deoxyribose phosphate aldolase yn	1070	6	0,4404	-1,18	-0,82	0,44	1,38	0,19	0,62	0,19	0	CYT	Core

D9Q659_CORP1	Formate acetyltransferase	15050,01	5	2,0751	1,05	0,73	0,15	0,65	0,06	1,35	0,06	1	CYT	Core
D9Q660_CORP1	Formate acetyltransferase 1 a	16865,06	36	1,1735	0,23	0,16	0,08	0,92	0,04	1,08	0,04	1	CYT	Core
D9Q662_CORP1	Putative uncharacterized protein	6026,61	4	1,2969	0,38	0,26	0,21	0,87	0,1	1,13	0,1	1	CYT	Core
D9Q666_CORP1	2,3 bisphosphoglycerate dependent phosphatase	58261,35	14	1,8589	0,89	0,62	0,08	0,7	0,04	1,3	0,04	1	CYT	Core
D9Q671_CORP1	Putative uncharacterized protein	5147,74	14	0,6376	-0,65	-0,45	0,12	1,22	0,06	0,78	0,06	0	MEM	Core
D9Q674_CORP1	DNA binding Excisionase protein	8240,56	5	0,5434	-0,88	-0,61	0,26	1,29	0,12	0,71	0,12	0	CYT	Core
D9Q681_CORP1	Glutamyl tRNA reductase er	2323,34	18	0,657	-0,61	-0,42	0,16	1,21	0,08	0,79	0,08	0	CYT	Core
D9Q682_CORP1	Porphobilinogen deaminase	10362,36	17	0,6839	-0,55	-0,38	0,13	1,19	0,06	0,81	0,06	0	CYT	Core
D9Q684_CORP1	Delta aminolevulinic acid dehydratase O	2498,52	13	0,5488	-0,87	-0,6	0,15	1,29	0,07	0,71	0,07	0	CYT	Core
D9Q687_CORP1	Uroporphyrinogen decarboxylase yn	1466,19	11	0,7634	-0,39	-0,27	0,19	1,13	0,09	0,87	0,09	0	SEC	Core
D9Q690_CORP1	Glutamate 1 semialdehyde 2,1 aminomutase	10069,48	21	1,6989	0,76	0,53	0,16	0,74	0,08	1,26	0,08	1	CYT	Core
D9Q691_CORP1	Probable phosphoglycerate mutase	6080	14	0,7634	-0,39	-0,27	0,19	1,13	0,09	0,87	0,09	0	CYT	Core
D9Q6A4_CORP1	Naphthoate synthase erium	1669,27	17	0,7558	-0,40	-0,28	0,15	1,14	0,07	0,86	0,07	0	CYT	Core
D9Q6B0_CORP1	Demethylmenaquinone methyltransferase O	2587,26	11	0,6637	-0,59	-0,41	0,22	1,2	0,1	0,8	0,1	0	CYT	Core
D9Q6B3_CORP1	Polypropenyl synthetase eriu	2584,38	13	2,1815	1,13	0,78	0,27	0,63	0,11	1,37	0,11	1	CYT	Core
D9Q6B4_CORP1	Preprotein translocase subunit SecE OS	7580,88	6	1,4333	0,52	0,36	0,28	0,82	0,14	1,18	0,14	1	MEM	Core
D9Q6B5_CORP1	Transcription antitermination protein n	10055,64	10	0,6313	-0,66	-0,46	0,11	1,23	0,05	0,77	0,05	0	CYT	Core
D9Q6B6_CORP1	50S ribosomal protein L11	56914,66	8	1,4918	0,58	0,4	0,11	0,8	0,06	1,2	0,06	1	CYT	Core
D9Q6B7_CORP1	50S ribosomal protein L1 e	36940,67	11	0,7866	-0,35	-0,24	0,08	1,12	0,04	0,88	0,04	0	CYT	Core
D9Q6B9_CORP1	N ethylmaleimide reductase ac	5881,91	19	0,7558	-0,40	-0,28	0,19	1,14	0,09	0,86	0,09	0	CYT	Core
D9Q6C0_CORP1	50S ribosomal protein L10	71009,23	12	1,6	0,68	0,47	0,07	0,77	0,03	1,23	0,03	1	CYT	Shared
D9Q6C1_CORP1	50S ribosomal protein L7 L12	69197,34	12	0,6065	-0,72	-0,5	0,07	1,25	0,03	0,75	0,03	0	CYT	Core
D9Q6D0_CORP1	DNA directed RNA polymerase subunit bet	20024,66	63	0,6637	-0,59	-0,41	0,06	1,2	0,03	0,8	0,03	0	CYT	Core
D9Q6D1_CORP1	DNA directed RNA polymerase subunit bet	22544,65	88	0,7047	-0,50	-0,35	0,04	1,17	0,02	0,83	0,02	0	CYT	Core
D9Q6E3_CORP1	30S ribosomal protein S7 e	70872,22	11	1,284	0,36	0,25	0,09	0,88	0,05	1,12	0,05	1	CYT	Core
D9Q6E4_CORP1	Elongation factor G erium	61222,3	44	1,4333	0,52	0,36	0,05	0,82	0,02	1,18	0,02	1	CYT	Core
D9Q6E5_CORP1	Elongation factor Tu erium	91926,84	28	1,4333	0,52	0,36	0,07	0,82	0,04	1,18	0,04	1	CYT	Core
D9Q6F2_CORP1	Putative uncharacterized protein	15017,67	9	0,6977	-0,52	-0,36	0,1	1,18	0,05	0,82	0,05	0	CYT	Core
D9Q6F3_CORP1	30S ribosomal protein S10	29376,59	10	0,8025	-0,32	-0,22	0,09	1,11	0,04	0,89	0,04	0	CYT	Core
D9Q6F4_CORP1	50S ribosomal protein L3 e	63911,54	12	0,7634	-0,39	-0,27	0,07	1,14	0,04	0,86	0,04	0	CYT	Core
D9Q6F5_CORP1	50S ribosomal protein L4 e	54542,38	13	1,5373	0,62	0,43	0,07	0,79	0,03	1,21	0,03	1	CYT	Core

D9Q6F6_CORP1	50S ribosomal protein L23	19865,59	7	0,6839	-0,55	-0,38	0,1	1,19	0,05	0,81	0,05	0	CYT	Core
D9Q6F7_CORP1	50S ribosomal protein L2 e	33268,52	18	1,1618	0,22	0,15	0,07	0,92	0,04	1,08	0,04	1	CYT	Core
D9Q6F8_CORP1	30S ribosomal protein S19	49674,58	9	1,1735	0,23	0,16	0,16	0,92	0,08	1,08	0,08	0,96	CYT	Core
D9Q6F9_CORP1	50S ribosomal protein L22	56645,38	10	1,5683	0,65	0,45	0,1	0,78	0,05	1,22	0,05	1	CYT	Shared
D9Q6G0_CORP1	30S ribosomal protein S3 e	50409,02	15	1,5068	0,59	0,41	0,06	0,8	0,03	1,2	0,03	1	CYT	Core
D9Q6G1_CORP1	50S ribosomal protein L16	26095,49	6	1,1972	0,26	0,18	0,13	0,91	0,06	1,09	0,06	0,98	CYT	Shared
D9Q6G2_CORP1	50S ribosomal protein L29	67728,64	8	2,0751	1,05	0,73	0,25	0,65	0,11	1,35	0,11	1	CYT	Core
D9Q6G3_CORP1	30S ribosomal protein S17	35515,99	8	0,625	-0,68	-0,47	0,14	1,23	0,07	0,77	0,07	0	CYT	Core
D9Q6G4_CORP1	Oligopeptide binding protein oppA	6409,05	29	1,6989	0,76	0,53	0,15	0,74	0,07	1,26	0,07	1	PSE	Core
D9Q6H0_CORP1	50S ribosomal protein L14	23934,85	7	0,8353	-0,26	-0,18	0,09	1,09	0,04	0,91	0,04	0	CYT	Core
D9Q6H1_CORP1	50S ribosomal protein L24	51692,45	6	0,7788	-0,36	-0,25	0,09	1,12	0,05	0,88	0,05	0	CYT	Core
D9Q6H2_CORP1	50S ribosomal protein L5 e	32970,07	11	1,8404	0,88	0,61	0,12	0,71	0,05	1,29	0,05	1	CYT	Core
D9Q6H7_CORP1	50S ribosomal protein L6 e	28305,79	12	1,4191	0,50	0,35	0,12	0,83	0,06	1,17	0,06	1	CYT	Core
D9Q6H8_CORP1	50S ribosomal protein L18	24484,4	7	0,8106	-0,30	-0,21	0,11	1,1	0,05	0,9	0,05	0	CYT	Core
D9Q6H9_CORP1	30S ribosomal protein S5 e	14713,58	7	1,284	0,36	0,25	0,15	0,88	0,07	1,12	0,07	1	CYT	Core
D9Q6I0_CORP1	50S ribosomal protein L30	33396,32	6	0,4916	-1,02	-0,71	0,15	1,34	0,07	0,66	0,07	0	CYT	Core
D9Q6I1_CORP1	50S ribosomal protein L15	41496,34	8	1,3231	0,40	0,28	0,12	0,86	0,06	1,14	0,06	1	CYT	Core
D9Q6I3_CORP1	Maltotriose binding protein a	12652,1	25	1,2969	0,38	0,26	0,13	0,87	0,06	1,13	0,06	1	PSE	Core
D9Q6I9_CORP1	Glycerol 3 phosphate transporting ATPas	7453,05	19	1,4191	0,50	0,35	0,16	0,83	0,08	1,17	0,08	1	CYT	Shared
D9Q6J1_CORP1	Adenylate kinase se	11815,02	9	1,6653	0,74	0,51	0,15	0,75	0,07	1,25	0,07	1	CYT	Core
D9Q6J2_CORP1	Neuraminidase Sialidase	27098,3	40	1,2969	0,38	0,26	0,06	0,87	0,03	1,13	0,03	1	SEC	Shared
D9Q6J3_CORP1	L D transpeptidase catalytic domain re	7349,33	10	0,6005	-0,74	-0,51	0,13	1,25	0,06	0,75	0,06	0	SEC	Core
D9Q6J4_CORP1	Translation initiation factor IF 1	23927,21	6	1,8221	0,87	0,6	0,12	0,71	0,06	1,29	0,06	1	CYT	Core
D9Q6J5_CORP1	30S ribosomal protein S13	33203,57	9	1,1618	0,22	0,15	0,1	0,93	0,05	1,07	0,05	0,99	CYT	Core
D9Q6J6_CORP1	30S ribosomal protein S11	34290,42	6	1,716	0,78	0,54	0,14	0,74	0,07	1,26	0,07	1	CYT	Core
D9Q6J7_CORP1	30S ribosomal protein S4 e	42436,14	14	1,522	0,61	0,42	0,08	0,79	0,04	1,21	0,04	1	CYT	Core
D9Q6J8_CORP1	DNA directed RNA polymerase subunit alp	76700,45	24	1,4623	0,55	0,38	0,05	0,81	0,03	1,19	0,03	1	CYT	Core
D9Q6L0_CORP1	50S ribosomal protein L13	47058,93	9	0,7408	-0,43	-0,3	0,07	1,15	0,03	0,85	0,03	0	CYT	Core
D9Q6L1_CORP1	30S ribosomal protein S9 e	25699,39	10	0,6376	-0,65	-0,45	0,08	1,22	0,04	0,78	0,04	0	CYT	Core
D9Q6L2_CORP1	Phosphoglcosamine mutase	907,75	16	1,3634	0,45	0,31	0,22	0,85	0,11	1,15	0,11	0,98	CYT	Core
D9Q6L8_CORP1	UPF0079 ATP binding protein a	577,85	6	0,5599	-0,84	-0,58	0,57	1,28	0,25	0,72	0,25	0,03	CYT	Core

D9Q6M0_CORP1	Putative uncharacterized protein	769,15	8	0,5169	-0,95	-0,66	0,29	1,32	0,13	0,68	0,13	0	CYT	Shared
D9Q6M3_CORP1	10 kDa chaperonin s	73111,66	9	1,477	0,56	0,39	0,13	0,81	0,06	1,19	0,06	1	CYT	Core
D9Q6M4_CORP1	60 kDa chaperonin s	100293,8	37	1,5527	0,63	0,44	0,05	0,78	0,02	1,22	0,02	1	CYT	Core
D9Q6M7_CORP1	Inosine 5 monophosphate dehydrogenase	5214,43	26	0,6188	-0,69	-0,48	0,11	1,23	0,05	0,77	0,05	0	CYT	Core
D9Q6M8_CORP1	Inosine 5 monophosphate dehydrogenase	13651,78	21	0,7118	-0,49	-0,34	0,09	1,17	0,04	0,83	0,04	0	CYT	Core
D9Q6N0_CORP1	GMP synthase glutamine hydrolyzing OS	18709,51	28	0,7047	-0,50	-0,35	0,06	1,17	0,03	0,83	0,03	0	CYT	Core
D9Q6N5_CORP1	Putative uncharacterized protein	2785,31	6	0,4771	-1,07	-0,74	0,22	1,35	0,09	0,65	0,09	0	PSE	Core
D9Q6N8_CORP1	Methionine import ATP binding protein M	3041,96	14	0,7047	-0,50	-0,35	0,13	1,17	0,06	0,83	0,06	0	CYT	Core
D9Q6P0_CORP1	D methionine binding lipoprotein metQ O	4568,85	14	0,6005	-0,74	-0,51	0,13	1,25	0,06	0,75	0,06	0	PSE	Core
D9Q6P2_CORP1	Manganese ABC transporter substrate bin	1444,48	15	0,7334	-0,45	-0,31	0,3	1,15	0,14	0,85	0,14	0,03	PSE	Core
D9Q6P6_CORP1	DtxR family transcriptional regulator O	2371,28	8	0,5117	-0,97	-0,67	0,19	1,32	0,08	0,68	0,08	0	CYT	Core
D9Q6P7_CORP1	Putative tRNA cytidine 34 2 O methyltransferase	1924,41	9	0,4868	-1,04	-0,72	0,23	1,34	0,1	0,66	0,1	0	CYT	Core
D9Q6P8_CORP1	Bifunctional protein Fold	10168,94	14	0,6771	-0,56	-0,39	0,1	1,19	0,05	0,81	0,05	0	CYT	Core
D9Q6Q3_CORP1	Hemin binding periplasmic protein hmuT	529,87	16	0,8106	-0,30	-0,21	0,18	1,1	0,09	0,9	0,09	0,01	PSE	Core
D9Q6Q7_CORP1	Isocitrate dehydrogenase NADP γ	28508,6	42	0,7483	-0,42	-0,29	0,06	1,14	0,03	0,86	0,03	0	CYT	Core
D9Q6R0_CORP1	Endonuclease Exonuclease phosphatase fa	4144,75	22	0,7047	-0,50	-0,35	0,17	1,18	0,08	0,82	0,08	0	CYT	Core
D9Q6R2_CORP1	Tryptophan tRNA ligase er	13272,39	18	0,8187	-0,29	-0,2	0,09	1,1	0,04	0,9	0,04	0	CYT	Core
D9Q6R3_CORP1	Ribonuclease BN like family a	530,11	8	1,2461	0,32	0,22	0,23	0,89	0,11	1,11	0,11	0,96	MEM	Core
D9Q6R6_CORP1	Putative uncharacterized protein	10723,88	18	0,5488	-0,87	-0,6	0,09	1,29	0,04	0,71	0,04	0	CYT	Core
D9Q6R8_CORP1	Uracil phosphoribosyltransferase	6010,76	9	0,5488	-0,87	-0,6	0,13	1,29	0,06	0,71	0,06	0	CYT	Core
D9Q6S0_CORP1	Phosphoglucomutase phosphomannomutase O	834,15	22	0,7711	-0,38	-0,26	0,23	1,13	0,11	0,87	0,11	0,02	CYT	Core
D9Q6S2_CORP1	Flavoprotein disulfide reductase	16892,25	23	0,6907	-0,53	-0,37	0,06	1,18	0,03	0,82	0,03	0	CYT	Core
D9Q6S3_CORP1	Pyruvate carboxylase erium	3082,51	53	0,6907	-0,53	-0,37	0,09	1,18	0,04	0,82	0,04	0	CYT	Core
D9Q6S6_CORP1	Acyl coenzyme A carboxylase a	30533,84	28	1,6323	0,71	0,49	0,06	0,76	0,03	1,24	0,03	1	CYT	Core
D9Q6S7_CORP1	Sulfurtransferase s	5084,87	22	1,9739	0,98	0,68	0,14	0,67	0,06	1,33	0,06	1	CYT	Core
D9Q6T0_CORP1	Putative uncharacterized protein	2023,9	7	0,6065	-0,72	-0,5	0,24	1,25	0,11	0,75	0,11	0	CYT	Shared
D9Q6T1_CORP1	Maf like protein Cp1002 0482	1351,96	5	0,5016	-1,00	-0,69	0,43	1,33	0,19	0,67	0,19	0	CYT	Core
D9Q6T2_CORP1	Ribokinase b	5644,6	9	0,4966	-1,01	-0,7	0,15	1,34	0,07	0,66	0,07	0	CYT	Core
D9Q6T5_CORP1	Propionyl CoA carboxylase beta chain 1	7525,24	25	1,1163	0,16	0,11	0,1	0,94	0,05	1,06	0,05	0,98	PSE	Core
D9Q6T7_CORP1	Biotin Acetyl CoA carboxylase ligase	1493,49	13	0,6126	-0,71	-0,49	0,22	1,24	0,1	0,76	0,1	0	CYT	Core
D9Q6T9_CORP1	Phosphoribosyl amino imidazole carboxyl	2790,22	18	0,5945	-0,75	-0,52	0,12	1,25	0,06	0,75	0,06	0	CYT	Core

D9Q6U0_CORP1	N5 carboxyaminoimidazole ribonucleotide	3141,09	7	0,827	-0,27	-0,19	0,18	1,09	0,09	0,91	0,09	0,02	CYT	Core
D9Q6U7_CORP1	Putative uncharacterized protein	2844,58	12	0,7483	-0,42	-0,29	0,27	1,14	0,13	0,86	0,13	0,04	CYT	Core
D9Q6U8_CORP1	Transcriptional regulator lytR yn	787,5	19	1,3231	0,40	0,28	0,14	0,86	0,07	1,14	0,07	1	PSE	Core
D9Q6U9_CORP1	dTDP Rha alpha D GlcNAc pyrophosphate p	1542,67	14	1,2214	0,29	0,2	0,22	0,9	0,11	1,1	0,11	0,96	CYT	Core
D9Q6V6_CORP1	Phosphomannomutase ManB er	10957,22	17	0,6313	-0,66	-0,46	0,07	1,23	0,04	0,77	0,04	0	CYT	Core
D9Q6V8_CORP1	Mannose 6 phosphate isomerase manA	3098,09	18	0,6065	-0,72	-0,5	0,13	1,25	0,06	0,75	0,06	0	CYT	Shared
D9Q6W2_CORP1	Adenosylhomocysteinase eri	5036,51	20	0,6771	-0,56	-0,39	0,13	1,19	0,06	0,81	0,06	0	CYT	Core
D9Q6W4_CORP1	DNA binding response regulator mtrA OS	6431,55	8	0,8025	-0,32	-0,22	0,12	1,11	0,06	0,89	0,06	0	CYT	Core
D9Q6W8_CORP1	Ribosomal protein S30AE family protein	47138,34	14	1,391	0,48	0,33	0,08	0,83	0,04	1,17	0,04	1	CYT	Core
D9Q6W9_CORP1	Protein translocase subunit SecA	13277,96	51	0,6637	-0,59	-0,41	0,08	1,2	0,04	0,8	0,04	0	CYT	Shared
D9Q6Z8_CORP1	Lon protease seudot	467,02	11	0,6376	-0,65	-0,45	0,28	1,22	0,13	0,78	0,13	0	SEC	Core
D9Q701_CORP1	UPF0182 protein Cp1002 0552 a	3348,79	37	0,6839	-0,55	-0,38	0,1	1,19	0,05	0,81	0,05	0	PSE	Core
D9Q717_CORP1	Methylmalonyl CoA carboxyltransferase 5	10172,94	23	1,31	0,39	0,27	0,15	0,87	0,07	1,13	0,07	1	CYT	Core
D9Q719_CORP1	Putative uncharacterized protein	17226,19	6	2,1598	1,11	0,77	0,23	0,63	0,1	1,37	0,1	1	CYT	Core
D9Q723_CORP1	Inositol 1 monophosphatase ImpA y	2746,43	11	0,657	-0,61	-0,42	0,16	1,21	0,08	0,79	0,08	0	CYT	Core
D9Q724_CORP1	Peptide chain release factor 2 yn	2091,61	20	0,6005	-0,74	-0,51	0,19	1,25	0,09	0,75	0,09	0	CYT	Shared
D9Q728_CORP1	Cell division ATP binding protein FtsE	12058,7	13	0,7945	-0,33	-0,23	0,16	1,12	0,08	0,88	0,08	0	CYT	Core
D9Q739_CORP1	Putative uncharacterized protein	30799,1	10	0,8694	-0,20	-0,14	0,11	1,07	0,05	0,93	0,05	0,02	MEM	Core
D9Q743_CORP1	Cold shock protein B erium	1489,77	7	0,5712	-0,81	-0,56	0,27	1,27	0,13	0,73	0,13	0	CYT	Core
D9Q749_CORP1	Putative uncharacterized protein	1683,14	13	1,9542	0,97	0,67	0,28	0,68	0,13	1,32	0,13	1	CYT	Core
D9Q752_CORP1	Citrate synthase se	74969,49	22	1,6323	0,71	0,49	0,06	0,76	0,03	1,24	0,03	1	CYT	Core
D9Q757_CORP1	2 5 diketo D gluconic acid reductase A	13545,55	20	0,625	-0,68	-0,47	0,1	1,23	0,05	0,77	0,05	0	CYT	Core
D9Q760_CORP1	Cation acetate symporter ActP yne	4858,05	11	1,1972	0,26	0,18	0,2	0,91	0,1	1,09	0,1	0,95	MEM	Core
D9Q780_CORP1	Thymidylate synthase erium	4708,55	11	0,7189	-0,48	-0,33	0,19	1,16	0,09	0,84	0,09	0	CYT	Core
D9Q781_CORP1	3 phosphoadenosine 5 phosphate phosph	10046,23	12	0,6188	-0,69	-0,48	0,09	1,24	0,04	0,76	0,04	0	CYT	Core
D9Q787_CORP1	Glucose 6 phosphate isomerase yne	16541,96	25	0,8869	-0,17	-0,12	0,09	1,06	0,04	0,94	0,04	0	CYT	Core
D9Q788_CORP1	Succinate semialdehyde dehydrogenase N	3515,83	27	1,5841	0,66	0,46	0,12	0,77	0,06	1,23	0,06	1	CYT	Core
D9Q793_CORP1	Phosphoribosylglycinamide formyltransfe	4504,02	10	1,682	0,75	0,52	0,22	0,75	0,1	1,25	0,1	1	CYT	Shared
D9Q794_CORP1	Bifunctional purine biosynthesis protei	10408,95	21	0,6977	-0,52	-0,36	0,11	1,18	0,05	0,82	0,05	0	CYT	Core
D9Q796_CORP1	Glutamate binding protein GluB yn	3543,34	17	0,6065	-0,72	-0,5	0,13	1,25	0,06	0,75	0,06	0	PSE	Core
D9Q7A2_CORP1	30S ribosomal protein S18	39472,24	4	1,7683	0,82	0,57	0,23	0,72	0,11	1,28	0,11	1	CYT	Core

D9Q7A4_CORP1	50S ribosomal protein L33	35026,86	5	1,2586	0,33	0,23	0,17	0,89	0,08	1,11	0,08	1	CYT	Shared
D9Q7A5_CORP1	50S ribosomal protein L28	23240,6	8	1,1275	0,17	0,12	0,13	0,94	0,07	1,06	0,07	0,96	CYT	Shared
D9Q7A6_CORP1	50S ribosomal protein L31	84419,1	4	0,7634	-0,39	-0,27	0,1	1,14	0,05	0,86	0,05	0	CYT	Core
D9Q7A7_CORP1	50S ribosomal protein L32	69177,47	3	0,8694	-0,20	-0,14	0,13	1,07	0,07	0,93	0,07	0,04	CYT	Core
D9Q7A8_CORP1	Two component system response regulator	36652,11	13	1,6989	0,76	0,53	0,1	0,74	0,05	1,26	0,05	1	CYT	Core
D9Q7A9_CORP1	Two component system sensor kinase prot	839,56	19	1,6161	0,69	0,48	0,27	0,77	0,13	1,23	0,13	1	PSE	Core
D9Q7B0_CORP1	Serine protease seu	3527,23	17	0,436	-1,20	-0,83	0,17	1,39	0,07	0,61	0,07	0	CYT	Core
D9Q7B3_CORP1	Large conductance mechanosensitive chan	24324,5	5	1,1618	0,22	0,15	0,13	0,92	0,06	1,08	0,06	1	MEM	Core
D9Q7B6_CORP1	UTP glucose 1 phosphate uridylyltransf	7356,45	13	0,4916	-1,02	-0,71	0,16	1,34	0,07	0,66	0,07	0	CYT	Core
D9Q7C5_CORP1	Putative uncharacterized protein	628,32	8	0,5066	-0,98	-0,68	0,38	1,32	0,16	0,68	0,16	0	MEM	Core
D9Q7C7_CORP1	Methionine tRNA ligase er	7626,54	27	0,5945	-0,75	-0,52	0,1	1,25	0,05	0,75	0,05	0	CYT	Core
D9Q7C9_CORP1	Resuscitation promoting factor RpfB OS	386,07	12	0,6188	-0,69	-0,48	0,46	1,23	0,21	0,77	0,21	0,04	SEC	Core
D9Q7D0_CORP1	Ribosomal RNA small subunit methyltrans	1326,57	13	1,8965	0,92	0,64	0,27	0,69	0,12	1,31	0,12	1	CYT	Shared
D9Q7D2_CORP1	ABC transporter ATP binding protein OS	576,81	21	1,284	0,36	0,25	0,28	0,88	0,14	1,12	0,14	0,95	CYT	Core
D9Q7D3_CORP1	Antibiotic biosynthesis monooxygenase O	12505,42	8	0,4868	-1,04	-0,72	0,47	1,34	0,2	0,66	0,2	0	CYT	Core
D9Q7D4_CORP1	Transcriptional regulatory protein PvdS	4890,75	17	0,657	-0,61	-0,42	0,14	1,21	0,07	0,79	0,07	0	CYT	Core
D9Q7D6_CORP1	Enoyl CoA hydratase erium	564,37	15	0,7558	-0,40	-0,28	0,29	1,14	0,14	0,86	0,14	0,05	CYT	Shared
D9Q7D7_CORP1	Putative uncharacterized protein	1218,44	15	0,7945	-0,33	-0,23	0,2	1,11	0,1	0,89	0,1	0,02	CYT	Core
D9Q7D8_CORP1	Glyceraldehyde 3 phosphate dehydrogenas	16713,74	20	1,6487	0,72	0,5	0,13	0,76	0,06	1,24	0,06	1	CYT	Core
D9Q7E0_CORP1	Proline iminopeptidase eri	9292,55	20	0,7047	-0,50	-0,35	0,12	1,17	0,06	0,83	0,06	0	CYT	Core
D9Q7E1_CORP1	Peptide chain release factor 3 yn	4085,95	26	1,682	0,75	0,52	0,21	0,75	0,1	1,25	0,1	1	CYT	Core
D9Q7E4_CORP1	Peptidyl tRNA hydrolase er	2310,46	11	0,7945	-0,33	-0,23	0,22	1,11	0,11	0,89	0,11	0,04	CYT	Core
D9Q7E7_CORP1	Peptidyl tRNA hydrolase er	2094,07	9	0,4449	-1,17	-0,81	0,33	1,38	0,14	0,62	0,14	0	CYT	Core
D9Q7E8_CORP1	50S ribosomal protein L25	13498,22	8	1,3364	0,42	0,29	0,13	0,86	0,06	1,14	0,06	1	CYT	Core
D9Q7E9_CORP1	Pullulanase	973,01	23	0,7118	-0,49	-0,34	0,15	1,17	0,07	0,83	0,07	0	CYT	Shared
D9Q7F0_CORP1	Ribose phosphate pyrophosphokinase	27819,05	16	0,7558	-0,40	-0,28	0,11	1,14	0,05	0,86	0,05	0	CYT	Core
D9Q7F1_CORP1	Bifunctional protein GlmU	1969,37	25	0,6313	-0,66	-0,46	0,12	1,23	0,06	0,77	0,06	0	CYT	Core
D9Q7F5_CORP1	TetR family transcriptional regulator O	813,86	8	0,6313	-0,66	-0,46	0,27	1,22	0,13	0,78	0,13	0	CYT	Core
D9Q7F9_CORP1	LpqU family protein erium	467,51	10	0,657	-0,61	-0,42	0,33	1,21	0,16	0,79	0,16	0,01	SEC	Core
D9Q7G0_CORP1	Enolase berc	108928,9	22	1,522	0,61	0,42	0,06	0,79	0,03	1,21	0,03	1	CYT	Core
D9Q7G3_CORP1	Ppx GppA phosphatase family a	713,3	12	0,7483	-0,42	-0,29	0,23	1,15	0,11	0,85	0,11	0,02	CYT	Core

D9Q7G7_CORP1	Transcription elongation factor GreA OS	38744,29	12	0,7408	-0,43	-0,3	0,1	1,15	0,05	0,85	0,05	0	CYT	Core
D9Q7G9_CORP1	Mycothiol conjugate amidase Mcay	1322,34	15	0,7945	-0,33	-0,23	0,16	1,11	0,08	0,89	0,08	0	CYT	Core
D9Q7H4_CORP1	Serine hydroxymethyltransferase y	51204,91	25	0,6126	-0,71	-0,49	0,05	1,24	0,02	0,76	0,02	0	CYT	Core
D9Q7H7_CORP1	Putative uncharacterized protein	1105,9	6	1,7116	0,78	0,54	0,24	0,74	0,11	1,26	0,11	1	CYT	Core
D9Q7I0_CORP1	Putative uncharacterized protein	3523,4	8	0,4724	-1,08	-0,75	0,2	1,36	0,09	0,64	0,09	0	PSE	Shared
D9Q7I1_CORP1	Phosphinothricin acetyltransferase YwnH	3798,2	11	0,7118	-0,49	-0,34	0,15	1,17	0,07	0,83	0,07	0	CYT	Core
D9Q7I4_CORP1	Fumarate hydratase class II a	42646,02	27	0,8694	-0,20	-0,14	0,06	1,07	0,03	0,93	0,03	0	CYT	Core
D9Q7I5_CORP1	Fructose 1,6 bisphosphatase a	8626,74	15	0,7408	-0,43	-0,3	0,09	1,15	0,04	0,85	0,04	0	CYT	Core
D9Q7I6_CORP1	Putative uncharacterized protein	2084,64	11	1,5373	0,62	0,43	0,39	0,79	0,18	1,21	0,18	0,97	MEM	Core
D9Q7I8_CORP1	4 hydroxy 3 methylbut 2 enyl diphosphat	3383,83	8	0,5886	-0,76	-0,53	0,18	1,26	0,09	0,74	0,09	0	CYT	Core
D9Q7J1_CORP1	GTP binding protein YchF e	13449,82	22	0,5827	-0,78	-0,54	0,08	1,26	0,04	0,74	0,04	0	CYT	Core
D9Q7K5_CORP1	Oligopeptide binding protein oppA	40589,02	37	1,391	0,48	0,33	0,06	0,84	0,03	1,16	0,03	1	PSE	Core
D9Q7L2_CORP1	GTP binding protein TypA BipA yne	4898,74	28	0,5945	-0,75	-0,52	0,06	1,25	0,03	0,75	0,03	0	CYT	Core
D9Q7L7_CORP1	N succinyl diaminopimelate aminotransfer	8892,76	16	0,6771	-0,56	-0,39	0,19	1,19	0,09	0,81	0,09	0	CYT	Core
D9Q7M1_CORP1	2,3,4,5 tetrahydropyridine 2,6 dicarbox	19268,63	15	0,6977	-0,52	-0,36	0,09	1,18	0,05	0,82	0,05	0	CYT	Core
D9Q7M4_CORP1	Succinyl diaminopimelate desuccinylase	3122,34	10	0,6839	-0,55	-0,38	0,21	1,19	0,1	0,81	0,1	0	CYT	Core
D9Q7M5_CORP1	Lysine decarboxylase erium	3593,51	12	0,6637	-0,59	-0,41	0,1	1,2	0,05	0,8	0,05	0	CYT	Core
D9Q7M6_CORP1	Dihydropteroate synthase e	389,33	18	0,5599	-0,84	-0,58	0,26	1,28	0,12	0,72	0,12	0	CYT	Core
D9Q7M9_CORP1	Putative uncharacterized protein	119011,8	4	0,5769	-0,79	-0,55	0,18	1,27	0,09	0,73	0,09	0	CYT	Core
D9Q7N0_CORP1	Ribosomal RNA methyltransferase y	6525,35	13	1,8776	0,91	0,63	0,17	0,7	0,08	1,3	0,08	1	CYT	Core
D9Q7N1_CORP1	Sucrose 6 phosphate hydrolase yne	7319,03	23	0,6505	-0,62	-0,43	0,1	1,21	0,05	0,79	0,05	0	CYT	Core
D9Q7N2_CORP1	Alpha acetolactate decarboxylase	1991,57	10	0,6505	-0,62	-0,43	0,18	1,21	0,08	0,79	0,08	0	CYT	Core
D9Q7N3_CORP1	Glycosyl transferase erium	2735,9	13	0,7558	-0,40	-0,28	0,26	1,14	0,13	0,86	0,13	0,04	CYT	Core
D9Q7N5_CORP1	O methyltransferase erium	2831,89	10	0,6126	-0,71	-0,49	0,18	1,24	0,08	0,76	0,08	0	CYT	Core
D9Q7N9_CORP1	Protein mrp	2230,48	12	1,2214	0,29	0,2	0,19	0,9	0,09	1,1	0,09	0,97	CYT	Core
D9Q7P1_CORP1	Magnesium transporter mgtE ac	1849,76	22	0,8025	-0,32	-0,22	0,14	1,11	0,07	0,89	0,07	0	CYT	Core
D9Q7P3_CORP1	2 oxoglutarate dehydrogenase E1 compone	19180,55	66	0,7711	-0,38	-0,26	0,05	1,13	0,03	0,87	0,03	0	CYT	Core
D9Q7P5_CORP1	Putative uncharacterized protein	6924,43	11	1,2092	0,27	0,19	0,21	0,91	0,1	1,09	0,1	0,97	CYT	Core
D9Q7P9_CORP1	Putative uncharacterized protein	7518,64	6	0,5543	-0,85	-0,59	0,19	1,28	0,09	0,72	0,09	0	CYT	Core
D9Q7Q4_CORP1	DEAD box helicase s	5478,66	26	0,6313	-0,66	-0,46	0,1	1,23	0,05	0,77	0,05	0	CYT	Core
D9Q7Q7_CORP1	Putative uncharacterized protein	928,51	4	0,5599	-0,84	-0,58	0,25	1,28	0,12	0,72	0,12	0	MEM	Core

D9Q7R8_CORP1	Putative uncharacterized protein	17774,3	12	0,6771	-0,56	-0,39	0,11	1,19	0,05	0,81	0,05	0	CYT	Core
D9Q7S0_CORP1	Lactate utilization protein A yne	17160,29	16	0,6005	-0,74	-0,51	0,1	1,25	0,05	0,75	0,05	0	CYT	Core
D9Q7S2_CORP1	Arginine tRNA ligase eriu	9831,17	27	1,5068	0,59	0,41	0,16	0,8	0,07	1,2	0,07	1	CYT	Core
D9Q7S6_CORP1	Putative uncharacterized protein	679,16	13	0,7118	-0,49	-0,34	0,29	1,17	0,14	0,83	0,14	0	CYT	Core
D9Q7S8_CORP1	Transcription termination factor Rho OS	7181,64	27	0,5945	-0,75	-0,52	0,08	1,25	0,04	0,75	0,04	0	CYT	Shared
D9Q7S9_CORP1	Peptide chain release factor 1 yn	1425,12	18	0,5543	-0,85	-0,59	0,13	1,29	0,06	0,71	0,06	0	CYT	Core
D9Q7T1_CORP1	tRNA threonylcarbamoyladenosine biosynt	3882,38	9	0,6376	-0,65	-0,45	0,27	1,22	0,13	0,78	0,13	0,01	CYT	Core
D9Q7T4_CORP1	ATP synthase subunit a eri	8370,34	3	1,2586	0,33	0,23	0,19	0,89	0,09	1,11	0,09	0,97	MEM	Core
D9Q7T6_CORP1	ATP synthase subunit b eri	11332,36	11	1,5841	0,66	0,46	0,13	0,77	0,06	1,23	0,06	1	MEM	Shared
D9Q7T7_CORP1	ATP synthase subunit delta ac	44543,4	21	0,8025	-0,32	-0,22	0,08	1,11	0,04	0,89	0,04	0	CYT	Core
D9Q7T8_CORP1	ATP synthase subunit alpha ac	50757,36	27	1,5683	0,65	0,45	0,07	0,78	0,03	1,22	0,03	1	CYT	Core
D9Q7T9_CORP1	ATP synthase gamma chain e	20432,64	18	1,6	0,68	0,47	0,14	0,77	0,06	1,23	0,06	1	CYT	Core
D9Q7U0_CORP1	ATP synthase subunit beta	58504,8	30	1,4918	0,58	0,4	0,05	0,8	0,02	1,2	0,02	1	CYT	Core
D9Q7U3_CORP1	Endonuclease NucS s	2434,09	14	0,6771	-0,56	-0,39	0,19	1,19	0,09	0,81	0,09	0	CYT	Core
D9Q7U4_CORP1	Methylmalonyl CoA epimerase a	671,04	7	0,4724	-1,08	-0,75	0,33	1,36	0,14	0,64	0,14	0	CYT	Core
D9Q7U9_CORP1	Ferric enterobactin transport ATP bindi	4320,85	13	0,6703	-0,58	-0,4	0,17	1,2	0,08	0,8	0,08	0	CYT	Core
D9Q7V1_CORP1	Putative uncharacterized protein	370,87	20	0,5827	-0,78	-0,54	0,2	1,26	0,09	0,74	0,09	0	CYT	Core
D9Q7V2_CORP1	Electron transfer flavo protein subunit	15215,76	13	0,6065	-0,72	-0,5	0,13	1,24	0,06	0,76	0,06	0	CYT	Core
D9Q7V3_CORP1	Electron transfer flavo protein subunit	17536,7	9	0,5769	-0,79	-0,55	0,14	1,27	0,06	0,73	0,06	0	CYT	Shared
D9Q7V4_CORP1	Cysteine desulfurase erium	1480,88	12	0,7334	-0,45	-0,31	0,2	1,15	0,1	0,85	0,1	0	CYT	Core
D9Q7V6_CORP1	tRNA specific 2 thiouridylase MnmA	905,37	15	0,4771	-1,07	-0,74	0,24	1,35	0,1	0,65	0,1	0	CYT	Core
D9Q7V7_CORP1	Putative uncharacterized protein	1535,7	18	0,5599	-0,84	-0,58	0,2	1,28	0,09	0,72	0,09	0	CYT	Shared
D9Q7V8_CORP1	DNA polymerase III subunit epsilon	1523,62	14	0,6126	-0,71	-0,49	0,23	1,24	0,11	0,76	0,11	0	CYT	Core
D9Q7V9_CORP1	DNA ligase b	1599,87	30	0,625	-0,68	-0,47	0,14	1,23	0,07	0,77	0,07	0	CYT	Core
D9Q7W0_CORP1	Putative uncharacterized protein	11030,96	6	0,5655	-0,82	-0,57	0,13	1,28	0,06	0,72	0,06	0	CYT	Core
D9Q7W2_CORP1	Glutamyl tRNA Gln amidotransferase sub	13475,3	30	0,5945	-0,75	-0,52	0,1	1,25	0,05	0,75	0,05	0	CYT	Core
D9Q7W3_CORP1	Mycothiol acetyltransferase a	2849,23	6	0,6505	-0,62	-0,43	0,38	1,21	0,18	0,79	0,18	0	CYT	Core
D9Q7W9_CORP1	Iron 3 hydroxamate binding protein fh	5235,71	19	1,1388	0,19	0,13	0,13	0,94	0,06	1,06	0,06	0,97	PSE	Core
D9Q7X1_CORP1	Aspartyl glutamyl tRNA Asn Gln amidotr	9318,35	26	0,657	-0,61	-0,42	0,08	1,21	0,04	0,79	0,04	0	CYT	Core
D9Q7X2_CORP1	Aldo keto reductase erium	2035,98	17	0,7189	-0,48	-0,33	0,19	1,16	0,09	0,84	0,09	0	CYT	Core
D9Q7X6_CORP1	Putative uncharacterized protein	6516,52	12	0,8781	-0,19	-0,13	0,14	1,06	0,07	0,94	0,07	0,05	MEM	Core

D9Q7X8_CORP1	Low molecular weight protein antigen 6	1360,27	9	1,4477	0,53	0,37	0,3	0,82	0,15	1,18	0,15	0,99	0	MEM	Core
D9Q7Y1_CORP1	Ketol acid reductoisomerase a	2043,98	16	0,625	-0,68	-0,47	0,15	1,23	0,07	0,77	0,07	0	0	CYT	Core
D9Q7Y5_CORP1	D 3 phosphoglycerate dehydrogenase	27949,83	27	0,7047	-0,50	-0,35	0,06	1,18	0,03	0,82	0,03	0	0	CYT	Core
D9Q7Z0_CORP1	2 hydroxyhepta 2 4 diene 1 7 dioate iso	3042,79	10	0,625	-0,68	-0,47	0,16	1,23	0,07	0,77	0,07	0	0	CYT	Core
D9Q7Z1_CORP1	Menaquinone specific isochorismate synt	787,97	16	0,7261	-0,46	-0,32	0,21	1,16	0,1	0,84	0,1	0	0	CYT	Shared
D9Q7Z2_CORP1	Glutamate tRNA ligase eri	9393,34	29	0,644	-0,63	-0,44	0,08	1,21	0,04	0,79	0,04	0	0	CYT	Core
D9Q801_CORP1	D alanine D alanine ligase a	10455,24	16	0,6771	-0,56	-0,39	0,11	1,19	0,05	0,81	0,05	0	0	CYT	Core
D9Q802_CORP1	Putative uncharacterized protein	858,5	14	1,9739	0,98	0,68	0,33	0,67	0,14	1,33	0,14	1	1	SEC	Core
D9Q808_CORP1	Ribosomal RNA small subunit methyltrans	534,61	8	2,1383	1,10	0,76	0,37	0,64	0,17	1,36	0,17	1	1	CYT	Core
D9Q813_CORP1	Serine threonine protein kinase PknD OS	605,97	7	0,5117	-0,97	-0,67	0,43	1,32	0,19	0,68	0,19	0,01	0	PSE	Shared
D9Q816_CORP1	DNA polymerase seu9	3369,43	38	0,6907	-0,53	-0,37	0,1	1,18	0,05	0,82	0,05	0	0	CYT	Core
D9Q818_CORP1	30S ribosomal protein S1 e	58315,71	36	0,6376	-0,65	-0,45	0,03	1,22	0,02	0,78	0,02	0	0	CYT	Core
D9Q820_CORP1	Phosphotransferase system II Component	49710	19	1,284	0,36	0,25	0,09	0,88	0,04	1,12	0,04	1	1	PSE	Shared
D9Q824_CORP1	Stress related protein eri	11795,76	12	0,7945	-0,33	-0,23	0,18	1,12	0,09	0,88	0,09	0	0	CYT	Core
D9Q826_CORP1	DoxX family protein erium	41704,48	12	0,8781	-0,19	-0,13	0,09	1,07	0,04	0,93	0,04	0	0	CYT	Core
D9Q828_CORP1	UvrABC system protein A er	1010,23	49	1,1853	0,25	0,17	0,13	0,92	0,06	1,08	0,06	0,99	0	CYT	Core
D9Q829_CORP1	Translation initiation factor IF 3	2709,33	8	0,7189	-0,48	-0,33	0,2	1,16	0,09	0,84	0,09	0	0	CYT	Core
D9Q831_CORP1	50S ribosomal protein L20	22871,22	9	1,477	0,56	0,39	0,1	0,81	0,05	1,19	0,05	1	1	CYT	Core
D9Q832_CORP1	Putative uncharacterized protein	13481,49	9	1,4333	0,52	0,36	0,18	0,82	0,09	1,18	0,09	1	1	PSE	Core
D9Q834_CORP1	Phenylalanine tRNA ligase alpha subuni	2175,21	15	0,7189	-0,48	-0,33	0,21	1,16	0,1	0,84	0,1	0	0	CYT	Core
D9Q835_CORP1	Phenylalanine tRNA ligase beta subunit	6665,97	36	0,6637	-0,59	-0,41	0,07	1,2	0,03	0,8	0,03	0	0	CYT	Core
D9Q841_CORP1	Arginine repressor	2244,2	8	0,4819	-1,05	-0,73	0,22	1,35	0,1	0,65	0,1	0	0	CYT	Core
D9Q842_CORP1	Argininosuccinate synthase ac	13335,77	25	0,7261	-0,46	-0,32	0,1	1,16	0,05	0,84	0,05	0	0	CYT	Core
D9Q845_CORP1	Tyrosine tRNA ligase eriu	14531,34	18	0,625	-0,68	-0,47	0,12	1,23	0,06	0,77	0,06	0	0	CYT	Core
D9Q846_CORP1	Tetratricopeptide TPR2 eri	8902,76	18	0,7711	-0,38	-0,26	0,19	1,13	0,09	0,87	0,09	0,01	0	CYT	Shared
D9Q847_CORP1	Haloacid dehalogenase HAD superfamily	3803,45	15	0,6637	-0,59	-0,41	0,14	1,2	0,07	0,8	0,07	0	0	CYT	Core
D9Q851_CORP1	DNA repair protein recN er	523,05	25	1,9348	0,95	0,66	0,17	0,68	0,07	1,32	0,07	1	1	CYT	Core
D9Q852_CORP1	Thiamin pyrophosphokinase catalytic do	4805,34	11	1,8965	0,92	0,64	0,17	0,69	0,08	1,31	0,08	1	1	PSE	Core
D9Q853_CORP1	Putative uncharacterized protein	3477,71	17	0,6977	-0,52	-0,36	0,19	1,18	0,09	0,82	0,09	0	0	PSE	Core
D9Q854_CORP1	ADP ribose pyrophosphatase ADPRase OS	472,62	8	0,5712	-0,81	-0,56	0,41	1,27	0,19	0,73	0,19	0,01	0	CYT	Core
D9Q856_CORP1	Chromosome partitioning ATPase protein	1311,45	10	1,2586	0,33	0,23	0,22	0,89	0,11	1,11	0,11	1	1	CYT	Core

D9Q861_CORP1	Adenosylmethionine 8 amino 7 oxononanoa	436,08	13	0,7047	-0,50	-0,35	0,3	1,17	0,15	0,83	0,15	0,01	CYT	Core
D9Q862_CORP1	ATP dependent dethiobiotin synthetase B	2236,46	8	0,4493	-1,15	-0,8	0,2	1,38	0,08	0,62	0,08	0	CYT	Core
D9Q864_CORP1	Pseudouridine synthase eri	2571,07	18	1,1972	0,26	0,18	0,17	0,91	0,08	1,09	0,08	0,96	CYT	Core
D9Q866_CORP1	GTPase Der b	2730,19	29	0,7334	-0,45	-0,31	0,17	1,15	0,08	0,85	0,08	0	CYT	Core
D9Q871_CORP1	Iron ABC transporter substrate binding	1977,02	17	1,477	0,56	0,39	0,27	0,81	0,13	1,19	0,13	0,98	PSE	Core
D9Q883_CORP1	Hydrolase alpha beta superfamily	2557,75	16	0,6703	-0,58	-0,4	0,18	1,2	0,08	0,8	0,08	0	CYT	Core
D9Q886_CORP1	Oxoglutarate dehydrogenase inhibitor OS	42598,09	11	0,6771	-0,56	-0,39	0,13	1,19	0,06	0,81	0,06	0	CYT	Core
D9Q887_CORP1	MerR family transcriptional regulator O	896,1	10	0,6703	-0,58	-0,4	0,34	1,2	0,16	0,8	0,16	0	CYT	Core
D9Q890_CORP1	Putative uncharacterized protein	4284,56	17	0,7189	-0,48	-0,33	0,1	1,16	0,05	0,84	0,05	0	SEC	Core
D9Q895_CORP1	6 phosphogluconate dehydrogenase decar	21563,62	21	0,6505	-0,62	-0,43	0,1	1,21	0,05	0,79	0,05	0	CYT	Core
D9Q896_CORP1	Thioesterase seudot	44507,53	8	0,8187	-0,29	-0,2	0,18	1,1	0,09	0,9	0,09	0,03	CYT	Core
D9Q899_CORP1	NADH dehydrogenase	15916,17	22	1,4623	0,55	0,38	0,06	0,81	0,03	1,19	0,03	1	PSE	Core
D9Q8A3_CORP1	Protein ycel seudot	1175,13	9	1,6487	0,72	0,5	0,25	0,76	0,12	1,24	0,12	1	SEC	Core
D9Q8A5_CORP1	Putative uncharacterized protein	24085,25	9	0,6376	-0,65	-0,45	0,17	1,22	0,08	0,78	0,08	0	CYT	Core
D9Q8A6_CORP1	Polypropenol phosphate mannose synthase d	6440,15	16	0,6313	-0,66	-0,46	0,12	1,23	0,06	0,77	0,06	0	CYT	Core
D9Q8B0_CORP1	Precorrin 3B synthase eriu	3910,99	16	0,6839	-0,55	-0,38	0,13	1,19	0,06	0,81	0,06	0	CYT	Core
D9Q8B1_CORP1	Precorrin 8X methyl mutase ac	18309,5	12	1,1972	0,26	0,18	0,17	0,91	0,08	1,09	0,08	0,97	CYT	Core
D9Q8B3_CORP1	Precorrin 6A reductase eri	4365,72	12	0,8106	-0,30	-0,21	0,18	1,1	0,09	0,9	0,09	0,02	CYT	Core
D9Q8B7_CORP1	Dipeptidase pepE se	2304,02	17	1,6161	0,69	0,48	0,31	0,76	0,15	1,24	0,15	1	CYT	Core
D9Q8C3_CORP1	Pup protein ligase erium	751,44	21	1,391	0,48	0,33	0,22	0,84	0,11	1,16	0,11	1	CYT	Core
D9Q8C7_CORP1	SAM dependent methyltransferase involve	3413,62	15	0,625	-0,68	-0,47	0,13	1,23	0,06	0,77	0,06	0	CYT	Core
D9Q8C8_CORP1	M18 family aminopeptidase	5595,5	17	0,8437	-0,25	-0,17	0,16	1,08	0,08	0,92	0,08	0,03	CYT	Core
D9Q8D1_CORP1	Formate tetrahydrofolate ligase	7887,69	23	0,657	-0,61	-0,42	0,1	1,21	0,05	0,79	0,05	0	CYT	Core
D9Q8D3_CORP1	Anaerobic C4 dicarboxylate transporter	1337,88	7	0,7711	-0,38	-0,26	0,24	1,13	0,12	0,87	0,12	0,03	MEM	Shared
D9Q8D4_CORP1	ATP phosphoribosyltransferase yne	3869,42	17	1,31	0,39	0,27	0,21	0,87	0,1	1,13	0,1	1	CYT	Core
D9Q8D9_CORP1	L cysteine 1D myo inositol 2 amino 2 de	2452,75	16	0,5769	-0,79	-0,55	0,17	1,27	0,08	0,73	0,08	0	CYT	Shared
D9Q8E3_CORP1	Dihydroorotate dehydrogenase quinone	3379,43	14	0,6313	-0,66	-0,46	0,13	1,23	0,06	0,77	0,06	0	CYT	Shared
D9Q8E6_CORP1	Phosphatidylethanolamine binding protei	5928,27	7	0,5827	-0,78	-0,54	0,23	1,26	0,11	0,74	0,11	0	CYT	Shared
D9Q8E8_CORP1	Dihydroxyacetone kinase family protein	10944,55	15	0,8781	-0,19	-0,13	0,16	1,06	0,08	0,94	0,08	0,04	PSE	Core
D9Q8E9_CORP1	Dihydroxyacetone kinase subununit	2233,25	7	0,827	-0,27	-0,19	0,21	1,09	0,1	0,91	0,1	0,05	CYT	Core
D9Q8F3_CORP1	Arginine ornithine transport system ATP	1479,63	16	1,6989	0,76	0,53	0,21	0,74	0,1	1,26	0,1	1	CYT	Core

D9Q8F4_CORP1	Methylmalonyl CoA mutase large subunit	5379,42	27	1,4918	0,58	0,4	0,11	0,8	0,05	1,2	0,05	1	CYT	Core
D9Q8F5_CORP1	Methylmalonyl CoA mutase small subunit	13427,82	24	1,1388	0,19	0,13	0,1	0,94	0,05	1,06	0,05	0,99	CYT	Core
D9Q8G2_CORP1	Ferrochelatase seed	739,51	14	0,7945	-0,33	-0,23	0,23	1,11	0,11	0,89	0,11	0,03	CYT	Core
D9Q8G5_CORP1	Aconitate hydratase erium	24922,95	42	0,7558	-0,40	-0,28	0,05	1,14	0,02	0,86	0,02	0	CYT	Shared
D9Q8G6_CORP1	HTH type transcriptional repressor AcnR	1202,19	13	2,1117	1,08	0,75	0,29	0,65	0,13	1,35	0,13	1	CYT	Core
D9Q8G7_CORP1	Glutamine amidotransferase class I	1662,95	8	0,6637	-0,59	-0,41	0,29	1,2	0,14	0,8	0,14	0	CYT	Core
D9Q8G8_CORP1	UPF0237 protein Cp1002 1078 a	21744,25	3	0,6771	-0,56	-0,39	0,35	1,19	0,16	0,81	0,16	0,01	CYT	Core
D9Q8G9_CORP1	UPF0210 protein Cp1002 1079 a	5707,24	20	1,1853	0,25	0,17	0,16	0,92	0,08	1,08	0,08	0,98	CYT	Core
D9Q8H7_CORP1	Cysteine desulfurase erium	9689,63	20	0,6977	-0,52	-0,36	0,13	1,18	0,06	0,82	0,06	0	CYT	Core
D9Q8H8_CORP1	FeS assembly ATPase SufC e	17070,38	12	0,6839	-0,55	-0,38	0,12	1,19	0,06	0,81	0,06	0	CYT	Core
D9Q8H9_CORP1	FeS cluster assembly protein SufD	27431,53	21	1,3231	0,40	0,28	0,1	0,86	0,05	1,14	0,05	1	CYT	Core
D9Q8I0_CORP1	FeS cluster assembly protein sufB	10542,63	26	0,7189	-0,48	-0,33	0,28	1,16	0,13	0,84	0,13	0,02	CYT	Core
D9Q8I7_CORP1	Transketolase seudo	6636,6	36	0,7261	-0,46	-0,32	0,07	1,16	0,04	0,84	0,04	0	CYT	Core
D9Q8I9_CORP1	Glucose 6 phosphate 1 dehydrogenase OS	4151,23	24	0,625	-0,68	-0,47	0,1	1,23	0,05	0,77	0,05	0	CYT	Core
D9Q8J0_CORP1	OxPP cycle protein opcA er	7522,19	18	0,6907	-0,53	-0,37	0,1	1,18	0,05	0,82	0,05	0	CYT	Core
D9Q8J1_CORP1	6 phosphogluconolactonase	5515	14	0,4916	-1,02	-0,71	0,13	1,34	0,06	0,66	0,06	0	CYT	Core
D9Q8J3_CORP1	Phosphoenolpyruvate carboxylase y	12781,1	49	1,2092	0,27	0,19	0,06	0,91	0,03	1,09	0,03	1	CYT	Core
D9Q8J4_CORP1	Triosephosphate isomerase	69536,66	18	0,8958	-0,16	-0,11	0,06	1,05	0,03	0,95	0,03	0	CYT	Core
D9Q8J5_CORP1	Phosphoglycerate kinase er	36185,14	27	1,284	0,36	0,25	0,13	0,88	0,06	1,12	0,06	1	CYT	Core
D9Q8J6_CORP1	Glyceraldehyde 3 phosphate dehydrogenas	80573,51	23	1,0725	0,10	0,07	0,06	0,96	0,03	1,04	0,03	0,98	CYT	Core
D9Q8J7_CORP1	Putative sporulation transcription regu	1183,86	18	0,7558	-0,40	-0,28	0,31	1,14	0,15	0,86	0,15	0,05	CYT	Core
D9Q8J9_CORP1	UPF0042 nucleotide binding protein Cp10	11452,26	22	1,2092	0,27	0,19	0,17	0,9	0,08	1,1	0,08	1	CYT	Core
D9Q8K2_CORP1	6 7 dimethyl 8 ribityllumazine synthase	4145,71	8	0,4868	-1,04	-0,72	0,22	1,34	0,1	0,66	0,1	0	CYT	Core
D9Q8K4_CORP1	Riboflavin synthase alpha chain y	930,73	6	0,5712	-0,81	-0,56	0,31	1,27	0,14	0,73	0,14	0	CYT	Core
D9Q8K6_CORP1	Ribulose phosphate 3 epimerase yn	1139,6	7	0,7558	-0,40	-0,28	0,26	1,14	0,13	0,86	0,13	0,01	CYT	Core
D9Q8K7_CORP1	Ribosomal RNA small subunit methyltrans	3936,59	21	1,1052	0,14	0,1	0,1	0,95	0,05	1,05	0,05	0,95	CYT	Core
D9Q8K9_CORP1	Peptide deformylase erium	1395,17	7	1,804	0,85	0,59	0,51	0,72	0,22	1,28	0,22	1	CYT	Core
D9Q8L1_CORP1	Sadenosylmethionine synthase yne	1988,09	20	1,1853	0,25	0,17	0,19	0,91	0,09	1,09	0,09	0,96	CYT	Core
D9Q8L3_CORP1	DNA directed RNA polymerase subunit ome	10132,82	5	0,4584	-1,13	-0,78	0,25	1,37	0,11	0,63	0,11	0	CYT	Core
D9Q8L8_CORP1	Carbamoyl phosphate synthase large chai	4964,02	46	0,8437	-0,25	-0,17	0,11	1,09	0,05	0,91	0,05	0	CYT	Core
D9Q8L9_CORP1	Carbamoyl phosphate synthase small chai	5554,07	15	0,7788	-0,36	-0,25	0,17	1,12	0,08	0,88	0,08	0	CYT	Core

D9Q8M0_CORP1	Dihydroorotate seud	1839,16	25	0,657	-0,61	-0,42	0,12	1,21	0,06	0,79	0,06	0	CYT	Core
D9Q8M1_CORP1	Aspartate carbamoyltransferase yn	371,33	18	0,7261	-0,46	-0,32	0,31	1,16	0,15	0,84	0,15	0,03	CYT	Core
D9Q8M2_CORP1	Bifunctional protein PyrR	1082,54	12	0,5945	-0,75	-0,52	0,28	1,25	0,13	0,75	0,13	0	CYT	Core
D9Q8M6_CORP1	Elongation factor P erium	30607,41	10	0,8025	-0,32	-0,22	0,09	1,11	0,04	0,89	0,04	0	CYT	Core
D9Q8M7_CORP1	Uncharacterized peptidase yqhT Metallo	27446,37	17	1,5841	0,66	0,46	0,12	0,77	0,06	1,23	0,06	1	CYT	Shared
D9Q8N1_CORP1	Chorismate synthase erium	2903,82	21	1,2712	0,35	0,24	0,17	0,88	0,09	1,12	0,09	1	CYT	Core
D9Q8N8_CORP1	Phosphotransferase enzyme family protei	1499,05	18	1,4918	0,58	0,4	0,17	0,8	0,08	1,2	0,08	1	CYT	Core
D9Q8N9_CORP1	Aspartate tRNA ligase eri	8875	29	0,6977	-0,52	-0,36	0,1	1,18	0,05	0,82	0,05	0	CYT	Core
D9Q8P0_CORP1	Zinc metallopeptidase eriu	2123,21	13	0,6126	-0,71	-0,49	0,15	1,24	0,07	0,76	0,07	0	PSE	Shared
D9Q8P6_CORP1	L serine dehydratase erium	787,73	14	0,7788	-0,36	-0,25	0,19	1,12	0,09	0,88	0,09	0	CYT	Core
D9Q8Q0_CORP1	Histidine tRNA ligase eri	4144,87	29	0,8437	-0,25	-0,17	0,12	1,08	0,06	0,92	0,06	0,01	CYT	Core
D9Q8Q2_CORP1	Probable thiol peroxidase	89849,24	9	0,6977	-0,52	-0,36	0,06	1,18	0,03	0,82	0,03	0	CYT	Core
D9Q8Q3_CORP1	Peptidyl prolyl cis trans isomerase B O	6363,67	11	0,7558	-0,40	-0,28	0,14	1,14	0,07	0,86	0,07	0	PSE	Core
D9Q8Q9_CORP1	Protein translocase subunit SecD	1521,09	16	1,6161	0,69	0,48	0,18	0,76	0,09	1,24	0,09	1	PSE	Shared
D9Q8R4_CORP1	Probable transcriptional regulatory pro	5667,73	14	0,5273	-0,92	-0,64	0,23	1,31	0,1	0,69	0,1	0	CYT	Core
D9Q8R8_CORP1	6 carboxyhexanoate CoA ligase yn	4618,69	15	0,5827	-0,78	-0,54	0,15	1,26	0,07	0,74	0,07	0	CYT	Core
D9Q8S4_CORP1	Hit Histidine triad family protein OS	2212,25	10	0,5434	-0,88	-0,61	0,22	1,29	0,1	0,71	0,1	0	CYT	Core
D9Q8S5_CORP1	Threonine tRNA ligase eri	5451,15	37	0,8521	-0,23	-0,16	0,09	1,08	0,05	0,92	0,05	0	CYT	Core
D9Q8S6_CORP1	Dyp type peroxidase family protein	1180,79	24	1,4049	0,49	0,34	0,26	0,83	0,12	1,17	0,12	0,99	CYT	Core
D9Q8S7_CORP1	Lipoprotein	37673,4	12	1,4477	0,53	0,37	0,09	0,82	0,04	1,18	0,04	1	PSE	Core
D9Q8T2_CORP1	Chlorite dismutase	36674,05	20	1,716	0,78	0,54	0,09	0,74	0,04	1,26	0,04	1	CYT	Core
D9Q8T3_CORP1	Putative uncharacterized protein	1247,22	8	1,6989	0,76	0,53	0,42	0,74	0,18	1,26	0,18	0,98	CYT	Core
D9Q8T5_CORP1	1 deoxy D xylulose 5 phosphate synthase	2183,21	32	0,7711	-0,38	-0,26	0,13	1,13	0,07	0,87	0,07	0	CYT	Core
D9Q8T6_CORP1	RNA methyltransferase TrmA family	325,54	14	0,5326	-0,91	-0,63	0,34	1,3	0,15	0,7	0,15	0	CYT	Core
D9Q8T8_CORP1	Putative uncharacterized protein	1693,61	11	1,9739	0,98	0,68	0,24	0,67	0,11	1,33	0,11	1	CYT	Core
D9Q8T9_CORP1	Deoxyuridine 5 triphosphate nucleotido	7379,32	9	0,5016	-1,00	-0,69	0,29	1,33	0,12	0,67	0,12	0	CYT	Core
D9Q8U0_CORP1	Putative uncharacterized protein	968,42	4	1,5841	0,66	0,46	0,42	0,78	0,2	1,22	0,2	0,98	MEM	Shared
D9Q8U1_CORP1	Putative uncharacterized protein	1316,34	7	0,463	-1,11	-0,77	0,45	1,36	0,19	0,64	0,19	0	CYT	Core
D9Q8U2_CORP1	Polyphosphate glucokinase	5342,55	11	0,6977	-0,52	-0,36	0,17	1,18	0,08	0,82	0,08	0	CYT	Core
D9Q8U3_CORP1	RNA polymerase sigma factor a	3408,18	22	1,8589	0,89	0,62	0,12	0,7	0,05	1,3	0,05	1	CYT	Core
D9Q8U6_CORP1	Putative uncharacterized protein	1676,76	7	0,436	-1,20	-0,83	0,5	1,39	0,21	0,61	0,21	0,01	CYT	Shared

D9Q8V0_CORP1	RNA polymerase sigma factor a	1047,88	16	0,6771	-0,56	-0,39	0,18	1,19	0,09	0,81	0,09	0	CYT	Core
D9Q8V1_CORP1	Diphtheria toxin repressor ac	45064,54	17	1,5841	0,66	0,46	0,09	0,77	0,04	1,23	0,04	1	CYT	Core
D9Q8V2_CORP1	UDP glucose 4 epimerase er	21656,98	18	0,6703	-0,58	-0,4	0,1	1,2	0,05	0,8	0,05	0	CYT	Core
D9Q8V4_CORP1	Proteasome assembly chaperones 2 PAC2	685,43	11	0,4966	-1,01	-0,7	0,3	1,33	0,13	0,67	0,13	0	CYT	Core
D9Q8V5_CORP1	Alkyl hydroperoxide reductase AhpD	80222,59	13	1,0942	0,13	0,09	0,07	0,96	0,03	1,04	0,03	0,99	CYT	Core
D9Q8V6_CORP1	Alkyl hydroperoxide reductase subunit C	33130,05	14	1,9155	0,94	0,65	0,16	0,69	0,07	1,31	0,07	1	CYT	Core
D9Q8W0_CORP1	Transcriptional repressor NrdR yn	2214,19	9	1,4477	0,53	0,37	0,3	0,82	0,14	1,18	0,14	0,99	CYT	Shared
D9Q8W3_CORP1	Galactitol utilization operon repressor	10063,69	15	1,2092	0,27	0,19	0,18	0,91	0,09	1,09	0,09	0,96	CYT	Core
D9Q8W4_CORP1	Phosphoenolpyruvate protein phosphotran	27878,12	29	0,8521	-0,23	-0,16	0,07	1,08	0,04	0,92	0,04	0	CYT	Core
D9Q8W9_CORP1	Phosphocarrier protein HPr ac	36269,17	4	1,391	0,48	0,33	0,11	0,84	0,05	1,16	0,05	1	CYT	Core
D9Q8X3_CORP1	GTPase HflX	760,86	22	0,6188	-0,69	-0,48	0,21	1,23	0,1	0,77	0,1	0	CYT	Core
D9Q8X4_CORP1	Putative uncharacterized protein	2408,27	7	0,4449	-1,17	-0,81	0,33	1,38	0,14	0,62	0,14	0	CYT	Core
D9Q8X6_CORP1	Diaminopimelate epimerase	3822,71	10	0,6376	-0,65	-0,45	0,2	1,22	0,09	0,78	0,09	0	CYT	Core
D9Q8X8_CORP1	Putative uncharacterized protein	442,34	12	0,7118	-0,49	-0,34	0,23	1,17	0,11	0,83	0,11	0,01	CYT	Core
D9Q8X9_CORP1	Putative uncharacterized protein	28382,21	28	0,8106	-0,30	-0,21	0,11	1,1	0,06	0,9	0,06	0	CYT	Core
D9Q8Y1_CORP1	Dimethylallyl adenosine tRNA methylthi	357,09	22	0,5488	-0,87	-0,6	0,27	1,29	0,12	0,71	0,12	0	CYT	Core
D9Q8Y3_CORP1	Protein RecA seudot	10572,09	23	0,7047	-0,50	-0,35	0,1	1,17	0,05	0,83	0,05	0	CYT	Core
D9Q8Y8_CORP1	Phage shock protein A IM30	25919,42	21	0,522	-0,94	-0,65	0,07	1,32	0,03	0,68	0,03	0	CYT	Core
D9Q8Z7_CORP1	Putative uncharacterized protein	338,24	11	0,7788	-0,36	-0,25	0,25	1,13	0,12	0,87	0,12	0,03	CYT	Core
D9Q8Z9_CORP1	Dihydrodipicolinate synthase	7808,15	14	0,74	-0,43	-0,3	0,16	1,15	0,08	0,85	0,08	0	CYT	Core
D9Q902_CORP1	Polyribonucleotide nucleotidyltransfera	26710,7	45	0,68	-0,55	-0,38	0,05	1,19	0,03	0,81	0,03	0	CYT	Core
D9Q904_CORP1	30S ribosomal protein S15	77045,36	6	1,34	0,42	0,29	0,11	0,86	0,05	1,14	0,05	1	CYT	Core
D9Q905_CORP1	Pyrimidine specific ribonucleoside hydr	8386,93	9	0,54	-0,88	-0,61	0,17	1,29	0,08	0,71	0,08	0	CYT	Core
D9Q906_CORP1	Riboflavin biosynthesis protein ribF OS	1142,3	14	0,81	-0,30	-0,21	0,15	1,1	0,08	0,9	0,08	0,01	CYT	Core
D9Q912_CORP1	Ribosome binding factor A	35736,72	11	0,71	-0,49	-0,34	0,14	1,17	0,07	0,83	0,07	0	CYT	Core
D9Q913_CORP1	Translation initiation factor IF 2	10185,58	32	0,79	-0,33	-0,23	0,07	1,12	0,04	0,88	0,04	0	CYT	Core
D9Q915_CORP1	Transcription elongation protein	3684,88	17	0,72	-0,48	-0,33	0,19	1,16	0,09	0,84	0,09	0	CYT	Core
D9Q916_CORP1	Ribosome maturation factor Rimp y	1112,36	3	0,64	-0,65	-0,45	0,31	1,22	0,14	0,78	0,14	0	CYT	Core
D9Q918_CORP1	Proline tRNA ligase erium	8226,83	30	0,69	-0,53	-0,37	0,11	1,18	0,05	0,82	0,05	0	CYT	Shared
D9Q920_CORP1	Uroporphyrinogen III methylase yn	980,03	8	0,54	-0,89	-0,62	0,31	1,3	0,14	0,7	0,14	0	CYT	Core
D9Q925_CORP1	Cob I yrinic acid a c diamide adenosy	16455,74	14	2,12	1,08	0,75	0,15	0,64	0,07	1,36	0,07	1	CYT	Core

D9Q928_CORP1	Probable malate quinone oxidoreductase	28995,92	30	0,81	-0,30	-0,21	0,1	1,1	0,05	0,9	0,05	0	CYT	Core
D9Q929_CORP1	Mycothione glutathione reductase	7195,19	18	1,21	0,27	0,19	0,13	0,91	0,07	1,09	0,07	1	CYT	Core
F9Y2X3_CORP1	Invasion associated protein p60 y	7046,85	25	0,66	-0,61	-0,42	0,22	1,21	0,1	0,79	0,1	0	CYT	Core
GLGE_CORP1	Alpha 1 4 glucan maltose 1 phosphate malt	2644,02	23	0,67	-0,58	-0,4	0,13	1,2	0,06	0,8	0,06	0	CYT	Core

(b) Core-genome analysis of 15 strains of *C. pseudotuberculosis*: shared = present in two or more strains; core = present in 15 strains of *C. pseudotuberculosis*

(c) CYT = cytoplasmic; MEM = membrane; PSE = potentially surface-exposed; SEC = secreted

Anexo/Annexe 3: Subjected Publications / Evidence Submission

A shift in the virulence potential of *Corynebacterium pseudotuberculosis* biovars *ovis* and *equi* after passage in a murine host demonstrated through comparative proteomics. (Submitted for publication in the journal: *Journal of Proteomics* – Online ISSN: 1874-3919) Silva, W.M., Dorella, F.A., Soares, S.C., Souza, G.H., Santos, A.V., Pimenta, A.M., Le Loir, Y., Miyoshi, A., Silva, A., Azevedo, V.

Elsevier Editorial System(tm) for Journal of Proteomics

Manuscript Number: JPROT-S-14-01015

Title: A shift in the virulence potential of *Corynebacterium pseudotuberculosis* biovars *ovis* and *equi* after passage in a murine host demonstrated through comparative proteomics

Article Type: Original Article

Keywords: *Corynebacterium pseudotuberculosis*; proteomic; caseous lymphadenitis; ulcerative lymphangitis; bacterial virulence; serial passage

Corresponding Author: Prof. Vasco Azevedo, Ph.D

Corresponding Author's Institution: Federal University of Minas Gerais

First Author: Wanderson M Silva, MSc

Order of Authors: Wanderson M Silva, MSc; Fernanda A Dorella, Ph.D; Siomar C Soares, Ph.D; Gustavo H Souza, Ph.D; Agenor V Santos, Ph.D; Adriano M Pimenta, Ph.D; Yves Le Loir, Ph.D; Anderson Miyoshi, Ph.D; Artur Silva, Ph.D; Vasco Azevedo, Ph.D

Abstract: *Corynebacterium pseudotuberculosis* is a pathogen subdivided into two biovars: *C. pseudotuberculosis ovis*, etiologic agent of caseous lymphadenitis in small ruminants, and *C. pseudotuberculosis equi*, which causes ulcerative lymphangitis in equines. For insight into biovar differences and to identify proteins that favor the virulence of this pathogen, we applied an experimental passage process using a murine model and high-throughput proteomics to evaluate the functional genome of the strains 1002_*ovis* and 258_*equi*. The experimental infection assays revealed that strain 258_*equi* exhibits higher virulence than strain 1002_*ovis*. However, recovering these strains from infected mice spleens induced a dramatic change in the strain 1002_*ovis* virulence potential, which became as virulent as strain 258_*equi* in a new infection challenge. The proteomic screening performed from the culture supernatant of these recovered strains, revealed 118 proteins differentially regulated in the strain 1002_*ovis* and 140 proteins differentially regulated in the strain 258_*equi*. In addition, this proteomic analysis revealed that

strain 1002_*ovis* and strain 258_*equi* produce different classes of proteins involved in detoxification process, pathogenesis and export pathways. The results indicate that the stains 1002_*ovis* and 258_*equi* use distinct mechanisms during infection. Moreover, this study enhances our understanding of the factors that may influence pathogenesis of *C. pseudotuberculosis*.

Suggested Reviewers: Sergio Costa Oliveira Ph.D
Immunology and Biochemistry , UFMG
scozeus@icb.ufmg.br

Mario Sergio Palma Ph.D
Center for the Study of Venoms and Venomous Animals, UNESP
mspålma@rc.unesp.br

Stanislav Dusko Ehrlich Ph.D
Unité de Génétique Microbienne, INRA
dusko.ehrlich@jouy.inra.fr

Opposed Reviewers: Michael C Fontaine
Ph.D, Moredun Research Institute
michael.fontaine@moredun.ac.uk

Anexo/Annexe 4: Curriculum vitae

Address to access this CV:<http://lattes.cnpq.br/1913484452322187>

Personal Information

Full name	Wanderson Marques Silva
Name used in Bibliographic Citations	SILVA, W. M.;SILVA, WANDERSON MARQUES;SILVA, WANDERSON M.;Wanderson M. Silva;Marques Silva, W;SILVA, WANDERSON M;Wanderson M Silva
Professional Address	Universidade Federal de Minas Gerais, Instituto de Ciências Biológicas Av. Antônio Carlos, 6627, Laboratorio de Genetica Celular e Molecular, Bloco Q3, sala 259 Pampulha - Belo Horizonte 31270910, MG - Brazil Phone number: 31 34092873
e-Mail	contact e-mail : silvamarques@yahoo.com.br alternative e-mail : wanderson.marques1@gmail.com

Formal Education

2011	Doctorate in Genetics. Universidade Federal de Minas Gerais, UFMG, Belo Horizonte, Brazil (Co-guardianship) Institut National de la Recherche Agronomique (Advisor : Yves Le Loir) Title: Estudo do genoma funcional de <i>Corynebacterium pseudotuberculosis</i> através de diferentes estratégias proteômicas Advisor: Vasco Ariston de Carvalho Azevedo Scholarship from : Coordenação de Aperfeiçoamento de Pessoal de Nível Superior <i>Knowledge areas : Molecular Genetics and of Microorganisms, Molecular Biology</i>
2009 - 2011	Professional Master's in Inovações Biofarmacêuticas. Universidade Federal de Minas Gerais, UFMG, Belo Horizonte, Brazil Title: Caracterização do exoproteoma de duas linhagens de <i>Corynebacterium pseudotuberculosis</i> através de 2D-DIGE e espectrometria de massa Advisor: Vasco Ariston de Carvalho Azevedo Scholarship from : Conselho Nacional de Desenvolvimento Científico e Tecnológico <i>Keywords: Corynebacterium pseudotuberculosis, Linfadenite Caseosa, Proteômica</i> <i>Knowledge areas : Molecular Genetics and of Microorganisms, Biochemistry</i>
2008 - 2009	Specialization in Microbiologia.

Universidade Federal de Minas Gerais, UFMG, Belo Horizonte, Brazil
Title: Novas perspectivas na elaboração de um diagnóstico subclínico para linfadenite caseosa através da técnica de Phage Display
Advisor: Vasco Ariston de Carvalho Azevedo

2004 - 2007 Bachelor's in Biomedicina.
Universidade José do Rosário Vellano, UNIFENAS, Alfenas, Brazil
Title: História da Arte da Linfadenite Caseosa e o Genoma de seu agente etiológico Corynebacterium pseudotuberculosis.
Advisor: Vasco Ariston de Carvalho Azevedo

Complementary Education

2013 - 2013	Short Term Course in Bioinformática Estrutural e Análises do Proteoma. Universidade Federal de Minas Gerais, UFMG, Belo Horizonte, Brazil
2012 - 2012	Short Term Course in Molecular Methods for Microbial Diagnosis. Universidade Federal de Minas Gerais, UFMG, Belo Horizonte, Brazil
2010 - 2010	Proteomic Analysis - CBAB/CABIO. Universidade Estadual Paulista Júlio de Mesquita Filho, UNESP, São Paulo, Brazil
2009 - 2009	Short Term Course in Aplicações da PCR Quantitativa em Tempo Real. Universidade Federal do Pará, UFPA, Belém, Brazil
2007 - 2007	Short Term Course in Citogenética molecular no diagnóstico e pesquisa. Sociedade Brasileira de Genética, SBG, Ribeirão Preto, Brazil
2007 - 2007	Short Term Course in Atualização Clínico-Patológica em HPV. Sociedade Brasileira de Patologia, SBP, São Paulo, Brazil
2004 - 2004	Short Term Course in 1º Seminário de Atualização em Biomedicina. Universidade José do Rosário Vellano, UNIFENAS, Alfenas, Brazil

Areas of Expertise

1. Pathological Anatomy and Clinical Pathology
2. Molecular Biology
3. Micro-organism genetic
4. Applied Microbiology

Languages

English	Understanding Functional , Speaking Functional , Writing Basic , Reading Fluent
Español	Understanding Fluent , Speaking Fluent , Writing Functional , Reading Fluent
Français	Understanding Functional , Speaking Functional , Writing Basic , Reading Functional

S, T & A Production

Bibliographic Production

Articles Published in Scientific Journals

1. **SILVA, WANDERSON M.**, SEYFFERT, NÚBIA, CIPRANDI, ALESSANDRA, SANTOS, AGENOR V., CASTRO, THIAGO L. P., PACHECO, LUIS G. C., BARH, DEBMALYA, LE LOIR, YVES, PIMENTA, ADRIANO M. C., MIYOSHI, ANDERSON, SILVA, ARTUR, AZEVEDO, VASCO
Differential Exoproteome Analysis of Two *Corynebacterium pseudotuberculosis* Biovar Ovis Strains Isolated from Goat (1002) and Sheep (C231). *Current Microbiology* (Print). , v.xx, p.xx - xx, 2013.
2. **SILVA, WANDERSON M.**, SEYFFERT, NÚBIA, SANTOS, AGENOR V., CASTRO, THIAGO L.P., PACHECO, LUIS G.C., SANTOS, ANDERSON R., CIPRANDI, ALESSANDRA, DORELLA, FERNANDA A., ANDRADE, HÉLIDA M., BARH, DEBMALYA, PIMENTA, ADRIANO M.C., SILVA, ARTUR, MIYOSHI, ANDERSON, AZEVEDO, VASCO
Identification of 11 new exoproteins in *Corynebacterium pseudotuberculosis* by comparative analysis of the exoproteome. *Microbial Pathogenesis*. , v.xx, p.xx - xx, 2013.
3. CIPRANDI, ALESSANDRA, **SILVA, WANDERSON MARQUES**, SANTOS, AGENOR VALADARES, CASTRO PIMENTA, ADRIANO MONTEIRO, CAREPO, MARTA SOFIA PEIXE, SCHNEIDER, MARIA PAULA CRUZ, AZEVEDO, VASCO, SILVA, ARTUR
Chromobacterium violaceum: Important Insights for Virulence and Biotechnological Potential by Exoproteomic Studies. *Current Microbiology*. , v.00, p.00 - 00, 2013.
4. CASTRO, T. L. P., SEYFFERT, N., Ramos, J., BARBOSA, S., CARVALHO, R. D. O., PINTO, A. C., CARNEIRO, A. R., **SILVA, W. M.**, PACHECO, L. G. C, DOWNSON, C., SCHNEIDER, M. P., MIYOSHI, A., AZEVEDO, V., SILVA, A.
Ion Torrent-based transcriptional assessment of a *Corynebacterium pseudotuberculosis* equi strain reveals denaturing high-performance liquid chromatography a promising rRNA depletion method.. *Microbial Biotechnology* (Online). , v.6, p.168 - 177, 2013.
5. PINTO, A. C., RAMOS, R. T. J., **SILVA, W. M.**, ROCHA, F. S., BARBOSA, S., MIYOSHI, A., SCHNEIDER, M. P., SILVA, A., AZEVEDO, V.
The core stimulon of *Corynebacterium pseudotuberculosis* strain 1002 identified using ab initio methodologies. *INTEGR BIOL-UK*. , v.00, p.00 - , 2012.
6. PACHECO, L. G. C, SUSAN,, SEYFFERT, N., SANTOS, A.R, CASTRO, T. L. P., **SILVA, W. M.**, SANTOS, A. V., SANTOS, S. G., FARIA, L. M., CARVALHO, M. A., PIMENTA, A., MEYER, R., SILVA, A., SCRIVENS, J. H., OLIVEIRA, S. C., MIYOSHI, A., DOWNSON, C. G., AZEVEDO, V.
A combined approach for comparative exoproteome analysis of *Corynebacterium pseudotuberculosis*.. *BMC Microbiology* (Online). , v.11, p.00 - 00, 2011.
7. SEYFFERT, N., PACHECO, L. G. C, **SILVA, W. M.**, CASTRO, T. L. P., SANTOS, A. V., SANTOS, A.R, McCulloch, J. A, RODRIGUES, M. R., SANTOS, S. G., FARIA, L. M., CARVALHO, M. A., PIMENTA, A., SILVA, A., MEYER, R., MIYOSHI, A., AZEVEDO, V.
Serological secretome analysis of *Corynebacterium pseudotuberculosis*. *Journal of Integrated OMICS*. , v.00, p.00 - 00, 2011.
8. CHAGAS, S. A. P., NUNES, M. B., SOUZA, R. T. P. E., **SILVA, W. M.**
Malacoplaquia na língua : relato de caso. *Brazilian journal of otorhinolaryngology* (Online). , v.75, p.910 - , 2009.
9. MORAES, PABLO M. R. O., SEYFFERT, NUBIA, **SILVA, WANDERSON M.**, CASTRO, THIAGO L. P., SILVA, RENATA F., LIMA, DANIELLE D., HIRATA, RAPHAEL, SILVA, ARTUR, MIYOSHI, ANDERSON, AZEVEDO, VASCO
Characterization of the Opp Peptide Transporter of *Corynebacterium pseudotuberculosis* and Its Role in Virulence and Pathogenicity. *BioMed Research International*. , v.2014, p.1 - 7, 2014.
10. PINTO, ANNE CYBELLE, DE SÁ, PABLO HENRIQUE, RAMOS, ROMMEL T, BARBOSA,

SILVANIRA, BARBOSA, HIVANA P, RIBEIRO, ADRIANA CARNEIRO, **SILVA, WANDERSON MARQUES**, ROCHA, FLÁVIA SOUZA, SANTANA, MARIANA PASSOS, DE PAULA CASTRO, THIAGO LUIZ, MIYOSHI, ANDERSON, SCHNEIDER, MARIA P, SILVA, ARTUR, AZEVEDO, VASCO
Differential transcriptional profile of *Corynebacterium pseudotuberculosis* in response to abiotic stresses. BMC Genomics. , v.15, p.14 - , 2014.

11. **SILVA, WANDERSON M**, CARVALHO, RODRIGO D, SOARES, SIOMAR C, BASTOS, ISABELA FS, FOLADOR, EDSON L, SOUZA, GUSTAVO HMF, LE LOIR, YVES, MIYOSHI, ANDERSON, SILVA, ARTUR, AZEVEDO, VASCO

Label-free proteomic analysis to confirm the predicted proteome of *Corynebacterium pseudotuberculosis* under nitrosative stress mediated by nitric oxide. BMC Genomics. , v.15, p.1065 - , 2014.

12. SEYFFERT, NUBIA, SILVA, RENATA FARIA, JARDIN, JULIEN, **SILVA, WANDERSON MARQUES**, DE PAULA CASTRO, THIAGO LUIZ, TARTAGLIA, NATAYME ROCHA, DE OLIVEIRA SANTANA, KARINA TALITA, PORTELA, RICARDO WAGNER, SILVA, ARTUR, MIYOSHI, ANDERSON, LE LOIR, YVES, AZEVEDO, VASCO

Serological proteome analysis of *Corynebacterium pseudotuberculosis* isolated from different hosts reveals novel candidates for prophylactics to control caseous lymphadenitis. Veterinary Microbiology (Amsterdam. Print). , v.6, p.00 - , 2014.

Book chapters published

1. SILVA, A., CARNEIRO, A. R., ABURJAILE, F., GUIMARAES, L. C., RAMOS, R. T., CASTRO, T. L. P., ABREU, V., **SILVA, WANDERSON M**, SCHNEIDER, M. P., AZEVEDO, V.

Comprehensive whole genome and transcriptome analysis for novel diagnostics In: Comprehensive whole genome and transcriptome analysis for novel diagnostics. 1 ed. London : Future Medicine, 2013, p. 64-76.

2. SOARES, S. C., RAMOS, R. T. J., **SILVA, W. M.**, OLIVEIRA, L. C., AMORIM, L. G., HIRATA Jr, R., MATTOS-GUARALDI, A. L., MIYOSHI, A., SILVA, A., AZEVEDO, V.

Corynebacterium pathogenic species in next-generation genomic era: the use of EDGAR and PIPS software and the importance of pathogenicity islands identification in pan-genomic analyses of pathogenic species. In: Microbial pathogens and strategies for combating them: science, technology and education. 1, 2013, v.3, p. 1584-1599.

Total of Production

Bibliographic Production

Articles published in scientific journal	12
Chapters published	2
Articles published in annals of events	19
Presentations in Events (Congress)	1

Academic Advisories

Academic Advisory - concluded (scientific initiation)	1
Participation in events (congress)	6
Participation in events (symposium)	2
Participation in events (other)	1